BIOLOGICAL FINGERPRINTING AND THERAPEUTIC EFFICACY OF *LANNEA COROMANDELICA* AND *TREVESIA PALMATA* IN TRINITROBENZENE SULFONIC ACID INDUCED ULCERATIVE COLITIS RAT MODEL

A THESIS SUBMITTED IN PARTIAL FULFILLMENT OF THE REQUIREMENTS FOR THE DEGREE OF DOCTOR OF PHILOSOPHY

BIDANCHI R. MOMIN

MZU REGISTRATION NO.: 7120 of 2014

Ph.D. REGISTRATION NO.: MZU/Ph.D./1105 of 03.05.2018

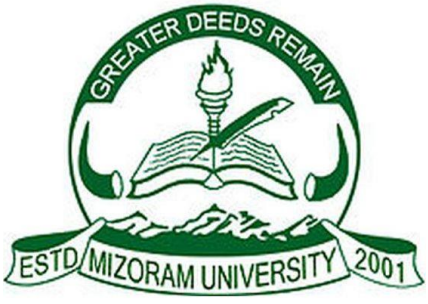

DEPARTMENT OF ZOOLOGY

SCHOOL OF LIFE SCIENCES

MARCH, 2025

BIOLOGICAL FINGERPRINTING AND THERAPEUTIC EFFICACY OF *LANNEA COROMANDELICA* AND *TREVESIA PALMATA* IN TRINITROBENZENE SULFONIC ACID INDUCED ULCERATIVE COLITIS RAT MODEL

BY

BIDANCHI R. MOMIN

Department of Zoology

SUPERVISOR

Prof. GURUSWAMI GURUSUBRAMANIAN

Submitted

In partial fulfillment of the requirement of the Degree of Doctor of Philosophy in Zoology of Mizoram University, Aizawl.

Department of Zoology
School of Life Sciences
MIZORAM UNIVERSITY
(*A Central University*)

Dr. G. Gurusubramanian Ph.D
Professor & Dean, SLS

Phone: 9862399411 (M)

CERTIFICATE

I certify that the thesis entitled "**Biological fingerprinting and therapeutic efficacy of *Lannea coromandelica* and *Trevesia palmata* in trinitrobenzene sulfonic acid induced ulcerative colitis rat model**" submitted to Mizoram University for the award of the degree of **Doctor of Philosophy** in **Zoology** by **Bidanchi R. Momin** bearing **MZU Regn. no. 7120 of 2014** and **Ph.D. Regn. No. MZU/Ph.D./1105 of 03.05.2018** is a record of dissertation work carried out under my guidance and supervision, and that this work has not formed the basis for the award of any degree, diploma or other titles in this university or any other university or institution of higher learning.

(Prof. G. Gurusubramanian)
Supervisor
Department of Zoology
Mizoram University
Aizawl-796004

DECLARATION

MIZORAM UNIVERSITY

MARCH, 2025

I **BIDANCHI R. MOMIN**, hereby declare that the subject matter of this thesis is the record of work done by me, that the contents of this thesis did not form basis of the award of any previous degree to me or to do the best of my knowledge to anybody else, and that the thesis has not been submitted by me for any research degree in any other University/Institute.

This is being submitted to the Mizoram University for the **Degree of Doctor of Philosophy in Zoology.**

(BIDANCHI R. MOMIN)

Department of Zoology
Mizoram University, Aizawl - 796004

(**Prof. H.T. LALREMSANGA**)
Head
Department of Zoology
Mizoram University
Aizawl - 796004

(**Prof. G. GURUSUBRAMANIAN**)
Supervisor
Department of Zoology
Mizoram University
Aizawl - 796004

ACKNOWLEDGEMENT

With immense gratitude and heartfelt appreciation, I extend my most sincere thanks to all those who have supported, guided, and encouraged me throughout my Ph.D. journey.

First and foremost, I express my deepest gratitude to God Almighty for His endless blessings, wisdom, and strength, which have sustained me throughout this journey. His grace has been my guiding light, enabling me to overcome challenges and successfully complete my research.

I am profoundly grateful to my supervisor, Prof. G. Gurusubramanian, for his invaluable guidance, unwavering support, and insightful mentorship. His encouragement and expertise have been instrumental in shaping my research and academic growth. I also extend my sincere thanks to Dr. Vikas Kumar Roy, Associate Professor, for his constant guidance, constructive suggestions, and support throughout this work.

I am deeply appreciative of Prof. H.T. Lalremsanga, Head of the Department of Zoology, Mizoram University, for his encouragement and support, as well as all the esteemed faculty members of the department for their guidance and cooperation. I also extend my sincere gratitude to the office staff for their assistance and support throughout my academic journey.

I am immensely thankful to Brilliant N. Marak, Dr. Manikandan Bose, Nisekhoto Nisa, Bhanushree Baishya, Dorshon Chakravarty, Andy Lalremruata, Behryl Ch. Marak, R. Lalremruata, Abdelgani Baraka, Saeed Ahmed Lasker, Sonia Chakma and Dr. Dinata Roy for their unwavering cooperation, valuable suggestions, and constant encouragement. Their support and camaraderie have made this journey more

enriching. My sincere appreciation also goes to my lab mates for their invaluable assistance and support during my research.

I extend my gratitude to the Department of Biotechnology, Ministry of Science and Technology, Government of India; Ministry of Tribal Affairs, Government of India; and the University Grants Commission (UGC) for their financial support, which made this research possible.

A special note of thanks to my mother and siblings, whose unconditional love, financial support, and unwavering belief in me have been my greatest source of strength. Their sacrifices and encouragement have been invaluable in this journey.

Lastly, I am deeply grateful to my friends, both near and far, for their constant emotional and mental support. Their encouragement and understanding have played a crucial role in keeping me motivated throughout this challenging yet rewarding journey.

-Bidanchi R. Momin

Table of Contents

LIST OF FIGURES

	coromandelica (Lc 10 mg/kg) and *Lannea coromandelica* (Lc 20 mg/kg). Datas are represented as Mean ± SEM (n = 5). Statistical comparison was performed using one-way ANOVA followed by Tukey's multiple comparison tests. The bar graph with a different letter means statistically significant difference at $p < 0.05$ and similar letters are not significant.	
Figure 48	*Lannea coromandelica* – induced suppression of inflammatory parameter in TNBS-treated rats. *Lannea coromandelica* (Lc 10 mg/kg) and *Lannea coromandelica* (Lc 20 mg/kg) decreased the high expression of TNF alpha (B), IL-6 (C) and iNOS (D) expression (A). *Lannea coromandelica* reduced the increase in NFkB-p65 (A) phosphorylation and inducible nitric oxide synthase (iNOS) (D) protein expression in TNBS-treated rats. Lannea coromandelica also increased the transcription factor PPAR gamma (E) and NOX2 (F) NADPH oxidase protein expression by the administration of Lannea coromandelica (Lc 10 mg/kg) and Lannea coromandelica (Lc 20 mg/kg). Datas are represented as Mean ± SEM (n = 5). Statistical comparison was performed using one-way ANOVA followed by Tukey's multiple comparison tests. The bar graph with a different letter means statistically significant difference at $p < 0.05$ and similar letters are not significant.	275

LIST OF TABLES

List Of Acronyms

%	Percentage
°C	Degree celsius
°F	Degree fahrenheit
µg	microgram
µl	microlitre
µm	micrometer
ABC	Avidin-biotinylated peroxidase complex
ADMET	Chemical absorption, distribution, metabolism, excretion, and toxicity
ATSDR	The Agency for Toxic Substances and Disease Registry
Bax	Apoptotic regulator
Bcl-2	B-cell lymphoma
CAT	Catalase
COX-2	Cyclooxygenase 2
CALP	Calprotection
DAB	3,3′-diaminobenzidine tetrachloride
DNA	Dioyribonucleic acid
DTNB	5,5’-dithiobis-(2-nitrobenzoic acid)
EDTA	Ethylene diamine tetraacetic acid
ECL	Enhanced chemiluminescence
GPx	Glutathione peroxidase
GSH	Reduced glutathione
GSSG	Glutathione disulfide
H_2O_2	Hydrogen Peroxide
IU/L	International unit per litre
IL-6	Interleukin-6

IL-10	Interleukin-10
K_2HPO_4	Dipotassium phosphate
Kg	Kilogram
KH_2PO_4	Monopotassium Phosphate
Lc	*Lannea coromandelica*
LCLE	Lannea coromandelica leaf extract
LPO	Lipid peroxidation
M	Molar concentration
MDA	3,4-Methylenedioxyamphetamine
MCE	Medicinal chemistry evolution
Mg	milligram
Min	minute
Ml	millilitre
mM	millimolar
MPO	Myeloperoxidase
MW	Molecular weight
Na_2HPO_4	Disodium phosphate
NaCl	Sodium Chloride
NADH	Nicotinamide adenine dinucleotide
NO	Nitric oxide
Nm	Nanomole
NFkB p65	Nuclear factor kappa B p65
NOAEL	No-observed adverse effect level
NOEL	No-observed effect level
OECD	Organization for Economic Cooperation and Development
p53	Tumour protein
PAGE	Polyacrylamide gel electrophoresis
PBS	Phosphate-buffered saline
PG-E2	Prostaglandin E2
pH	Power of Hydrogen
PPAR-α	Peroxisome proliferator-activated receptor (PPAR)-alpha

PVDF	Polyvinylidene fluoride
QED	Quantitative estimate of druglikeness
QSAR	Quantitative structure-activity relationships
ROS	Reactive Oxygen Species
Rpm	Revolutions per minute
RT-PCR	Reverse Transcriptase Polymerase Chan Reaction
SAscore	Synthetic accessibility score
SDS	Sodium dodecyl sulphate
Sec	Second
SOD	Superoxide dismutase
TBA	Thiobarbituric acid
TBARS	Thiobarbituric acid reactive substances
TCA	Tetracyclic acid
Tris-HCl	Tris hydrochloride
TNBS	Trintitrobenzenesulfonic acid
Tp	*Trevesia palmata*
TPLE	Trevesia palmata
TNF-α	Tumour Necrosis Factor alpha
UV-VIS	Ultraviolet visible
Wt	Weight

CHAPTER 1

GENERAL INTRODUCTION

I. GENERAL INTRODUCTION

1.1. Ulcerative Colitis: A Comprehensive Review

Ulcerative colitis (UC) is a chronic inflammatory bowel disease (IBD) characterized by inflammation and ulceration of the colonic mucosa. It is one of the two main forms of IBD, the other being Crohn's disease. UC typically presents with symptoms such as bloody diarrhoea, abdominal pain, urgency, and tenesmus, which can significantly impair patients' quality of life (Lamb et al., 2019). Despite advances in understanding its pathogenesis and treatment, UC remains a challenging condition to manage, requiring a multidisciplinary approach for optimal care (Taku et al., 2020).

UC is most commonly diagnosed in young adults aged 15 to 35 years, although it can occur at any age. The incidence and prevalence of UC vary geographically, with higher rates reported in Western countries such as North America and Europe (Pizzorno et a., 2016). However, UC incidence is rising globally, including in developing regions undergoing rapid industrialization and westernization (Mendell et al., 2023).

The exact aetiology of UC remains incompletely understood, but it is believed to result from a complex interplay between genetic susceptibility, environmental factors, dysregulated immune responses, and alterations in the gut microbiota (Tanwar et al., 2023; Caioni et al., 2021). Genetic studies have identified numerous susceptibility loci associated with UC, implicating aberrant immune activation and epithelial barrier dysfunction in disease pathogenesis. Environmental factors such as diet, smoking, and antibiotic use also contribute to UC risk, highlighting the importance of gene-environment interactions (Porter et al., 2020; Di Sabatino et al., 2012).

UC typically presents with a relapsing-remitting course, characterized by periods of active inflammation interspersed with periods of remission (Kaushal et al., 2017). Common symptoms include bloody diarrhoea, abdominal pain, urgency, tenesmus, and fatigue. The severity and extent of disease vary among patients, ranging from

mild, limited colitis to severe, extensive colonic involvement (Gros and Kaplan, 2023; Choi et al., 2018).

The diagnosis of UC is based on a combination of clinical symptoms, endoscopic findings, histopathological evaluation, and exclusion of other causes of colonic inflammation (Kovari et al., 2022; Gajendran et al., 2019). Endoscopy with mucosal biopsy remains the gold standard for diagnosis, allowing direct visualization of colonic mucosal inflammation and histological assessment of disease severity (Van der Laan et al., 2021; Waldner et al., 2017).

The goals of UC treatment are to induce and maintain remission, alleviate symptoms, prevent disease complications, and improve patients' quality of life. Treatment strategies vary depending on disease severity, extent, and patient factors. Therapeutic options include amino-salicylates, corticosteroids, immunomodulators, biologic agents, and surgical intervention in refractory cases or complications such as toxic megacolon or colorectal cancer (Cai et al., 2021).

UC is associated with various complications, including toxic megacolon, intestinal perforation, strictures, colorectal cancer, and extraintestinal manifestations such as arthritis, dermatologic conditions, and hepatobiliary disorders. Close monitoring and appropriate management are essential to prevent and mitigate these complications (Eder et al., 2023; Higuchi et al., 2016).

Ulcerative colitis is a complex inflammatory bowel disease with significant clinical implications (Orlando et al., 2013). Advances in understanding its aetiology, pathogenesis, and treatment have improved outcomes for patients with UC. However, challenges remain in optimizing disease management, particularly in refractory cases or those with complications (Elhag et al., 2022; Ashton et al., 2019). Further research is needed to elucidate the underlying mechanisms of UC and develop novel therapeutic approaches aimed at achieving long-term remission and improving patients' overall well-being.

1.2. Review of Trinitrobenzene Sulfonic Acid (TNBS) as a Drug for Establishing Ulcerative Colitis Rat Models

Trinitrobenzene sulfonic acid (TNBS) is a well-established chemical agent used to induce experimental colitis in animal models, particularly rats, to mimic the pathophysiological features of human ulcerative colitis (UC) (Chamanara et al., 2019). UC is a chronic inflammatory bowel disease characterized by inflammation and ulceration of the colonic mucosa (Gajendran et al., 2019). The TNBS-induced colitis model has been widely utilized in preclinical research to investigate the pathogenesis of UC, evaluate potential therapeutic interventions, and elucidate underlying mechanisms of disease progression (Roy et al., 2023; Hu et al. 2021).

TNBS induces colitis through a two-step process involving haptenization and immune activation. Following rectal administration, TNBS haptenizes colonic proteins, leading to the formation of hapten-protein complexes recognized by the immune system as foreign antigens. This triggers an exaggerated T cell-mediated immune response, characterized by the activation of pro-inflammatory cytokines, such as tumour necrosis factor-alpha (TNF-α), interleukin-1 beta (IL-1β), and interleukin-6 (IL-6). The subsequent recruitment of immune cells, including macrophages, neutrophils, and T lymphocytes, results in mucosal inflammation, epithelial damage, and ulcer formation, closely resembling the histopathological features of human UC.

The TNBS-induced colitis model exhibits several key characteristics reminiscent of human UC (Silva et al., 2022; Antoniou et al., 2016), including:

i) Transmural Inflammation: TNBS administration leads to inflammation extending through the entire thickness of the colonic wall, resembling the transmural inflammation observed in UC (Silva et al., 2022; Calabresi et al., 2019).

ii) Mucosal Ulceration: TNBS-induced colitis results in mucosal ulceration, erosion, and crypt distortion, consistent with the ulcerative lesions observed in human UC (Catana et al., 2018; Yang et al., 2016).

iii) Inflammatory Cytokine Production: TNBS stimulates the production of pro-inflammatory cytokines within the colonic mucosa, contributing to the perpetuation of mucosal inflammation and tissue damage (de Oliveira et al., 2021; Ortiz et al., 2020).

iv) Immune Cell Infiltration: TNBS-induced colitis is characterized by the infiltration of immune cells, including neutrophils, macrophages, and T lymphocytes, into the colonic mucosa, reflecting the immune cell infiltrates observed in human UC lesions (Hambardikar et al., 2022; Alizade Naini et al., 2021).

The TNBS-induced colitis model serves as a valuable tool for preclinical drug development in UC. It allows researchers to evaluate the efficacy and safety of potential therapeutic interventions, including anti-inflammatory agents, immunomodulators, and biologic agents, in a controlled experimental setting. Moreover, the model enables the investigation of novel mechanisms underlying UC pathogenesis and the identification of potential therapeutic targets for disease intervention (Silva et al., 2022; Antoniou et al., 2016).

Trinitrobenzene sulfonic acid (TNBS) has emerged as a widely utilized drug for establishing ulcerative colitis rat models in preclinical research. By recapitulating key histopathological features of human UC, the TNBS-induced colitis model provides a valuable platform for investigating disease mechanisms, evaluating therapeutic interventions, and advancing our understanding of UC pathogenesis (Silva et al., 2022; Magro et al., 2021). However, it is essential to acknowledge the limitations of the model and consider complementary approaches to ensure the translational relevance of preclinical findings to human disease.

1.3. An Overview of Sulfasalazine as a Therapeutic Agent for Treating Ulcerative Colitis, Highlighting its Mechanism of Action, Clinical Efficacy and Safety Profile

Ulcerative colitis (UC) is a chronic inflammatory bowel disease characterized by inflammation and ulceration of the colonic mucosa, leading to debilitating symptoms such as abdominal pain, diarrhoea, and rectal bleeding. Management of UC aims to

induce and maintain remission, alleviate symptoms, and improve patients' quality of life (Taku et al., 2020). Sulfasalazine, a classic disease-modifying anti-rheumatic drug (DMARD), has been a cornerstone of UC therapy for decades. Its efficacy in UC treatment has been well-documented, making it a widely used first-line therapy in clinical practice (Choi and Fenando, 2020).

Sulfasalazine is a prodrug composed of sulfapyridine and 5-aminosalicylic acid (5-ASA) (Beiranvand,2021; Couto et al., 2010). Upon oral administration, sulfasalazine reaches the colon intact, where colonic bacteria enzymatically cleave it into its active metabolites. 5-ASA, the primary active component, exerts its therapeutic effects by modulating inflammatory pathways within the intestinal mucosa (Chu et al., 2023; Abdu-Allah et al., 2016). It inhibits the production of pro-inflammatory cytokines, such as tumour necrosis factor-alpha (TNF-α) and interleukin-1 beta (IL-1β), and suppresses the activity of nuclear factor-kappa B (NF-κB), a key transcription factor involved in inflammatory gene expression. Additionally, 5-ASA possesses antioxidant properties, scavenging reactive oxygen species (ROS) and reducing oxidative stress within the colonic mucosa (Hwang et al., 2019; Sakthivel et al., 2013; Lakey and Cawston, 2009).

Clinical trials and observational studies have consistently demonstrated the efficacy of sulfasalazine in inducing and maintaining remission in patients with mild to moderate UC. It has been shown to alleviate symptoms such as bloody diarrhoea, abdominal pain, and urgency, and promote mucosal healing. Sulfasalazine is often used as first-line therapy in UC management, particularly in patients with left-sided or extensive colitis. However, its efficacy may be limited in patients with severe disease or those who are refractory to treatment (Yoshino et al., 2016; Wang et al., 2016).

Sulfasalazine is generally well-tolerated, with common adverse effects including gastrointestinal disturbances (nausea, vomiting, abdominal discomfort), headache, and hypersensitivity reactions. Notably, sulfasalazine can cause reversible oligospermia and infertility in men due to its sulfapyridine component. Regular

monitoring of blood counts and liver function tests is recommended during sulfasalazine therapy to detect potential hematologic and hepatic adverse effects.

Sulfasalazine remains a cornerstone therapy for the treatment of ulcerative colitis, owing to its well-established efficacy and safety profile. By targeting inflammatory pathways and oxidative stress within the colonic mucosa, sulfasalazine provides symptomatic relief and promotes mucosal healing in patients with UC (Choi and Fenando, 2020; Yoshino et al., 2016). However, its use may be limited by adverse effects and intolerance in some individuals. Further research exploring novel therapeutic agents and treatment strategies is warranted to improve outcomes and optimize UC management.

1.4. Exploring the Medicinal Value of *Lannea coromandelica* and *Trevesia palmata* in Mizoram, India: A Review

Mizoram, a northeastern state of India, is blessed with a rich biodiversity, including a variety of medicinal plants that have been integral to the traditional healing practices of its indigenous communities (Ralte et al., 2024). Among these plants, *Lannea coromandelica* (Swathi and Lakshman, 2022) and *Trevesia palmata* (Reddy et al., 2011) hold particular significance due to their diverse pharmacological properties and traditional uses in managing various ailments. This review aims to explore the medicinal value of *L. coromandelica* and *T. palmata* in Mizoram, shedding light on their traditional uses, phytochemical composition, pharmacological activities, and potential therapeutic applications.

In Mizoram, *L. coromandelica* (locally known as "Tawitawsuak") and *T. palmata* (known as "Kawhtebel") have been traditionally employed as important remedies for generations. Various parts of these plants, including leaves, bark, roots, and fruits, are utilized to treat a wide array of health conditions. Traditional healers in Mizoram utilize these plants for ailments such as gastrointestinal disorders, respiratory infections, skin diseases, fevers, wounds, and inflammatory conditions (Swathi and Lakshman, 2022; Reddy et al., 2011).

In Mizoram, *Trevesia palmata*, locally known as "Kawhtebel," holds cultural significance and is traditionally used for various medicinal purposes. While scientific research specific to the medicinal use of *T. palmata* in Mizoram may be limited, its traditional medicinal applications have been documented. Some researchers have reported the various medicinal uses of *T. palmata* in Mizoram. The roots are traditionally used in Mizoram to treat digestive ailments such as diarrhea, dysentery, and stomachaches. The root extracts are believed to possess anti-diarrheal and anti-dysenteric properties. In traditional Mizo medicine, it is used to alleviate symptoms of respiratory disorders such as coughs, colds, and bronchitis. The leaves or roots may be prepared as decoctions or infusions for respiratory relief. *T. palmata* is also employed for its purported wound healing properties. The crushed leaves or roots may be applied topically to wounds, cuts, and skin infections to promote healing and prevent infection. The plant may also be used to reduce inflammation and swelling associated with various conditions. Extracts from *T. palmata* leaves or roots are applied externally to inflamed areas for relief. Traditional healers in Mizoram may recommend *T. palmata* preparations to reduce fever and alleviate pain. The plant's anti-pyretic and analgesic properties are believed to contribute to its effectiveness in managing these symptoms (Manoharan et al., 2023; Rahman et al., 2014 and Rai et al., 2011).

The traditional knowledge surrounding the medicinal uses of *L. coromandelica* and *T. palmata* reflects the deep-rooted connection between nature and healthcare practices in Mizoram. It's important to note that while these two plants have a long history of traditional medicinal use in Mizoram and other regions, scientific research on its efficacy and safety is still limited. Further studies are needed to validate its traditional uses, identify active compounds, and understand its pharmacological mechanisms. Additionally, caution should be exercised when using any herbal remedies, and consultation with healthcare professionals is advisable, especially for serious or chronic health conditions.

Both *L. coromandelica* and *T. palmata* are rich sources of bioactive compounds, including polyphenols, flavonoids, terpenoids, alkaloids, and saponins.

Phytochemical analyses have revealed the presence of these secondary metabolites in various plant parts, contributing to their pharmacological activities. The diverse chemical composition of these plants underscores their potential therapeutic versatility and highlights their importance in traditional medicine systems (Jared et al., 2024; Vaou et al., 2021).

Studies investigating the pharmacological activities of *L. coromandelica* and *T. palmata* have demonstrated a wide range of beneficial effects. These include anti-inflammatory, antioxidant, antimicrobial, antidiabetic, analgesic, and wound healing properties. The anti-inflammatory and antioxidant activities of these plants are particularly noteworthy, as they play crucial roles in managing inflammatory conditions and reducing oxidative stress-induced damage. Additionally, their antimicrobial properties make them valuable agents against infectious diseases prevalent in Mizoram (Gonfa et al., 2023 and Rodríguez-Yoldi, 2021).

The medicinal value of *L. coromandelica* and *T. palmata* extends to various health conditions prevalent in Mizoram and beyond. Their anti-inflammatory and antioxidant properties make them potential candidates for managing inflammatory bowel diseases, skin disorders, respiratory infections, and metabolic disorders such as diabetes. Furthermore, their antimicrobial activities suggest applications in treating microbial infections, while their wound healing properties may aid in the management of cutaneous injuries.

L. coromandelica and *T. palmata* represent valuable medicinal plants with significant therapeutic potential in Mizoram, India. Their traditional uses, phytochemical composition, and pharmacological activities highlight their importance in indigenous healthcare systems and underscore the need for further research to explore their full therapeutic potential. By integrating traditional knowledge with modern scientific approaches, efforts can be made to harness the medicinal value of these plants for the benefit of the population in Mizoram and beyond, thereby preserving traditional healing practices and promoting public health.

1.5. Significance of Biological Fingerprinting of Herbal Plants and Therapeutic Approach in Treating Trinitrobenzene Sulfonic Acid (TNBS) Induced Ulcerative Colitis

Ulcerative colitis (UC) is a chronic inflammatory disorder characterized by inflammation of the colon and rectum, resulting in symptoms such as abdominal pain, diarrhoea, rectal bleeding, and weight loss. Despite advancements in treatment options, including conventional drugs such as corticosteroids, immunosuppressants, and biologics, many patients continue to experience inadequate symptom control, adverse effects, and disease relapse. Hence, there is a growing interest in exploring complementary and alternative therapies derived from natural sources, particularly medicinal plants, for the management of UC (Tripathi and Feuerstein, 2019).

Lannea coromandelica and *Trevesia palmata* are two such medicinal plants known for their potential therapeutic properties. *L. coromandelica*, commonly known as "Indian ash tree" or "Gum Arabic tree," belongs to the family Anacardiaceae and is widely distributed throughout India and other parts of Asia. Various parts of *L. coromandelica*, including the bark, leaves, and gum resin, have been traditionally used in Ayurvedic medicine for their anti-inflammatory, antioxidant, and gastroprotective effects (Reddy et al., 2011). *T. palmata*, belonging to the family Araliaceae, is commonly found in tropical regions of Asia and Africa. Its roots and leaves have been used in traditional medicine for their anti-inflammatory, antimicrobial, and wound-healing properties (Rahman et al., 2014).

In recent years, there has been an increasing interest in investigating the therapeutic potential of *L. coromandelica* an d *T. palmata* in experimental models of UC. Trinitrobenzene sulfonic acid (TNBS)-induced colitis in rats is a well-established model that closely mimics the pathophysiology and clinical features of human UC. This model involves the intrarectal administration of TNBS, which induces colonic inflammation characterized by mucosal damage, infiltration of inflammatory cells, and production of pro-inflammatory cytokines (Antoniou et al., 2016).

Several preclinical studies have evaluated the therapeutic efficacy of *L. coromandelica* and *T. palmata* in TNBS-induced colitis rat models, shedding light on their potential mechanisms of action and pharmacological properties. Both *L. coromandelica* and *T. palmata* have demonstrated significant anti-inflammatory effects in TNBS-induced colitis rats, as evidenced by a reduction in colonic inflammation, histological damage, and levels of pro-inflammatory cytokines such as tumour necrosis factor-alpha (TNF-α), interleukin-6 (IL-6), and interleukin-1β (IL-1β). Oxidative stress plays a crucial role in the pathogenesis of UC (Liu et al., 2024 and Varzandeh et al., 2024). Studies have shown that *L. coromandelica* and *T. palmata* possess potent antioxidant properties, scavenging reactive oxygen species (ROS) and enhancing endogenous antioxidant defences, thereby protecting against oxidative damage in the colon of TNBS-induced colitis rats (Kumar and Jain, 2015; Manik et al., 2013; Arifin et al., 2017 and Rahman et al., 2014).

L. coromandelica and *T. palmata* may exert gastroprotective effects by enhancing mucosal integrity, stimulating mucus production, and inhibiting the activity of inflammatory enzymes such as cyclooxygenase (COX) and inducible nitric oxide synthase (iNOS) in the colon. Both plants may also exhibit immunomodulatory effects by regulating the balance between pro-inflammatory and anti-inflammatory cytokines, modulating the activity of immune cells such as macrophages and T lymphocytes, and suppressing the nuclear factor-kappa B (NF-κB) signalling pathway, which plays a central role in inflammation.

This experiment is significant for advancing our understanding of herbal medicine mechanisms, developing targeted therapies, ensuring product quality, and ultimately improving patient outcomes in UC management.

In conclusion, the biological fingerprinting and therapeutic efficacy of *L. coromandelica* and *T. palmata* in the TNBS-induced UC rat model offers promising prospects as evidenced by their anti-inflammatory, antioxidant, gastroprotective and immunomodulatory effects for the development of novel therapeutic agents for UC management. By elucidating the chemical composition and pharmacological effects

of these plants, researchers can identify potential lead compounds for further investigation and clinical development. Additionally, the preclinical evaluation of *L. coromandelica* and *T. palmata* in UC models contributes to our understanding of their therapeutic mechanisms and may pave the way for the development of botanical-based therapies for UC in the future, particularly those who are refractory to conventional therapies or seek natural remedies with fewer adverse effects.

1.6. Isolation, Characterization and Identification of Bioactive Compounds: An Overview

Isolation, characterization and identification of bioactive compounds from *Lannea coromandelica* and *Trevesia palmata* involve a multi-step process that typically includes extraction, chromatographic separation, and spectroscopic analysis. Gas chromatography-mass spectrometry (GC-MS), liquid chromatography-mass spectrometry (LC-MS), and infrared spectroscopy (IR) are commonly employed techniques for the identification and characterization of bioactive compounds in plant extracts (Altemimi et al., 2017). An overview of each step involved in the process are as follows:

A) Extraction: The first step involves the extraction of bioactive compounds from the plant material (e.g., leaves, bark, roots) using suitable solvents such as methanol, ethanol, or water. Various extraction techniques, including maceration, Soxhlet extraction, and ultrasound-assisted extraction, can be employed to obtain a crude extract rich in bioactive compounds (Jha and Sit, 2022).

B) Fractionation and purification: The crude extract is then fractionated using chromatographic techniques such as column chromatography or preparative high-performance liquid chromatography (HPLC). This step involves the separation of compounds based on their polarity, size, and chemical properties. Fractions containing bioactive compounds are collected and further purified to isolate individual compounds of interest (Abubakar and Haque, 2020).

C) Chromatographic analysis (GC-MS and LC-MS):

i) Gas Chromatography-Mass Spectrometry (GC-MS): GC-MS is a powerful analytical technique used for the separation and identification of volatile and semi-volatile compounds. The sample is injected into a gas chromatograph, where compounds are separated based on their volatility and affinity for the stationary phase. The separated compounds are then ionized and analyzed by mass spectrometry, allowing for the identification of individual compounds based on their mass spectra and retention times (Bubli et al., 2021).

ii) Liquid Chromatography-Mass Spectrometry (LC-MS): LC-MS is employed for the analysis of non-volatile and polar compounds. In this technique, the sample is separated by liquid chromatography, and the eluent is introduced into the mass spectrometer for analysis. LC-MS allows for the identification of compounds based on their mass-to-charge ratio (m/z) and fragmentation patterns, providing valuable information about the molecular structure of the compounds (Lopez-Fernandez et al., 2020).

D) Spectroscopic analysis (IR):

i) Infrared Spectroscopy (IR): IR spectroscopy is used to analyse the functional groups present in organic compounds based on their absorption of infrared radiation. The sample is irradiated with infrared light, and the absorption bands corresponding to different functional groups are recorded. IR spectra provide information about the molecular structure and chemical composition of the compounds, allowing for their identification and characterization (Valand et al., 2020).

E) Identification and characterization: The data obtained from chromatographic and spectroscopic analyses are used to identify and characterize the bioactive compounds present in the plant extracts. This may involve comparing the retention times and mass spectra obtained from GC-MS and LC-MS analyses with those of reference standards or databases. Additionally, the interpretation of IR spectra helps in elucidating the functional groups and molecular structure of the compounds (El Sayed et al., 2020).

By employing a combination of chromatographic and spectroscopic techniques, researchers can isolate, characterize, and identify bioactive compounds from *Lannea coromandelica* and *Trevesia palmata* extracts, providing valuable insights into their chemical composition and potential pharmacological activities.

1.7. Computational Study of the Phytochemical and Pharmacological Bio-Activities of Herbal Plants

Lannea coromandelica (Indian ash tree) and *Trevesia palmata* are two medicinal plants that have been traditionally used in various systems of medicine for their therapeutic properties. Both plants are known to possess a wide range of bioactive compounds, including polyphenols, flavonoids, terpenoids, and alkaloids, which contribute to their pharmacological activities (Swathi and Lakshman, 2022; Reddy et al., 2011). With the increasing interest in natural products as potential sources of new drugs, computational approaches have emerged as valuable tools for the prediction and evaluation of the phytochemical composition and pharmacological bio-activities of medicinal plants (Thomford et al., 2018).

Computational methods, including molecular docking, molecular dynamics simulations and quantitative structure-activity relationship (QSAR) modelling, allow for the in-silico analysis of plant-derived compounds and their interactions with biological targets. These methods enable researchers to predict the binding affinity, mode of interaction, and pharmacological effects of bioactive molecules, thus guiding the design and optimization of new drug candidates (Shah et al., 2024; Lahyaoui et al., 2023).

In this experiment, computational approaches can be used to predict the phytochemical profile of *L. coromandelica* and *T. palmata* leaves by screening their chemical constituents against databases of known natural products. This allows for the identification of novel bioactive compounds and the elucidation of their chemical structures.

Molecular docking studies can help identify potential biological targets of the bioactive compounds present in *L. coromandelica* and *T. palmata* leaves. By

simulating the binding of these compounds to target proteins involved in disease pathways, such as inflammatory mediators or enzymes, computational methods provide insights into their potential pharmacological activities (Jiao et al., 2021; Yadav et al., 2021).

Pharmacophore modelling and virtual screening techniques can be employed to identify lead compounds from *L. coromandelica* and *T. palmata* leaves with desired pharmacological properties. By comparing the pharmacophore features of bioactive molecules against databases of chemical compounds, virtual screening facilitates the discovery of novel drug candidates with improved efficacy and selectivity (Giordano et al., 2022).

The computational methods also allow for the prediction of pharmacokinetic properties, such as absorption, distribution, metabolism, and excretion (ADME), of bioactive compounds from *L. coromandelica* and *T. palmata* leaves. These predictions help prioritize lead compounds for further experimental validation based on their drug-likeness and bioavailability (Wu et al., 2020 and Rai et al., 2023).

Overall, computational studies provide valuable insights into the phytochemical composition and pharmacological bio-activities of *L. coromandelica* and *T. palmata* leaves, offering a rational approach for the discovery and development of new therapeutic agents. Integrating computational and experimental approaches enables a more comprehensive understanding of the medicinal properties of these plants and accelerates the drug discovery process for the treatment of various diseases (Singh and Bharadvaja, 2021; Duarte et al., 2019).

1.8. Implication of Acute and Sub-acute Studies

Lannea coromandelica (Indian ash tree) and *Trevesia palmata* (Snowflake tree) are medicinal plants widely used in traditional medicine for various therapeutic purposes (Malu et al., 2024; Manoharan et al., 2023; Victoria et al., 2019). While these plants are renowned for their pharmacological benefits, it is imperative to assess their safety profiles, particularly regarding acute and sub-acute toxicity, before considering their therapeutic applications in humans.

Acute toxicity refers to the adverse effects of a single exposure to a substance, while sub-acute toxicity involves repeated exposures over a relatively short duration, typically up to 28 days in animal studies (Lakshmanan, 2022).

Understanding the toxicological effects of *L. coromandelica* and *T. palmata* extracts is crucial for determining safe dosage regimens and potential risks associated with their use. Toxicity studies in animal models, such as rats, provide valuable insights into the adverse effects of these plants on various organ systems and help establish the margin of safety for human consumption.

Acute toxicity studies aim to determine the lethal dose (LD50) or the dose at which adverse effects are observed following a single administration of the test substance. These studies involve administering increasing doses of *L. coromandelica* and *T. palmata* extracts to rats and monitoring their clinical signs, mortality, and gross pathological changes over a specified observation period. The LD50 value provides an estimate of the acute toxicity of the extracts and helps establish initial safety guidelines for subsequent sub-acute toxicity evaluations.

Sub-acute toxicity studies involve repeated administrations of *L. coromandelica* and *T. palmata* extracts to rats over a defined period, typically ranging from 14 to 28 days. These studies assess the potential adverse effects of prolonged exposure to the extracts on various physiological, biochemical, and histopathological parameters. Rats are divided into different treatment groups receiving different doses of the extracts, along with a control group receiving a vehicle or placebo. Parameters evaluated in sub-acute toxicity studies include body weight changes, haematological and biochemical parameters, organ weights, and histopathological alterations in vital organs (Lakshmanan, 2022; Subramanian et al., 2018).

Acute and sub-acute toxicity assessments of *L. coromandelica* and *T. palmata* extracts in rats provide crucial data on their safety profiles and potential hazards associated with their use. These studies help identify safe dosage ranges and potential toxic effects of the extracts, guiding their appropriate use in traditional medicine and therapeutic applications. By systematically evaluating the toxicity of these medicinal

plants, researchers can ensure their safe and effective utilization for the management of various health conditions while minimizing the risk of adverse effects in humans.

1.9. Comprehensive Appraisal of Modulatory, Anti-inflammatory and Antioxidant Effects of Phytocompounds Isolated from *Lannea coromandelica* and *Trevesia palmata* in Trinitrobenzene Sulphonic Acid (TNBS)-Induced Ulcerative Colitis Rat Model

Ulcerative colitis (UC) is a chronic inflammatory bowel disease characterized by inflammation and ulceration of the colonic mucosa, leading to various clinical symptoms and complications. Oxido-nitrosative stress, dysregulated inflammation, altered transcription factor activity, and increased apoptosis are key pathological features contributing to the pathogenesis of UC. Despite advances in conventional therapies, many patients experience inadequate symptom control and adverse effects. Therefore, there is growing interest in exploring alternative treatment options, including medicinal plants, for the management of UC.

Lannea coromandelica and *Trevesia palmata* are two medicinal plants known for their diverse pharmacological properties, including anti-inflammatory, antioxidant, and cytoprotective effects. Phytocompounds derived from these plants, such as polyphenols, flavonoids, and terpenoids, have shown potential in modulating various cellular pathways involved in inflammation, oxidative stress and cell survival (Swathi and Lakshman, 2022; Reddy et al., 2011). However, their specific effects and mechanisms of action in the context of UC pathology require further investigation.

Individual biomarker levels are known to vary, even among patients with the same level of disease activity. As a result, in addition to assessing biomarker levels at baseline and during therapy, it is crucial to monitor changes in these biomarkers throughout the disease's clinical course (Plevris and Lees, 2022), which is especially useful for detecting recurrence and treatment response. Despite this, no prospective studies have been conducted to track the various biomarkers in connection to changes in disease activity. Understanding the link between disease activity and biomarkers is critical for monitoring changes in disease activity; nevertheless, this

information is currently unapproachable. For instance, faecal calprotectin (FC) is an efficient biomarker for assessing mucosal healing, it has a high numerical variability and may not accurately reflect treatment-induced changes in disease activity (Tatsumi et al., 2023; Sipponen et al., 2010; Kolho et al., 2006).

Several biomarkers have been shown to correlate with disease activity in UC. Calprotectin is an inflammation-associated protein found mostly in neutrophilic cytoplasm; its presence in faeces suggests that neutrophils move to the gastrointestinal system during inflammation (Tatsumi et al., 2023; Smith & Gaya, 2012). FC predicts endoscopic activity with a high sensitivity (Mosli et al., 2015). However, it is challenging to utilize this biomarker as a measure of treatment response because the change in FC levels after treatment initiation varies greatly between patients (Magalhaes et al., 2023; Mylemans et al., 2021; Regueiro et al., 2011).

Excessive production of reactive oxygen species (ROS) and reactive nitrogen species (RNS) leads to oxidative and nitrosative stress, contributing to tissue damage and inflammation in UC. Phytocompounds with antioxidant and free radical scavenging properties may counteract oxidative and nitrosative stress, protecting against colonic injury.

Dysregulated immune responses and pro-inflammatory cytokine production play pivotal roles in UC pathogenesis. Phytocompounds with anti-inflammatory properties may modulate inflammatory signalling pathways, reduce cytokine secretion, and attenuate colonic inflammation.

Transcription factors such as nuclear factor-kappa B (NF-κB) and activator protein-1 (AP-1) are key regulators of inflammatory gene expression in UC (Kim et al., 2019 and Checker et al., 2012). Phytocompounds may modulate the activity of these transcription factors, thereby influencing the expression of pro-inflammatory genes and dampening the inflammatory response.

Dysregulated apoptosis of colonic epithelial cells contributes to mucosal damage and ulcer formation in UC (Wan et al., 2022; Patankar and Becker, 2020).

Phytocompounds with cytoprotective effects may regulate apoptotic signalling pathways, promoting cell survival and mucosal integrity (Shehata et al., 2020; Zhao et al., 2018).

This study aims to investigate the modulatory, anti-inflammatory and antioxidant effects of phytocompounds isolated from *L. coromandelica* and *T. palmata* in a trinitrobenzene sulphonic acid (TNBS)-induced ulcerative colitis rat model.

Phytocompounds isolated from the leaves of *L. coromandelica* and *T. palmata* using appropriate extraction technique (cold extraction) were used for this experiment. UC was induced in rats using TNBS, a well-established model that closely mimics the clinical and histopathological features of human UC.

The rats were divided into different treatment groups, including a control group, TNBS-induced colitis group, sulfasalazine treated group and two groups receiving phytocompounds of 10 mg/kg and 20 mg/kg isolated from the leaves of *L. coromandelica* and *T. palmata*. The phytocompounds were administered orally at various doses for a specified duration.

The effects of phytocompounds on colonic inflammation, mucosal damage, and histopathological changes were evaluated. This includes assessing parameters such as disease activity index (DAI), colon weight/length ratio, and histological scoring of colon tissues.

Evaluation of oxido-nitrosative stress markers, including lipid peroxidation products and nitric oxide levels, were assessed in colonic tissues.

The anti-inflammatory effects of phytocompounds were assessed by measuring levels of pro-inflammatory cytokines (e.g., TNF-α, IL-6, IL-1β) in colonic tissues using ELISA and western blot. Additionally, antioxidant enzyme activities and levels of oxidative stress markers (e.g., malondialdehyde) were measured to evaluate the antioxidant effects of phytocompounds.

Analysis of transcription factor activity (i.e., NF-κB activity) and quantification of apoptosis was evaluated using western blot analysis in colonic tissues.

This study aims to provide insights into the modulatory effects, anti-inflammatory, and antioxidant effects of phytocompounds isolated from *L. coromandelica* and *T. palmata* in a TNBS-induced ulcerative colitis rat model. The findings may elucidate the therapeutic potential of these medicinal plants and guide the development of novel treatments for UC targeting multiple pathological pathways.

2.0. Active Components of *Lannea coromandelica* and *Trevesia palmata* Protecting Against Ulcerative Colitis Through Gut-Microbiota Dependence

Ulcerative colitis (UC) is a chronic inflammatory bowel disease characterized by inflammation and ulceration of the colonic mucosa. Emerging evidence suggests that alterations in the gut microbiota composition and function play a critical role in the pathogenesis of UC. The interplay between host factors and the gut microbiota influences mucosal immune responses, barrier function, and inflammatory processes, thereby impacting UC susceptibility and severity. Consequently, therapeutic strategies targeting the gut microbiota have gained attention as potential treatments for UC (Guo et al., 2020; do Nascimento et al., 2020 and Sankarasubramanian, et al., 2020).

Lannea coromandelica and *Trevesia palmata* are medicinal plants known for their diverse pharmacological properties, including anti-inflammatory, antioxidant, and immunomodulatory effects. The main active components of these plants, such as polyphenols, flavonoids, and terpenoids, have shown promise in ameliorating UC symptoms in experimental models. Recent studies have highlighted the potential role of the gut microbiota in mediating the protective effects of these phytocompounds against UC (Victoria et al., 2019; Alam et al., 2017; Rahman et al., 2016; Rahman et al., 2014; De Tommasi et al., 2000).

This chapter aims to explore the primary active components of *L. coromandelica* and *T. palmata* and their protective effects against UC, with a focus on the gut-microbiota dependence of these effects.

Gut-Microbiota Dysbiosis, is a hallmark of UC. Imbalances in beneficial and pathogenic bacterial populations contribute to mucosal inflammation and disease

progression in UC (Alshehri et al., 2021). Targeting the gut microbiota with natural compounds may restore microbial homeostasis and alleviate UC symptoms.

Phytocompounds derived from *L. coromandelica* and *T. palmata* have been tested to modulate the gut microbiota composition and function. These compounds may promote the growth of beneficial bacteria, inhibit the growth of pathogenic bacteria, and enhance microbial diversity, thereby exerting protective effects against UC.

The gut microbiota interacts with the host immune system and epithelial barrier, influencing immune responses, inflammatory signalling, and mucosal integrity (Barbara et al., 2021; Chen et al., 2021 and Yu et al., 2012). Phytocompounds from *L. coromandelica* and *T. palmata* may modulate host-microbiota interactions by regulating immune cell function, cytokine production, and barrier function, thereby mitigating UC-associated inflammation and tissue damage.

Understanding the gut-microbiota dependence of the protective effects of main active components from *L. coromandelica* and *T. palmata* against UC holds significant therapeutic implications. Further research elucidating the mechanisms underlying these interactions will pave the way for the development of novel microbiota-targeted therapies for UC management. By harnessing the therapeutic potential of medicinal plants and their bioactive constituents, clinicians may offer patients safer and more effective treatment options for UC while minimizing adverse effects associated with conventional therapies.

II. OBJECTIVES

- Isolation, characterization and identification of bioactive compounds from *Lannea coromandelica* and *Trevesia palmata* through chromatographic and spectroscopic analyses (GC-MS, LC-MS and IR)
- Computational study of the phytochemical and pharmacological bio-activities of *Lannea coromandelica* and *Trevesia palmata* leaves
- To appraise the modulatory, anti-inflammatory and antioxidant effects of phytocompounds isolated from *Lannea coromandelica* and *Trevesia palmata* in trinitrobenzene sulphonic acid (TNBS)-induced ulcerative colitis rat model

III. OVERALL EXPERIMENTAL DESIGN

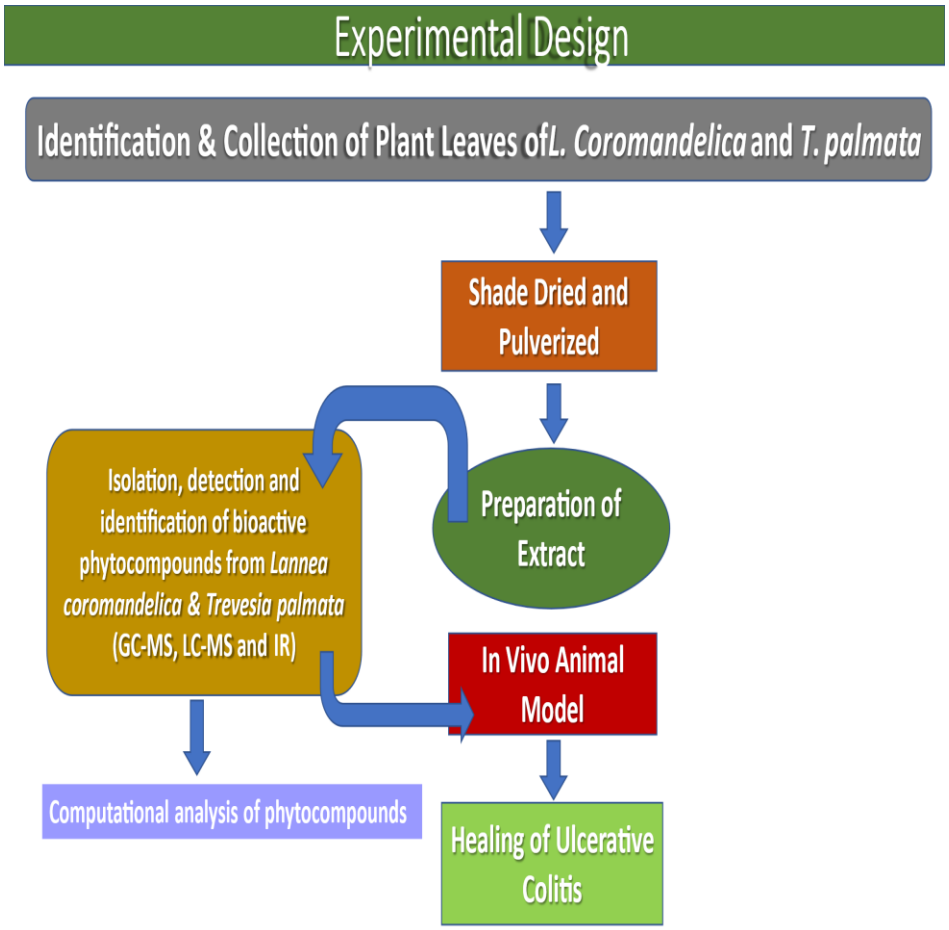

Figure 1: Schematic diagram of the overall experimental design.

IV. REFERENCES

Abdu-Allah, H. H., El-Shorbagi, A. N., Abdel-Moty, S. G., El-Awady, R., & Abdel-Alim, A. A. (2016). 5-Aminosalyclic acid (5-ASA): a unique anti-inflammatory salicylate. Med Chem (Los Angeles), 6(5), 306-15.

Abubakar, A. R., & Haque, M. (2020). Preparation of medicinal plants: Basic extraction and fractionation procedures for experimental purposes. Journal of Pharmacy and Bioallied Sciences, 12(1), 1-10.

Alam, M. B., Kwon, K. R., Lee, S. H., & Lee, S. H. (2017). Lannea coromandelica (houtt.) merr. induces heme oxygenase 1 (HO-1) expression and reduces oxidative stress via the p38/c-jun n-terminal kinase–nuclear factor erythroid 2-related factor 2 (p38/JNK–Nrf2)-mediated antioxidant pathway. International journal of molecular sciences, 18(2), 266.

Alizade Naini, M., Mehrvarzi, S., Zargari-Samadnejadi, A., Tanideh, N., Ghorbani, M., Dehghanian, A., Hasanzarrini, M., Banaee, F., Koohi-Hosseinabadi, O., Irajie, C. & Iraji, A. (2021). The antioxidant and anti-inflammatory effects of Quercus brantii extract on TNBS-induced ulcerative colitis in rats. Evidence-based Complementary and Alternative Medicine, 2021.

Alshehri, D., Saadah, O., Mosli, M., Edris, S., Alhindi, R., & Bahieldin, A. (2021). Dysbiosis of gut microbiota in inflammatory bowel disease: Current therapies and potential for microbiota-modulating therapeutic approaches. Bosnian Journal of Basic Medical Sciences, 21(3), 270.

Altemimi, A., Lakhssassi, N., Baharlouei, A., Watson, D. G., & Lightfoot, D. A. (2017). Phytochemicals: Extraction, isolation, and identification of bioactive compounds from plant extracts. Plants, 6(4), 42.

Antoniou, E., Margonis, G. A., Angelou, A., Pikouli, A., Argiri, P., Karavokyros, I., Papalois, A. & Pikoulis, E. (2016). The TNBS-induced colitis animal model: An overview. Annals of medicine and surgery, 11, 9-15.

Arifin, M. T., Sultana, N., Mukharjee, S. K., & Hossain, M. T. (2017). In vitro antioxidant, brine shrimp lethality and antibacterial activities of methanol extract of Trevesia palmata leaves. Journal of Noakhali Science and Technology University, 1(2), 49-54.

Ashton, J. J., Green, Z., Kolimarala, V., & Beattie, R. M. (2019). Inflammatory bowel disease: long-term therapeutic challenges. Expert Review of Gastroenterology & Hepatology, 13(11), 1049-1063.

Barbara, G., Barbaro, M. R., Fuschi, D., Palombo, M., Falangone, F., Cremon, C., Marasco, G & Stanghellini, V. (2021). Inflammatory and microbiota-related regulation of the intestinal epithelial barrier. Frontiers in nutrition, 8, 718356.

Beiranvand, M. (2021). A review of the biological and pharmacological activities of mesalazine or 5-aminosalicylic acid (5-ASA): an anti-ulcer and anti-oxidant drug. Inflammopharmacology, 29(5), 1279-1290.

Bubli, S. Y., Haque, F., & Khan, M. S. (2021). Gas Chromatography and Mass Spectroscopy (GC-MS) Technique for Food Analysis. Techniques to Measure Food Safety and Quality: Microbial, Chemical, and Sensory, 195-217.

Cai, Z., Wang, S., & Li, J. (2021). Treatment of inflammatory bowel disease: a comprehensive review. Frontiers in medicine, 8, 765474.

Caioni, G., Viscido, A., d'Angelo, M., Panella, G., Castelli, V., Merola, C., Frieri, G., Latella, G., Cimini, A. & Benedetti, E. (2021). Inflammatory bowel disease: New insights into the interplay between environmental factors and PPARγ. International Journal of Molecular Sciences, 22(3), 985.

Calabresi, M. F., Tanimoto, A., Próspero, A. G., Mello, F. P., Soares, G., Di Stasi, L. C., & Miranda, J. R. (2019). Changes in colonic contractility in response to inflammatory bowel disease: Long-term assessment in a model of TNBS-induced inflammation in rats. Life sciences, 236, 116833.

Catana, C. S., Magdas, C., Tabaran, F. A., Craciun, E. C., Deak, G., Magdas, V. A., Cozma, V., Gherman, C.M., Berindan-Neagoe, I. & Dumitrascu, D. L. (2018). Comparison of two models of inflammatory bowel disease in rats. Adv. Clin. Exp. Med, 27, 599-607.

Chamanara, M., Rashidian, A., Mehr, S. E., Dehpour, A. R., Shirkohi, R., Akbarian, R., Abdollahi, A. & Rezayat, S. M. (2019). Melatonin ameliorates TNBS-induced colitis in rats through the melatonin receptors: involvement of TLR4/MyD88/NF-κB signalling pathway. Inflammopharmacology, 27, 361-371.

Checker, R., Sandur, S. K., Sharma, D., Patwardhan, R. S., Jayakumar, S., Kohli, V., Sethi, G., Aggarwal, B.B & Sainis, K. B. (2012). Potent anti-inflammatory activity of ursolic acid, a triterpenoid antioxidant, is mediated through suppression of NF-κB, AP-1 and NF-AT. PloS one, 7(2), e31318.

Chen, Y., Cui, W., Li, X., & Yang, H. (2021). Interaction between commensal bacteria, immune response and the intestinal barrier in inflammatory bowel disease. Frontiers in Immunology, 12, 761981.

Choi, J., & Fenando, A. (2020). Sulfasalazine. Bookshelf ID: NBK557809. PMID:32491741.

Choi, Y. S., Kim, W. J., Kim, J. K., Kim, D. S., & Lee, D. H. (2018). Efficacy of topical 5-aminosalicylate monotherapy in patients with ulcerative proctitis with skip inflammation. Journal of Gastroenterology and Hepatology, 33(6), 1200-1206.

Chu, X. Y., & Ho, P. C. (2023). Intestinal Microbiome and Its Impact on Metabolism and Safety of Drugs. Oral Bioavailability and Drug Delivery: From Basics to Advanced Concepts and Applications, 483-500.

Couto, D., Ribeiro, D., Freitas, M., Gomes, A., Lima, J. L., & Fernandes, E. (2010). Scavenging of reactive oxygen and nitrogen species by the prodrug sulfasalazine and its metabolites 5-aminosalicylic acid and sulfapyridine. Redox Report, 15(6), 259-267.

de Oliveira, R. G., Damazo, A. S., Antonielli, L. F., Miyajima, F., Pavan, E., Duckworth, C. A., da Silva Lima, J.C., Arunachalam, K. & de Oliveira Martins, D. T. (2021). Dilodendron bipinnatum Radlk. extract alleviates ulcerative colitis induced by TNBS in rats by reducing inflammatory cell infiltration, TNF-α and IL-1β concentrations, IL-17 and COX-2 expressions, supporting mucus production and promotes an antioxidant effect. Journal of Ethnopharmacology, 269, 113735.

De Tommasi, N., Autore, G., Bellino, A., Pinto, A., Pizza, C., Sorrentino, R., & Venturella, P. (2000). Antiproliferative Triterpene Saponins from Trevesia p almata. Journal of natural products, 63(3), 308-314.

Di Sabatino, A., Biancheri, P., Rovedatti, L., MacDonald, T. T., & Corazza, G. R. (2012). Recent advances in understanding ulcerative colitis. Internal and emergency medicine, 7, 103-111.

do Nascimento, R. D. P., da Fonseca Machado, A. P., Galvez, J., Cazarin, C. B. B., & Junior, M. R. M. (2020). Ulcerative colitis: Gut microbiota, immunopathogenesis and application of natural products in animal models. Life sciences, 258, 118129.

Duarte, Y., Márquez-Miranda, V., Miossec, M. J., & González-Nilo, F. (2019). Integration of target discovery, drug discovery and drug delivery: a review on computational strategies. Wiley Interdisciplinary Reviews: Nanomedicine and Nanobiotechnology, 11(4), e1554.

Eder, P., Lodyga, M., Gawron-Kiszka, M., Dobrowolska, A., Gonciarz, M., Hartleb, M., Kłopocka, M., Małecka-Wojciesko, E., Radwan, P., Reguła, J. and Zagorowicz, E. & Rydzewska, G. (2023). Guidelines for the management of ulcerative colitis. Recommendations of the Polish Society of Gastroenterology and the Polish National Consultant in Gastroenterology. Gastroenterology Review/Przegląd Gastroenterologiczny, 18(1).

El Sayed, A. M., Basam, S. M., El-Naggar, E. M. B. A., Marzouk, H. S., & El-Hawary, S. (2020). LC–MS/MS and GC–MS profiling as well as the antimicrobial effect of leaves of selected Yucca species introduced to Egypt. Scientific reports, 10(1), 17778.

Elhag, D. A., Kumar, M., Saadaoui, M., Akobeng, A. K., Al-Mudahka, F., Elawad, M., & Al Khodor, S. (2022). Inflammatory bowel disease treatments and

predictive biomarkers of therapeutic response. International journal of molecular sciences, 23(13), 6966.

Gajendran, M., Loganathan, P., Jimenez, G., Catinella, A. P., Ng, N., Umapathy, C., Ziade, N. & Hashash, J. G. (2019). A comprehensive review and update on ulcerative colitis. Disease-a-month, 65(12), 100851.

Giordano, D., Biancaniello, C., Argenio, M. A., & Facchiano, A. (2022). Drug design by pharmacophore and virtual screening approach. Pharmaceuticals, 15(5), 646.

Gonfa, Y. H., Tessema, F. B., Bachheti, A., Rai, N., Tadesse, M. G., Singab, A. N., Chaubey, K.K. & KumarBachheti, R. (2023). Anti-inflammatory activity of phytochemicals from medicinal plants and their nanoparticles: A review. Current Research in Biotechnology, 100152.

Gros, B., & Kaplan, G. G. (2023). Ulcerative colitis in adults: A review. Jama, 330(10), 951-965.

Guo, X. Y., Liu, X. J., & Hao, J. Y. (2020). Gut microbiota in ulcerative colitis: insights on pathogenesis and treatment. Journal of digestive diseases, 21(3), 147-159.

Hambardikar, V. R., & Mandlik, D. S. (2022). Protective effect of naringin ameliorates TNBS-induced colitis in rats via improving antioxidant status and pro-inflammatory cytokines. Immunopharmacology and Immunotoxicology, 44(3), 373-386.

Higuchi, L., Regan, B. & Bousvaros, A. (2016). Ulcerative Colitis. In: Guandalini, S., Dhawan, A., Branski, D. (eds) Textbook of Pediatric Gastroenterology, Hepatology and Nutrition. Springer, Cham. https://doi.org/10.1007/978-3-319-17169-2_30

Hu, Y., Ye, Z., Wu, M., She, Y., Li, L., Xu, Y., Qin, K., Hu, Z., Yang, M., Lu, F. & Ye, Q. (2021). The communication between intestinal microbiota and ulcerative colitis: an exploration of pathogenesis, animal models, and potential therapeutic strategies. Frontiers in Medicine, 8, 766126.

Hwang, Y. J., Nam, S. J., Chun, W., Kim, S. I., Park, S. C., Kang, C. D., & Lee, S. J. (2019). Anti-inflammatory effects of apocynin on dextran sulfate sodium-induced mouse colitis model. PLoS One, 14(5), e0217642.

Jared Misonge, O., Gervason Apiri, M., James Onsinyo, M., & Vincent Obaga, N. (2024). Ethnomedicinal uses, phytochemistry, and pharmacology of the genus Sarcophyte: a review. Frontiers in Pharmacology, 14, 1301672.

Jha, A. K., & Sit, N. (2022). Extraction of bioactive compounds from plant materials using combination of various novel methods: A review. Trends in Food Science & Technology, 119, 579-591.

Jiao, X., Jin, X., Ma, Y., Yang, Y., Li, J., Liang, L., ... & Li, Z. (2021). A comprehensive application: Molecular docking and network pharmacology for the prediction of bioactive constituents and elucidation of mechanisms of action in component-based Chinese medicine. Computational Biology and Chemistry, 90, 107402.

Kaushal, P., Somwaru, A. S., Charabaty, A., & Levy, A. D. (2017). MR enterography of inflammatory bowel disease with endoscopic correlation. Radiographics, 37(1), 116-131.

Kim, T. W., Shin, J. S., Chung, K. S., Lee, Y. G., Baek, N. I., & Lee, K. T. (2019). Anti-Inflammatory mechanisms of Koreanaside A, a lignan isolated from the flower of Forsythia koreana, against LPS-induced macrophage activation and DSS-induced colitis mice: the crucial role of AP-1, NF-κB, and JAK/STAT signaling. Cells, 8(10), 1163.

Kolho, K. L., Raivio, T., Lindahl, H., & Savilahti, E. (2006). Fecal calprotectin remains high during glucocorticoid therapy in children with inflammatory bowel disease. Scandinavian journal of gastroenterology, 41(6), 720-725.

Kovari, B., Bathori, A., Friedman, M. S., & Lauwers, G. Y. (2022). Histologic diagnosis of inflammatory bowel diseases. Advances in Anatomic Pathology, 29(1), 48-61.

Kumar, T., & Jain, V. (2015). Appraisal of total phenol, flavonoid contents, and antioxidant potential of folkloric Lannea coromandelica using in vitro and in vivo assays. Scientifica, 2015.

Lahyaoui, M., El-Idrissi, H., Saffaj, T., Ihssane, B., Saffaj, N., Mamouni, R., & Rodi, Y. K. (2023). QSAR modeling, molecular docking and molecular dynamic simulation of phosphorus-substituted quinoline derivatives as topoisomerase I inhibitors. Arabian Journal of Chemistry, 16(6), 104783.

Lakey, R. L., & Cawston, T. E. (2009). Sulfasalazine blocks the release of proteoglycan and collagen from cytokine stimulated cartilage and down-regulates metalloproteinases. Rheumatology, 48(10), 1208-1212.

Lakshmanan, M. (2022). Preclinical Toxicity Studies. In Introduction to Basics of Pharmacology and Toxicology: Volume 3: Experimental Pharmacology: Research Methodology and Biostatistics (pp. 625-648). Singapore: Springer Nature Singapore.

Lamb, C. A., Kennedy, N. A., Raine, T., Hendy, P. A., Smith, P. J., Limdi, J. K., Hayee, B.H., Lomer, M.C., Parkes, G.C., Selinger, C., Barrett, K.J. & IBD Guidelines eDelphi Consensus Group. (2019). British Society of Gastroenterology consensus guidelines on the management of inflammatory bowel disease in adults. Gut, 68(Suppl 3), s1-s106.

Liu, C., Qi, X., Li, D., Zhao, L., Li, Q., Mao, K., Shen, G., Ma, Y. & Wang, R. (2024). Limosilactobacillus fermentum HF06-derived paraprobiotic and

postbiotic alleviate intestinal barrier damage and gut microbiota disruption in mice with ulcerative colitis. Journal of the Science of Food and Agriculture, 104(3), 1702-1712.

Lopez-Fernandez, O., Dominguez, R., Pateiro, M., Munekata, P. E., Rocchetti, G., & Lorenzo, J. M. (2020). Determination of polyphenols using liquid chromatography–tandem mass spectrometry technique (LC–MS/MS): A review. Antioxidants, 9(6), 479.

Magalhaes, D., Peyrin-Biroulet, L., Estevinho, M. M., Danese, S., & Magro, F. (2023). Pursuing neutrophils: systematic scoping review on blood-based biomarkers as predictors of treatment outcomes in inflammatory bowel disease. Therapeutic Advances in Gastroenterology, 16, 17562848231155987.

Magro, F., Dias-Pereira, P., Morato, M., & Duartearaújo, M. (2021). 2, 4, 6-trinitrobenzenesulfonic acid-induced colitis in Rattus norgevicus: a categorization proposal. Exp. Anim, 70(2), 245-256.

Malu, Q., Caldeira, G. I., Catarino, L., Indjai, B., da Silva, I. M., Lima, B., & Silva, O. (2024). Ethnomedicinal, Chemical, and Biological Aspects of Lannea Species—A Review. Plants, 13(5), 690.

Manik, M. K., Wahid, M. A., Islam, S. M. A., Pal, A., & Ahmed, K. T. (2013). A comparative study of the antioxidant, antimicrobial and thrombolytic activity of the bark and leaves of Lannea coromandelica (Anacardiaceae). International Journal of Pharmaceutical Sciences and Research, 4(7), 2609.

Manoharan, A. L., Jagadeesan, G., Nataraj, G., Muniyandi, K., Guruswami, G., Arunachalam, K., & Thangaraj, P. (2023). Efficacy of Trevesia palmata (Roxb. ex Lindl.) Vis. Extract on MG 63 cell lines and arthritis-induced animal models. Journal of Ethnopharmacology, 300, 115742.

Mendell, A., Le, K., Vannabouathong, C., & Mahood, Q. (2023). An overview of emerging trends and technologies in ulcerative colitis. Canadian Journal of Health Technologies, 3(7).

Mosli, M. H., Zou, G., Garg, S. K., Feagan, S. G., MacDonald, J. K., Chande, N., Sandborn, W.J. & Feagan, B. G. (2015). C-reactive protein, fecal calprotectin, and stool lactoferrin for detection of endoscopic activity in symptomatic inflammatory bowel disease patients: a systematic review and meta-analysis. Official journal of the American College of Gastroenterology| ACG, 110(6), 802-819.

Mylemans, M., Nevejan, L., Van Den Bremt, S., Stubbe, M., Vander Cruyssen, B., Moulakakis, C., Berthold, H., Konrad, C., Bossuyt, X. & Van Hoovels, L. (2021). Circulating calprotectin as biomarker in neutrophil-related inflammation: pre-analytical recommendations and reference values according to sample type. Clinica Chimica Acta, 517, 149-155.

Orlando, A., Guglielmi, F. W., Cottone, M., Orlando, E., Romano, C., & Sinagra, E. (2013). Clinical implications of mucosal healing in the management of patients with inflammatory bowel disease. Digestive and Liver Disease, 45(12), 986-991.

Ortiz, T., Argüelles-Arias, F., Illanes, M., García-Montes, J. M., Talero, E., Macias-Garcia, L., Alcudia, A., Vazquez-Roman, V., Motilva, V. & De-Miguel, M. (2020). Polyphenolic maqui extract as a potential nutraceutical to treat TNBS-induced Crohn's disease by the regulation of antioxidant and anti-inflammatory pathways. Nutrients, 12(6), 1752.

Patankar, J. V., & Becker, C. (2020). Cell death in the gut epithelium and implications for chronic inflammation. Nature reviews Gastroenterology & hepatology, 17(9), 543-556.

Pizzorno, J. E., Murray, M. T., & Joiner-Bey, H. (2016). The Clinician's handbook of natural medicine E-book. Elsevier Health Sciences.

Plevris, N., & Lees, C. W. (2022). Disease monitoring in inflammatory bowel disease: evolving principles and possibilities. Gastroenterology, 162(5), 1456-1475.

Porter, R. J., Kalla, R., & Ho, G. T. (2020). Ulcerative colitis: Recent advances in the understanding of disease pathogenesis. F1000Research, 9.

Rahman, K. H., Nandi, J. K., Sultana, S., Rahman, S., Hossan, S., & Rahmatullah, M. (2014). Phytochemical screening, antihyperglycemic and analgesic activity studies with methanol extract of Trevesia palmata leaves. World J Pharm Pharmaceut Sci, 3(10), 91-101.

Rahman, M., Khatun, A., Uddin, S. J., & Shilpi, J. A. (2016). Comparative effect of Lannea coromandelica (Houtt.) Merr. leaves and stem barks on acetic acid induced pain model in mice and chromagenic reagents: exploring the analgesic potential and phytochemical groups. Pharmacologyonline, 1(1), 146-152.

Rai, M., Singh, A. V., Paudel, N., Kanase, A., Falletta, E., Kerkar, P., P., Heyda, J., Barghash, R.F., Singh, S.P. & Soos, M. (2023). Herbal concoction unveiled: a computational analysis of phytochemicals' pharmacokinetic and toxicological profiles using novel approach methodologies (NAMs). Current Research in Toxicology, 5, 100118.

Rai, P. K., & Lalramnghinglova, H. (2011). Ethnomedicinal plants of India with special reference to an Indo-Burma hotspot region: An overview. Ethnobotany Research and Applications, 9, 379-420.

Ralte, L., Sailo, H., & Singh, Y. T. (2024). Ethnobotanical study of medicinal plants used by the indigenous community of the western region of Mizoram, India. Journal of Ethnobiology and Ethnomedicine, 20(1), 2.

Reddy, A. K., Joy, J. M., & Kumara, C. A. (2011). Available online through www. jpronline. info. Journal of Pharmacy Research, 4(3), 577-579.

Regueiro, M., Kip, K. E., Schraut, W., Baidoo, L., Sepulveda, A. R., Pesci, M., El-Hachem, S., Harrison, J. & Binion, D. (2011). Crohn's disease activity index does not correlate with endoscopic recurrence one year after ileocolonic resection. Inflammatory bowel diseases, 17(1), 118-126.

Rodríguez-Yoldi, M. J. (2021). Anti-inflammatory and antioxidant properties of plant extracts. Antioxidants, 10(6), 921.

Roy, S., Dhaneshwar, S., Mahmood, T., Kumar, S., & Saxena, S. K. (2023). Pre-clinical investigation of protective effect of nutraceutical D-glucosamine on TNBS-induced colitis. Immunopharmacology and immunotoxicology, 45(2), 172-184.

Sakthivel, K. M., & Guruvayoorappan, C. (2013). Amentoflavone inhibits iNOS, COX-2 expression and modulates cytokine profile, NF-κB signal transduction pathways in rats with ulcerative colitis. International immunopharmacology, 17(3), 907-916.

Sankarasubramanian, J., Ahmad, R., Avuthu, N., Singh, A. B., & Guda, C. (2020). Gut microbiota and metabolic specificity in ulcerative colitis and Crohn's disease. Frontiers in medicine, 7, 606298.

Shah, M., Patel, M., Shah, M., Patel, M., & Prajapati, M. (2024). Computational transformation in drug discovery: A comprehensive study on molecular docking and quantitative structure activity relationship (QSAR). Intelligent Pharmacy.

Shehata, A. M., Saadeldin, I. M., Tukur, H. A., & Habashy, W. S. (2020). Modulation of heat-shock proteins mediates chicken cell survival against thermal stress. Animals, 10(12), 2407.

Silva, I., Solas, J., Pinto, R., & Mateus, V. (2022). Chronic experimental model of TNBS-induced colitis to study inflammatory bowel disease. International Journal of Molecular Sciences, 23(9), 4739.

Singh, H., & Bharadvaja, N. (2021). Treasuring the computational approach in medicinal plant research. Progress in Biophysics and Molecular Biology, 164, 19-32.

Sipponen, T., Bjorkesten, C. G. A., Farkkila, M., Nuutinen, H., Savilahti, E., & Kolho, K. L. (2010). Faecal calprotectin and lactoferrin are reliable surrogate markers of endoscopic response during Crohn's disease treatment. Scandinavian journal of gastroenterology, 45(3), 325-331.

Smith, L. A., & Gaya, D. R. (2012). Utility of faecal calprotectin analysis in adult inflammatory bowel disease. World journal of gastroenterology: WJG, 18(46), 6782.

Subramanian, K., Sankaramourthy, D., & Gunasekaran, M. (2018). Toxicity studies related to medicinal plants. In Natural Products and Drug Discovery (pp. 491-505). Elsevier.

Swathi, S., & Lakshman, K. (2022). Photochemistry and Pharmacological Bio-Activities of Lannea coromandelica: A Review. Innovare Journal of Medical Science, 10(5).

Taku, K., Britta, S., Chen, W. S., Ferrante, M., Shen, B., Bernstein, C. N., Silvio, D., Laurent, P.B. & Toshifumi, H. (2020). Ulcerative colitis (primer). Nature Reviews: Disease Primers, 6(1).

Tanwar, H., Gnanasekaran, J. M., Allison, D., Chuang, L. S., He, X., Aimetti, M., Baima, G., Costalonga, M., Cross, R.K., Sears, C., Mehandru, S. & Thumbigere-Math, V. (2023). Unraveling the link between periodontitis and inflammatory bowel disease: challenges and outlook. ArXiv.

Tatsumi, Y., Kakimoto, K., Hara, A., Mizuta, N., Numa, K., Kinoshita, N., Nakazawa, K., Koshiba, R., Hirata, Y., Ota, K., Miyazaki, T. & Nishikawa, H. (2023). Biomarkers for Monitoring of Changes in Disease Activity in Ulcerative Colitis. Journal of Clinical Medicine, 12(22), 7165.

Thomford, N. E., Senthebane, D. A., Rowe, A., Munro, D., Seele, P., Maroyi, A., & Dzobo, K. (2018). Natural products for drug discovery in the 21st century: innovations for novel drug discovery. International journal of molecular sciences, 19(6), 1578.

Tripathi, K., & Feuerstein, J. D. (2019). New developments in ulcerative colitis: latest evidence on management, treatment, and maintenance. Drugs in context, 8.

Valand, R., Tanna, S., Lawson, G., & Bengtström, L. (2020). A review of Fourier Transform Infrared (FTIR) spectroscopy used in food adulteration and authenticity investigations. Food Additives & Contaminants: Part A, 37(1), 19-38.

Van der Laan, J. J., Van der Waaij, A. M., Gabriëls, R. Y., Festen, E. A., Dijkstra, G., & Nagengast, W. B. (2021). Endoscopic imaging in inflammatory bowel disease: current developments and emerging strategies. Expert Review of Gastroenterology & Hepatology, 15(2), 115-126.

Vaou, N., Stavropoulou, E., Voidarou, C., Tsigalou, C., & Bezirtzoglou, E. (2021). Towards advances in medicinal plant antimicrobial activity: A review study on challenges and future perspectives. Microorganisms, 9(10), 2041.

Varzandeh, R., Khezri, M. R., Esmaeilzadeh, Z., Jafari, A., & Ghasemnejad-Berenji, M. (2024). Protective effects of topiramate on acetic acid-induced colitis in rats through the inhibition of oxidative stress. Naunyn-Schmiedeberg's Archives of Pharmacology, 397(2), 1141-1149.

Victoria, S., RIPANS, A., Sailo, N., Lahlenmawia, H., Shantabi, L., & Selesih, A. (2019). Effect of trevesia palmata on some biochemical and haematological parameters. International Journal of Engineering Applied Sciences and Technology, 4(3), 610-614.

Waldner, M. J., Rath, T., Schürmann, S., Bojarski, C., & Atreya, R. (2017). Imaging of mucosal inflammation: current technological developments, clinical implications, and future perspectives. Frontiers in Immunology, 8, 1256.

Wan, Y., Yang, L., Jiang, S., Qian, D., & Duan, J. (2022). Excessive apoptosis in ulcerative colitis: crosstalk between apoptosis, ROS, ER stress, and intestinal homeostasis. Inflammatory bowel diseases, 28(4), 639-648.

Wang, Y., Parker, C. E., Feagan, B. G., & MacDonald, J. K. (2016). Oral 5-aminosalicylic acid for maintenance of remission in ulcerative colitis. Cochrane Database of Systematic Reviews, (5).

Wu, F., Zhou, Y., Li, L., Shen, X., Chen, G., Wang, X., Liang, X., Tan, M. & Huang, Z. (2020). Computational approaches in preclinical studies on drug discovery and development. Frontiers in chemistry, 8, 726.

Yadav, R., Hasan, S., Mahato, S., Celik, I., Mary, Y. S., Kumar, A., Dhamija, P., Sharma, A., Choudhary, N., Chaudhary, P.K. and Kushwah, A.S. & Chaudhary, J. K. (2021). Molecular docking, DFT analysis, and dynamics simulation of natural bioactive compounds targeting ACE2 and TMPRSS2 dual binding sites of spike protein of SARS CoV-2. Journal of molecular liquids, 342, 116942.

Yang, Y., He, J., Suo, Y., Lv, L., Wang, J., Huo, C., ... & Zhang, Y. (2016). Anti-inflammatory effect of taurocholate on TNBS-induced ulcerative colitis in mice. Biomedicine & Pharmacotherapy, 81, 424-430.

Yoshino, T., Sono, M., & Yazumi, S. (2016). Usefulness of sulfasalazine for patients with refractory-ulcerative colits. BMJ Open Gastroenterology, 3(1), e000103.

Yu, L. C. H., Wang, J. T., Wei, S. C., & Ni, Y. H. (2012). Host-microbial interactions and regulation of intestinal epithelial barrier function: From physiology to pathology. World journal of gastrointestinal pathophysiology, 3(1), 27.

Zhao, Y., Hu, X., Zuo, X., & Wang, M. (2018). Chemopreventive effects of some popular phytochemicals on human colon cancer: A review. Food & function, 9(9), 4548-4568.

CHAPTER 2

Isolation, characterization and identification of bioactive compounds from *Lannea coromandelica* and *Trevesia palmata* through chromatographic and spectroscopic analyses (GC-MS, LC-MS and IR)

2.1. INTRODUCTION

Plants produce numerous secondary metabolites, which are biosynthetically derived from primary metabolites and are a major source of microbicides, insecticides, and many pharmaceutical medications (Pang et al., 2021). For a long time, medicinal plants or their secondary metabolites have played a vital role in human society's disease-fighting efforts. Plant extracts have long been utilised as sources of bioactive compounds and for their therapeutic properties. Investigating the potential of plant extracts in a range of fields, such as medicine, cosmetics, and food, has gained a lot of attention recently (Sultana et al., 2023). The majority of plants have evolved special defences against hostile environments to make up for their immobility. The production of secondary metabolites is a crucial component of their coping strategies. Apart from their function in protecting plants from invaders, they also have the ability to treat illnesses, and their application by people dates back before written records were created. It has been well documented in the literature over the past few decades that medicinal plants can be used as a natural source of anti-inflammatory chemicals (Adeosun and Loots, 2024). Because of the unrivalled availability of chemical variety, natural products derived from medicinal plants, whether as pure compounds or standardised extracts, give limitless prospects for novel therapeutic leads. Interest in edible plants has developed worldwide as a result of an increasing desire for chemical variety in screening programmes, as well as the search for therapeutic medications from natural sources. Botanical and herbal preparations for therapeutic purposes contain a variety of bioactive chemicals (Sasidharan et al., 2011). This research focuses on the analytical approaches that involve the extraction, isolation, and characterisation of active components in *Lannea coromandelica* and *Trevesia palmata* methanolic plant extracts. In this experiment the compounds obtained are characterized using diverse identification techniques such as Gas Chromatography Mass Spectroscopy (GCMS), Liquid Chromatography Mass Spectroscopy (LCMS) and Fourier Transform Infrared (FTIR).

2.1.1. *Lannea coromandelica*: A medicinal plant

Lannea coromandelica (L. coromandelica) from the family Anacardiaceae is one of the strongest medicinal herbs (Gunjal et al., 2021). In Mizoram, India, the tree is known as Tawitawsuak and the bark is traditionally used as an astringent in ulcers and sores, while the leaves is beneficial in treating swellings, injuries, bruises, sprains, and body aches. *L. coromandelica* is widely used as a therapeutic herb around the globe. Several representatives of this genus are used in ethnomedicine as astringents, helping with antioxidant, anti-inflammatory, and anti-diabetic properties, as well as other physiological functions. Furthermore, the medicinal effects of Lannea species have been recognised in a number of scientific studies (Swathi and Lakshman,2022; Manik et al., 2013).

Several investigations confirm that the therapeutic actions of *L. coromandelica* can b e connected to the presence of a broad range of secondary metabolites and bioactive compounds. Previous studies have also been conducted where the in-vitro release kinetics of graft matrices from *L. coromandelica* gum was used for the treatment of colonic disorders by 5-ASA (Mate et al., 2020). Several studies have also demonstrated its efficacy in treating a variety of ailments (Swathi and Lakshman, 2022; Islam et al., 2022; Hussain et al., 2021; Weerapreeyakul et al., 2016) by pertaining phytochemical properties of pharmacological significance.

Figure 2: *Lannea coromandelica* plant.

2.1.2 *Trevesia palmata*: An overview

Trevesia palmata (Roxb. ex Lindl.) Vis. (Family: Araliaceae; Common Name: Snowflake Aralia) is mostly found in northeastern India and has several ethnobotanical significances. The leaves and fruits of *T. palmata*, locally known as kawhtebel in Mizoram, are edible and used for treating stomachache and high blood pressure; especially the Mizo consume the leaf juice for treating dyspepsia (Lalfakzuala et al., 2007) and eaten as a leafy vegetable (Angami et al., 2006). The stem and root are used by Laotians of the Kry ethnic minority as a lactagogue, as well as for perineal healing, stomachache relief, uterine retraction and postpartum care. Peninsular Malaysians appear to employ them in the treatment of bone fractures and skin disorders (Lamxay et al., 2011). In Vietnam, the leaf and fruits that contain rich oleanane-type saponins have long been utilised to reduce body heat and treat severe inflammations (Thao et al., 2018). *T. palmata* contains a variety of primary and secondary metabolites, including polyphenols, alkaloids, terpenes, phytosterols, and organosulfur compounds. Triterpenoid saponins and lactone glycoside phytocompounds produced have been reported to have antiproliferative activities in several malignant cells (Kim et al., 2018; De Tommasi et al., 2000). Furthermore, *T. palmata* has exhibited antihyperglycemic, antithrombotic, and anti-arthritic potential (Rahman et al., 2014; Sayeed et al., 2014).

Figure 3: *Trevesia palmata* plant.

2.1.3. Plant Secondary Metabolites

Plant secondary metabolites (PSMs) have a variety of roles, including defence against diseases, pests, and herbivores; reaction to environmental challenges; and promoting organismal relationships (Pang et al., 2021). Secondary metabolism, unlike primary metabolism, refers to metabolic pathways and their associated tiny molecular products that are not needed for the organism's development and reproduction (Yang et al., 2018). PSMs are bioactive molecules from plant sources that are spontaneously formed in all parts of plants, including bark, roots, leaves, flower stems, fruits and seeds, and include active components (Cragg and Newman, 2001). They are a diverse group of chemicals produced by secondary metabolic processes which are a broad collection of structurally varied chemicals derived from either primary metabolites or intermediates in the metabolic processes of these primary metabolites (Piasecka et al., 2015). The medicinal value of a plant is determined by some of its chemical elements, which have a specific physiological influence on the body. PSMs are divided into numerous broad molecular families based on their biosynthesis processes, including phenolics, terpenoids, steroids, alkaloids, and flavonoids (Kessler and Kalske, 2018).

Plant secondary metabolites play a variety of tasks, including plant growth and development, innate immunity (Piasecka et al., 2015), defensive response signalling (Isah, 2019), and responsiveness to environmental stresses (Yang et al., 2018). Furthermore, PSMs serve critical activities such as repelling pests and pathogens, acting as signals for plant-microorganism symbiosis, and modifying microbial populations associated with hosts (Guerrieri et al., 2019). Many PSMs have a positive impact on human health (Ullrich et al., 2019; Fakhri et al., 2020) and agricultural production, which is extremely beneficial to the economy. However, the roles of several PSMs remain unknown. Although numerous PSMs and protein-metabolite complexes have been discovered, their biological roles have not been verified (Kosmacz et al., 2020). Several notable reviews summarise current studies indicating the distinct actions of PSMs and stress the need for functional

comprehension of the plant metabolome (Zhou and Pichersky, 2020; Kosmacz et al., 2020; Fang et al., 2019).

2.1.4. Analytical methods in plant metabolites analysis

Plant metabolomics techniques have been utilised to uncover functional secondary metabolites and metabolic pathways for both fundamental and practical research. These strategies contribute to a more thorough understanding of how plant metabolic networks are regulated. The most commonly used methods include gas chromatography (GC)-mass spectrometry (-MS) (GC-MS), liquid chromatography-MS (LC-MS), capillary electrophoresis-MS (CE-MS), nuclear magnetic resonance spectroscopy (NMR), Fourier transform-near-infrared (FT-NIR) spectroscopy, MS imaging (MSI), and live single-cell -MS (LSC-MS). These approaches are frequently used in tandem since they can offer largely complementary information by evaluating several types of metabolites. Several outstanding technical reviews (Tahir et al., 2019; Lu et al., 2017) and comprehensive procedures (Zhalnina et al., 2018) on the application of these analytical tools in metabolomics research have been published.

Most classic investigations of PSMs use extracts of typical plant tissues as the primary materials reflecting average plant cells in a certain tissue or organ (Masuda et al., 2018). Because of the large size of the samples, it is often difficult to distinguish between PSMs produced by host plants and their associated microorganisms. However, there is currently a growing interest in limiting PSM analysis to the single-cell level, allowing for the isolation of plant cells from potentially related microbial cells (Pang et al., 2021).

Secondary metabolites are bioactive molecules from plant sources that are spontaneously formed in all parts of plants, including bark, roots, leaves, flower stems, fruits, and seeds, and include active components. (Ogunsina et al., 2020; Cragg and Newman, 2001). The medicinal value of a plant is determined by some of its chemical elements, which have a specific physiological influence on the body. Flavonoids, alkaloids, terpenoids, tannins, and steroids are among the most important bioactive plant elements (Edeoga etal., 2005). Understanding plant chemical

components is important not only for the discovery of therapeutic drugs, but also because such data can identify novel drug sources (Ranilla et al., 2010). The type of solvent used in the extraction process has a major impact on the detection of biologically active compounds in plant material. As a result, it is vital to utilise a range of solvents while screening plant materials for phytochemical components (Nortjie et al., 2022; Abubakar and Haque, 2020; Altemimi et al., 2017).

The Anacardiaceae family includes Lannea plants, which are used in traditional medicine to treat infectious disorders. The bark decoction of *L. coromandelica* is used to cure a variety of ailments. It is also used topically as an astringent in ulcers and sores, while the leaves are useful in treating swellings, injuries, bruises, sprains, and body aches (Swathi and Lakshman,2022). *T. palmata* belonging to Araliaceae family, is also used as a medicine locally to treat stomachache, high blood pressure and dyspepsia (Lalfakzuala et al., 2007). Several literature reviews have proved the efficiency of these two plants in pharmacology but some of the age-old ethnomedicinal practices have not been thoroughly confirmed.

For the past decade, a number of historical improvements in analytical techniques, such as GC-MS, LC-MS, and FTIR, have been used as a dominant tool for identifying and determining plant components (Ingle et al., 2022; Federica et al., 2018). The current study was conducted to validate the bioactive compounds present in the methanolic extract of *L. coromandelica* and *T. palmata* using GC-MS, LC-MS, and FTIR techniques, which may provide insight into its use to determine the compounds responsible for the observed activities as a traditional medicine.

2.2. REVIEW OF LITERATURE

Many physiologically active chemicals can be found in medicinal plants (Babich et al., 2024). Plants, according to Nikam et al. (2012) and Mishra and Tiwari (2011), are analogous to factories that synthesise exceedingly complex and unusual molecules for a variety of medical and non-medical applications. The complex phytochemical combinations seen in herbal or plant-based medicines have been proven to be superior to be isolated or intentionally modified single molecules from natural

sources (Rodriguez-Concepcion et al., 2018; Ekor, 2014; Carmona and Pereira, 2013). As a result, the usage of herbal goods and supplements has surged over the last three decades, as an increasing number of people resort to them for a variety of health-related concerns. However, manufacturing herbal medicine is a methodical and slow procedure (WHO, 2017; Ekor, 2014).

According to Newmaster et al. (2013) and Kunle et al. (2012), this herbal medication manufacturing involves three fundamental processes: (i) identifying herbs using macroscopical and microscopical traits; (ii) evaluating medications to validate their authenticity and purity; and (iii) standardisation. Standardization of herbal formulations includes all quality control methods carried out during the manufacturing process, such as sample preparation, phytochemical evaluation, and microbiological, biological, and toxicological testing (Newmaster et al., 2013; Kunle et al., 2012; Rodriguez-Concepcion et al., 2006). Procedures and criteria are also used to ensure that all herbal formulations and products are effective, safe, and of high quality (Balekundri and Mannur, 2020; WHO, 2017; Yadav et al., 2011).

The State Medicinal Plants Board - Mizoram has listed several medicinal plants from Mizoram, Northeast India, with the aim of cultivating, conserving, researching, developing and promoting the medicinal plants sector in the state. Among the medicinal plants on the list, *L. coromandelica* and *T. palmata* have been identified as species with uses in Mizoram that are being described for the first time. Furthermore, both plants come into the category, lower risk/conservation dependant (LR). Records have also been kept on the usage of both species, with the bark of the *L. coromandelica* tree used as an astringent and to treat ulcers and sores, and the leaves used to treat swellings, sprains, and bodily aches. Similarly, crushed leaf juice of *T. palmata* is used to treat colic, stomachache, and excessive blood pressure (State Medicinal Plants Board- Mizoram, 2001).

In traditional medicine practices, various parts of Trevesia palmata, including its roots, leaves, and fruits, are utilized for their medicinal properties. The plant contains bioactive compounds that are believed to have therapeutic effects. In Mizoram, as

well as in other regions where it grows, *T. palmata* may be used in traditional remedies for various ailments such as digestive disorders, respiratory problems, skin conditions, and more. Additionally, research studies have been conducted to explore the pharmacological potential of *T. palmata* extracts for their antimicrobial, antioxidant, anti-inflammatory, and other medicinal properties. While traditional use of *T. palmata* has been documented in various regions, including Mizoram, scientific research on its medicinal properties is relatively limited compared to more extensively studied medicinal plants. However, some studies have investigated the potential pharmacological activities of *T. palmata* and its constituents. Research has shown that extracts from *T. palmata* possess antimicrobial properties against various bacterial and fungal pathogens. For example, a study published in the journal "African Journal of Microbiology Research" evaluated the antimicrobial activity of *T. palmata* leaf extracts and found significant inhibitory effects against several pathogenic bacteria and fungi. Some studies have suggested that *T. palmata* extracts may exhibit anti-inflammatory effects. In one study published in the "Journal of Pharmacy Research," researchers investigated the anti-inflammatory activity of *T. palmata* leaf extracts using in vitro and in vivo models. The results indicated potential anti-inflammatory properties, which could be attributed to the presence of bioactive compounds. *T. palmata* has been investigated for its antioxidant potential, which is attributed to its ability to scavenge free radicals and reduce oxidative stress. Several studies have assessed the antioxidant activity of *Trevesia palmata* extracts using various assays, such as DPPH scavenging assay and total antioxidant capacity assay.

While these studies provide some scientific evidence supporting the traditional use of *Trevesia palmata* for medicinal purposes, more research is needed to fully elucidate its pharmacological properties, identify active constituents, and evaluate its safety and efficacy in clinical settings. Additionally, traditional knowledge and practices regarding the use of *Trevesia palmata* should be respected and further documented to preserve indigenous medicinal traditions.

2.2.1. Significance of standardising herbal formulations and their analytical techniques

Herbal remedies produced from medicinal plants have recognised therapeutic capabilities, but commercialization remains difficult in poor nations due to variable extraction procedures and varied composition in different batches (Sachan et al., 2016; Ekor et al., 2014). Thus, standardised herbal formulas seek to ensure uniform quality (Wang et al., 2023; Balekundri and Mannur, 2020). The phytochemical assessment is an important stage in standardising plant-derived therapeutic products. This entails identifying and quantifying bioactive components in plant extracts. Academicians were prompted to use a variety of analytical methodologies in order to identify the most important bioactive chemicals in plant extracts (Altemimi et al., 2017). Chromatography, sensors, spectroscopy, and spectrometry, as well as combinations of the two, are the most commonly employed techniques (Lozada-Ramirez, et al., 2021).

Mass spectrometry (MS) is a prevailing qualitative and quantitative analytical technique for identifying and quantifying a wide range of therapeutically imperative analytes. When mass spectrometers are used with gas or liquid chromatographs, they extend analytical capabilities to a diverse therapeutic application. Furthermore, due to its ability to detect and quantify proteins, MS is an important analytical tool in the field of proteomics (Garg and Zubair, 2023).

Infrared spectroscopy (IR), in conjunction with other techniques, aids in the production of conclusive analysis results. It is a method of qualitative and quantitative analysis that is fast, time-saving, cost-effective, accurate and non-destructive. This method has been applied for quantitative analysis of compounds in complex matrices such as plant-based medicine and supplements supported by chemometrics techniques (Junaedi et al., 2021)

2.2.2. Benefits and uses of plant secondary metabolites

Plants have a futuristic secondary metabolism that generates a large number of nonvital yet significant chemicals for adaptation to their surroundings. These molecules, known as secondary metabolites or natural products, exhibit a variety of biological activities such as antibiotic, antifungal, antiviral, herbicide, insecticide, anticancer, antioxidant, and antidiabetic properties (Hussein and El-Anssary, 2019). Chemically, these molecules pertain to several classes of compounds including flavonoids, alkaloids, terpenoids, tannins, and steroids, which are among the most important bioactive plant elements. Furthermore, these compounds have pharmacological properties such as reducing capillary fragility and permeability, as well as antioxidant, anti-inflammatory, antimutagenic, anticarcinogenic and antiedema effects (Roy et al., 2022).

The use of spectroscopic and spectrometric techniques to isolate, quantify, and describe bioactive chemicals for pharmacological and toxicological evaluations of medicinal plants is now a widespread and required activity in herbal medicine and pharmacognosy. As technology progresses, more varied approaches are being used, most of which are combined to provide the best diagnosis and information about a metabolite of interest (Lozada-Ramirez et al., 2021; Alseekh et al., 2021).

The phytochemical profile of extracts obtained using rigorous chromatographic and spectroscopic procedures are assessed throughout the examination. Highly-technical setups such as liquid and gas chromatography in conjunction with mass spectroscopy (LC/GC-MS) and Fourier transform infrared (FTIR) spectroscopic imaging are used in this experiment for the analysis of plant metabolites.

The purpose of this study was to examine the properties of plant extracts and the composition of plant raw materials derived from the leaves of *L. coromandelica* and *T. palmata*, which are commonly used in Mizoram to treat various diseases and ailments. Furthermore, this study also evaluates various vegetal products utilising chromatographic, spectroscopic, and spectrometric techniques to measure, separate,

and identify bioactive components in extracts, with an emphasis on research for future analysis.

2.3. MATERIALS AND METHODS

2.3.1. Identification and collection of the plants sample

The leaf of *L. coromandelica* and *T. palmata* was collected from Tanhril forest in Aizawl, Mizoram. The sample was identified, confirmed and submitted in the Department of Environmental Science's herbarium, Mizoram university, Aizawl, Mizoram, India under accession number 653 (A1481) and 1543 (3575).

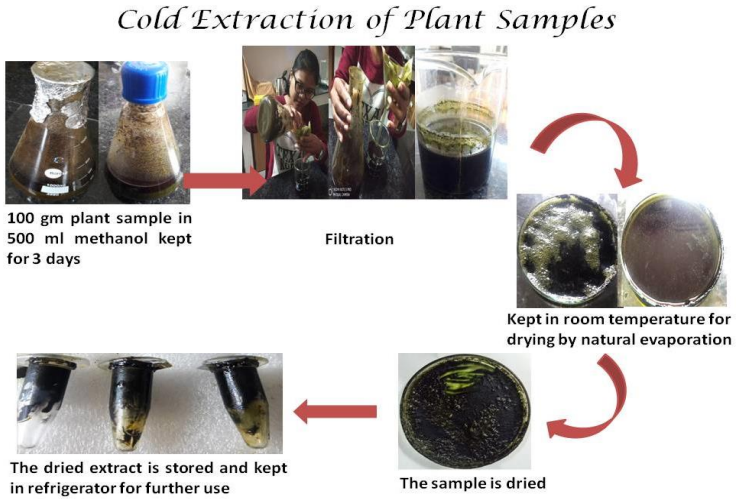

Figure 4: Workflow of the leaf extract preparation.

2.3.2. Preparation and processing of leaves

L. coromandelica and *T. palmata* leaves were collected, cleaned, chopped and dried in shade by air at room temperature (22ºC), after which they were powdered using a fine blender for extraction. The cold extraction process of the powdered plant samples was then carried out. Briefly, 100 gm of plant samples were dissolved in 500 ml of 100 % methanol and kept in a conical flask at room temperature for 72 h. The samples are then filtered using Whatman No. 1 filter papers and a rotary evaporator was used to condense the filtrate into a dark brownish-green semi-solid extract. The dried extract obtained was then stored for further use at 4ºC.

2.3.3. Gas chromatography-mass spectrometry (GC–MS) analytical conditions and analysis

Lannea coromandelica leaf extract (LCLE) and *Trevesia palmata* leaf extract (TPLE) were analyzed on a GCMS-2010 Shimadzu system (Shimadzu, Japan) in EI mode at 70 eV with a Restek-5MS column (30 0.25 mm film thickness 0.25 m). The carrier gas was pure helium gas (99.99 percent pure), flowing at a constant rate of 1 mL/min. For GC-MS spectrum detection, an electron ionisation energy technique was chosen, with a high ionisation energy of 70 eV (electron Volts), a scan length of 0.2 s, and fragments ranging from 40 to 650 (m/z). The injector temperature was maintained at 260°C, and the injection volume was 2 µL (split ratio: 10:1). The flow control mode was linear at a pressure of 99.3 kPa. The total and column flow rates were 16.3 mL/min and 1.21 mL/min, respectively. The temperature of the column oven was initially set at 120°C for two minutes, then increased by 10°C every minute until it reached 280°C, and finally to 300°C for 20 minutes. The chromatogram and mass spectra were assessed using the Xcalibur™ software included in the GC-MS/LC-MS system. The phytochemical contents of the test samples were determined by comparing their retention time (min), peak area, peak height, and mass spectral patterns to those of authentic compounds stored in the National Institute of Standards and Technology (NIST) library, which contains over 62,000 patterns and Dr. Duke's ethnobotanical phytochemical databases12. The spectra of the unknown component were compared to those of the known components in the NIST collection. The phytochemicals' names, molecular weights, and structures were determined.

2.3.4. Liquid chromatography-mass spectrometry (LC-MS/MS) classification

The Acquity Ultra Performance Liquid Chromatography (ACQUITY UPLC H-Class) equipment was used with an auto sampler and a binary pump (Waters, USA) connected to a 10L loop. The separation of phytocompounds from LCLE and TPLE was studied under a variety of chromatographic conditions, such as mobile phase composition, flow rate, and injection volume at various gradient programmes. Several mobile phase mixtures, including acetonitrile-water, methanol-water, and

acetonitrile-0.1% (v/v) formic acid aqueous solution, were evaluated in the gradient programme at a flow rate of 1.5 mL/min. The best separation conditions were determined to be 0-300 bar column pressure and 30°C column temperature. The compounds were separated at 30°C with an Acquity CSH C18 column (2.1 mm x 100 mm x 1.7 m). Two solvents, 0.1% (v/v) formic acid in water (A) and methanol (B), were used to accomplish gradient elution at a flow rate of 1.5 ml/min. The gradient programme started with 5% (B) at 0-1 min, then increased to 30% (B) at 6-12 min, 60% (B) at 12-16 min, 80% (B) at 16-20 min, and 5% (B) at 26-30 min. The sample injection volume was 10 µL. The MS analysis on the Water UPLC-TQD Mass Spectrometer (XEVOTQD#QCA1232) was carried out using data-dependent automated switching between MS and MS/MS acquisition modes. Positive and negative ionization modes were used to record the spectra, with a mass acquisition range of 150-2000 m/z.

2.3.5. FT-IR Analysis

Functional groups were identified using Fourier transform infrared spectroscopy (FTIR). The methanolic leaf extracts were analyzed using FTIR (Shimadzu, Kyoto, Japan, IR Affinity1), with a scan range of 400 to 4000 cm-1 and a resolution of 4 cm-1.

2.4. RESULTS

The methanolic crude extract from the LCLE and TPLE were analyzed by GCMS, LCMS, and FTIR.

2.4.1. GCMS analysis

Using the peak retention time, peak area (%), peak height (%) and mass spectral fragmentation patterns of the known compounds listed in the NIST library, the bioactive compounds present in the methanol LCLE were identified as 13 distinct peaks on the GC-MS chromatogram (**Figure 5**). The phytoconstituents in the methanolic LCLE were found to be Caryophyllene, Phenol, 3,5-bis(1,1-dimethylethyl)-, Diethyl Phthalate, Phenol, 2,4-bis(1,1-dimethylethyl)-5-methyl-,

Pentadecanoic acid, Oxirane, tetradecyl-, cis-9-Hexadecenal, Phytol, 9-Eicosene, (E)-, 1-Hexadecanol, Bis(2-ethylhexyl) phthalate, Phenol, 2,4-bis(1,1-dimethylethyl)-, 5,11,17,23-Tetratert-butylpentacyclo [19.3.1.1] (Table 1).

Likewise, the phytoconstituents of the methanolic TPLE were identified as 9 distinct peaks on the GC-MS chromatogram (**Figure 6**). These are Neophytadiene, Diethyl Phthalate, Pentadecanoic acid, Linoleic Acid, Phytol, gamma.-Tocopherol, dl-.alpha.-Tocopherol, Beta-Sitosterol and alpha.-Amyrin.

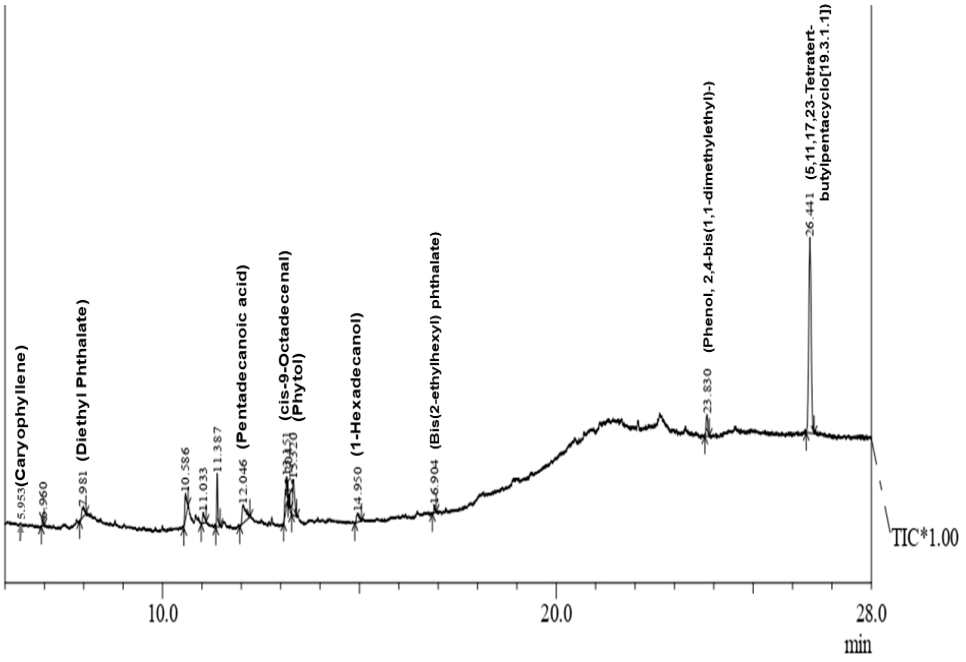

Figure 5: GC-MS Chromatogram of methanolic leaf extract of *Lannea coromandelica.*

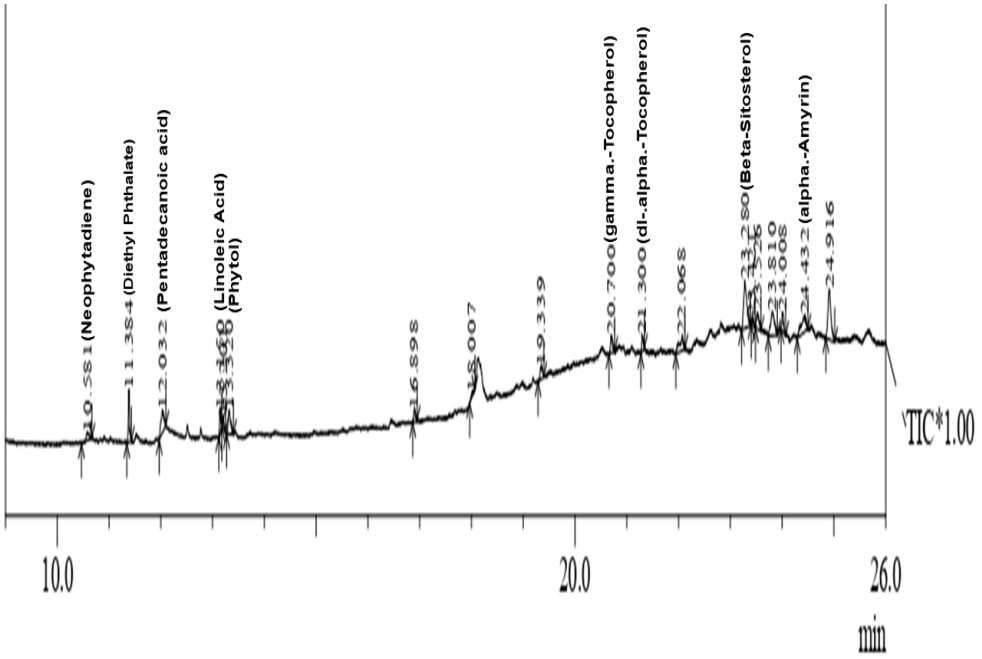

Figure 6: GC-MS Chromatogram of methanolic leaf extract of *Trevesia palmata*.

Table 1: Bioactive compounds identified in the methanol leaf extract of *Lannea coromandelica* using GC-MS.

Sl. no.	Compounds	Pub-Chem CID	Area %	Formula	Retention time	Mass spectrum (m/z)	Molecular weight (g/mol)	Class of Compound	Biological activities
1.	Caryophyllene	5281515	0.73	$C_{15}H_{24}$	5.953	204	204.35	Sesquiterpenoids	Antimicrobial, anticarcinogenic, antiinflammatory, antioxidant, anxiolytic like and local anesthetic
2.	Phenol, 3,5-bis(1,1-dimethylethyl)-	70825	0.73	$C_{14}H_{22}O$	6.960	206	206.32	Phenolic	Anti-biofilm and antifungal activities
3.	Diethyl Phthalate	6781	5.23	$C_{12}H_{14}O_4$	7.981	222	222.24	Benzoic acid esters	Antiviral, antioxidant, insecticidal, cytotoxic, antihyperglycemic, antibacterial, antifungal activity
4.	Phenol, 2,4-bis(1,1-dimethylethyl)-5-methyl-	10346	6.53	$C_{15}H_{24}O$	11.387	220	220.35	Phenolic	Antibacterial and antioxidant
5.	Pentadecanoic acid	13849	6.7 7	$C_{15}H_{30}O_2$	12.046	242	242.40	Fatty acids	Antibacterial and antifungal activity
6.	Oxirane, tetradecyl-	23741	6.77	$C_{16}H_{32}O$	13.151	240	240.42	Fatty acyls	Antibacterial, antifungal, antisporicidal and antivirus
7.	cis-9-Hexadecenal	5364643	0.88	$C_{16}H_{30}O$	13.204	238	238.41	Fatty acids	Antifungal
8.	Phytol	5280435	2.47	$C_{20}H_{40}O$	13.320	296	296.5	Acyclic diterpene alcohols	Metabolism-modulating, antioxidant, apoptosis, antiinflammatory, immunomodulatory and antimicrobial effects

9.	9-Eicosene, (E)-	5365037	2.47	$C_{20}H_{40}$	14.950	280	280.5	Fatty acids	Medicinal values and a hypotensive effect on blood pressure. It is also antimicrobial and antioxidant.
10.	1-Hexadecanol	2682	0.98	$C_{16}H_{34}O$	14.950	242	242.44	Fatty acids	Antibacterial and antioxidant activities
11.	Bis(2-ethylhexyl) phthalate	8343	0.98	$C_{24}H_{38}O_4$	16.904	390	390.6	Benzoic acid esters	Apoptosis inhibitor and an androstane receptor agonist
12.	Phenol, 2,4-bis(1,1-dimethylethyl)-	7311	4.11	$C_{14}H_{22}O$	23.830	206	206.32	Phenolics	Antioxidant, anti-inflammatory, antibacterial, antifungal and anticancer
13.	4-tert-Butylcalix[4]arene	335377	52.36	$C_{44}H_{56}O_4$	26.441	648	648.9	Tertiary alcohols	Antibacterial

Table 2: Bioactive compounds identified in the methanol leaf extract of *Trevesia palmata* using GC-MS.

Sl. no.	Compounds	Pub-Chem CID	Area %	Formula	Retention time	Mass spectrum (m/z)	Molecular weight (g/mol)	Class of compounds	Biological activities
1.	Neophytadiene	10446	2.36	$C_{20}H_{38}$	10.581	278	278.5	Sesquiterpenoids	Anti-inflammatory, antimicrobial, enzyme inhibitor, a plant and an algal metabolite
2.	Diethyl Phthalate	545303	7.07	$C_{17}H_{24}O_3$	11.384	276	276.4	Benzoic acid esters	Radical scavenger, antioxidant and anti-inflammatory
3.	Pentadecanoic acid	8042	6.63	$C_{17}H_{34}O_2$	12.032	270	270.5	Fatty acids	Antibacterial activity of long chain fatty acids
4.	Linoleic Acid	5280450	2.95	$C_{18}H_{32}O_2$	13.150	280	280.4	Fatty acid	Mucomembranous protector and antimicrobial
5.	Phytol	5280435	5.62	$C_{20}H_{40}O$	13.320	296	296.5	Acyclic Diterpenoids	Mucomembranous protector, lipid metabolism regulator, antiulcerative and peroxidase inhibitor
6.	gamma.-Tocopherol	92729	3.27	$C_{28}H_{48}O_2$	20.700	416	416.7	Tocopherols	Free radical scavenger and antioxidant
7.	dl-.alpha.-Tocopherol	2116	2.49	$C_{29}H_{50}O_2$	21.300	430	430.7	Tocopherols	Free radical scavenger, antioxidant and anti-inflammatory
8.	Beta-Sitosterol	222284	5.49	$C_{29}H_{50}O$	23.280	414	414.7	Phytosterols	An antioxidant, a plant and a mouse metabolite
9.	alpha.-Amyrin	73170	7.71	$C_{30}H_{50}O$	24.432	426	426.7	Triterpenoids	Antineoplastic, antiinflammatory, antiulcerative, membrane integrity antagonist and gastrin inhibitor

2.4.2. LCMS analysis

Based on the results of the LC-MS/MS analysis, alkaloids, flavonoids, carotenoids, phenols, fatty acids and terpenoid saponins constituted the majority of the phytocompounds that were extracted from methanolic LCLE. In the positive (**Fig. 7**) and negative (**Fig. 8**) ion modes, 16 peaks identified as major phytochemicals were found in the LC-MS/MS chromatogram of the methanol extract from *L. coromandelica* leaves. The PubChem ID, accurate and exact masses, RT, a molecular formula of the deprotonated molecules [M-H]*, mass spectrum (m/z), class of coumpounds and biological activities corresponding to each compound are shown in Table 3 with ID 1–18. Seven flavonoids were identified using LC-MS/MS including Hesperetin, 7-O-Methylquercetin-3-O-galactoside-6"-rhamnoside, Kaempferol, Quercetin-3-O-rutinoside, Kaempferol 7-neohesperidoside, Kaempferol-3-O-rutinoside and Luteolin-6-C-glucoside. Two triterpenoid saponins were identified including Asiaticoside and Diatoxanthin. Five carotenoids were identified including Beta-Carotene, gamma-Carotene, zeta-Carotene, Zeaxanthin and Lutein. One alkaloid i.e., Nantenine, phenolic i.e., Chlorogenic acid, tannin i.e., [Gallocatechin-(4alpha->8)]2-catechin and fatty acids such as Linoleic Acid are also identified using LC-MS/MS.

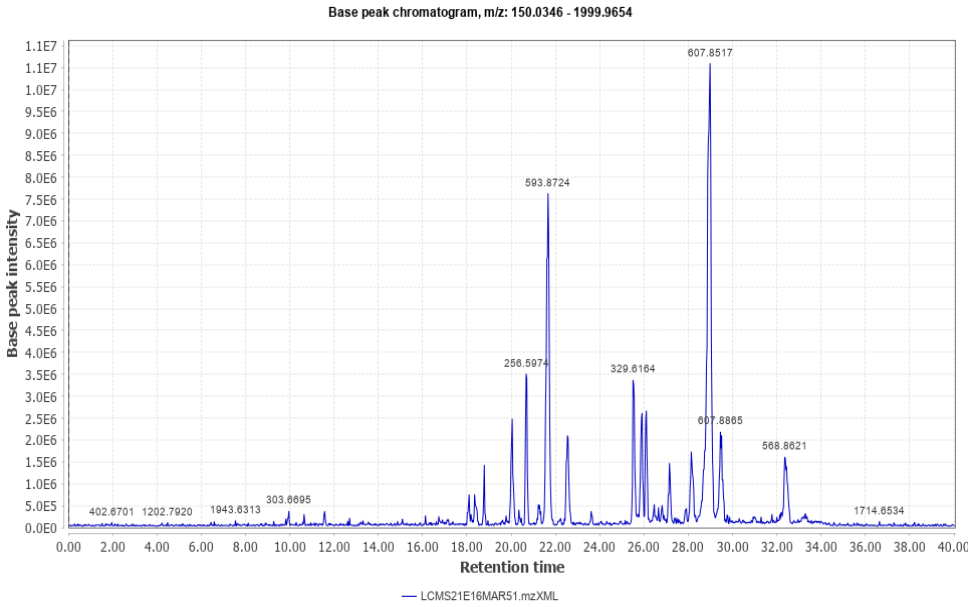

Figure 7: Total Ion Chromatogram of methanolic leaf extract of *Lannea coromandelica* (Positive Mode)

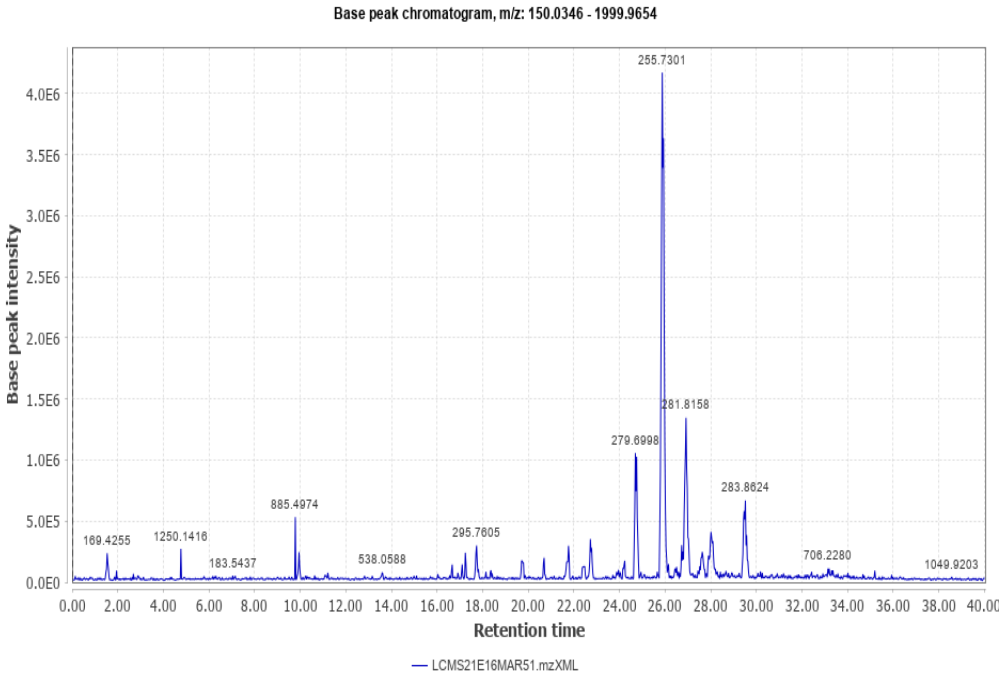

Figure 8: Total Ion Chromatogram of methanolic leaf extract of *Lannea coromandelica* (Negative Mode)

Table 3: Bioactive compounds identified in the methanol leaf extract of *Lannea coromandelica* by using LCMS.

ID	Compounds	Pub-Chem CID	Formula	Retention time	Mass spectrum (m/z)	Molecular weight (g/mol)	Class of Coumpounds	Biological activities
1.	Hesperetin	72281	$C_{16}H_{14}O_6$	9.96	303	302.28	Flavonoids	Anti-inflammatory, antioxidant, antibacterial, anticancer, anti-hepatic fibrosis and immune regulation
2.	Nantenine	197001	$C_{20}H_{21}NO_4$	16.31	339	339.4	Alkaloids	Antagonist against a wide range of MDMA and anticonvulsant
3.	7-O-Methylquercetin-3-O-galactoside-6"-rhamnoside	56995003	$C_{34}H_{42}O_{20}$	18.10	770	770.7	Flavonoids	Anticancer and antimicrobial
4.	Kaempferol	5280863	$C_{15}H_{10}O_6$	18.19	286	286.24	Flavonoids	Antibacterial, antifungal, antiprotozoal, anti-inflammatory and antioxidant
5.	Quercetin-3-O-rutinoside	5280805	$C_{27}H_{30}O_{16}$	19.77	610	610.5	Flavonoids	Anti-inflammatory
6.	Beta-Carotene	5280489	$C_{40}H_{56}$	21.23	535	536.9	Carotenoids	Biological pigment, a provitamin a, a plant metabolite, a human metabolite, a mouse metabolite and an antioxidant
7.	gamma-Carotene	5280791	$C_{40}H_{56}$	21.34	537	536.9	Carotenoids	Antiulcerative, antioxidant, anticarcinogenic, antiinflammatory and antibacterial
8.	Kaempferol 7-neohesperidoside	5483905	$C_{27}H_{30}O_{15}$	21.67	595	594.5	Flavonoids	Free radical scavenger, antiprotozoal, antioxidant, antiinflammatory, antibacterial and anticancer
9.	Kaempferol-3-O-rutinoside	5318767	$C_{27}H_{30}O_{15}$	22.54	594	594.5	Flavonoids	Free radical scavenger, antioxidant, antiprotozoal, antihemorrhagic and anti-inflammatory and antibacterial
10.	zeta-Carotene	5280788	$C_{40}H_{60}$	25.50	542	540.9	Carotenoids	Mucomembranous protector, antineoplastic, antioxidant, antiinflammatory, gastrin inhibitor and antiulcerative
11.	[Gallocatechin-(4alpha->8)]2-catechin	14890508	$C_{45}H_{38}O_{20}$	29.51	899	898.8	Tannins	Free radical scavenger, chemopreventive, antimutagenic, mucomembranous protector, antihemorrhagic, antioxidant, and anticarcinogenic

12.	Diatoxanthin	6440986	$C_{40}H_{54}O_2$	32.00	568	566.9	Triterpenoid saponins	Antineoplastic and cytochrome p450 stimulant
13.	Zeaxanthin	5280899	$C_{40}H_{56}O_2$	32.14	570	568.9	Carotenoids	Antineoplastic, oxidoreductase inhibitor, growth stimulant, chemopreventive, oxidizing agent, proliferative diseases treatment, antioxidant, chemoprotective and antiulcerative
14.	Lutein	5281243	$C_{40}H_{56}O_2$	32.19	570	568.9	Carotenoids	Reductant, antineoplastic, chemopreventive, antiulcerative, cytochrome p450 stimulant and oxidoreductase inhibitor
15.	Paclitaxel	36314	$C_{47}H_{51}NO_{14}$	32.36	852	853.9	Alkaloids	Antineoplastic, cytostatic and anticancer
16.	Chlorogenic acid	1794427	$C_{16}H_{18}O_9$	1.53	353	354.31	Phenolic	Free radical scavenger, anticarcinogenic, chemopreventive, antioxidant, antineoplastic and mucomembranous protector
17.	Luteolin-6-C-glucoside	114776	$C_{21}H_{20}O_{11}$	4.77	448	448.4	Flavonoids	Membrane permeability inhibitor, free radical scavenger, antihemorrhagic, antioxidant, antimutagenic, antineoplastic and antiprotozoal (leishmania)
18.	Linoleic Acid	5280450	$C_{18}H_{32}O_2$	24.75	279	280.4	Omega-6 fatty acids	Mucomembranous protector, prostaglandin-E2 9-reductase inhibitor, antimutagenic, reductant, antithrombotic, antiinflammatory, cytoprotectant and antihypoxic

The methanolic crude extract from the leaves of *T. palmata* analyzed by LCMS identified several phytochemicals through both the positive and negative ion mode which are shown in figure 9 and 10. The phytochemical analysis of LCLE by the LC-MS showed 17 major phytochemicals (Table 4). The PubChem ID, accurate and exact masses, RT, a molecular formula of the deprotonated molecules [M-H]*, mass spectrum (m/z), class of compounds and biological activities corresponding to each compound are shown in Table 3 with ID 1–17. These compounds contain six flavonoids including Icariin, Apigenin-6-C-glucoside-7-O-glucoside, Kaempferol 3-O-sophoroside, Kaempferol-3-O-rutinoside, Kaempferol 4'-methyl ether 3-(4Rha-rhamnosylrutinoside) and Quercetin 3-O-[2"-O-(6'"-O-p-coumaroyl)-b-D-glucopyranosyl]-a-L-rhamnopyranoside. Four triterpenoid saponins are also present including Asiaticoside, Bacoside A3, Hederacoside C and alpha-Hederin. Three carotenoids were also identified including Zeaxanthin, Lutein and zeta-Carotene. One fatty acid (Linolenic acid), alkaloids (Oxyacanthine), biphenols (Honokiol) and coumarin (Isofraxidin) were also identified in TPLE using LC-MS/MS analysis.

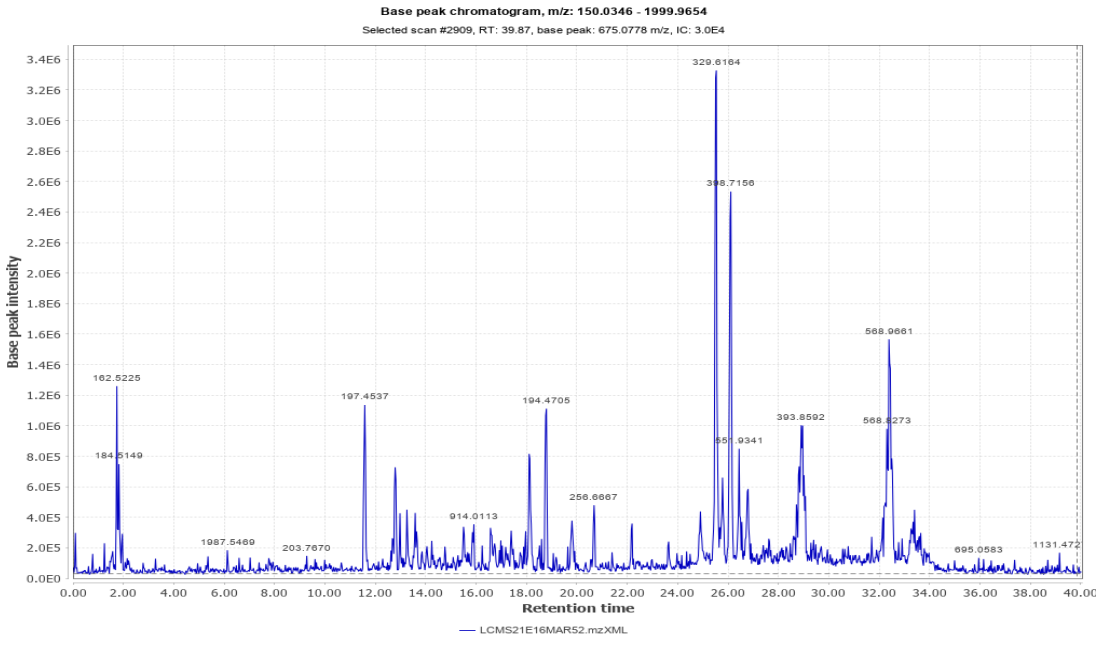

Figure 9: Total Ion Chromatogram of methanolic leaf extract of *Trevesia palmata* (Positive Mode)

Table 4: Bioactive compounds identified in the methanol leaf extract of *Trevesia palmata* by using LCMS.

ID	Compounds	Pub-Chem CID	Formula	Retention time	Mass spectrum (m/z)	Molecular weight (g/mol)	Class of Compounds	Biological activities
1.	Icariin	5318997	$C_{33}H_{40}O_{15}$	12.99	676	676.7	Flavonoid	Free radical scavenger, proliferative diseases treatment, antiprotozoal, antioxidant, antiinflammatory, antibacterial, antithrombotic and antimycobacterial
2.	Apigenin-6-C-glucoside-7-O-glucoside	4636593	$C_{27}H_{30}O_{15}$	17.43	594	594.5	Flavonoid	Free radical scavenger, antioxidant, antineoplastic, antiprotozoal, proliferative diseases treatment, antimycobacterial, antibacterial, antiinflammatory, gastritis treatment and antiulcerative
3.	Kaempferol 3-O-sophoroside	5282155	$C_{27}H_{30}O_{16}$	25.74	610	610.5	Flavonoid	Barrier integrity activity, inhibitory activity on cell adhesion and migration to endothelial cells by blocking the activation of NF-κB expression and production of TNF-α
4.	Kaempferol-3-O-rutinoside	5318767	$C_{27}H_{30}O_{15}$	17.03	594	594.5	Flavonoid	Analgesic and anti-inflammatory activities
5.	Kaempferol 4'-methyl ether 3-(4Rha-rhamnosylrutinoside)	44257995	$C_{34}H_{42}O_{19}$	1.82	754	754.7	Flavonoid	A member of flavonoids and a glycoside, antioxidant and antimicrobial
6.	Quercetin 3-O-[2"-O-(6"'-O-p-coumaroyl)-b-D-glucopyranosyl]-a-L-rhamnopyranoside	10169367	$C_{36}H_{36}O_{18}$	28.66	756	756.7 `	Flavonoid	Free radical scavenger, proliferative diseases treatment, antiprotozoal, antioxidant, antineoplastic, antiinflammatory, antithrombotic, antihemorrhagic, antibacterial and antiulcerative
7.	Asiaticoside	11954171	$C_{48}H_{78}O_{19}$	13.64	959	959.1	Triterpenoid Saponin	Antiinflammatory, antioxidant, antibacterial, anti-tumour and immunomodulatory activities.

8.	Bacoside A3	91827005	$C_{47}H_{76}O_{18}$	15.50	930	929.1	Triterpenoid saponin	Antiprotozoal (leishmania), antioxidant, chemopreventive, antineoplastic and antiprotozoal.
9.	Hederacoside C	5280788	$C_{40}H_{60}$	25.50	1221	1221.4	Triterpenoid saponin	Mucomembranous protector, antineoplastic, antioxidant, antiinflammatory, gastrin inhibitor and antiulcerative
10.	alpha-Hederin	11954171	$C_{48}H_{78}O_{19}$	30.93	751	751.0	Triterpenoid saponin	Wound healing agent, chemopreventive, antiprotozoal (leishmania), membrane integrity antagonist, antiinflammatory, antineoplastic, antiulcerative, immunostimulant, immunosuppressant and antithrombotic
11.	Zeaxanthin	5280899	$C_{40}H_{56}O_2$	32.14	570	568.9	Carotenoid	Antineoplastic, oxidoreductase inhibitor, growth stimulant, chemopreventive, oxidizing agent, antioxidant, chemoprotective and antiulcerative
12.	Lutein	5281243	$C_{40}H_{56}O_2$	32.19	570	568.9	Carotenoid	Reductant, antineoplastic, chemopreventive, antiulcerative, cytochrome p450 stimulant and oxidoreductase inhibitor
13.	zeta-Carotene	5280788	$C_{40}H_{60}$	25.50	542	540.9	Carotenoid	Mucomembranous protector, antineoplastic, antioxidant, antiinflammatory, gastrin inhibitor and antiulcerative
14.	Linolenic acid	5280934	$C_{18}H_{30}O_2$	16.98	279	278.4	Fatty acids	Mucomembranous protector, antiinflammatory, antisecretoric, mucositis treatment and antithrombotic
15.	Oxyacanthine	442333	$C_{37}H_{40}N_2O_6$	28.46	608	608.7	Alkaloids	Histamine release stimulant, spasmolytic, oxygen scavenger, fibrinogen receptor antagonist and antitussive
16.	Honokiol	72303	$C_{18}H_{32}O_2$	11.58	266	266.3	Neolignan biphenols	Potent antioxidative, anti-inflammatory, antiangiogenic, anticancer and antimicrobial activities
17.	Isofraxidin	5318565	$C_{11}H_{10}O_5$	1.74	222	222.19	Coumarin	Anti-inflammatory

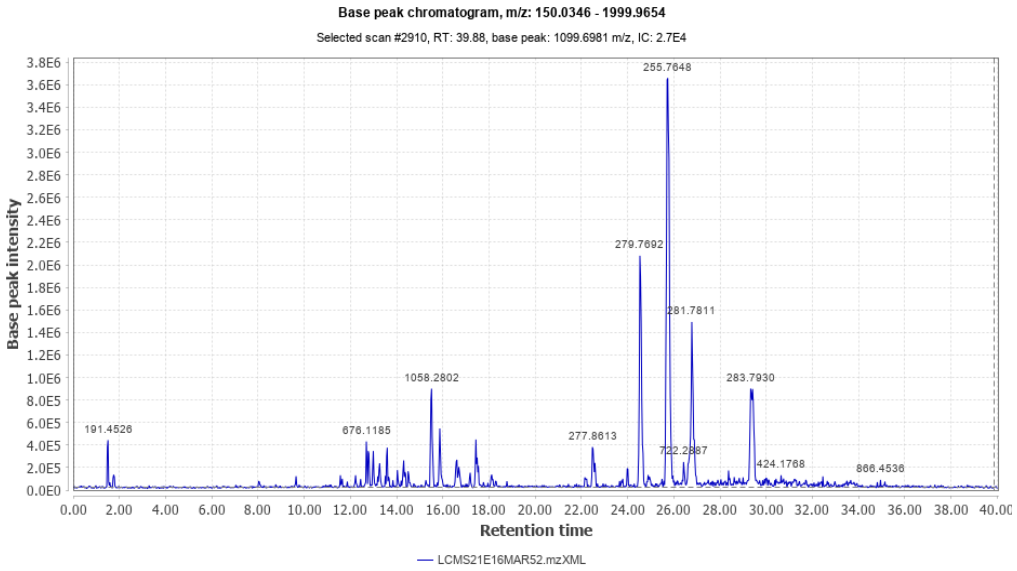

Figure 10: Total Ion Chromatogram of methanolic extract of *Trevesia palmata* (Negative Mode)

2.4.3. FT-IR analysis

FTIR spectroscopy of methanolic leaf extracts were done to determine the functional groups of isolated substances.

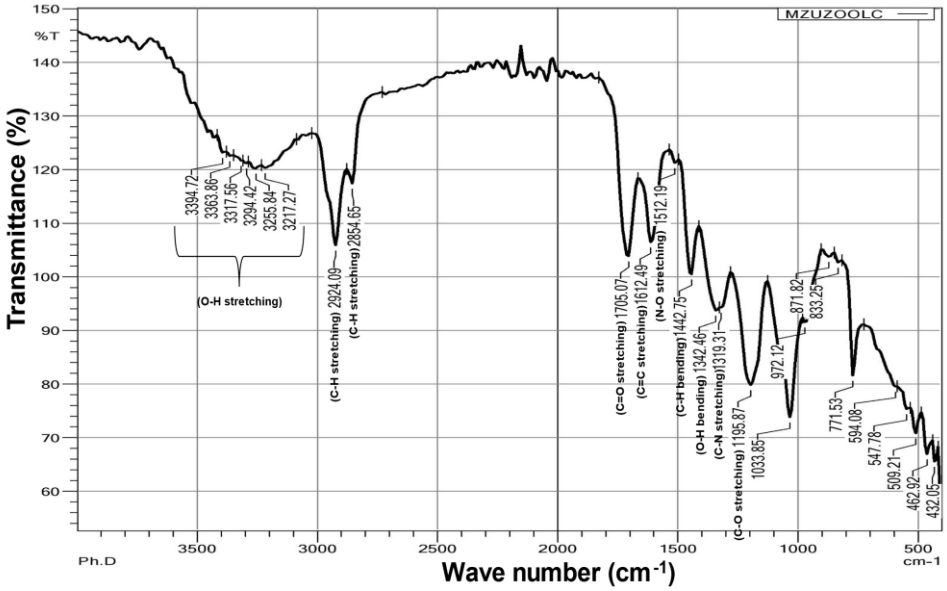

Figure 11: FTIR Chromatogram of *Lannea coromandelica*.

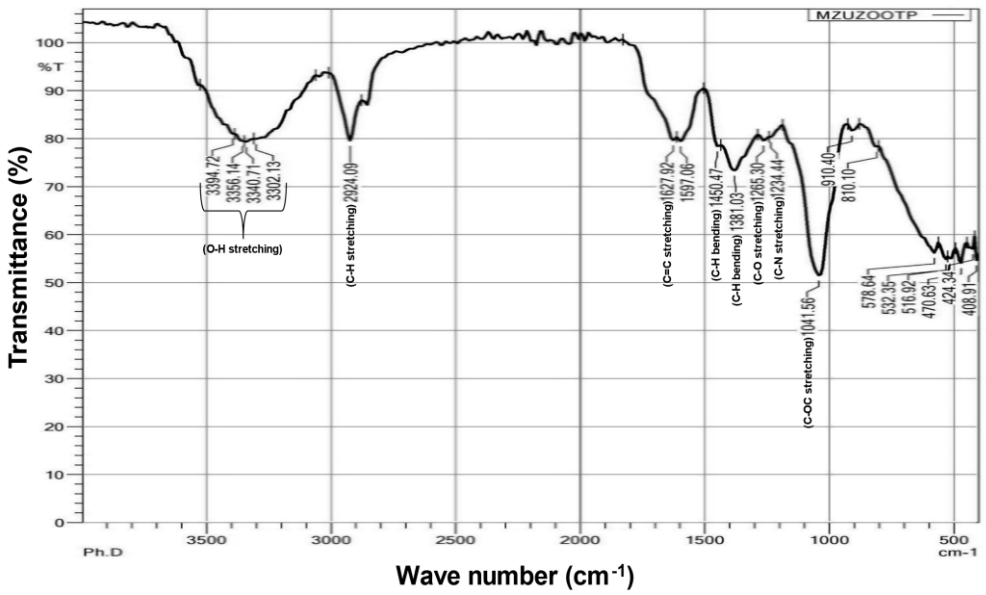

Figure 12: FTIR Chromatogram of *Trevesia palmata*.

In FTIR analysis of *L. coromandelica* (**Figure 11**), the presence of -OH functional groups are responsible for the broad absorption band at 3394-3317 cm^{-1}. The sharp absorption bands at 2924 cm^{-1} and 2854 cm^{-1} indicate C-H stretching. The absorption band at 1705 cm-1 indicates the presence of phytochemicals containing C=O functional groups, such as aldehydic, ketonic, ester, or carboxylic groups. Furthermore, the absorption bands at 1612 cm^{-1}, 1512 cm^{-1}, and 1319 cm^{-1} indicate the presence of C=C, N-O, and C-N stretching frequencies, respectively.

Similarly, in *T. palmata* (**Figure 12**) FTIR analysis shows a broad absorption band at 3394-3302 cm^{-1}, indicating the presence of -OH functional groups. The sharp absorption band at 2924 cm^{-1} indicates C-H stretching. The medium absorption band at 1627 cm^{-1} indicates the presence of C=C stretching. The (-C-O-C-) stretching at 1041 cm^{-1} suggests the presence of phytocompounds containing ether functional groups.

2.5. DISCUSSION

The identification of bioactive compounds in natural extracts is crucial for understanding their potential therapeutic or pharmacological effects. Research involving the isolation, characterization, and identification of bioactive compounds from plants like *Lannea coromandelica* and *Trevesia palmata* often employs a combination of chromatographic and spectroscopic techniques, including Gas Chromatography-Mass Spectrometry (GC-MS), Liquid Chromatography-Mass Spectrometry (LC-MS), and Infrared Spectroscopy (IR). These methods enable researchers to separate, analyze, and identify various compounds present in plant extracts (Sasidharan et al., 2011).

GC-MS is used to separate and identify volatile and semi-volatile compounds present in the extract. Compounds are separated based on their retention times in the gas chromatograph and identified by their mass spectra. LC-MS is utilized for the separation and identification of non-volatile and semi-volatile compounds. It provides high sensitivity and resolution for a wide range of compounds. IR Spectroscopy is employed to analyze the functional groups present in the isolated compounds. It helps in identifying characteristic absorption bands corresponding to various chemical bonds, aiding in structural elucidation. The data obtained from chromatographic and spectroscopic analyses are compared with reference databases, authentic standards, and literature to identify and characterize the bioactive compounds present in the plant extracts. Once the compounds were identified, further studies were conducted to evaluate their biological activities, such as antioxidant, antimicrobial, anti-inflammatory, or cytotoxic properties. Finally, the structures of bioactive compounds are elucidated based on the analytical data obtained, including MS fragmentation patterns, retention times, and UV-Vis spectra. This multi-step process involving chromatographic and spectroscopic techniques allows researchers to isolate, identify, and characterize bioactive compounds from plant extracts, providing insights into their potential medicinal and therapeutic applications. This study highlights the significance of using analytical tools to assess the potential health benefits of plant-based diets.

Nowadays, the use of medicinal plants for alleviating diseases is growing day by day around the world especially in Asia. Fewer side effects of medicinal plants play a big role for the popularity of the medicinal plants (Manik et al., 2013). Several studies have reported the ethnomedicinal uses of both *L. coromandelica* and *T. palmata*. Several representatives of this genus are used in ethnomedicine as astringents, helping with antioxidant, anti-inflammatory, and anti-diabetic properties, as well as other physiological functions (Swathi and Lakshman, 2022; Reddy et al., 2011).

The presence of phytochemicals in the plant extracts revealed that, tannins are known to be useful in the treatment of inflamed or ulcerated tissues and they have remarkable antioxidant, antibacterial, anticancer and anti-inflammatory activity (Tong et al., 2022; Demarque et al., 2018). Flavonoids possess antibacterial, antiviral, antioxidant, anti-inflammatory, antimutagenic, and anticarcinogenic properties. Due to their various therapeutic applications, various pharmaceutical companies have exploited different plants for the production of flavonoids (Roy et al., 2022). Flavonoids serve as health promoting compound as a result of its anion radicals (Dias et al., 2021; Panche et al., 2016). Terpenoids were also detected in the extract which have significant biological and pharmacological activities, and they play essential roles in various physiological processes in plants and animals. They exhibit potent anti-inflammatory, anticancer, antimicrobial and antioxidant activities (Wang et al., 2023). Phenolic compounds are a class of organic compounds that contain a phenol group, which consists of a hydroxyl (-OH) group bonded to an aromatic benzene ring. The presence of phenolic compounds has garnered significant attention in medicinal use due to their diverse biological activities and potential health benefits. They posses potent and promising antioxidant, anti-inflammatory, antimicrobial and anticancer activity as well. Many phenolic compounds exhibit anti-inflammatory properties by inhibiting the production of inflammatory mediators and modulating inflammatory pathways. These compounds can help alleviate symptoms associated with inflammatory conditions such as arthritis, inflammatory bowel disease, and asthma (Sun and Shahrajabian, 2023; Tungmunnithum et al., 2018). Fatty acids, essential components of the human diet, play crucial roles in various physiological processes and have been investigated for their therapeutic effects on a range of

diseases. Omega-3 fatty acids also exhibit anti-inflammatory properties, which can be beneficial in managing inflammatory conditions such as rheumatoid arthritis, inflammatory bowel disease (IBD), and asthma. They can reduce the production of pro-inflammatory cytokines and eicosanoids, leading to decreased inflammation and symptom relief (Elyasi et al., 2019). Alkaloids were also detected in this plant study. These are a diverse group of naturally occurring chemical compounds that contain nitrogen atoms, often found in plants. They possess a wide range of pharmacological activities including antimicrobial (inhibiting the growth and replication of pathogens, making them useful in the treatment of infections), anticancer (inhibiting tumour growth, inducing apoptosis (programmed cell death), and interfering with cancer cell signalling pathways), antioxidant (scavenging free radicals and reducing oxidative stress in the body) and anti-inflammatory activities as well (Heinrich et al., 2021). Phytosterols have been shown to possess anti-inflammatory effects, which may be beneficial in managing inflammatory conditions (Vilahur et al., 2019). Tocopherols and carotenoids also possess potent antioxidant activity that can contribute to overall health and may help prevent or manage various diseases (Crupi et al., 2023; Miazek et al., 2022). These observations support the usefulness of this plant in folklore remedies in the treatment of immune dysregulation, epithelial barrier dysfunction, microbiota dysbiosis and oxidative stress.

It's important to note that the presence of these compounds suggests potential bioactivity, but further studies would be needed to determine their exact biological effects, mechanisms of action, and potential applications in medicine or other fields. Additionally, the concentrations of these compounds in the extracts may influence their biological activity, which warrants further investigation.

2.6. SUMMARY

- Research involving the isolation, characterization, and identification of bioactive compounds from plants like *Lannea coromandelica* and *Trevesia palmata* often employs a combination of chromatographic and spectroscopic techniques, including Gas Chromatography-Mass Spectrometry (GC-MS), Liquid Chromatography-Mass Spectrometry (LC-MS), and Infrared Spectroscopy (IR).

- The data obtained from chromatographic and spectroscopic analyses are compared with reference databases, authentic standards, and literature to identify and characterize the bioactive compounds present in the plant extracts.
- Finally, the structures of bioactive compounds are elucidated based on the analytical data obtained, including MS fragmentation patterns, retention times, and UV-Vis spectra.
- This multi-step process involving chromatographic and spectroscopic techniques allows researchers to isolate, identify, and characterize bioactive compounds from plant extracts, providing insights into their potential medicinal and therapeutic applications.
- This study highlights the significance of using analytical tools to assess the potential health benefits of plant-based diets.
- The presence of phenolic compounds has garnered significant attention in medicinal use due to their diverse biological activities and potential health benefits.
- Many phenolic compounds exhibit anti-inflammatory properties by inhibiting the production of inflammatory mediators and modulating inflammatory pathways.
- Alkaloids were also detected in this plant study.
- These are a diverse group of naturally occurring chemical compounds that contain nitrogen atoms, often found in plants.
- They possess a wide range of pharmacological activities including antimicrobial (inhibiting the growth and replication of pathogens, making them useful in the treatment of infections), anticancer (inhibiting tumor growth, inducing apoptosis (programmed cell death), and interfering with cancer cell signaling pathways), antioxidant (scavenging free radicals and reducing oxidative stress in the body) and anti-imflammatory activities as well.
- Phytosterols have been shown to possess anti-inflammatory effects, which may be beneficial in managing inflammatory conditions.
- Tocopherols and carotenoids also posseses potent antioxidant activity that can contribute to overall health and may help prevent or manage various diseases.
- These observations support the usefulness of this plant in folklore remedies in the treatment of immune dysregulation, epithelial barrier dysfunction, microbiota dysbiosis and oxidative stress.

- It's important to note that the presence of these compounds suggests potential bioactivity, but further studies would be needed to determine their exact biological effects, mechanisms of action, and potential applications in medicine or other fields.
- Additionally, the concentrations of these compounds in the extracts may influence their biological activity, which warrants further investigation.

2.7. CONCLUSION

The utilization of chromatographic and spectroscopic techniques, such as GC-MS, LC-MS, and IR, in isolating and characterizing bioactive compounds from plants like *Lannea coromandelica* and *Trevesia palmata* underscores their potential medicinal and therapeutic significance. The presence of various compounds, including phenolic compounds, alkaloids, phytosterols, tocopherols, and carotenoids, suggests a wide range of pharmacological activities, including anti-inflammatory, antimicrobial, anticancer, and antioxidant properties. These findings support the traditional medicinal uses of these plants in treating conditions related to immune dysregulation, epithelial barrier dysfunction, microbiota dysbiosis, and oxidative stress. However, further research is needed to fully elucidate the biological effects, mechanisms of action, and potential applications of these compounds in medicine or other fields, considering the influence of compound concentrations on their biological activity.

2.8. REFERENCES

Abubakar, A. R., & Haque, M. (2020). Preparation of medicinal plants: Basic extraction and fractionation procedures for experimental purposes. Journal of pharmacy & bioallied sciences, 12(1), 1.

Adeosun, W. B., & Loots, D. T. (2024). Medicinal Plants against Viral Infections: A Review of Metabolomics Evidence for the Antiviral Properties and Potentials in Plant Sources. *Viruses*, *16*(2), 218.

Alseekh, S., Aharoni, A., Brotman, Y., Contrepois, K., D'Auria, J., Ewald, J., C. Ewald, J., Fraser, P.D., Giavalisco, P., Hall, R.D. & Heinemann, M. (2021). Mass spectrometry-based metabolomics: a guide for annotation, quantification and best reporting practices. Nature methods, 18(7), 747-756.

Altemimi, A., Lakhssassi, N., Baharlouei, A., Watson, D. G., & Lightfoot, D. A. (2017). Phytochemicals: Extraction, isolation, and identification of bioactive compounds from plant extracts. Plants, 6(4), 42.

Angami, A., Gajurel, P. R., Rethy, P., Singh, B., & Kalita, S. K. (2006). Status and potential of wild edible plants of Arunachal Pradesh.

Babich, O. O., Samsuev, I. G., Tsibulnikova, A. V., Zemlyakova, E. S., Popov, A. D., Ivanova, S. A., Noskova S. Y., & Sukhikh, S. A. (2024). Properties of plant extracts and component composition: column chromatography and IR spectroscopy. Food and Raw Materials, 12(2), 373-387.

Balekundri, A., & Mannur, V. (2020). Quality control of the traditional herbs and herbal products: A review. Future Journal of Pharmaceutical Sciences, 6, 1-9.

Carmona, F., & Pereira, A. M. S. (2013). Herbal medicines: old and new concepts, truths and misunderstandings. Revista Brasileira de Farmacognosia, 23(2), 379-385.

Cragg, G. M., & Newman, D. J. (2001). Natural product drug discovery in the next millennium. Pharmaceutical biology, 39(sup1), 8-17.

Crupi, P., Faienza, M. F., Naeem, M. Y., Corbo, F., Clodoveo, M. L., & Muraglia, M. (2023). Overview of the potential beneficial effects of carotenoids on consumer health and well-being. Antioxidants, 12(5), 1069.

De Tommasi, N., Autore, G., Bellino, A., Pinto, A., Pizza, C., Sorrentino, R., & Venturella, P. (2000). Antiproliferative Triterpene Saponins from Trevesia p almata. Journal of natural products, 63(3), 308-314.

Demarque, D. P., Callejon, D. R., Oliveira, G. G. D., Silva, D. B., Carollo, C. A., & Lopes, N. P. (2018). The role of tannins as antiulcer agents: a fluorescence-imaging based study. Revista Brasileira de Farmacognosia, 28, 425-432.

Dias, M. C., Pinto, D. C., & Silva, A. M. (2021). Plant flavonoids: Chemical characteristics and biological activity. Molecules, 26(17), 5377.

Edeoga, H. O., Okwu, D. E., & Mbaebie, B. O. (2005). Phytochemical constituents of some Nigerian medicinal plants. African journal of biotechnology, 4(7), 685-688.

Ekor, M. (2014). The growing use of herbal medicines: issues relating to adverse reactions and challenges in monitoring safety. Frontiers in pharmacology, 4, 177.

Elyasi, H., Sepahvand, A., Rahimi, H., Nafari, A., Azizi, S., Khadem, E., ... & Bahmani, M. (2019). Fatty Acids and Herbal Medicine. Current Traditional Medicine, 5(3), 246-256.

Fakhri, S., Moradi, S. Z., Farzaei, M. H., & Bishayee, A. (2022). Modulation of dysregulated cancer metabolism by plant secondary metabolites: A mechanistic review. In Seminars in cancer biology (Vol. 80, pp. 276-305). Academic Press.

Fang, C., Fernie, A. R., & Luo, J. (2019). Exploring the diversity of plant metabolism. Trends in Plant Science, 24(1), 83-98.

Federica, B., Leopold, I., Termopoli, V., & Lucia, M. (2018). Advances in MS-Based Analytical Methods: Innovations and Future Trends. Journal of Analytical Methods in Chemistry, 2018:2084567. doi: 10.1155/2018/2084567.

Garg, E., & Zubair, M. (2023). Mass Spectrometer. In StatPearls [Internet]. StatPearls Publishing. https://www.ncbi.nlm.nih.gov/books/NBK589702/

Guerrieri, A., Dong, L., & Bouwmeester, H. J. (2019). Role and exploitation of underground chemical signaling in plants. Pest management science, 75(9), 2455-2463.

Gunjal, J. N., Patil, M. S., & K. P. Chittam, P. (2021). Lannea coromandelica: An overview. *International Journal of Pharmaceutical and Biological Science Archive*, *9*(1), 102-107.

Heinrich, M., Mah, J., & Amirkia, V. (2021). Alkaloids used as medicines: Structural phytochemistry meets biodiversity—An update and forward look. Molecules, 26(7), 1836.

Hussain, M. I., Shill, S., Barman, S. K., & Jahan, K. (2021). Assessment of preliminary phytochemical screening, cytotoxic and hypoglycemic activity of lannea coromandelica bark extract. Pharmacologyonline, 2, 89-96.

Hussein, R. A., & El-Anssary, A. A. (2019). Plants secondary metabolites: the key drivers of the pharmacological actions of medicinal plants. Herbal medicine, 1(3).

Ingle, R. G., Zeng, S., Jiang, H., & Fang, W. J. (2022). Current developments of bioanalytical sample preparation techniques in pharmaceuticals. Journal of Pharmaceutical Analysis, 12(4), 517-529.

Isah, T. (2019). Stress and defense responses in plant secondary metabolites production. Biological research, 52.

Islam, F., Mitra, S., Nafady, M. H., Rahman, M. T., Tirth, V., Akter, A., ... & El-Kholy, S. S. (2022). Neuropharmacological and antidiabetic potential of lannea coromandelica (houtt.) merr. Leaves extract: an experimental analysis. Evidence-Based Complementary and Alternative Medicine, 2022.

Junaedi, E. C., Lestari, K., & Muchtaridi, M. (2021). Infrared spectroscopy technique for quantification of compounds in plant-based medicine and supplement. Journal of Advanced Pharmaceutical Technology & Research, 12(1), 1.

Kessler, A., & Kalske, A. (2018). Plant secondary metabolite diversity and species interactions. Annual Review of Ecology, Evolution, and Systematics, 49, 115-138.

Kim, B., Han, J. W., Thi Ngo, M., Le Dang, Q., Kim, J. C., Kim, H., & Choi, G. J. (2018). Identification of novel compounds, oleanane-and ursane-type

triterpene glycosides, from Trevesia palmata: their biocontrol activity against phytopathogenic fungi. Scientific reports, 8(1), 14522.
Kosmacz, M., Sokołowska, E. M., Bouzaa, S., & Skirycz, A. (2020). Towards a functional understanding of the plant metabolome. Current opinion in plant biology, 55, 47-51.
Kunle, Oluyemisi, F., Egharevba, Henry, O., Ahmadu, & Peter, O. (2012). Standardization of herbal medicines-A review. International journal of biodiversity and conservation, 4(3), 101-112.
Lalfakzuala, R., Lalramnghinglova, H., & Kayang, H. (2007). Ethnobotanical usages of plants in western Mizoram.
Lamxay, V., de Boer, H. J., & Björk, L. (2011). Traditions and plant use during pregnancy, childbirth and postpartum recovery by the Kry ethnic group in Lao PDR. Journal of Ethnobiology and Ethnomedicine, 7, 1-16.
Lozada-Ramirez, J. D., Ortega-Regules, A. E., Hernández, L. R., & Anaya de Parrodi, C. (2021). Spectroscopic and spectrometric applications for the identification of bioactive compounds from vegetal extracts. Applied Sciences, 11(7), 3039.
Manik, M. K., Wahid, M. A., Islam, S. M. A., Pal, A., & Ahmed, K. T. (2013). A comparative study of the antioxidant, antimicrobial and thrombolytic activity of the bark and leaves of Lannea coromandelica (Anacardiaceae). International Journal of Pharmaceutical Sciences and Research, 4(7), 2609.
Mate, C. J., Mishra, S., & Srivastava, P. K. (2020). In vitro release kinetics of graft matrices from Lannea coromandelica (Houtt) gum for treatment of colonic diseases by 5-ASA. *International journal of biological macromolecules*, *149*, 908-920.
Miazek, K., Beton, K., Śliwińska, A., & Brożek-Płuska, B. (2022). The effect of β-carotene, tocopherols and ascorbic acid as anti-oxidant molecules on human and animal in vitro/in vivo studies: A review of research design and analytical techniques used. Biomolecules, 12(8), 1087.
Mishra, B. B., & Tiwari, V. K. (2011). Natural products: an evolving role in future drug discovery. European journal of medicinal chemistry, 46(10), 4769-4807.
Newmaster, S. G., Grguric, M., Shanmughanandhan, D., Ramalingam, S., & Ragupathy, S. (2013). DNA barcoding detects contamination and substitution in North American herbal products. BMC medicine, 11, 1-13.
Nikam, P. H., Kareparamban, J., Jadhav, A., & Kadam, V. (2012). Future trends in standardization of herbal drugs. Journal of applied pharmaceutical science, (Issue), 38-44.
Nortjie, E., Basitere, M., Moyo, D., & Nyamukamba, P. (2022). Extraction methods, quantitative and qualitative phytochemical screening of medicinal plants for antimicrobial textiles: a review. Plants, 11(15), 2011.
Ogunsina O. I., Ayedogbon O. S., & Adekahunsi A. J. (2020). GC-MS Analysis of Bioactive Components of Methanolic Stem Bark Extract of Lannea acida (Anacardiaceae). Global Scientific Journals, 8(4), 2320-9186.
Panche, A. N., Diwan, A. D., & Chandra, S. R. (2016). Flavonoids: an overview. Journal of nutritional science, 5, e47.

Pang, Z., Chen, J., Wang, T., Gao, C., Li, Z., Guo, L., & Cheng, Y. (2021). Linking plant secondary metabolites and plant microbiomes: a review. Frontiers in Plant Science, 12, 621276.

Piasecka, A., Jedrzejczak-Rey, N., & Bednarek, P. (2015). Secondary metabolites in plant innate immunity: conserved function of divergent chemicals. New Phytologist, 206(3), 948-964.

Rahman, K. H., Nandi, J. K., Sultana, S., Rahman, S., Hossan, S., & Rahmatullah, M. (2014). Phytochemical screening, antihyperglycemic and analgesic activity studies with methanol extract of Trevesia palmata leaves. World J Pharm Pharmaceut Sci, 3(10), 91-101.

Ranilla, L. G., Kwon, Y. I., Apostolidis, E., & Shetty, K. (2010). Phenolic compounds, antioxidant activity and in vitro inhibitory potential against key enzymes relevant for hyperglycemia and hypertension of commonly used medicinal plants, herbs and spices in Latin America. Bioresource technology, 101(12), 4676-4689.

Reddy, A. K., Joy, J. M., & Kumara, C. A. (2011). Available online through www. jpronline. info. Journal of Pharmacy Research, 4(3), 577-579.

Rodriguez-Concepcion, M., Avalos, J., Bonet, M. L., Boronat, A., Gomez-Gomez, L., Hornero-Mendez, D., Limon, C., Meléndez-Martínez, A. J., Olmedilla-Alonso, B., Palou, A., Ribot, J., Rodrigo, M. J., Zacarias, L., & Zhu, C. (2018). A global perspective on carotenoids: Metabolism, biotechnology, and benefits for nutrition and health. Progress in lipid research, 70, 62-93.

Roy, A., Khan, A., Ahmad, I., Alghamdi, S., Rajab, B. S., Babalghith, A. O., Alshahrani, M.Y., Islam, S., & Islam, M. R. (2022). Flavonoids a bioactive compound from medicinal plants and its therapeutic applications. BioMed Research International, 2022.

Sachan, A. K., Vishnoi, G., & Kumar, R. (2016). Need of standardization of herbal medicines in modern era. International Journal of Phytomedicine, 8(3), 300-307.

Sasidharan, S., Chen, Y., Saravanan, D., Sundram, K. M., & Latha, L. Y. (2011). Extraction, isolation and characterization of bioactive compounds from plants' extracts. African journal of traditional, complementary and alternative medicines, 8(1).

Sayeed, M. A., Faruk, M., Chowdhury, A. I., & Rusti, A. (2014). Thrombolytic and Anti-arthritic Activities of Methanolic Extract of Trevesia palmata. J. Sci. Technol, 5(9), 119-124.

State Medicinal Plants Board- Mizoram. (2001). (Under National Medicinal Plants Board), Directorate Of AYUSH, Health & Family Welfare Department, Government of Mizoram. List of Medicinal Plants Board – Mizoram.

Sultana, H., Chetia, A., Saikia, A., & Khan, N. J. (2023). An updated review on extraction, isolation, and identification of bioactive compounds from plant extracts. *Sch Acad J Pharm*, *12*(7).

Sun, W., & Shahrajabian, M. H. (2023). Therapeutic potential of phenolic compounds in medicinal plants—Natural health products for human health. Molecules, 28(4), 1845.

Swathi, S., & Lakshman, K. (2022). Photochemistry and Pharmacological Bio-Activities of Lannea coromandelica: A Review. Innovare Journal of Medical Science, 10(5).

Thao, L. T. T., Quyen, D., Vu, D. B., Tai, B. H., & Van Kiem, P. (2018). New acetylated saponins from the leaves of Trevesia palmata. Natural Product Communications, 13(4), 1934578X1801300407.

Tong, Z., He, W., Fan, X., & Guo, A. (2022). Biological function of plant tannin and its application in animal health. Frontiers in veterinary science, 8, 803657.

Tungmunnithum, D., Thongboonyou, A., Pholboon, A., & Yangsabai, A. (2018). Flavonoids and other phenolic compounds from medicinal plants for pharmaceutical and medical aspects: An overview. Medicines, 5(3), 93.

Ullrich, C. I., Aloni, R., Saeed, M. E., Ullrich, W., & Efferth, T. (2019). Comparison between tumors in plants and human beings: Mechanisms of tumor development and therapy with secondary plant metabolites. Phytomedicine, 64, 153081.

Vadivel, K., Thangabalan, B., Narayana, K. V., Chetanajessygrace, B., Praveen Kumar, D., & Manohar, B. S. (2012). Preliminary phytochemical evaluation of leaf extracts of lannea corommandelica L. Int J Pharmacol Res, 2(2), 64-68.

Vilahur, G., Ben-Aicha, S., Diaz-Riera, E., Badimon, L., & Padro, T. (2019). Phytosterols and inflammation. Current Medicinal Chemistry, 26(37), 6724-6734.

Wang, H., Chen, Y., Wang, L., Liu, Q., Yang, S., & Wang, C. (2023). Advancing herbal medicine: enhancing product quality and safety through robust quality control practices. Frontiers in Pharmacology, 14.

Wang, Q., Zhao, X., Jiang, Y., Jin, B., & Wang, L. (2023). Functions of Representative Terpenoids and Their Biosynthesis Mechanisms in Medicinal Plants. Biomolecules, 13(12), 1725.

Weerapreeyakul, N., Junhom, C., Barusrux, S., & Thitimetharoch, T. (2016). Induction of apoptosis in human hepatocellular carcinoma cells by extracts of Lannea coromandelica (Houtt.) Merr. and Diospyros castanea (Craib) Fletcher. Chinese Medicine, 11(1), 1-10.

World Health Organization. (2017). WHO guidelines for selecting marker substances of herbal origin for quality control of herbal medicines. WHO Expert Committee on Specification for Pharmaceutical Preparations: Fifty-first report. Geneva: World Health Organization.

Yadav, P., Mahour, K., & Kumar, A. (2011). Standardization and evaluation of herbal drug formulations. Journal of Advanced Laboratory Research in Biology, 2(4), 161-166.

Yang, L., Wen, K. S., Ruan, X., Zhao, Y. X., Wei, F., & Wang, Q. (2018). Response of plant secondary metabolites to environmental factors. Molecules, 23(4), 762.

Zhou, F., & Pichersky, E. (2020). More is better: the diversity of terpene metabolism in plants. Current opinion in plant biology, 55, 1-10.

Chapter 3

Computational study of the phytochemical and pharmacological bio-activities of *Lannea coromandelica* and *Trevesia palmata* leaves

3.1. INTRODUCTION

There are several ways for two or more substances to interact with biological systems. Chemical reactions in a mixture can be predicted using perceptions of concentration or dose addition for substances with the same mechanism of action (MOA) and/or same target of effect. Chemicals that operate on a variety of biological targets may be suitable for response augmentation. Both hypotheses are only valid when there is no chemical contact. In contrast, when chemicals combine in a combination, they cause synergy or potentiation if an activating enzyme is activated or a detoxifying enzyme inhibited. Individual chemical competition at the biological target site, on the other hand, results in antagonism. Experimental models are time-consuming and costly. The experimenter's task is complicated by the variety of mixes and the need to test several organisms from different environments in order to acquire toxicity data. As a result, computational approaches are critical for filling toxicity data gaps, selecting compounds, finding toxicity pathways, risk assessment and management (Kar and Leszczynski, 2022).

Pharmaceutical corporations employ medicinal plants to produce medications. However, two major obstacles impede the use of plants until they are commercialised: safety and efficacy (van Wyk and Prinsloo, 2020). Preclinical toxicity and adverse medication responses cause roughly one-third of product failures (Van Norman, 2019). Time, money, and labour are the three most major barriers to evaluating the toxicity of drugs utilising in vivo and in vitro approaches. Toxicology evaluation utilising computational methodologies facilitates early drug development by enabling for the discovery of substances with no experimental data (Pognan et al., 2023). These methods also provide an alternative to animal-based toxicology research.

In silico prediction techniques use the physiochemical features of a substance to estimate its activity in a specific biological system. To anticipate the relative activities of a compound's structure, mathematical models such as structure activity relationship (SAR) and quantitative structure activity relationship (QSAR) are used (Kar and Leszczynski, 2022). SAR and quantitative structure activity relationship

(QSAR) strategies have been primarily used by a number of regulatory agencies, including those in the agrochemical, educational, food, and health care sectors, to handle the toxicological evaluation of a major substance found in nature, with clear annotation. As a result, SAR/QSAR programmes are recognised as effective, substantial, and improved core prediction tools in systems biology. They may give beneficial approaches for increasing our understanding of the potentially detrimental effects of phytochemicals (Nisa et al., 2023).

Several academic and commercial SAR/QSAR modelling programmes and packages, including VEGA-HUB, Toxicity Estimation Software Tool, Toxtree, the OECD QSAR Toolbox, and the Online Chemical Modelling Environment (OCHEM), have been described for defining a wide range of toxicological activities (Dinata et al., 2024; Ranjith Kumar et al., 2019). Unlike the previously described QSAR models, the read-through strategy-based tools VEGAHUB, TEST, and QSAR toolbox produce realistic, repeatable, transparent, and verifiable findings (Kumar et al., 2019).

Natural compounds, as a leading compound, have been extensively researched in various industries. Because they may also have other side effects, determining their toxicity is critical. Computational methods can overcome the primary challenges of assessing the toxicity of substances using in vivo and in vitro techniques, such as time, money, labour, and the use of animal models (Barba-Ostria et al., 2022).

Although the plants leaf both *Lannea coromandelica* and *Trevesia palmata* has a significant economic potential, its exploitation has yet to be thoroughly explored in terms of its toxicity and food safety. In Utilizing the TEST, OECD QSAR toolkit, VEGA-HUB, Toxtree and PASS tools, phytocompounds from L. coromandelica and T. palmata will be assessed for toxicity, food safety risk assessment, and biological activity.

A collection of computational approaches can be considered for toxicity modelling of the mixture. The most prominent one is quantitative structure–activity relationship (QSAR) which is an established method for toxicity prediction (Kar and Leszczynski, 2022). Other methods like machine learning approaches, structural

alerts and rule-based models, read-across, docking, and molecular dynamics have the potential to evaluate risk assessment, identify the biological pathways of toxicity, interaction, and binding.

3.1.1. COX-2 and its significance

Cyclooxygenase-2 (COX-2), plays a significant role in the inflammatory response within the body. It is an enzyme involved in the synthesis of prostaglandins, which are lipid compounds that mediate inflammation, pain, and fever. COX-2 is not constitutively expressed in most tissues under normal conditions, but its expression is induced in response to inflammatory stimuli such as cytokines, growth factors, and other pro-inflammatory mediators. This selective expression makes COX-2 a target for anti-inflammatory drugs.

Inflammation is a natural defence mechanism of the body in response to injury, infection, or irritation. However, excessive or prolonged inflammation can lead to tissue damage and contribute to various chronic diseases such as arthritis, cardiovascular disease, and cancer. COX-2 is upregulated at sites of inflammation, where it catalyzes the conversion of arachidonic acid into prostaglandins, particularly prostaglandin E2 (PGE2), which promotes inflammation by causing vasodilation, increasing vascular permeability, and sensitizing pain receptors (Kulesza et al., 2023).

Nonsteroidal anti-inflammatory drugs (NSAIDs) and selective COX-2 inhibitors are widely used as anti-inflammatory agents. Traditional NSAIDs, such as aspirin and ibuprofen, inhibit both COX-1 and COX-2 enzymes, leading to potential side effects such as gastrointestinal ulcers and bleeding due to inhibition of COX-1, which is constitutively expressed in the stomach and plays a role in maintaining gastrointestinal mucosal integrity. Selective COX-2 inhibitors, such as celecoxib, target only the COX-2 enzyme, thus reducing the risk of gastrointestinal adverse effects (Bokhtia et al., 2023).

By targeting COX-2, anti-inflammatory drugs can inhibit the production of prostaglandins and attenuate the inflammatory response, providing relief from pain, swelling, and redness associated with inflammation. Additionally, inhibition of COX-

2 has been implicated in the prevention and treatment of various inflammatory conditions, including rheumatoid arthritis, osteoarthritis, and inflammatory bowel disease (Zarghi and Arfaei, 2011).

COX-2 expression levels can serve as biomarkers for assessing the severity of inflammation and monitoring the efficacy of anti-inflammatory therapies. Techniques such as immunohistochemistry, western blotting, and quantitative polymerase chain reaction (qPCR) are used to measure COX-2 expression in tissues and cells, aiding in the diagnosis and management of inflammatory diseases.

Precisely, COX-2 plays a crucial role in the inflammatory process, and its selective inhibition is a key strategy for anti-inflammatory therapy and disease management. Detection and modulation of COX-2 activity are important for understanding and treating inflammatory disorders effectively (Szweda et al., 2020).

3.1.2. TNF, IL-6 and iNOS an inflammatory marker

Tumor necrosis factor (TNF), interleukin-6 (IL-6), and inducible nitric oxide synthase (iNOS) are indeed well-known inflammatory markers commonly studied in the context of various inflammatory conditions and diseases.

TNF is a cytokine involved in systemic inflammation and is produced chiefly by activated macrophages, although it can be synthesized by many other cell types such as lymphoid cells, mast cells, endothelial cells, and fibroblasts. It plays a crucial role in regulating immune cells and initiating the inflammatory response. Elevated levels of TNF are associated with various inflammatory diseases such as rheumatoid arthritis, inflammatory bowel disease, psoriasis, and sepsis (Jang et al., 2021).

IL-6 is another cytokine involved in the regulation of immune response and inflammation. It is produced by various cells including macrophages, T cells, B cells, fibroblasts, endothelial cells, and keratinocytes. IL-6 has diverse functions including promoting B cell proliferation, differentiation of T cells, and stimulation of acute phase protein production in the liver. Elevated levels of IL-6 are found in inflammatory conditions such as rheumatoid arthritis, systemic lupus erythematosus, and certain cancers (Aliyu et al., 2022; Tanaka et al., 2014).

iNOS is an enzyme responsible for producing nitric oxide (NO) in response to various stimuli including inflammatory cytokines. Nitric oxide is a signalling molecule involved in a wide range of physiological processes, including vasodilation, neurotransmission, and host defence against pathogens. In the context of inflammation, increased iNOS expression leads to the production of high levels of NO, which can exert cytotoxic effects on pathogens but also contribute to tissue damage and inflammation. iNOS expression is often upregulated in inflammatory conditions such as sepsis, inflammatory bowel disease, and asthma (Forstermann and Sessa, 2012).

Medicinal plants contain an extensive diversity of secondary metabolites that have a wide range of biological activities (A. Hussein and A. El-Anssary, 2019). In this study, we chose two medicinal plants with antiulcerative, antiinflammatory and antimicrobial properties, i.e., *Lannea coromandelica* and *Trevesia palmata* for virtual screening to identify a potential compound that can inhibit the target protein of ulcerative colitis. Molecular docking was performed to confirm the binding posture.

3.2. REVIEW OF LITERATURE

A computational study of the phytochemical constituents from *Lannea coromandelica* and *Trevesia palmata* leaves likely involves several key steps and methodologies. The first step involves gathering data on known phytochemical constituents present in *L. coromandelica* and *T. palmata* leaves from existing literature, databases, or experimental studies. Using computational tools and databases, the chemical structures of these phytochemical constituents would be retrieved and compiled.

Molecular docking involves predicting the binding modes and affinity of small molecules (phytochemical constituents) with target proteins or receptors associated with specific biological activities. In this case, docking studies could be performed to predict the interactions between the identified phytochemicals and proteins relevant to the treatment of diseases like ulcerative colitis (Agu et al., 2023).

Pharmacophore modelling involves identifying the essential structural and chemical features necessary for a molecule to interact with a biological target. This approach

could be used to elucidate the pharmacophoric features of the phytochemical constituents and their relevance to therapeutic activity (Giordano et al., 2022).

Ligand-based virtual screening involves comparing the structural and physicochemical properties of known active compounds with those of the phytochemical constituents to identify potential bioactive molecules. This approach could help prioritize phytochemicals for further experimental validation (Vazquez et al., 2020).

Absorption, distribution, metabolism, excretion, and toxicity (ADME/Tox) prediction involves assessing the pharmacokinetic and toxicological properties of molecules. Computational tools can be used to predict these properties for the identified phytochemical constituents, aiding in the selection of candidates with favourable pharmacological profiles. Finally, the results obtained from computational studies were analyzed and interpreted to identify promising phytochemical constituents with potential therapeutic applications, such as in the treatment of ulcerative colitis (Xiong et al., 2021).

3.2.1. COX-2, TNF-α, IL-6 and iNOS in ulcerative colitis

Ulcerative colitis (UC) is a type of inflammatory bowel disease (IBD) characterized by chronic inflammation of the colon and rectum (Gajendran et al., 2019). Several inflammatory markers, including cyclooxygenase-2 (COX-2), tumor necrosis factor-alpha (TNF- α), interleukin-6 (IL-6), and inducible nitric oxide synthase (iNOS), are implicated in the pathogenesis and progression of UC (Gandhi et al., 2023).

Cyclooxygenase-2 (COX-2) is an enzyme involved in the production of prostaglandins, which are lipid mediators with various physiological functions, including inflammation and regulation of gastrointestinal mucosal integrity. COX-2 expression is upregulated during inflammation, including in UC, where it contributes to the production of prostaglandins that exacerbate inflammation and contribute to tissue damage. Inhibiting COX-2 activity is a therapeutic strategy for managing UC symptoms and reducing inflammation (Spisni et al., 2015).

Tumor necrosis factor (TNF) is a pro-inflammatory cytokine produced by various cells, including macrophages and T cells. Elevated levels of TNF are found in the inflamed mucosa of individuals with UC. TNF plays a central role in the pathogenesis of UC by promoting inflammation, disrupting epithelial barrier function, and recruiting inflammatory cells to the site of inflammation. Therapies targeting TNF, such as anti-TNF antibodies, have been effective in inducing and maintaining remission in UC patients (Peyrin-Biroulet et al., 2021).

Interleukin-6 (IL-6) is a pleiotropic cytokine involved in the regulation of immune responses, acute-phase reactions, and inflammation. Elevated levels of IL-6 are observed in the serum and colonic mucosa of UC patients during active disease. L-6 contributes to the perpetuation of inflammation in UC by stimulating the production of acute-phase proteins, promoting T cell activation, and inducing the differentiation of pro-inflammatory Th17 cells. Targeting IL-6 signaling pathways represents a potential therapeutic approach for UC management (Peyrin-Biroulet et al., 2021; Cao et al., 2021).

Inducible nitric oxide synthase (iNOS) is an enzyme responsible for the production of nitric oxide (NO) in response to inflammatory stimuli. Increased iNOS expression and NO production are observed in the inflamed colonic mucosa of UC patients. NO has various effects in the gastrointestinal tract, including modulation of intestinal motility, regulation of mucosal blood flow, and modulation of immune responses. However, excessive NO production by iNOS can contribute to mucosal injury and inflammation in UC. Modulating iNOS activity may offer therapeutic benefits in UC by reducing inflammation and promoting mucosal healing (Soufli et al., 2016).

In summary, COX-2, TNF, IL-6, and iNOS are key inflammatory mediators implicated in the pathogenesis of ulcerative colitis. Targeting these molecules or their downstream pathways represents promising therapeutic strategies for managing UC and achieving remission.

Overall, a computational study of the phytochemical constituents from *L. coromandelica* and *T. palmata* leaves would leverage various computational approaches to elucidate their potential biological activities and mechanisms of action,

providing valuable insights for further experimental validation and drug discovery efforts.

3.3. MATERIALS AND METHODS

A total of 31 phytocompounds of *Lannea coromandelica* and 26 phytocompounds of *Trevesia palmata* leaves were identified and collected from various research papers from PubMed (https://pubmed.ncbi.nlm.nih.gov). PubMed is a free search engine that mainly accesses the MEDLINE database, which contains references and abstracts on biomedical and life sciences subjects. The database is managed by the National Institutes of Health's United States National Library of Medicine as part of the Entrez information retrieval system. PubChem is a public chemical information resource created and managed by the National Centre for Biotechnology Information (NCBI) at the National Library of Medicine (NLM), which is part of the National Institutes of Health (NIH) in the United States. It compiles descriptions of chemical compounds and their biological activity from more than 500 data sources and makes this knowledge available to the public for free. The SMILES format, as well as the PubChem CID, Class of Compound, Chemical Formula, and Molecular Weight of a total of 31 phytocompounds of *L. coromandelica* and 26 phytocompounds of *T. palmata*, were collected and retrieved from PubChem (National Institutes of Health's open chemistry database).

3.3.1. Toxicity Prediction by QSAR TEST Toolbox

All the 27 phytocompounds identified from plant leaves of Lannea coromandelica against the giant, free-living ciliate, the fathead minnow, and rat using Toxicity Estimation Software Tool (TEST), (https://epa.figshare.com/articles/software/Toxicity_Estimation_Software Tool TEST /21379365) was developed to allow users to easily estimate the toxicity of chemicals from the structure of a compound using Quantitative Structure Activity Relationships (QSARs) methodologies. Mathematical models called Toxicity Estimation Software Tool (TEST) QSARs are used to predict amounts of toxicity based on molecular descriptors, or the physical properties of chemical structures. Here, the research was conducted using NOAEL of repeated dosage toxicity and reproductive toxicity. For

this investigation, the consensus technique was used since it incorporates all of the previously mentioned models for toxicity prediction.

3.3.2. Prediction of activity spectra for substances (PASS)

PASS is an online software that may be used to assess the potential binding affinity of organic drug-like molecules based on their structural properties. All phytochemicals underwent PASS analysis (Filimonov et al., 2014). It uses multilevel neighbourhood of atom (MNA) descriptors and a Bayesian algorithm to predict the activity of organic compounds using a structure-activity relationship (SAR) model for a large number of pharmaceutical drugs.

3.3.3. Protein retrieval and preparation

The three-dimensional structures of COX-2 (PDB ID: 3NTG, Fig.), TNF-α (PDB ID: 2AZ5, Fig.), IL-6 (PDB ID: 1ALU, Fig.), and iNOS (PDB ID: 1M8D, Fig. 1) were retrieved from the Research Collaboratory for Structural Bioinformatics (RCSB) Protein Data Bank (PDB) at a resolution of 1.62 Å. UCSF Chimaera 1.15 (https:// www. cgl. ucsf. edu/ chime ra/) was used to construct the crystal structures of COX-2, TNF-α, IL-6, and iNOS receptors prior to docking (Pettersen et al. 2004). The co-crystallized ligand, water molecules, and metal ions were all removed from the target proteins. Polar hydrogen atoms and partial charges have been introduced into the formations. The shortened side chains were restored and Gasteiger charges were added to the target proteins using the in-built dock prep programme (Opo et al. 2021).

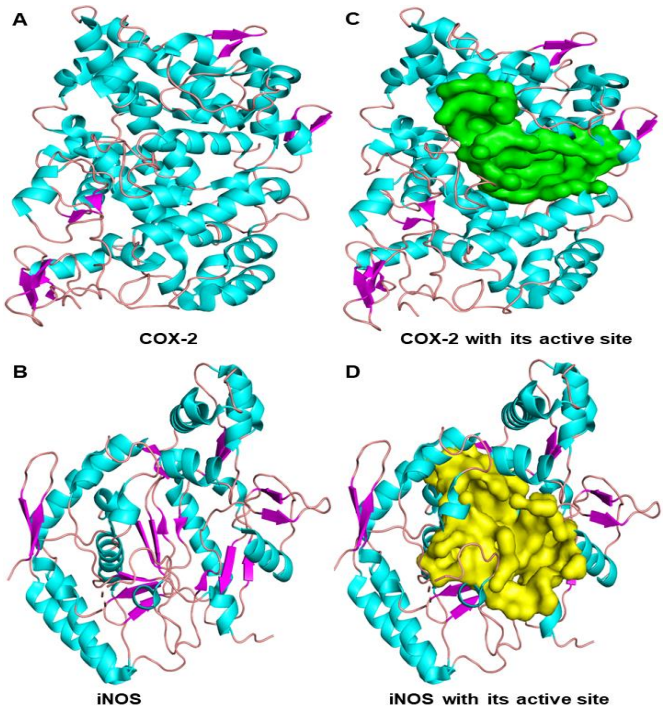

Figure 13: Preparation of target receptors, as well as identification and characterization of active sites in COX-2 and iNOS receptors, for molecular docking studies. The COX-2 (A) and iNOS (B) target receptors have been prepared (removal of co-crystallized ligand, water molecules, and metal ions from the target receptor; addition of polar hydrogen atoms and partial charges to the target receptor; and repairing of the truncated side chains and adding Gasteiger charges to the target receptor using the in-built Dock Prep tool) for docking using UCSF Chimaera software. Figure C) and D) shows active site prediction in the COX-2 (green colour) and iNOS (yellow colour) receptors by fpocket web server.

3.3.4. Physicochemical properties of the receptors

Expasy-ProtParam was used to assess the physicochemical parameters of COX-2, TNF-α, IL-6, and iNOS receptors (http://web. expasy. org/protparam/). The amino acid sequence of COX-2, TNF-α, IL-6, and iNOS receptors was downloaded in FASTA format from RCSB PDB and used as input for the webserver to compute several parameters such as theoretical PI, amino acid composition, atomic composition, extinction coefficient, estimated half-life, instability index, aliphatic index, and grand average of hydropathicity (GRAVY) (Gasteiger et al., 2005).

3.3.5. Protein active site prediction

The discovery and characterisation of pockets in a protein structure is a critical step in a molecular docking investigation. The fpocket web server (https://biose rv. rpbs. univ- paris- dider ot. fr/ services/ fpock et/) was used to identify the active site or pocket of the prepared COX-2, TNF-α, IL-6, and iNOS receptors. The fpocket tool uses Voronoi tessellation and α-spheres to identify protein active pockets. The fpocket successfully detected 94% and 92% of known protein binding sites inside the top three pockets (Schmidtke et al., 2010). The receptor was assigned to the best-ranked pocket (Pocket 0) from the fpocket results. The results were visualised using Schrödinger's Pymol 2.4.0 (http:// www. pymol. org/ pymol).

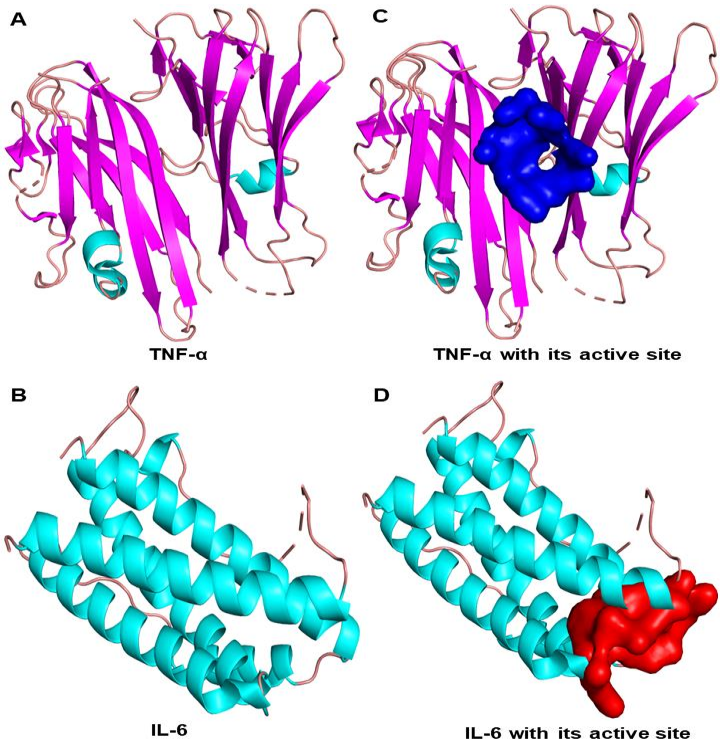

Figure 14: Preparation of the target receptors for TNF-α and IL-6 identified and characterised with their active sites. To dock with UCSF Chimaera software, the TNF-α (A) and IL-6 (B) target receptors were prepared by removing co-crystallized ligands, water molecules, and metal ions, adding polar hydrogen atoms and partial charges, and repairing truncated side chains and Gasteiger charges. Figures C and D show active site prediction for TNF-α (blue) and IL-6 (red colour) receptors by fpocket web server.

3.3.6. Molecular docking

The molecular docking was done in PyRx - Python prescription 0.8 using the AutoDock Vina plug-in programme (Trott and Olson 2010). GA run (number of genetic algorithms, 250) and eval (number of energy evaluations, 25000000) were altered, while other choices docking parameters remained unchanged. The AutoGrid programme was used to create the grid box for grid mapping. The "Vina wizard control" option loaded the target COX-2, TNF-α, IL-6, and iNOS receptors, as well as ligand molecules. The active pocket residue of the receptor molecule was named, shown, and classified using the PyRx virtual screening software's "molecules" function to perform point-specific molecular docking. Following categorization, a grid box was mapped on the receptor. The centre point's measurements for COX-2 are x (45.3951), y (22.7384), and z (30.0723), while the grid area's dimensions are x (30.0191), y (30.0609), and z (30.0723). The centre point's measurements for iNOS are x (124.213), y (112.677) and z (22.3046), while the grid area's dimensions are x (30.0328), y (30.0078) and z (30.0557. The centre point's measurements for IL-6 are x (11.2608), y (33.7931), and z (5.9736), while the grid area's dimensions are x (30.0298), y (30.0613), and z (30.0479). The centre point's measurements for TNF-α are x (12.4509), y (114.6905), and z (95.7405), while the grid area's dimensions are x (30.0609), y (30.0335), and z (30.5265). Following the grid mapping generation, the AutoDock Vina programme was created and executed. The AutoDock Vina Lamarckian algorithm (LGA) uses a tight clustering technique with an RMSD tolerance of 1.0 Å to generate 200 conformers for each ligand (Fuhrmann et al., 2010). The generated clusters were accurately sorted by the lowest binding energy (the most stable conformer) and arranged hierarchically. The docking results were examined on the "analyse results" page and saved in CSV format (Comma Separated Values). The interaction with the lowest binding affinity (kcal/mol) was chosen as the optimal conformation for each ligand. The top four protein-ligand interactions were selected for further investigation. The chosen interactions were visualised using BIOVIA Discovery Studio Visualizer v21.1.0.20298 (https:// disco ver.3ds. com/ disco). very-studio-visualizer-download (Biovia, 2015) and PyMol software (Schrödinger and DeLano, 2020).

3.3.7. Evaluation of various Pharmacokinetics (PK) and pharmacodynamics properties

Lannea coromandelica, and *Trevesia palmata* ligand compounds were retrieved from the PubChem database (https://pubchem.ncbi.nlm.nih.gov/) using the standard SMILES format. SwissADME (http://www.swissadme.ch) and Molinspiration Cheminformatics (https://www.molinspiration.com) tools were used to predict the ADMET features, lipophilicity, water solubility, drug likeness bioactivity score (DLBS), and pharmacokinetics-bioactivity, as well as medicinal chemistry, drug likeness bioavailability score and pharmacokinetics. SWISSADME and Molinspiration Cheminformatics tools evaluate the ligand molecules using the Lipinski rule of 5 (LOR5), which states that an active oral medication must meet the following criteria: ADMET default range—Molecular weight (MW): 100-600 hydrogen atoms; number of hydrogen bond acceptors (nHA): 0–12; number of hydrogen bond donors (nHD): 0-7; number of rotatable bonds (nRot): 0-11 (amide C-N bonds are excluded from being taken into account in certain contexts because of their high rotational energy barrier); number of rings (nRing): 0-6; number of rigid bonds as opposed to rotatable bonds (nRig): 0-30; flexibility: Flexibility = nRot / nRig; Topological polar surface area (TPSA) (Å2): 0-140, based on Veber rule; logarithm of aqueous solubility value (LogS): -4 to 0.5 log mol/L; logarithm of the n-octanol/water distribution coefficient (LogP): 0 to 3 log mol/L; logarithm of the n-octanol/water distribution coefficients at pH=7.4 (LogD7.4): 1 to 3 log mol/L (Daina et al., 2014; Ertl et al., 2000; Lipinski, 2004; Lipinski et al., 2001; Veber et al., 2002). The drug-likeness bioactivity score (DLBS) of the ligand molecule was predicted using the criteria of GPCR ligand, ion channel modulator, nuclear receptor ligand, kinase inhibitor, protease inhibitor, enzyme inhibitor, and cytochrome P450 inhibitors and scored as follows: The Molinspiration cheminformatics server (Daina & Zoete, 2016) classified medicines as active (score >0), moderately active (5.0 to 0.0), or inactive (scoring <5.0). The SwissADME programme was used to calculate pharmacokinetic bioactivity parameters such as gastrointestinal (GI) absorption, blood brain barrier (BBB) permeability, and P-glycoprotein substrate (P-gp). The SwissADME method was used to forecast skin permeability (Log Kp), and a lower

Log Kp value indicates less penetration to the skin, making it an attractive medication candidate (Potts & Guy, 1992). The zero alert of PAINS and the Brenk filter (which aids in categorising the ligand molecule) indicate whether or not the ligand molecule responds to the biological assays (PAINS), as well as ensuring the accepted toxic level, chemical reactivity, and metabolically unstable or enduring properties that are responsible for poor pharmacokinetics (Brenk) (Baell & Holloway, 2010; Brenk et al., 2008). The synthetic accessibility score is a metric for assessing the ease of synthesis of drug-like compounds, with a value of 1 indicating extremely easy synthesis and a score of 10 indicating very difficult synthesis (Ertl & Schuffenhauer, 2009). A bioavailability score of greater than 0.10 indicates oral bioavailability according to Lipinski's principles and is deemed a suitably absorbable molecule orally (Martin, 2005).

3.4. RESULTS

In LCLE 31 phytocompounds with a predominance of alkaloids, flavonoids, phenolic, terpenoids and fatty acids were identified using GC-MS and LC-MS/MS analysis. Also, in TPLE 26 phytocompounds were identified with numerous flavonoids, triterpenoid saponins, carotenoid, fatty acid, alkaloid, biphenols and coumarin by GC-MS and LC-MS/MS investigation. Each of these compounds exhibit distinct biological activities, making them potentially useful for various applications in pharmaceuticals, cosmetics, and other industries.

QSAR Tool Software allows testing of Repeated dose toxicity and Reproductive toxicity in a cost-efficient way. ADMETLab 2.0 provides findings in a variety of forms, including a downloadable PDF version. PASS Online gives access to predict the potential biological properties of phytocompounds which are evaluated on the Way2Drug web server. The parameters listed below were predicted for 31 compounds identified from *Lannea coromandelica* namely: Paclitaxel, Quercetin-3-O-rutinoside, Kaempferol 7-neohesperidoside, Kaempferol-3-O-rutinoside, Kaempferol, Chlorogenic acid, zeta-Carotene, Hesperetin, [Gallocatechin-(4alpha->8)]2-catechin, Caryophyllene, Luteolin-6-C-glucoside, 7-O-Methylquercetin-3-O-galactoside-6"-rhamnoside, Diatoxanthin, Zeaxanthin, Beta-Carotene, Lutein 9-

Eicosene, (E)-, Phytol, Nantenine, gamma-Carotene, 4-tert-Butylcalix[4]arene, Diethyl Phthalate, cis-9-Hexadecenal, Phenol, 2,4-bis(1,1-dimethylethyl)-, Phenol, 3,5-bis(1,1-dimethylethyl)-, Phenol, 2,4-bis(1,1-dimethylethyl)-5-methyl-, Pentadecanoic acid, Bis(2-ethylhexyl) phthalate, Oxirane, tetradecyl-, Linoleic Acid, and 1-Hexadecanol. The parameters listed below were predicted for 26 compounds identified from *Trevesia palmata* namely: Quercetin 3-O-[2"-O-(6"'-O-p-coumaroyl)-b-D-glucopyranosyl]-a-L-rhamnopyranoside, Kaempferol-3-O-rutinoside, Icariin, Oxyacanthine, Kaempferol 3-O-sophoroside, Asiaticoside, alpha.-Amyrin, Apigenin-6-C-glucoside-7-O-glucoside, gamma.-Tocopherol, Kaempferol 4'-methyl ether 3-(4Rha-rhamnosylrutinoside), Honokiol, Beta-Sitosterol, alpha-Hederin, Lutein, zeta-Carotene, Hederacoside C, Zeaxanthin, Bacoside A3, Neophytadiene, dl-.alpha.-Tocopherol, Phytol, Linolenic acid, Linoleic Acid, Diethyl Phthalate, Isofraxidin and Pentadecanoic acid.

3.4.1. Metabolism, Repeated dose toxicity and Reproductive toxicity

Table 5 outlines the potential metabolic interactions of compounds derived from *Lannea coromandelica* and Table 6 outlines the metabolic interactions of compounds from *Trevesia palmata* with various cytochrome P450 (CYP) enzymes, including CYP1A2, CYP2C19, CYP2C9, CYP2D6, and CYP3A4. These interactions can have significant implications for the toxicity and pharmacokinetics of these compounds. Repeated dose toxicity in terms of the no-observed-adverse-effect level (NOAEL) in milligrams per kilogram of body weight (mg/kg) and reproductive toxicity of identified compounds were also shown in the tables.

In *L. coromandelica,* the CYP 1A2 inhibitor of 11 compounds is 0.0-0.1, 9 compounds range from 0.1-0.3, 5 compounds range from 0.3-0.7 and 6 compounds range from 0.7-1.0. CYP 1A2 substrate of 9 compounds is 0.0, 10 compounds range from 0.1-0.3, 5 compounds range from 0.3-0.7, and 7 compounds range from 0.7-1.0. CYP2C19 inhibitor of 15 compounds is 0.0, 4 compounds range from 0.1-0.3, 7 compounds range from 0.3-0.7, and 5 compounds range from 0.7-1.0. CYP2C19 substrate of 18 compounds is 0.0, 3 compounds range from 0.1-0.3, 1 compound range from 0.3-0.7 and 9 compounds range from 0.7-1.0. CYP2C9 inhibitor of 13

compounds is 0.0, 7 compounds range from 0.1-0.3, 8 compounds range from 0.3-0.7, 3 compounds range from 0.7-1.0. CYP2C9 substrate of 2 compounds range is 0.0, 4 compounds range from 0.1-0.3, 9 compounds range from 0.3-0.7 and 16 compounds range from 0.7-1.0. CYP2D6 inhibitor of 16 compounds is 0.0, 4 compounds range from 0.1-0.3, 5 compounds range from 0.3-0.7 and 6 compounds range from 0.7-1.0. CYP2D6 substrate of 8 compounds is 0.0, 11 compounds range from 0.1-0.3, 2 compounds range from 0.3-0.7, and 10 compounds range from 0.7-1.0. CYP3A4 inhibitor of 16 compounds is 0.0, 6 compounds range from 0.1-0.3, 6 compounds range from 0.3-0.7, and 3 compound range from 0.7-1.0. CYP3A4 substrate of 14 compounds is 0.0, 6 compounds range from 0.1-0.3, 5 compounds range from 0.3-0.7, and 6 compounds range from 0.7-1.0 (Table 5). The data suggests that compounds from *L. coromandelica* can interact with several CYP enzymes, either inhibiting or being metabolized (acting as substrates) by these enzymes. This metabolic activity can influence the breakdown and clearance of these compounds from the body, affecting their overall toxicity and pharmacological effects. Repeated dose toxicity refers to the adverse effects that occur after repeated exposure to a substance over a prolonged period. Toxicity levels are categorized based on the no-observed-adverse-effect level (NOAEL) in milligrams per kilogram of body weight (mg/kg). Compounds are labelled as either "Toxic" or "Non-toxic" based on their NOAEL values. A higher NOAEL generally indicates lower toxicity, while a lower NOAEL suggests higher toxicity upon repeated exposure. In the context of compounds from *L. coromandelica*, the interactions with various CYP enzymes may influence their accumulation in the body upon repeated dosing. Depending on whether these compounds are metabolized or inhibit the activity of specific CYP enzymes, they may exhibit different patterns of toxicity over time. For instance, if a compound is a substrate for a CYP enzyme responsible for its metabolism, inhibition of that enzyme could lead to increased systemic exposure and potential toxicity upon repeated dosing (Table 5). Reproductive toxicity refers to adverse effects on the reproductive system, including fertility, foetal development, and reproductive organs. The potential effects of compounds from *L. coromandelica* on reproductive toxicity could be influenced by their metabolic interactions with CYP enzymes. Metabolism of these compounds can affect their distribution to

reproductive organs, placental transfer to the fetus, and clearance from the body, all of which can impact reproductive health and fetal development. Out of 31 compounds in *L. coromandelica* 14 compounds are found to be toxic and 17 compounds are found to be non-toxic to the reproductive organs (Table 5).

In table 6, *T. palmata* implications of the data in terms of metabolic activity, repeated dose toxicity, and reproductive toxicity were shown. The CYP 1A2 inhibitor of 18 compounds is 0.0-0.1, 2 compounds range from 0.1-0.3, 4 compounds range from 0.3-0.7 and 2 compounds range from 0.7-1.0. CYP 1A2 substrate of 7 compounds is 0.0, 10 compounds range from 0.1-0.3, 6 compounds range from 0.3-0.7, and 3 compounds range from 0.7-1.0. CYP2C19 inhibitor of 19 compounds is 0.0, 2 compounds range from 0.1-0.3, 4 compounds range from 0.3-0.7, and 1 compound range from 0.7-1.0. CYP2C19 substrate of 10 compounds is 0.0, 3 compounds range from 0.1-0.3, 3 compound range from 0.3-0.7 and 10 compounds range from 0.7-1.0. CYP2C9 inhibitor of 18 compounds is 0.0, 4 compounds range from 0.1-0.3, 4 compounds range from 0.3-0.7 and no compounds were present at high range from 0.7-1.0. CYP2C9 substrate of 4 compounds range is 0.0, 2 compounds range from 0.1-0.3, 9 compounds range from 0.3-0.7 and 11 compounds range from 0.7-1.0. CYP2D6 inhibitor of 19 compounds is 0.0, 3 compounds range from 0.1-0.3, 3 compounds range from 0.3-0.7 and 1 compounds range from 0.7-1.0. CYP2D6 substrate of 6 compounds is 0.0, 11 compounds range from 0.1-0.3, 3 compounds range from 0.3-0.7, and 6 compounds range from 0.7-1.0. CYP3A4 inhibitor of 14 compounds is 0.0, 9 compounds range from 0.1-0.3, 3 compounds range from 0.3-0.7, and no compounds were present ranging from 0.7-1.0. CYP3A4 substrate of 13 compounds is 0.0, 6 compounds range from 0.1-0.3, 1 compound range from 0.3-0.7, and 6 compounds range from 0.7-1.0 (Table 6). The data indicates whether each compound acts as an inhibitor or substrate for each CYP enzyme. The compounds with lower values (0.0-0.3) are less likely to inhibit the enzyme's activity, while those with higher values (0.7-1.0) are more potent inhibitors. Substrates are

Table 5: Prediction of Metabolic activity, Repeated dose toxicity and Reproductive toxicity of compounds identified from *Lannea coromandelica* using VEGA HUB and OECD QSAR platforms.

Compounds	Metabolism										Repeated dose toxicity	Reproductive toxicity
	CYP 1A2 inhibitor	CYP 1A2 substrate	CYP2 C19 inhibitor	CYP2 C19 substrate	CYP2 C9 inhibitor	CYP2 C9 substrate	CYP2 D6 inhibitor	CYP2 D6 substrate	CYP3 A4 inhibitor	CYP3 A4 substrate	NOAEL (mg/kg)	
Caryophyllene	0.107 --	0.309 -	0.11 --	0.933 +++	0.215 --	0.452 -	0.013 ---	0.89 ++	0.047 ---	0.361 -	25.1	Toxic
Phenol, 3,5-bis(1,1-dimethylethyl)-	0.944 +++	0.886 ++	0.86 ++	0.709 ++	0.701 ++	0.859 ++	0.909 +++	0.663 +	0.567 +	0.527 +	1.4586	Non-toxic
Diethyl Phthalate	0.980 +++	0.53 +	0.911 +++	0.095 ---	0.764 ++	0.21 --	0.286 --	0.181 --	0.111 --	0.159 --	37.32	Toxic
Phenol, 2,4-bis(1,1-dimethylethyl)-5-methyl-	0.862 ++	0.945 +++	0.613 +	0.835 +	0.499 -	0.858 ++	0.874 ++	0.9 +++	0.519 +	0.664 +	1.887	Non-toxic
Pentadecanoic acid	0.298 --	0.199 --	0.146 --	0.154 --	0.213 --	0.988 +++	0.007 ---	0.06 ---	0.02 ---	0.021 ---	201.37	Non-toxic
Oxirane, tetradecyl-	0.340 -	0.221 --	0.348 -	0.077 ---	0.115 --	0.793 ++	0.094 ---	0.084 ---	0.187 --	0.064 ---	1.272	Non-toxic
cis-9-Hexadecenal	0.612 +	0.198 --	0.452 -	0.066 ---	0.304 -	0.936 +++	0.3 --	0.237 --	0.39 -	0.05 ---	2.0095	Non-toxic
Phytol	0.401 -	0.18 --	0.314 -	0.11 --	0.464 -	0.951 +++	0.053 ---	0.038 ---	0.164 --	0.119 --	108.75	Non-toxic
9-Eicosene, (E)-	0.209 --	0.17 --	0.316 -	0.06 ---	0.102 --	0.959 +++	0.269 --	0.072 ---	0.235 --	0.032 ---	1.1902	Non-toxic

1-Hexadecanol	0.416 -	0.195 --	0.365 -	0.056 ---	0.132 --	0.939 +++	0.025 ---	0.049 ---	0.166 --	0.043 ---	169.79	Non-toxic
Bis(2-ethylhexyl) phthalate	0.208 --	0.305 -	0.749 ++	0.061 ---	0.277 --	0.161 --	0.788 ++	0.12 --	0.733 ++	0.106 --	1.4665	Toxic
Phenol, 2,4-bis(1,1-dimethylethyl)-	0.907 +++	0.935 +++	0.77 ++	0.779 ++	0.633 +	0.872 ++	0.885 ++	0.864 ++	0.429 -	0.669 +	1.5578	Non-toxic
4-tert-Butylcalix[4]arene	0.009 ---	0.907 +++	0.43 -	0.123 --	0.06 ---	0.804 ++	0.009 ---	0.849 ++	0.074 ---	0.933 +++	2.0011	Non-toxic
Hesperetin	0.912 +++	0.857 ++	0.722 +++	0.063 ---	0.792 ++	0.923 +++	0.605 +	0.678 +	0.815 ++	0.201 --	84.73	Toxic
Nantenine	0.649 +	0.962 +++	0.278 --	0.939 +++	0.017 ---	0.801 ++	0.667 +	0.936 +++	0.681 ++	0.922 +++	4.08	Toxic
7-O-Methylquercetin-3-O-galactoside-6"-rhamnoside	0.002 ---	0.03 ---	0.007 ---	0.06 ---	0.0 ---	0.349 -	0.002 ---	0.163 --	0.004 ---	0.002 ---	6.84	Non-toxic
Kaempferol	0.972 +++	0.11 --	0.181 --	0.046 ---	0.653 +	0.867 + +	0.722 + +	0.283 --	0.697 +	0.08 ---	110.97	Toxic
Quercetin-3-O-rutinoside	0.013 ---	0.026 ---	0.011 ---	0.05 ---	0.002 ---	0.246 --	0.007 ---	0.155 --	0.013 ---	0.003 ---	3683.98	Toxic
Beta-Carotene	0.107 --	0.788 ++	0.054 ---	0.989 +++	0.012 ---	0.643 +	0.842 ++	0.986 +++	0.08 ---	0.924 +++	33.85	Non-toxic
gamma-Carotene	0.169 --	0.169 --	0.056 ---	0.989 +++	0.016 ---	0.687 +	0.571 +	0.983 +++	0.039 ---	0.92 +++	47.42	Non-toxic
Kaempferol 7-neohesperidoside	0.013 ---	0.023 ---	0.009 ---	0.056 ---	0.001 ---	0.192 ---	0.007 ---	0.15 --	0.012 ---	0.007 ---	1628.96	Toxic
Kaempferol-3-O-rutinoside	0.012 ---	0.028 ---	0.013 ---	0.055 ---	0.001 ---	0.598 +	0.008 ---	0.159 --	0.013 ---	0.005 ---	1628.96	Toxic
zeta-Carotene	0.261 --	0.192 --	0.088 ---	0.975 +++	0.052 ---	0.954 +++	0.153 --	0.943 +++	0.134 --	0.642 +	62.42	Non-toxic

[Gallocatechin-(4alpha->8)]2-catechin	0.001 ---	0.071 ---	0.005 ---	0.03 ---	0.126 --	0.375 -	0.0 ---	0.14 --	0.009 ---	0.494 --	8.80	Non-toxic
Diatoxanthin	0.146 --	0.096 ---	0.047 ---	0.064 ---	0.409 -	0.843 ++	0.003 ---	0.073 ---	0.009 ---	0.207 --	17.21	Toxic
Zeaxanthin	0.040 ---	0.62 +	0.045 ---	0.98 +++	0.008 ---	0.375 -	0.615 +	0.976 +++	0.007 ---	0.929 +++	161.33	Toxic
Lutein	0.026 ---	0.531 +	0.06 ---	0.976 +++	0.024 ---	0.576 +	0.377 -	0.969 +++	0.031 ---	0.921 +++	1138.6	Non-toxic
Paclitaxel	0.003 ---	0.039 ---	0.057 ---	0.086 ---	0.398 -	0.1 ---	0.006 ---	0.091 ---	0.605 +	0.638 +	3.04	Toxic
Chlorogenic acid	0.036 ---	0.042 ---	0.023 ---	0.053 ---	0.016 ---	0.511 +	0.003 ---	0.156 --	0.03 ---	0.022 ---	1138.6	Non-toxic
Luteolin-6-C-glucoside	0.041 ---	0.041 ---	0.013 ---	0.052 ---	0.012 ---	0.282 --	0.008 ---	0.175 --	0.025 ---	0.012 ---	1855.22	Toxic
Linoleic Acid	0.235 --	0.171 --	0.086 ---	0.066 ---	0.43 -	0.988 +++	0.006 ---	0.019 ---	0.085 ---	0.019 ---	235.32	Toxic

For the classification endpoints, the prediction probability values are transformed into six symbols: 0-0.1 (- - -), 0.1-0.3 (- -), 0.3-0.5 (-), 0.5-0.7 (+), 0.7- 0.9 (++), and 0.9-1.0 (+++). CYP 1A2 / 2C19 /2C9 / 2D6 / 3A4 substrate: 0.0: non CYP substrate; 0.1–0.3: low CYP substrate; 0.3–0.7: medium CYP substrate; 0.7–1.0: high CYP substrate; **CYP 1A2 / 2C19 / 2C9 / 2D6 / 3A4 inhibitor**: 0.0: non CYP inhibitor; 0.1–0.3: low CYP inhibitor; 0.3–0.7: medium CYP inhibitor; 0.7–1.0: high CYP inhibitor

NOAEL: No observed adverse effect levels. The highest concentration or amount of a chemical at which a population exposed to it experiences no discernible negative effects (VEGA HUB)

Reproductive toxicity: Predicts the possible harm that a specific chemical agent will have on both male and female fertility as well as the development of the children (OECD QSAR)

Table 6: Prediction of Metabolic activity, Repeated dose toxicity and Reproductive toxicity of compounds identified from *Trevesia palmata* using VEGA HUB and OECD QSAR platforms.

Compounds	**Metabolism**										**Repeated dose toxicity**	**Reproductive toxicity**
	CYP 1A2 inhibitor	**CYP 1A2 substrate**	**CYP 2C19 inhibitor**	**CYP2C19 substrate**	**CYP2C9 inhibitor**	**CYP 2C9 substrate**	**CYP 2D6 inhibitor**	**CYP2D6 substrate**	**CYP 3A4 inhibitor**	**CYP 3A4 substrate**	**NOAEL (mg/kg)**	
Icariin	0.012 ---	0.057 ---	0.005 ---	0.153 --	0.001 ---	0.528 +	0.015 ---	0.188 --	0.013 ---	0.014 ---	1336.22	Toxic
Apigenin-6-C-glucoside-7-O-glucoside	0.007 ---	0.014 ---	0.004 ---	0.061 ---	0.0 ---	0.405 -	0.001 ---	0.148 --	0.003 ---	0.003 ---	4229.49	Toxic
Kaempferol 3-O-sophoroside	0.0 ---	0.04 ---	0.001 ---	0.209 ---	0.0 ---	0.062 --	0.003 ---	0.284 --	0.001 ---	0.207 ---	2949.8	Toxic
Kaempferol-3-O-rutinoside	0.012 ---	0.028 ---	0.013 ---	0.055 ---	0.001 ---	0.598 +	0.008 ---	0.159 --	0.013 ---	0.005 ---	651.79	Non-toxic
Kaempferol 4'-methyl ether 3-(4Rha-rhamnosylrutinoside)	0.002 ---	0.035 ---	0.009 ---	0.069 ---	0.0 ---	0.393 -	0.004 ---	0.171 --	0.006 ---	0.004 ---	2581.28	Non-toxic
Mm m m mmQuercetin 3-O-[2"-O-(6"'-O-p-coumaroyl)-b-D-glucopyranosyl]-a-L-rhamnopyranoside	---	---	---	---	---	+	--	--	---	---	2409.6	Toxic
gamma.-Tocopherol	0.1 ---	0.208 --	0.316 -	0.89 ++	0.16 --	0.948 +++	0.219 --	0.277 --	0.331 -	0.138 --	82.58	Toxic

dl-.alpha.-Tocopherol	0.068 ---	0.209 --	0.185 --	0.932 +++	0.123 --	0.959 +++	0.033 ---	0.178 --	0.212 --	0.129 --	108.63	Toxic
Asiaticoside	0.0 ---	0.132 --	0.0 ---	0.221 --	0.0 ---	0.04 ---	0.0 ---	0.072 --	0.015 ---	0.025 ---	17241.29	Non-toxic
Bacoside A3	0.0 ---	0.13 -	0.0 ---	0.501 +	0.0 ---	0.038 ---	0.0 ---	0.081 ---	0.039 ---	0.032 ---	2388.41	Toxic
Hederacoside C	0.0 ---	0.065 ---	0.0 ---	0.063 ---	0.0 ---	0.028 ---	0.0 ---	0.067 ---	0.008 ---	0.002 ---	68566.6	Non-toxic
alpha.-Amyrin	0.026 ---	0.454 -	0.064 ---	0.97 +++	0.097 ---	0.187 --	0.039 ---	0.585 +	0.217 --	0.745 ++	25.56	Toxic
Phytol	0.401 -	0.18 --	0.314 -	0.11 --	0.464 -	0.951 +++	0.053 ---	0.038 ---	0.164 --	0.119 --	108.75	Non-toxic
alpha-Hederin	0.0 ---	0.527 +	0.001 ---	0.815 ++	0.002 ---	0.081 ---	0.0 ---	0.125 --	0.039 ---	0.051 ---	905.93	Non-toxic
Neophytadiene	0.442 -	0.2 --	0.352 -	0.557 +	0.498 -	0.934 +++	0.058 ---	0.072 ---	0.349 -	0.186 --	34.24	Non-toxic
Zeaxanthin	0.04 ---	0.62 +	0.045 ---	0.98 +++	0.008 ---	0.375 -	0.615 +	0.976 +++	0.007 ---	0.929 +++	161.33	Toxic
Lutein	0.026 ---	0.531 +	0.06 ---	0.976 +++	0.024 ---	0.576 +	0.377 -	0.969 +++	0.031 ---	0.921 +++	161.33	Toxic
zeta-Carotene	0.261 --	0.192 --	0.088 ---	0.975 +++	0.052 ---	0.954 +++	0.153 --	0.943 +++	0.134 --	0.642 +	66.42	Toxic
Isopropyl Tetradecanoate	0.42 -	0.191 --	0.449 -	0.067 ---	0.282 --	0.951 +++	0.045 ---	0.012 ---	0.24 --	0.067 ---	107.46	Non-toxic
Linoleic Acid	0.235 --	0.171 --	0.086 ---	0.066 ---	0.43 -	0.988 +++	0.006 ---	0.086 ---	0.085 ---	0.019 ---	235.32	Non-toxic
Linolenic acid	0.11 --	0.156 --	0.03 ---	0.065 ---	0.282 --	0.986 +++	0.006 ---	0.122 --	0.122 --	0.024 ---	1628.96	Toxic
Oxyacanthine	0.052 ---	0.968 +++	0.06 ---	0.973 +++	0.031 ---	0.543 +	0.016 ---	0.957 +++	0.055 ---	0.956 +++	0.4004	Toxic

Honokiol	0.97 +++	0.341 -	0.84 ++	0.064 ---	0.622 +	0.868 ++	0.955 +++	0.945 +++	0.597 +	0.247 --	27.23	Toxic
Beta-Sitosterol	0.044 ---	0.491 -	0.074 ---	0.958 +++	0.096 ---	0.314 -	0.005 ---	0.409 -	0.202 --	0.784 ++	68.24	Toxic
Thalsimine	0.043 ---	0.967 +++	0.093 ---	0.963 +++	0.077 ---	0.816 ++	0.001 ---	0.936 +++	0.146 --	0.958 +++	0.8002	Toxic
Isofraxidin	0.965 +++	0.103 +++	0.103 --	0.332 -	0.062 ---	0.768 ++	0.506 +	0.629 +	0.219 --	0.297 --	80.61	Toxic

For the classification endpoints, the prediction probability values are transformed into six symbols: 0-0.1 (- - -), 0.1-0.3 (- -), 0.3-0.5 (-), 0.5-0.7 (+), 0.7- 0.9 (++), and 0.9-1.0 (+++). CYP 1A2 / 2C19 /2C9 / 2D6 / 3A4 substrate: 0.0: non CYP substrate; 0.1–0.3: low CYP substrate; 0.3–0.7: medium CYP substrate; 0.7–1.0: high CYP substrate; **CYP 1A2 / 2C19 / 2C9 / 2D6 / 3A4 inhibitor**: 0.0: non CYP inhibitor; 0.1–0.3: low CYP inhibitor; 0.3–0.7: medium CYP inhibitor; 0.7–1.0: high CYP inhibitor

NOAEL: No observed adverse effect levels. The highest concentration or amount of a chemical at which a population exposed to it experiences no discernible negative effects (VEGA HUB)

Reproductive toxicity: Predicts the possible harm that a specific chemical agent will have on both male and female fertility as well as the development of the children (OECD QSAR).

compounds that are metabolized by the enzyme, while inhibitors are compounds that inhibit the enzyme's activity, potentially affecting the metabolism of other substances. Toxicity levels vary among the compounds (given in mg/kg in Table 6), with some being classified as toxic based on their NOAEL values, indicating potential adverse effects upon repeated exposure. A lower NOAEL generally indicates higher toxicity, while a higher NOAEL suggests lower toxicity. Compounds with higher inhibition of CYP enzymes may have altered metabolism, potentially leading to toxicity upon repeated exposure, depending on their NOAEL values. compounds classified as toxic may potentially exhibit adverse effects on reproductive health if exposure occurs during critical periods of reproduction or development. Out of 26 compounds, 17 compounds were classified as toxic which may have implications for reproductive health based on their NOAEL values and 9 compounds were classified as non-toxic to the reproductive organs.

Overall, the data suggests that compounds from *L. coromandelica* and *T. palmata* can interact with various CYP enzymes, potentially influencing their metabolism and toxicity. The extent of metabolic activity and toxicity varies among the compounds and depends on their interactions with specific CYP enzymes.

3.4.2. PASS Online Prediction

The PASS (Prediction of Activity Spectra for Substances) Prediction table provides information on the predicted biological activities of various compounds. Each compound is evaluated for its potential activity across multiple categories, with values assigned for both the probability of activity (Pa) and the probability of inactivity (Pi). In the present study, compounds with pa > 0.7 (70%) were identified to exhibit significant biological action. Table 7 shows the probable activity (pa) and inactivity (pi) values of the compounds for activities such as anti-ulcerative, transcription factor NF kappa B inhibitor, antioxidant, free radical scavenger, anti-inflammatory, anti-protozoal, membrane integrity antagonist, and anti-neoplastic in *L. coromandelica* phytocompounds. Whereas, Table 8 illustrates the PASS Prediction for *T. palmata* phytocompounds.

PASS Online Prediction for *L. coromandelica* are summarized in Table 7. A total of 8 Biological activities descriptors, based on the structure of organic compounds were predicted for 31 compounds. For “Anti-Ulcerative” activity, 5 compounds have Pa>0.7, 13 compounds with 0.4< Pa<0.7, and 7 compounds with Pa<0.4, and their probability to be active (Pa) is greater than the probability to be inactive (Pi) (Pa>Pi). For “Transcription factor NFkB inhibitor” activity, no compounds were present for Pa>0.7, 2 compounds with 0.4< Pa<0.7, and 26 compounds with Pa<0.4, and their probability to be active (Pa) is less than the probability to be inactive (Pi) (Pa<Pi). For “Antioxidant” activity, 13 compounds have Pa>0.7, 6 compounds with 0.4< Pa<0.7, and 10 compounds with Pa<0.4, and their probability to be active (Pa) is greater than the probability to be inactive (Pi) (Pa>Pi). For “Free-radical scavenger” activity, 9 compounds have Pa>0.7, 6 compounds with 0.4< Pa<0.7, and 14 compounds with Pa<0.4, and their probability to be active (Pa) is greater than the probability to be inactive (Pi) (Pa>Pi). For “Anti-inflammatory” activity, 8 compounds have Pa>0.7, 17 compounds with 0.4< Pa<0.7, and 2 compounds with Pa<0.4, and their probability to be active (Pa) is greater than the probability to be inactive (Pi) (Pa>Pi). For “Anti-protozoal” activity, 1 compound has Pa>0.7, 19 compounds with 0.4< Pa<0.7, and 8 compounds with Pa<0.4, and their probability to be active (Pa) is greater than the probability to be inactive (Pi) (Pa>Pi). For “Membrane integrity antagonist” activity, 10 compounds with Pa>0.7, 8 compounds with 0.4< Pa<0.7, and 4 compounds with Pa<0.4, and their probability to be active (Pa) is greater than the probability to be inactive (Pi) (Pa>Pi). For “Antineoplastic” activity, 8 compounds have Pa>0.7, 1 compound with 0.4<Pa<0.7 and 11 compounds with Pa<0.4, and their probability to be active (Pa) is less than the probability to be inactive (Pi) (Pa<Pi).

PASS Online Prediction for *T. palmata* are summarized in Table 8. A total of 8 Biological activities descriptors, based on the structure of organic compounds were predicted for 26 compounds. For “Antineoplastic" activity, 15 compounds have Pa>0.7, 3 compounds with 0.4< Pa<0.7, and 8 compounds with Pa<0.4, and their probability to be active (Pa) is greater than the probability to be inactive (Pi) (Pa>Pi). For “Antiulcerative” activity, 8 compounds were present for Pa>0.7, 12 compounds

Table 7: PASS Online prediction of phytocompounds identified from *Lannea coromandelica* using Way2Drug webserver (way2drug.com/passonline/predict.php).

Compounds	Anti-ulcerative		Transcription factor NF kappa B inhibitor		Antioxidant		Free radical scavenger		Anti-Inflammatory		Anti-protozoal		Membrane integrity antagonist		Anti-neoplastic	
	Pa	Pi	Pa	Pi	Pa	Pi	Pa	Pi	Pa	Pi	Pa	Pi	Pa	Pi	Pa	Pi
Caryophyllene	-	-	0.686	0.003	0.144	0.110	-	-	0.759	0.009	0.578	0.006	-	-	0.343	0.027
Phenol, 3,5-bis(1,1-dimethylethyl)-	0.342	0.072	0.204	0.026	0.469	0.008	0.512	0.010	0.610	0.029	0.493	0.025	0.732	0.012	0.274	0.169
Diethyl Phthalate	0.493	0.024	0.301	0.012	0.135	0.120	0.217	0.063	0.475	0.064	0.021	0.005	0.710	0.013	-	-
Phenol, 2,4-bis(1,1-dimethylethyl)-5-methyl-	0.335	0.075	0.146	0.048	0.489	0.007	0.478	0.012	0.664	0.021	0.435	0.037	0.759	0.010	-	-
Pentadecanoic acid	0.525	0.019	0.105	0.091	0.222	0.045	0.315	0.027	0.515	0.052	0.451	0.033	0.781	0.008	-	-
Oxirane, tetradecyl-	0.362	0.062	0.108	0.087	0.145	0.109	0.190	0.085	0.377	0.030	0.392	0.052	0.598	0.025	-	-
cis-9-Hexadecenal	0.313	0.088	0.140	0.053	0.146	0.107	0.192	0.083	0.250	0.212	0.413	0.044	0.334	0.096	-	-
Phytol	0.736	0.005	0.172	0.036	0.475	0.008	0.318	0.027	0.458	0.070	0.601	0.014	0.273	0.132	0.389	0.108
9-Eicosene, (E)-	0.545	0.016	0.190	0.030	0.296	0.031	0.281	0.027	0.622	0.027	0.474	0.028	0.615	0.023	-	-
1-Hexadecanol	0.476	0.028	0.138	0.054	0.229	0.043	0.265	0.040	0.498	0.058	0.550	0.019	0.814	0.006	-	-
Bis(2-ethylhexyl) phthalate	0.339	0.073	0.118	0.074	0.134	0.122	0.160	0.116	0.537	0.046	0.276	0.120	0.563	0.031	-	-
Phenol, 2,4-bis(1,1-dimethylethyl)-	0.346	0.069	0.166	0.039	0.525	0.006	0.532	0.009	0.762	0.009	0.525	0.021	0.769	0.009	-	-

4-tert-Butylcalix[4]arene	-	-	0.145	0.049	0.283	0.027	0.288	0.033	0.618	0.028	0.436	0.036	0.683	0.016	0.530	0.530
Hesperetin	0.599	0.011	0.384	0.007	0.746	0.004	0.878	0.002	0.640	0.024	0.180	0.129	0.653	0.018	0.325	0.029
Nantenine	0.233	0.163	-	-	-	-	0.206	0.071	-	-	0.206	0.189	-	-	0.173	0.035
7-O-Methylquercetin-3-O-galactoside-6"-rhamnoside	-	-	0.286	0.013	0.897	0.003	0.993	0.000	-	-	-	-	0.852	0.004	0.858	0.006
Kaempferol	0.487	0.026	0.286	0.013	0.856	0.003	0.771	0.003	0.676	0.019	0.554	0.018	0.530	0.037	0.791	0.013
Quercetin-3-O-rutinoside	0.586	0.012	0.253	0.016	0.923	0.003	0.988	0.001	0.728	0.013	0.484	0.011	0.758	0.010	0.169	0.038
Beta-Carotene	0.627	0.009	0.136	0.055	0.775	0.004	0.306	0.029	0.690	0.017	0.551	0.019	-	-	0.163	0.074
gamma-Carotene	0.875	0.003	0.190	0.030	0.858	0.003	0.457	0.013	0.732	0.012	0.523	0.021	-	-	0.157	0.077
Kaempferol 7-neohesperidoside	0.617	0.010	0.314	0.011	0.880	0.003	0.982	0.001	0.717	0.014	0.536	0.008	0.851	0.004	0.197	0.025
Kaempferol-3-O-rutinoside	0.586	0.012	0.222	0.021	0.924	0.003	0.984	0.001	0.743	0.011	0.492	0.011	0.810	0.006	0.169	0.038
zeta-Carotene	0.712	0.005	0.185	0.032	0.812	0.003	0.446	0.014	0.754	0.010	0.246	0.073	-	-	0.126	0.095
[Gallocatechin-(4alpha->8)]2-catechin	-	-	0.454	0.005	0.875	0.003	0.940	0.001	-	-	-	-	0.227	0.169	-	-
Diatoxanthin	0.514	0.021	-	-	0.643	0.004	0.265	0.040	0.410	0.090	0.313	0.092	-	-	0.886	0.005
Zeaxanthin	0.718	0.006	0.136	0.055	0.766	0.004	0.449	0.014	0.675	0.019	0.483	0.027	-	-	0.920	0.005
Paclitaxel	-	-	-	-	-	-	-	-	-	-	-	-	-	-	0.990	0.003
Lutein	0.815	0.004	0.150	0.046	0.609	0.004	0.205	0.072	0.463	0.068	0.252	0.140	-	-	0.913	0.005
Chlorogenic acid	0.54	0.017	0.218	0.023	0.785	0.004	0.856	0.002	0.598	0.03	0.65	0.01	0.30	0.11	0.778	0.01

	2									2	5	1	4	2		4
Luteolin-6-C-glucoside	0.367	0.060	0.250	0.017	0.818	0.003	0.871	0.002	0.496	0.056	0.705	0.009	0.537	0.036	0.805	0.011
Linoleic Acid	0.658	0.007	0.137	0.055	0.314	0.021	0.315	0.027	0.730	0.012	0.400	0.049	0.567	0.030	-	-

Pa (probability "to be active") estimates the chance that the studied compound is belonging to the sub-class of active compounds (resembles the structures of molecules, which are the most typical in a sub-set of "actives" in PASS training set).

Pi (probability "to be inactive") estimates the chance that the studied compound is belonging to the sub-class of inactive compounds (resembles the structures of molecules, which are the most typical in a sub-set of "inactives" in PASS training set).

Probability to be active (Pa) should be greater than **Probability to be inactive (Pi)**

If Pa > 0.7, the substance is very likely to exhibit the activity in experiment, but chances of the substance being the analogue of a known pharmaceutical agent is also high. If 0.4 < Pa <0.7 the substance is likely to exhibit the activity in experiment, but the probability is less. If Pa < 0.4, the substance is unlikely to exhibit the activity in experiment. However, if the presence of this activity is confirmed in the experiment the substance might be a new chemical entity.

Table 8: PASS analysis of phytocompounds from *Trevesia palmata* using way2drug Pass Prediction (http://www.way2drug.com/passonline/predict.php).

Compounds	Antineoplastic		Antiulcerative		Antioxidant		Free radical scavenger		Antiinflammatory		Antiprotozoal		Transcription factor NF kappa B inhibitor		Membrane integrity antagonist	
	Pa	Pi	Pa	Pi	Pa	Pi	Pa	Pi	Pa	Pi	Pa	Pi	Pa	Pi	Pa	Pi
Icariin	0.830	0.009	0.624	0.009	0.835	0.003	0.990	0.001	0.732	0.012	0.867	0.004	0.456	0.005	0.610	0.023
Apigenin-6-C-glucoside-7-O-glucoside	0.833	0.002	0.390	0.049	0.865	0.003	0.924	0.002	0.571	0.038	0.788	0.005	0.170	0.038	0.657	0.018
Kaempferol 3-O-sophoroside	0.862	0.006	0.581	0.013	0.926	0.003	0.977	0.001	0.751	0.010	0.919	0.003	0.267	0.014	0.828	0.005
Kaempferol-3-O-rutinoside	0.851	0.007	0.586	0.012	0.924	0.003	0.984	0.001	0.743	0.011	0.898	0.003	0.222	0.021	0.810	0.006
Kaempferol 4'-methyl ether 3-(4Rha-rhamnosylrutinoside)	0.855	0.006	0.619	0.009	0.876	0.003	0.987	0.001	0.716	0.014	0.936	0.002	0.211	0.024	0.858	0.004
7,9-Di-tert-butyl-1-oxaspiro(4,5)deca-6,9-diene-2,8-dione	0.367	0.118	-	-	0.284	0.026	-	-	0.247	0.123	0.559	0.018	-	-	0.487	0.047
Quercetin 3-O-[2"-O-(6"'-O-p-coumaroyl)-b-D-glucopyranosyl]-a-L-rhamnopyranoside	0.870	0.005	0.643	0.008	0.908	0.003	0.996	0.000	0.754	0.010	0.970	0.001	0.562	0.004	0.667	0.017
gamma.-Tocopherol	0.072	0.069	0.566	0.014	0.927	0.0003	0.757	0.003	0.775	0.008	-	-	0.104	0.093	-	-
dl-.alpha.-Tocopherol	0.262	0.022	0.666	0.006	0.967	0.002	0.607	0.005	0.814	0.006	-	-	-	-	-	-

Asiaticoside	0.899	0.005	0.895	0.002	0.636	0.004	0.197	0.078	0.901	0.004	0.961	0.002	0.367	0.008	0.903	0.003
Bacoside A3	0.841	0.008	-	-	0.857	0.003	-	-	0.470	0.066	0.995	0.001	0.155	0.044	0.565	0.030
Hederacoside C	0.919	0.005	0.936	0.002	0.677	0.004	0.322	0.026	0.849	0.005	0.950	0.002	0.518	0.004	0.952	0.001
alpha.-Amyrin	0.901	0.005	0.840	0.003	0.411	0.011	-	-	0.889	0.004	0.878	0.003	0.667	0.003	0.839	0.005
Neophytadiene	0.548	0.057	0.585	0.012	0.374	0.014	-	-	-	-	0.460	0.031	0.181	0.033	0.245	0.241
Phytol	0.389	0.108	0.736	0.005	0.475	0.008	0.318	0.027	0.458	0.070	0.601	0.014	0.172	0.036	0.273	0.132
alpha-Hederin	0.914	0.005	0.873	0.003	0.575	0.005	0.265	0.040	0.839	0.005	0.948	0.002	0.683	0.003	0.971	0.001
Zeaxanthin	0.920	0.005	0.718	0.005	0.766	0.004	0.449	0.014	0.675	0.019	0.297	0.057	0.136	0.055	-	-
Lutein	0.913	0.005	0.815	0.004	0.609	0.004	0.205	0.072	0.463	0.068	0.252	0.140	0.150	0.046	-	-
zeta-Carotene	0.903	0.005	0.712	0.005	0.812	0.003	0.446	0.014	0.754	0.010	0.335	0.079	0.185	0.032	-	-
Isopropyl Tetradecanoate	0.071	0.069	0.515	0.021	0.227	0.043	-	-	0.446	0.074	0.483	0.027	-	-	0.782	0.008
Linoleic Acid	0.301	0.020	0.657	0.007	0.314	0.021	-	-	0.730	0.012	0.400	0.049	0.137	0.055	0.567	0.030
Linolenic acid	-	-	0.656	0.007	0.364	0.015	0.281	0.035	0.804	0.006	0.350	0.071	0.120	0.071	0.480	0.049
Oxyacanthine	0.309	0.147	-	-	0.178	0.071	0.289	0.033	0.397	0.097	-	-	0.132	0.059	-	-
Honokiol	0.345	0.128	0.471	0.029	0.421	0.010	0.479	0.012	0.515	0.052	0.494	0.025	0.387	0.007	-	-
Beta-Sitosterol	0.411	0.100	-	-	0.178	0.072	-	-	0.467	0.067	0.316	0.090	0.101	0.098	0.553	0.033

Thalsimine	0.454	0.086	-	-	-	-	-	-	0.319	0.144	0.194	0.111	-	-	-	-
Isofraxidin	0.755	0.018	0.295	0.103	0.579	0.005	0.750	0.003	0.710	0.015	0.392	0.051	0.471	0.005	0.639	0.020

Pa (probability "to be active") estimates the chance that the studied compound is belonging to the sub-class of active compounds (resembles the structures of molecules, which are the most typical in a sub-set of "actives" in PASS training set).

Pi (probability "to be inactive") estimates the chance that the studied compound is belonging to the sub-class of inactive compounds (resembles the structures of molecules, which are the most typical in a sub-set of "inactives" in PASS training set).

Probability to be active (Pa) should be greater than **Probability to be inactive (Pi)**

If Pa > 0.7, the substance is very likely to exhibit the activity in experiment, but chances of the substance being the analogue of a known pharmaceutical agent is also high. If 0.4 < Pa <0.7 the substance is likely to exhibit the activity in experiment, but the probability is less. If Pa < 0.4, the substance is unlikely to exhibit the activity in experiment. However, if the presence of this activity is confirmed in the experiment the substance might be a new chemical entity.

with 0.4< Pa<0.7, and 2 compounds with Pa<0.4, and their probability to be active (Pa) is greater than the probability to be inactive (Pi) (Pa>Pi). For “Antioxidant” activity, 11 compounds have Pa>0.7, 8 compounds with 0.4< Pa<0.7, and 7 compounds with Pa<0.4, and their probability to be active (Pa) is greater than the probability to be inactive (Pi) (Pa>Pi). For “Free-radical scavenger” activity, 8 compounds have Pa>0.7, 4 compounds with 0.4< Pa<0.7, and 7 compounds with Pa<0.4, and their probability to be active (Pa) is greater than the probability to be inactive (Pi) (Pa>Pi). For “Anti-inflammatory” activity, 14 compounds have Pa>0.7, 8 compounds with 0.4< Pa<0.7, and 3 compounds with Pa<0.4, and their probability to be active (Pa) is greater than the probability to be inactive (Pi) (Pa>Pi). For “Anti-protozoal” activity, 11 compound has Pa>0.7, 6 compounds with 0.4< Pa<0.7, and 7 compounds with Pa<0.4, and their probability to be active (Pa) is greater than the probability to be inactive (Pi) (Pa>Pi). For “Transcription factor NFkB inhibitor” activity, 0 compounds with Pa>0.7, 6 compounds with 0.4< Pa<0.7 and 17 compounds with Pa<0.4, and their probability to be active (Pa) is less than the probability to be inactive (Pi) (Pa<Pi). For “Membrane integrity antagonist” activity, 8 compounds have Pa>0.7, 9 compounds with 0.4<Pa<0.7 and 2 compounds with Pa<0.4, and their probability to be active (Pa) is greater than the probability to be inactive (Pi) (Pa>Pi).

3.4.3. Molecular Docking

The calculated binding affinity of each ligand to the COX-2, iNOS, TNF-α and IL-6 receptors, measured in kilocalories per mole (kcal/mol) are shown from table 9 to table 16. A lower binding affinity value indicates stronger binding between the ligand and the receptor.

Table 9 represents the binding affinities of various ligands derived from *Lannea coromandelica* when docked against the COX-2 receptor. Ligands with higher negative values (e.g., Paclitaxel, Quercetin-3-O-rutinoside, Kaempferol 7-neohesperidoside) exhibit stronger binding affinities to the COX-2 receptor, suggesting potential efficacy in modulating COX-2 activity. Ligands with moderately negative values (e.g., Kaempferol-3-O-rutinoside, Kaempferol,

Chlorogenic acid) may also have significant interactions with the receptor, albeit slightly weaker than strong binders. Ligands with less negative values (e.g., Phytol, Nantenine, gamma-Carotene) exhibit weaker binding affinities and may have less significant interactions with the COX-2 receptor. Ligands with values close to or above zero (e.g., 4-tert-Butylcalix[4]arene, Diethyl Phthalate, cis-9-Hexadecenal) are less likely to bind strongly to the COX-2 receptor under the conditions tested.

Table 9: Binding affinities of the ligands identified from *Lannea coromandelica* docked against COX-2 receptor obtained from autodock vina.

Ligand	**PubChem ID**	**Binding affinity value (kcal/mol)**
Paclitaxel	36314	-10.3
Quercetin-3-O-rutinoside	5280805	-9.3
Kaempferol 7-neohesperidoside	5483905	-9.1
Kaempferol-3-O-rutinoside	5318767	-8.9
Kaempferol	5280863	-8.8
Chlorogenic acid	1794427	-8.5
zeta-Carotene	5280788	-8.2
Hesperetin	72281	-8.1
[Gallocatechin-(4alpha->8)]2-catechin	14890508	-8.1
Caryophyllene	5281515	-8.0
Luteolin-6-C-glucoside	114776	-8.0
7-O-Methylquercetin-3-O-galactoside-6"-rhamnoside	56995003	-7.6
Diatoxanthin	6440986	-7.6
Zeaxanthin	5280899	-7.6
Beta-Carotene	5280489	-7.5
Lutein	5281243	-7.4
9-Eicosene, (E)-	5365037	-7.3
Phytol	5280435	-7.2
Nantenine	197001	-7.1
gamma-Carotene	5280791	-6.9
4-tert-Butylcalix[4]arene	335377	-6.8
Diethyl Phthalate	6781	-6.7
cis-9-Hexadecenal	5364643	-6.5
Phenol, 2,4-bis(1,1-dimethylethyl)-	7311	-6.5
Phenol, 3,5-bis(1,1-dimethylethyl)-	70825	-6.1
Phenol, 2,4-bis(1,1-dimethylethyl)-5-methyl-	10346	-6.1
Pentadecanoic acid	13849	-6.1
Bis(2-ethylhexyl) phthalate	8343	-6.1
Oxirane, tetradecyl-	23741	-6.0
Linoleic Acid	5280450	-6.0
1-Hexadecanol	2682	-5.7

Table 10 provides the results of molecular docking studies indicating the binding affinities of various ligands derived from *Trevesia palmata* when docked against the COX-2 receptor. Ligands with higher negative values (e.g., Quercetin 3-O-[2"-O-(6"'-O-p-coumaroyl)-b-D-glucopyranosyl]-a-L-rhamnopyranoside, Kaempferol-3-O-rutinoside) exhibit strong binding affinities to the COX-2 receptor, suggesting potential efficacy in modulating COX-2 activity. Ligands with moderately negative values (e.g., Icariin, Oxyacanthine, Kaempferol 3-O-sophoroside) may also have significant interactions with the receptor, albeit slightly weaker than strong binders. Ligands with less negative values (e.g., Linoleic Acid, Diethyl Phthalate, Isofraxidin) exhibit weaker binding affinities and may have less significant interactions with the COX-2 receptor. Ligands with values close to or above zero (e.g., Pentadecanoic acid) are less likely to bind strongly to the COX-2 receptor under the conditions tested.

Table 9 and 10 provides insights into the potential efficacy of various compounds derived from *L. coromandelica* and *T. palmata* in modulating COX-2 activity, which could be valuable in drug discovery and development efforts targeting inflammatory pathways.

Table 10: Binding affinities of the ligands identified from *Trevesia palmata* docked against COX-2 receptor obtained from autodock vina.

Ligand	**PubChem ID**	**Binding affinity value (kcal/mol)**
Quercetin 3-O-[2"-O-(6"'-O-p-coumaroyl)-b-D-glucopyranosyl]-a-L-rhamnopyranoside	10169367	-9.9
Kaempferol-3-O-rutinoside	5318767	-8.9
Icariin	5318997	-8.7
Oxyacanthine	442333	-8.7
Kaempferol 3-O-sophoroside	5282155	-8.5
Asiaticoside	11954171	-8.5
alpha.-Amyrin	73170	-8.4
Apigenin-6-C-glucoside-7-O-glucoside	4636593	-8.4
gamma.-Tocopherol	92729	-8.2
Kaempferol 4'-methyl ether 3-(4Rha-rhamnosylrutinoside)	44257995	-8.1
Honokiol	72303	-8.0
Beta-Sitosterol	222284	-7.9

alpha-Hederin	11954171	-7.9
Lutein	5281243	-7.7
zeta-Carotene	5280788	-7.7
Hederacoside C	5280788	-7.6
Zeaxanthin	5280899	-7.5
Bacoside A3	91827005	-7.3
Neophytadiene	10446	-7.2
dl-.alpha.-Tocopherol	2116	-7.2
Phytol	5280435	-7.1
Linolenic acid	5280934	-7.1
Linoleic Acid	5280450	-6.8
Diethyl Phthalate	545303	-6.7
Isofraxidin	5318565	-6.5
Pentadecanoic acid	8042	-6.1

Table 11 presents the results of molecular docking studies showing the binding affinities of various ligands derived from *Lannea coromandelica* when docked against the iNOS (Inducible Nitric Oxide Synthase) receptor. Ligands with highly negative values (e.g., Quercetin-3-O-rutinoside, Paclitaxel) exhibit strong binding affinities to the iNOS receptor, indicating potential efficacy in modulating iNOS activity. Ligands with moderately negative values (e.g., Kaempferol-3-O-rutinoside, Kaempferol 7-neohesperidoside) also demonstrate significant interactions with the receptor, albeit slightly weaker than strong binders. Ligands with less negative values (e.g., Linoleic Acid, Phenol derivatives) exhibit weaker binding affinities and may have less significant interactions with the iNOS receptor. Ligands with values close to or above zero (e.g., Pentadecanoic acid, 1-Hexadecanol) are less likely to bind strongly to the iNOS receptor under the conditions tested.

Table 11: Binding affinities of the ligands identified from *Lannea coromandelica* docked against iNOS receptor obtained from autodock vina

Ligand	**PubChem ID**	**Binding affinity value (kcal/mol)**
Quercetin-3-O-rutinoside	5280805	-11.4
Paclitaxel	36314	-11.4
Kaempferol-3-O-rutinoside	5318767	-10.8
Kaempferol 7-neohesperidoside	5483905	-10.0
Nantenine	197001	-9.5
Hesperetin	72281	-9.3

Kaempferol	5280863	-9.3
zeta-Carotene	5280788	-9.2
[Gallocatechin-(4alpha->8)]2-catechin	14890508	-9.1
7-O-Methylquercetin-3-O-galactoside-6"-rhamnoside	56995003	-8.9
Luteolin-6-C-glucoside	114776	-8.9
Chlorogenic acid	1794427	-8.1
Beta-Carotene	5280489	-8.0
Diatoxanthin	6440986	-7.9
Zeaxanthin	5280899	-7.9
Lutein	5281243	-7.8
Diethyl Phthalate	6781	-7.4
Bis(2-ethylhexyl) phthalate	8343	-7.4
gamma-Carotene	5280791	-7.4
4-tert-Butylcalix[4]arene	335377	-7.3
9-Eicosene, (E)-	5365037	-7.0
Linoleic Acid	5280450	-7.0
Phenol, 2,4-bis(1,1-dimethylethyl)-	7311	-6.9
Phenol, 3,5-bis(1,1-dimethylethyl)-	70825	-6.8
Phenol, 2,4-bis(1,1-dimethylethyl)-5-methyl-	10346	-6.8
Caryophyllene	5281515	-6.6
Phytol	5280435	-6.6
cis-9-Hexadecenal	5364643	-6.4
Pentadecanoic acid	13849	-6.1
1-Hexadecanol	2682	-6.1
Oxirane, tetradecyl-	23741	-6.0

Table 12 provides the results of molecular docking studies indicating the binding affinities of various ligands derived from *Trevesia palmata* when docked against the iNOS (Inducible Nitric Oxide Synthase) receptor. Ligands with highly negative values (e.g., Kaempferol-3-O-rutinoside, Quercetin 3-O-[2"-O-(6"'-O-p-coumaroyl)-b-D-glucopyranosyl]-a-L-rhamnopyranoside) exhibit strong binding affinities to the iNOS receptor, indicating potential efficacy in modulating iNOS activity. Ligands with moderately negative values (e.g., Oxyacanthine, Asiaticoside, Kaempferol 4'-methyl ether 3-(4Rha-rhamnosylrutinoside)) also demonstrate significant interactions with the receptor, albeit slightly weaker than strong binders. Ligands with less negative values (e.g., Linoleic Acid, Diethyl Phthalate, Phytol) exhibit weaker binding affinities and may have less significant interactions with the iNOS receptor.

Ligands with values close to or above zero (e.g., Pentadecanoic acid) are less likely to bind strongly to the iNOS receptor under the conditions tested.

Table 12: Binding affinities of the ligands identified from *Trevesia palmata* docked against iNOS receptor obtained from autodock vina.

Ligand	**PubChem ID**	**Binding affinity value (kcal/mol)**
Kaempferol-3-O-rutinoside	5318767	-11.3
Quercetin 3-O-[2"-O-(6"'-O-p-coumaroyl)-b-D-glucopyranosyl]-a-L-rhamnopyranoside	10169367	-11.0
Oxyacanthine	442333	-10.9
Asiaticoside	11954171	-10.4
Kaempferol 4'-methyl ether 3-(4Rha-rhamnosylrutinoside)	44257995	-10.3
zeta-Carotene	5280788	-10.0
alpha-Hederin	11954171	-9.9
alpha.-Amyrin	73170	-9.8
Icariin	5318997	-9.8
Kaempferol 3-O-sophoroside	5282155	-9.7
Beta-Sitosterol	222284	-9.1
Apigenin-6-C-glucoside-7-O-glucoside	4636593	-9.0
Bacoside A3	91827005	-9.0
Honokiol	72303	-9.0
Hederacoside C	5280788	-8.7
dl-.alpha.-Tocopherol	2116	-8.2
Zeaxanthin	5280899	-8.0
Lutein	5281243	-8.0
gamma.-Tocopherol	92729	-7.8
Diethyl Phthalate	545303	-7.4
Phytol	5280435	-7.3
Linolenic acid	5280934	-7.3
Isofraxidin	5318565	-7.3
Neophytadiene	10446	-7.2
Linoleic Acid	5280450	-6.5
Pentadecanoic acid	8042	-6.1

Table 11 and 12 data provides insights into the potential efficacy of various compounds derived from *L. coromandelica* and *T. palmata* in modulating iNOS activity, which could be valuable in drug discovery and development efforts targeting inflammatory pathways.

Table 13: Binding affinities of the ligands identified from *Lannea coromandelica* docked against TNF-α receptor obtained from autodock vina.

Ligand	PubChem ID	Binding affinity value (kcal/mol)
4-tert-Butylcalix[4]arene	335377	-9.5
Paclitaxel	36314	-9.1
Kaempferol 7-neohesperidoside	5483905	-9.0
[Gallocatechin-(4alpha->8)]2-catechin	14890508	-8.9
7-O-Methylquercetin-3-O-galactoside-6"-rhamnoside	56995003	-8.5
Nantenine	197001	-8.5
9-Eicosene, (E)-	5365037	-8.3
Kaempferol-3-O-rutinoside	5318767	-8.1
Luteolin-6-C-glucoside	114776	-8.0
Beta-Carotene	5280489	-7.8
Quercetin-3-O-rutinoside	5280805	-7.6
zeta-Carotene	5280788	-7.6
Hesperetin	72281	-7.5
Zeaxanthin	5280899	-7.5
Lutein	5281243	-7.5
Caryophyllene	5281515	-7.4
Diatoxanthin	6440986	-7.3
Kaempferol	5280863	-7.2
gamma-Carotene	5280791	-7.2
Chlorogenic acid	1794427	-7.1
Diethyl Phthalate	6781	-6.2
Phytol	5280435	-6.0
Phenol, 2,4-bis(1,1-dimethylethyl)-5-methyl-	10346	-6.0
Phenol, 2,4-bis(1,1-dimethylethyl)-	7311	-5.8
Phenol, 3,5-bis(1,1-dimethylethyl)-	70825	-5.8
Pentadecanoic acid	13849	-5.5
Linoleic Acid	5280450	-5.4
Bis(2-ethylhexyl) phthalate	8343	-5.3
cis-9-Hexadecenal	5364643	-5.2
1-Hexadecanol	2682	-5.2
Oxirane, tetradecyl-	23741	-4.8

Table 13 represents the results of molecular docking studies indicating the binding affinities of various ligands derived from *L. coromandelica* when docked against the TNF-α (Tumor Necrosis Factor-alpha) receptor. Ligands with highly negative values (e.g., 4-tert-Butylcalix[4]arene, Paclitaxel, Kaempferol 7-neohesperidoside) exhibit

strong binding affinities to the TNF-α receptor, suggesting potential efficacy in modulating TNF-α activity. Ligands with moderately negative values (e.g., [Gallocatechin-(4alpha->8)]2-catechin, 7-O-Methylquercetin-3-O-galactoside-6''-rhamnoside, Nantenine) also demonstrate significant interactions with the receptor, albeit slightly weaker than strong binders. Ligands with less negative values (e.g., Chlorogenic acid, Diethyl Phthalate, Phytol) exhibit weaker binding affinities and may have less significant interactions with the TNF-α receptor. Ligands with values close to or above zero (e.g., Pentadecanoic acid, Linoleic Acid, Bis(2-ethylhexyl) phthalate) are less likely to bind strongly to the TNF-α receptor under the conditions tested.

Table 14: Binding affinities of the ligands identified from *Trevesia palmata* docked against TNF-α receptor obtained from autodock vina.

Ligand	**PubChem ID**	**Binding affinity value (kcal/mol)**
Asiaticoside	11954171	-10.0
alpha.-Amyrin	73170	-9.4
Oxyacanthine	442333	-9.3
Hederacoside C	5280788	-9.2
Quercetin 3-O-[2''-O-(6'''-O-p-coumaroyl)-b-D-glucopyranosyl]-a-L-rhamnopyranoside	10169367	-9.0
Beta-Sitosterol	222284	-8.6
Honokiol	72303	-8.6
Icariin	5318997	-8.3
Kaempferol-3-O-rutinoside	5318767	-8.1
Kaempferol 4'-methyl ether 3-(4Rha-rhamnosylrutinoside)	44257995	-8.1
alpha-Hederin	11954171	-8.0
Apigenin-6-C-glucoside-7-O-glucoside	4636593	-7.9
Lutein	5281243	-7.8
Bacoside A3	91827005	-7.7
gamma.-Tocopherol	92729	-7.6
Zeaxanthin	5280899	-7.6
dl-.alpha.-Tocopherol	2116	-7.4
Kaempferol 3-O-sophoroside	5282155	-7.4
zeta-Carotene	5280788	-7.2
Diethyl Phthalate	545303	-6.2
Isofraxidin	5318565	-6.2
Phytol	5280435	-5.9
Linoleic Acid	5280450	-5.6

Neophytadiene	10446	-5.5
Pentadecanoic acid	8042	-5.5
Linolenic acid	5280934	-5.5

Table 14 represents the results of molecular docking studies indicating the binding affinities of various ligands derived from *T. palmata* when docked against the TNF-α (Tumor Necrosis Factor-alpha) receptor. Ligands with highly negative values (e.g., Asiaticoside, alpha.-Amyrin, Oxyacanthine) exhibit strong binding affinities to the TNF-α receptor, suggesting potential efficacy in modulating TNF-α activity. Ligands with moderately negative values (e.g., Hederacoside C, Quercetin 3-O-[2"-O-(6"'-O-p-coumaroyl)-b-D-glucopyranosyl]-a-L-rhamnopyranoside, Beta-Sitosterol) also demonstrate significant interactions with the receptor, albeit slightly weaker than strong binders. Ligands with less negative values (e.g., Diethyl Phthalate, Isofraxidin, Phytol) exhibit weaker binding affinities and may have less significant interactions with the TNF-α receptor. Ligands with values close to or above zero (e.g., Linoleic Acid, Pentadecanoic acid, Linolenic acid) are less likely to bind strongly to the TNF-α receptor under the conditions tested.

Overall, table 13 and 14 data provide insights into the potential efficacy of various compounds derived from *L. coromandelica* and *T. palmata* in modulating TNF-α activity, which could be valuable in drug discovery and development efforts targeting inflammatory pathways.

Table 15: Binding affinities of the ligands identified from *Trevesia palmata* docked against IL-6 receptor obtained from autodock vina.

Ligand	**PubChem ID**	**Binding affinity value (kcal/mol)**
Kaempferol-3-O-rutinoside	5318767	-8.1
Kaempferol 3-O-sophoroside	5282155	-7.5
Asiaticoside	11954171	-7.1
Apigenin-6-C-glucoside-7-O-glucoside	4636593	-7.0
Icariin	5318997	-6.9
alpha-Hederin	11954171	-6.9
Beta-Sitosterol	222284	-6.7
alpha.-Amyrin	73170	-6.7
Kaempferol 4'-methyl ether 3-(4Rha-	44257995	-6.6

rhamnosylrutinoside)		
Quercetin 3-O-[2"-O-(6"'-O-p-coumaroyl)-b-D-glucopyranosyl]-a-L-rhamnopyranoside	10169367	-6.6
Hederacoside C	5280788	-6.5
Oxyacanthine	442333	-6.5
Bacoside A3	91827005	-6.4
Honokiol	72303	-5.9
Zeaxanthin	5280899	-5.7
Lutein	5281243	-5.7
zeta-Carotene	5280788	-5.6
Isofraxidin	5318565	-5.6
Pentadecanoic acid	8042	-5.5
gamma.-Tocopherol	92729	-5.3
Diethyl Phthalate	545303	-5.1
dl-.alpha.-Tocopherol	2116	-5.1
Phytol	5280435	-4.8
Linolenic acid	5280934	-4.7
Linoleic Acid	5280450	-4.5
Neophytadiene	10446	-4.2

Table 15 represents the results of molecular docking studies indicating the binding affinities of various ligands derived from *T. palmata* when docked against the IL-6 (Interleukin-6) receptor. Ligands with highly negative values (e.g., Kaempferol-3-O-rutinoside, Kaempferol 3-O-sophoroside, Asiaticoside) exhibit strong binding affinities to the IL-6 receptor, suggesting potential efficacy in modulating IL-6 activity. Ligands with moderately negative values (e.g., Apigenin-6-C-glucoside-7-O-glucoside, Icariin, alpha-Hederin) also demonstrate significant interactions with the receptor, albeit slightly weaker than strong binders. Ligands with less negative values (e.g., Linolenic acid, Linoleic Acid, Phytol) exhibit weaker binding affinities and may have less significant interactions with the IL-6 receptor. Ligands with values close to or above zero (e.g., Neophytadiene) are less likely to bind strongly to the IL-6 receptor under the conditions tested.

Table 16: Binding affinities of the ligands identified from *Lannea coromandelica* docked against iNOS receptor obtained from autodock vina.

Ligand	**PubChem ID**	**Binding affinity value (kcal/mol)**
Paclitaxel	36314	-11.4
Quercetin-3-O-rutinoside	5280805	-11.4
Kaempferol-3-O-rutinoside	5318767	-10.8
Kaempferol 7-neohesperidoside	5483905	-10.0
[Gallocatechin-(4alpha->8)]2-catechin	14890508	-10.0
9-Eicosene, (E)-	5365037	-9.8
Nantenine	197001	-9.5
Kaempferol	5280863	-9.3
Hesperetin	72281	-9.3
zeta-Carotene	5280788	-9.2
Luteolin-6-C-glucoside	114776	-8.9
7-O-Methylquercetin-3-O-galactoside-6"-rhamnoside	56995003	-8.9
Chlorogenic acid	1794427	-8.1
Beta-Carotene	5280489	-8.0
4-tert-Butylcalix[4]arene	335377	-8.0
Diatoxanthin	6440986	-7.9
Zeaxanthin	5280899	-7.9
Lutein	5281243	-7.8
gamma-Carotene	5280791	-7.4
Diethyl Phthalate	6781	-7.4
Linoleic Acid	5280450	-7.0
Caryophyllene	5281515	-6.6
Phytol	5280435	-6.6
Bis(2-ethylhexyl) phthalate	8343	-6.5
cis-9-Hexadecenal	5364643	-6.4
Phenol, 2,4-bis(1,1-dimethylethyl)-	7311	-6.3
Phenol, 3,5-bis(1,1-dimethylethyl)-	70825	-6.3
Phenol, 2,4-bis(1,1-dimethylethyl)-5-methyl-	10346	-6.2
Pentadecanoic acid	13849	-6.1
1-Hexadecanol	2682	-6.1
Oxirane, tetradecyl-	23741	-6.0

Table 16 presents the results of molecular docking studies indicating the binding affinities of various ligands derived from *L. coromandelica* when docked against the iNOS (inducible Nitric Oxide Synthase) receptor. Ligands with highly negative values including Paclitaxel and Quercetin-3-O-rutinoside exhibit strong binding

affinities to the iNOS receptor, suggesting potential efficacy in modulating iNOS activity. Ligands with moderately negative values including Kaempferol-3-O-rutinoside, Kaempferol 7-neohesperidoside and [Gallocatechin-(4alpha->8)]2-catechin also demonstrate significant interactions with the receptor, albeit slightly weaker than strong binders. Ligands with less negative values including Linoleic Acid, Caryophyllene and Phytol exhibit weaker binding affinities and may have less significant interactions with the iNOS receptor. Ligands with values close to or above zero including Pentadecanoic acid, 1-Hexadecanol and Oxirane, tetradecyl- are less likely to bind strongly to the iNOS receptor under the conditions tested.

Table 15 and 16 data provides insights into the potential efficacy of various compounds derived from *T. palmata* and *L. coromandelica* in modulating iNOS activity, which could be valuable in drug discovery and development efforts targeting inflammatory pathways.

Table 17: Binding affinity and the residues involved in the interaction of plant phytochemicals of *Lannea coromandelica* and *Trevesia palmata* with COX-2, iNOS, TNF and IL-6.

Compounds	Binding affinity (kcal/mol)	Residues involved in H-bond	Residues involved in other interactions (π···anion, π···cation, π···σ, π···π, π···alkyl)
		Cox-2	
Paclitaxel	-10.3	Gln189, His200, His374	Val281, Leu377, Val277, His372, Val433, Lys197, Val430, His193
Quercetin-3-O-rutinoside	-9.3	Thr192, Thr198, His374, As368, Tyr371	His193, His200, His372
Kaempferol 7-neohesperidoside	-9.1	Ala185, His374, Asn368, Phe196	Ala188, His193, His372

Quercetin 3-O-[2''-O-(6'''-O-p-coumaroyl)-b-D-glucopyranosyl]-a-L-rhamnopyranoside	-9.9	Asn368, Phe196	Ala188, Val433, Ala436, His374
	iNOS		
Quercetin-3-O-rutinoside	-11.4	Tyr367, Gln257, Glu371, Asn364	Leu203, Phe363, Trp188, Cys194, Ala191
Paclitaxel	-11.4	--	Met349, Arg193, Ala191, Phe363, Trp188, Cys194, Pro344, Tyr367
Oxyacanthine	-10.9	--	Tyr485, Met349, Val346, Phe363, Cys194, Trp188, Ala191, Pro344
Kaempferol-3-O-rutinoside	-11.3	--	Ala191, Cys194, Phe363, Trp188, Leu203
Quercetin 3-O-[2''-O-(6'''-O-p-coumaroyl)-b-D-glucopyranosyl]-a-L-rhamnopyranoside	-11.0	Arg193, Gly365, Arg382	Phe363, Trp188, Leu203, Pro344, Glu371
	TNF-α		
Hederacoside C	-9.2	Gly121, Lys98 (A), Lys98 (B), Tyr119	Val123, Leu57, Tyr59, Tyr119
Asiaticoside	-10.0	Lys98 (A), Lys98 (B), Glu116, Tyr115, Ser99	Tyr119 (A), Tyr119 (B)
Oxyacanthine	-9.3	--	Tyr119, Ser60
4-tert-Butylcalix[4]arene	-9.5	Leu120	Tyr119, Tyr59, Leu57
	IL6		
Kaempferol-3-O-rutinoside	-8.1	Glu42, Glu106, Gln156,	Lys46, Ser47, Asp160

		Arg104, Gln159, Gln152, Asn103

This table (Table 17) provides valuable insights into the molecular interactions between plant phytochemicals and inflammatory targets, including COX-2, iNOS, TNF-α, and IL-6, which could have implications for potential therapeutic interventions targeting inflammation-related diseases.

Binding Affinity (kcal/mol) column indicates the strength of the binding interaction between the phytochemical compounds and the respective protein targets. Lower values indicate stronger binding affinity. Residues involved in H-bond are the specific amino acid residues within the protein target that form hydrogen bonds with the phytochemical compounds during the binding process. Residues involved in other interactions (π···anion, π···cation, π···σ, π···π, π···alkyl) column lists the amino acid residues involved in other types of interactions, such as pi interactions (π), which are important for stabilizing the protein-ligand complex. Table 17 provides the data predicting the binding affinity and the residues involved in interactions between various compounds and specific protein targets.

Cyclooxygenase-2 (COX-2): Compounds like Paclitaxel, Quercetin-3-O-rutinoside, Kaempferol 7-neohesperidoside, and Quercetin 3-O-[2''-O-(6'''-O-p-coumaroyl)-b-D-glucopyranosyl]-a-L-rhamnopyranoside exhibit varying degrees of binding affinity with COX-2. They form hydrogen bonds and other interactions with specific amino acid residues within the COX-2 binding site. Paclitaxel binds with a binding affinity of -10.3 kcal/mol. Interacts with residues Gln189, His200, His374 through hydrogen bonds, and with residues Val281, Leu377, Val277, His372, Val433, Lys197, Val430, His193 through other interactions. Quercetin-3-O-rutinoside binds with a binding affinity of -9.3 kcal/mol. Forms hydrogen bonds with Thr192, Thr198, His374, As368, Tyr371, and interacts with His193, His200, His372 through other interactions. Kaempferol 7-neohesperidoside binds with a binding affinity of -9.1 kcal/mol. Involves hydrogen bonds with Ala185, His374, Asn368, Phe196, and interacts with Ala188, His193, His372 through other interactions. Quercetin 3-O-[2''-

O-(6'''-O-p-coumaroyl)-b-D-glucopyranosyl]-a-L-rhamnopyranoside binds with a binding affinity of -9.9 kcal/mol. Forms hydrogen bonds with Asn368, Phe196, and interacts with Ala188, Val433, Ala436, His374 through other interactions (Figure 15).

Inducible Nitric Oxide Synthase (iNOS): Compounds such as Quercetin-3-O-rutinoside, Paclitaxel, Oxyacanthine, Kaempferol-3-O-rutinoside, and Quercetin 3-O-[2''-O-(6'''-O-p-coumaroyl)-b-D-glucopyranosyl]-a-L-rhamnopyranoside
demonstrate strong binding affinity with iNOS, forming hydrogen bonds and other interactions with key amino acid residues within the protein. Quercetin-3-O-rutinoside binds with a binding affinity of -11.4 kcal/mol. Forms hydrogen bonds with Tyr367, Gln257, Glu371, Asn364, and interacts with Leu203, Phe363, Trp188, Cys194, Ala191 through other interactions. Paclitaxel binds with a binding affinity of -11.4 kcal/mol. Interacts with Met349, Arg193, Ala191, Phe363, Trp188, Cys194, Pro344, Tyr367. Oxyacanthine binds with a binding affinity of -10.9 kcal/mol. Interacts with Tyr485, Met349, Val346, Phe363, Cys194, Trp188, Ala191, Pro344. Kaempferol-3-O-rutinoside binds with a binding affinity of -11.3 kcal/mol. Interacts with Ala191, Cys194, Phe363, Trp188, Leu203. Quercetin 3-O-[2''-O-(6'''-O-p-coumaroyl)-b-D-glucopyranosyl]-a-L-rhamnopyranoside binds with a binding affinity of -11.0 kcal/mol. Interacts with Arg193, Gly365, Arg382, Phe363, Trp188, Leu203, Pro344, Glu371 (Figure 16).

Tumor Necrosis Factor-alpha (TNF-α): Phytochemicals like Hederacoside C, Asiaticoside, Oxyacanthine, and 4-tert-Butylcalix[4]arene exhibit interactions with TNF-α, forming hydrogen bonds and other interactions with specific amino acid residues. Hederacoside C binds with a binding affinity of -9.2 kcal/mol. Forms hydrogen bonds with Gly121, Lys98, Tyr119, and interacts with Val123, Leu57, Tyr59, Tyr119 through other interactions. Asiaticoside binds with a binding affinity of -10.0 kcal/mol. Forms hydrogen bonds with Lys98, Glu116, Tyr115, Ser99, and interacts with Tyr119 through other interactions. Oxyacanthine binds with a binding affinity of -9.3 kcal/mol. Interacts with Tyr119, Ser60. 4-tert-Butylcalix[4]arene binds with a binding affinity of -9.5 kcal/mol. Interacts with Leu120, Tyr119, Tyr59, Leu57 (Figure 17).

Interleukin-6 (IL-6): Kaempferol-3-O-rutinoside shows binding with IL-6, forming hydrogen bonds and other interactions with specific amino acid residues within the protein. Kaempferol-3-O-rutinoside binds with a binding affinity of -8.1 kcal/mol. Forms hydrogen bonds with Glu42, Glu106, Gln156, Arg104, Gln159, Gln152, Asn103, and interacts with Lys46, Ser47, Asp160 (Figure 18).

These results provide insights into the potential binding interactions of various compounds with their respective protein targets, which could be useful in drug discovery and development processes.

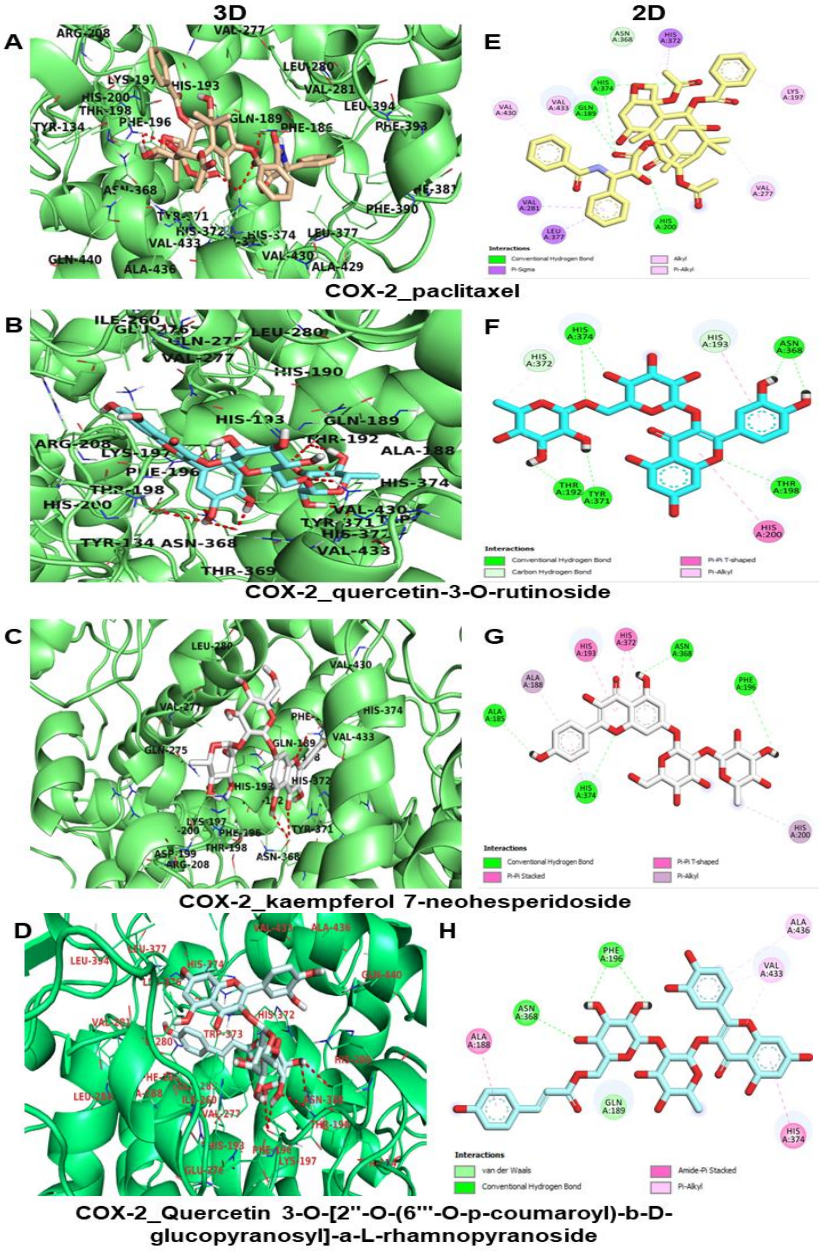

Figure 15: Three dimensional (3D) and two dimensional (2D) docking poses showing the interactions of the active site residues of COX-2 receptor with the top hit potential bioactive compounds from *Lannea coromandelica* and *Trevesia palmata* leaf extract products (ligands). (A, E) Paclitaxel (binding affinity −10.3 kcal/mol); (B, F) Quercetin-3-O-rutinoside (binding affinity −9.3 kcal/mol); (C, G) Kaempferol 7-neohesperidoside (binding affinity −9.1 kcal/mol); and (D, H) Quercetin 3-O-[2''-O-(6'''-O-p-coumaroyl)-b-D-glucopyranosyl]-a-L-rhamnopyranoside (binding affinity −9.9 kcal/mol). COX-2: Cyclooxygenase-2.

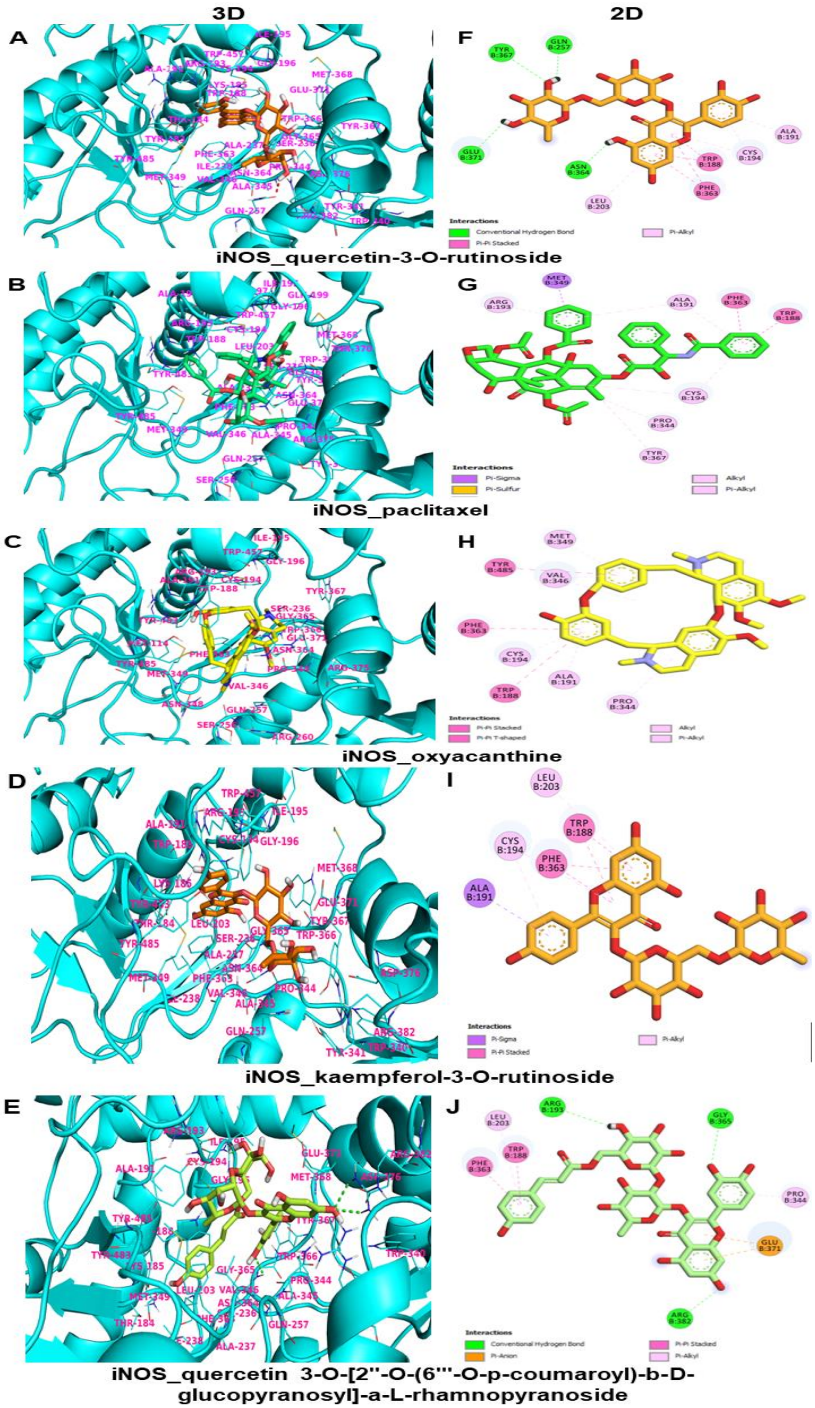

Figure 16: Three dimensional (3D) and two dimensional (2D) docking poses showing the interactions of the active site residues of iNOS receptor with the top hit potential bioactive compounds from *Lannea coromandelica* and *Trevesia palmata* leaf extract products (ligands). (A, F) Quercetin-3-O-rutinoside (binding affinity –11.4 kcal/mol); (B, G) Paclitaxel (binding affinity –11.4 kcal/mol); (C, H)

Oxyacanthine (binding affinity –10.9 kcal/mol); and (D, I) Kaempferol-3-O-rutinoside (binding affinity −11.3 kcal/mol) and (E, J) Quercetin 3-O-[2"-O-(6"'-O-p-coumaroyl)-b-D-glucopyranosyl]-a-L-rhamnopyranoside (binding affinity −11.0 kcal/mol). iNOS: Inducible nitric oxide synthase.

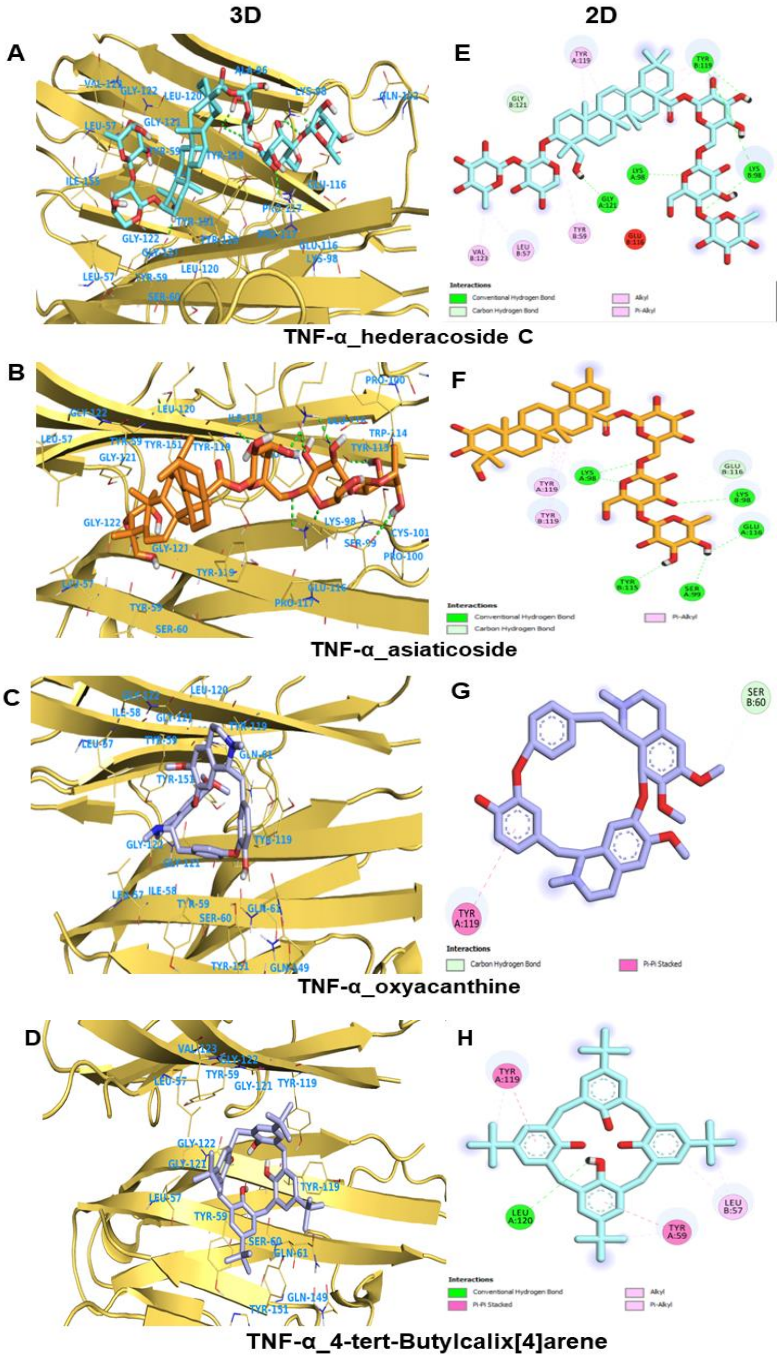

Figure 17: Three dimensional (3D) and two dimensional (2D) docking poses showing the interactions of the active site residues of TNF-α receptor with the top hit

potential bioactive compounds from *Lannea coromandelica* and *Trevesia palmata* leaf extract products (ligands). (A, E) Hederacoside C (binding affinity –9.2 kcal/mol); (B, F) Asiaticoside (binding affinity –10.0 kcal/mol); (C, G) Oxyacanthine (binding affinity –9.3 kcal/mol); and (D, H) 4-tert-Butylcalix[4]arene (binding affinity −9.5 kcal/mol). TNF- α: Tumor necrosis factor alpha.

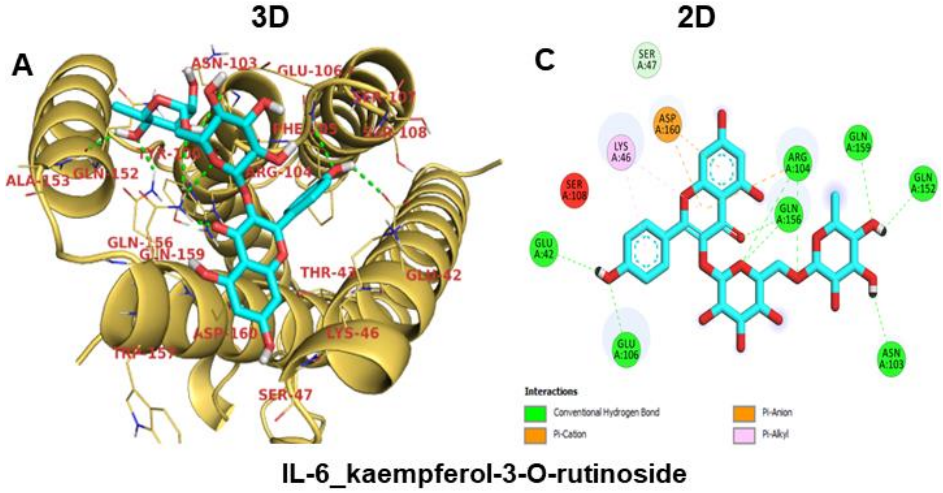

Figure 18: Three dimensional (3D) and two dimensional (2D) docking poses showing the interactions of the active site residues of TNF-α receptor with the top hit potential bioactive compounds of *Trevesia palmata* leaf extract products (ligands). (A, C) Kaempferol-3-O-rutinoside (binding affinity −8.1 kcal/mol). IL-6: Interleukin-6

4.4. Physicochemical properties

Physicochemical properties are summarized in Table 18 and 19.

Table 18 shows the result of physicochemical properties for phytochemicals derived from *L. coromandelica*. The ideal molecular weight is between 100 and 600 hydrogen atoms (Da). The molecular weight of the 26 compounds ranges from 200-600 Da. Out of 31 compounds, 25 compounds have 0-12 number of hydrogen bond acceptor (nHA) which is in the optimal range and 6 compounds namely 7-O-Methylquercetin-3-O-galactoside-6"-rhamnoside, Quercetin-3-O-rutinoside, Kaempferol 7-neohesperidoside, Kaempferol-3-O-rutinoside, [Gallocatechin-

(4alpha->8)]2-catechin and Paclitaxel have (nHA) more than the optimal range. The number of hydrogen bond donors is determined based on the total of all OHs and NHs. The ideal range is 0-7. 25 compounds have an optimal range of (nHD), while 6 compounds namely 7-O-Methylquercetin-3-O-galactoside-6"-rhamnoside, Quercetin-3-O-rutinoside, Kaempferol 7-neohesperidoside, Kaempferol-3-O-rutinoside, [Gallocatechin-(4alpha->8)]2-catechin and Luteolin-6-C-glucoside have (nHD) more than the optimal value. The optimal range for the number of rotatable (nRot) bonds ranges from 0-11, out of which 20 compounds are under the optimal range, while 11 compounds exceed the optimal range. Number of rotatable rings (nRing) ideal range is 0-6, in which 29 compounds are under the optimal range and 2 compounds including [Gallocatechin-(4alpha->8)]2-catechin and Paclitaxel shows higher than the optimal range. A number of rigid bonds (nRig) as opposed to rotatable bonds should range between 0-30. 27 compounds are under the optimal range which enables the molecule to establish a stable conformation at its target while 4 compounds including 4-tert-Butylcalix[4]arene, 7-O-Methylquercetin-3-O-galactoside-6"-rhamnoside, [Gallocatechin-(4alpha->8)]2-catechin and Paclitaxel showed higer than the optimal range. The Flexibility is calculated as (nRot) divided by (nRig). Flexibility values represent the degree of molecular flexibility of each compound. Compounds with higher flexibility values tend to have greater degrees of freedom in their molecular structures, allowing them to adopt a wider range of conformations. Compounds with lower flexibility values may have more rigid molecular structures, which can impact their interactions with biological targets and their overall pharmacological properties. The flexibility of a compound can influence its bioavailability, metabolism, and potential therapeutic effects. The topological polar surface area (TPSA) optimal range is 0-140, in which 23 compounds are under the optimal range and 8 compounds exceed the ideal range. The logarithm of aqueous solubility (logS) ideal value ranges from -4 to 0.5 log mol/L. 12 compounds out of 31 are under the optimal range. The logarithm of the n-octanol/water distribution coefficient (LogP) ideal value ranges from 0 to 3 log mol/L. Of 31 compounds, only 5 compounds are under the ideal range. The logarithm of the n-octanol/water distribution coefficients (LogD7.4) at pH=7.4 optimal value ranges from 1 to 3 log mol/L. Only 12 compounds are under the ideal range.

Table 18: Physicochemical property prediction of compounds identified from *Lannea coromandelica* using ADMETlab 2.0 webserver (https://admetmesh.scbdd.com/service/evaluation/cal).

Compound	M.W (g/mol)	nHA	nHD	nRot	nRing	nRig	Flexibility	TPSA	LogS	LogP	LogD7.4
Caryophyllene	220.180	1	0	0	3	15	0.000	12.530	- 5.153	4.474	4.143
Phenol, 3,5-bis(1,1-dimethylethyl)-	206.17	1	1	2	1	6	0.333	20.23	-4.426	5.045	4.567
Diethyl Phthalate	222.090	4	0	6	4	8	0.750	52.600	- 2.513	2.681	2.736
Phenol, 2,4-bis(1,1-dimethylethyl)-5-methyl-	220.18	1	1	2	1	6	0.333	20.23	-4.954	5.155	4.509
Pentadecanoic acid	242.220	2	1	13	0	1	13.000	37.300	- 4.814	6.283	3.135
Oxirane, tetradecyl-	240.250	1	0	13	1	3	4.333	12.530	-6.526	6.795	4.319
cis-9-Hexadecenal	238.23	1	0	13	0	2	6.500	17.070	-5.569	6.171	4.141
Phytol	296.310	1	1	13	0	1	13.000	20.230	- 6.641	7.764	5.599
9-Eicosene, (E)-	280.31	0	0	16	0	1	16.000	0.0	-7.262	9.512	5.011
1-Hexadecanol	242.260	1	1	14	0	0	-	20.230	- 6.475	6.773	3.956
Bis(2-ethylhexyl) phthalate	390.28	4	0	16	1	8	2.000	52.6	-5.291	7.337	5.716
Phenol, 2,4-bis(1,1-dimethylethyl)-	206.17	1	1	2	1	6	0.333	20.23	-4.599	4.832	4.333
4-tert-Butylcalix[4]arene	648.420	4	4	4	5	32	0.125	80.920	-5.190	10.072	5.642
Hesperetin	302.080	6	3	2	3	18	0.111	96.220	- 3.975	2.473	2.600
Nantenine	339.150	5	0	2	5	24	0.083	40.160	- 3.014	3.054	2.944
7-O-Methylquercetin-3-O-galactoside-6"-rhamnoside	770.230	20	11	9	6	36	0.250	317.350	-3.756	-0.928	1.082
Kaempferol	286.050	6	4	1	3	18	0.056	111.130	- 3.624	2.656	2.233
Quercetin-3-O-rutinoside	610.150	16	10	6	5	30	-	269.430	- 3.928	-0.763	0.695
Beta-Carotene	536.440	0	0	10	2	21	0.476	0.000	- 7.973	11.150	6.646
gamma-Carotene	536.440	0	0	13	1	17	0.765	0.000	- 7.805	11.108	6.304

Kaempferol 7-neohesperidoside	594.160	15	9	6	5	30	0.200	249.200	- 3.687	-0.393	0.974
Kaempferol-3-O-rutinoside	594.500	15	9	6	5	30	0.200	249.200	- 3.952	-0.553	1.052
zeta-Carotene	540.900	0	0	18	0	11	1.636	0.000	- 7.536	12.135	6.763
[Gallocatechin-(4alpha->8)]2-catechin	898.200	20	17	5	9	51	0.098	371.600	-3.977	1.873	1.251
Diatoxanthin	566.410	2	2	8	2	21	0.381	40.460	- 7.085	9.078	5.727
Zeaxanthin	568.430	2	2	10	2	21	-	40.460	- 7.119	9.238	5.660
Lutein	568.430	2	2	10	2	21	0.476	40.460	- 6.746	9.133	5.672
Paclitaxel	853.330	15	4	15	7	44	0.341	221.290	-4.080	3.153	1.939
Chlorogenic acid	354.100	9	6	5	2	15	0.333	164.750	- 1.198	-0.162	0.005
Luteolin-6-C-glucoside	448.100	11	8	3	4	24	-	201.280	- 3.702	-0.021	0.111
Linoleic Acid	280.240	2	1	14	0	3	4.667	37.300	- 5.230	6.652	3.580

MW: The ideal molecular weight is between 100 and 600 hydrogen atoms (Da); **nHA**: The number of hydrogen bond acceptors is computed based on the total of all O and N. The ideal value is 0–12. **nHD**: The number of hydrogen bond donors is determined based on the total of all OHs and NHs. The ideal range is 0-7. **nRot**: The number of rotatable bonds. Amide C-N bonds are excluded from being taken into account in certain contexts because of their high rotational energy barrier. Optimal:0-11. **nRing**: Number of rings. Ideal value:0-6. **nRig**: Number of rigid bonds as opposed to rotatable bonds. Optimum value:0-30. **Flexibility**: Flexibility = nRot / nRig. **TPSA**: Topological polar surface area ($Å^2$). Total of the polar fragments' tabulated surface contributions. Optimal: 0-140, based on Veber rule. **LogS**: The logarithm of aqueous solubility value. Compounds in the range from -4 to 0.5 log mol/L will be considered the compound is water soluble. **LogP**: The logarithm of the n-octanol/water distribution coefficient. Compounds in the range from 0 to 3 log

mol/L will be considered the compound is membrane permeable and bind to the target. **LogD7.4**: The logarithm of the n-octanol/water distribution coefficients at pH=7.4. Compounds in the range from 1 to 3 log mol/L will be considered to dissolve in bodily fluid and successfully penetrate the bio-membrane

Table 19: Physicochemical property prediction of compounds identified from *Trevesia palmata* using ADMETlab webserver (https://admetmesh.scbdd.com/service/evaluation/cal)

Compounds	M.W	nHA	nHD	nRot	nRing	nRig	Flexibility	TPSA	LogS	LogP	LogD7.4
Icariin	676.240	15	8	9	5	31	0.290	238.20	-3.781	1.587	2.066
Apigenin-6-C-glucoside-7-O-glucoside	594.160	15	10	6	5	30	0.200	260.20	-3.489	- 0.893	0.153
Kaempferol 3-O-sophoroside	610.15	16	10	7	5	30	0.233	269.43	-3.418	- 1.071	0.249
Kaempferol-3-O-rutinoside	594.160	15	9	6	5	30	0.200	249.20	-3.952	- 0.553	1.052
Kaempferol 4'-methyl ether 3-(4Rha-rhamnosylrutinoside)	754.23	19	10	9	6	36	0.25	297.12	-3.864	- 0.666	1.371
7,9-Di-tert-butyl-1-oxaspiro(4,5)deca-6,9-diene-2,8-dione	276.170	3	0	2	2	13	0.154	43.370	-4.720	3.915	3.576
Quercetin 3-O-[2"-O-(6"'-O-p-coumaroyl)-b-D-glucopyranosyl]-a-L-rhamnopyranoside	756.190	18	10	10	6	38	0.263	295.73	-4.359	1.619	2.098
gamma.-Tocopherol	416.370	2	1	12	2	11	1.091	29.460	-6.926	9.347	6.556
dl-.alpha.-Tocopherol	430.380	2	1	12	2	11	1.091	29.460	-6.500	9.624	6.351
Asiaticoside	256.11	3	1	4	2	13	0.308	38.69	-4.012	3.831	3.798
Bacoside A3	928.500	18	10	10	9	46	0.217	276.140	-2.208	1.434	1.731

Hederacoside C	1220.62	26	15	14	10	57	0.246	412.820	-1.498	- 0.542	1.418
alpha.-Amyrin	426.390	1	1	0	5	26	0.000	20.230	-6.357	7.352	5.667
Neophytadiene	222.05	5	1	2	2	12	0.167	68.9	-2.39	0.942	1.125
Phytol	296.5	1	14	0	3	4.67	37.300	-5.230	6.652	3.580	5.599
alpha-Hederin	750.460	12	7	6	7	39	0.154	195.60	-3.323	3.348	3.653
Zeaxanthin	568.430	2	2	10	2	21	0.476	40.460	-7.119	9.238	5.660
Lutein	568.430	2	2	10	2	21	0.476	40.460	-6.746	9.133	5.672
zeta-Carotene	540.470	0	0	18	0	11	1.636	0.000	-7.536	12.135	6.763
Isopropyl Tetradecanoate	270.260	2	0	14	0	1	14.000	26.300	-6.508	6.768	4.637
Linoleic Acid	280.240	2	1	14	0	3	4.667	37.300	-5.230	6.652	3.580
Linolenic acid	278.220	2	1	13	0	4	3.250	37.300	-4.973	6.156	3.690
Oxyacanthine	608.290	8	1	3	8	42	0.071	72.860	-4.152	5.476	4.091
Honokiol	266.130	2	2	5	2	14	266.130	40.460	-4.176	4.870	3.787
Beta-Sitosterol	414.390	1	1	6	4	20	0.300	20.230	-7.052	7.663	6.329
Thalsimine	636.280	9	0	5	8	42	0.119	80.210	-6.390	6.281	3.910
Isofraxidin	424.140	10	3	1	6	27	0.037	148.820	-3.522	0.928	0.892

MW: The ideal molecular weight is between 100 and 600 hydrogen atoms (Da). **nHA**: The number of hydrogen bond acceptors is computed based on the total of all O and N. The ideal value is 0–12. **nHD**: The number of hydrogen bond donors is determined based on the total of all OHs and NHs. The ideal range is 0-7. **nRot**: The number of rotatable bonds. Amide C-N bonds are excluded from being taken into account in certain contexts because of their high rotational energy barrier. Optimal:0-11. **nRing**: Number of rings. Ideal value:0-6. **nRig**: Number of rigid bonds as opposed to rotatable bonds. Optimum value:0-30. **Flexibility**: Flexibility = nRot / nRig. **TPSA**: Topological polar surface area ($Å^2$). Total of the polar fragments' tabulated surface contributions. Optimal: 0-140, based on Veber rule. **LogS**: The logarithm of aqueous solubility value. Compounds in the range from -4 to 0.5 log mol/L will be considered the compound is water soluble. **LogP**: The logarithm of the n-octanol/water distribution coefficient. Compounds in the range from 0 to 3 log mol/L will be considered the compound is membrane permeable and bind to the target. **LogD7.4**: The logarithm of the n-octanol/water distribution coefficients at pH=7.4. Compounds in the range from 1 to 3 log mol/L will be considered to dissolve in bodily fluid and successfully penetrate the bio-membrane

Table 19 shows the result of physicochemical properties for phytochemicals derived from *T. palmata*. The ideal molecular weight is between 100 and 600 hydrogen atoms (Da). The molecular weight of the 16 compounds ranges from 200-600 Da. Out of 26 compounds, 19 compounds have 0-12 number of hydrogen bond acceptor (nHA) which is in the optimal range and 7 compounds namely Icariin, Apigenin-6-C-glucoside-7-O-glucoside, Kaempferol 3-O-sophoroside, Kaempferol 4'-methyl ether 3-(4Rha-rhamnosylrutinoside), Quercetin 3-O-[2"-O-(6'"-O-p-coumaroyl)-b-D-glucopyranosyl]-a-L-rhamnopyranoside, Bacoside A3 and Hederacoside C have (nHA) more than the optimal range. The number of hydrogen bond donors is determined based on the total of all OHs and NHs. The ideal range is 0-7. 18 compounds have an optimal range of (nHD), while 8 compounds namely 7 Icariin, Apigenin-6-C-glucoside-7-O-glucoside, Kaempferol 3-O-sophoroside, Kaempferol-3-O-rutinoside, Kaempferol 4'-methyl ether 3-(4Rha-rhamnosylrutinoside), Quercetin 3-O-[2"-O-(6'"-O-p-coumaroyl)-b-D-glucopyranosyl]-a-L-rhamnopyranoside, Bacoside A3, Hederacoside C and Phytol have (nHD) more than the optimal value. The optimal range for the number of rotatable (nRot) bonds ranges from 0-11, out of which 20 compounds are under the optimal range, while 11 compounds exceed the optimal range. Number of rotatable rings (nRing) ideal range is 0-6, in which 22 compounds are under the optimal range and 4 compounds including Bacoside A3, Hederacoside C, alpha-Hederin and Oxyacanthine shows higher than the optimal range. A number of rigid bonds (nRig) as opposed to rotatable bonds should range between 0-30. 17 compounds are under the optimal range which enables the molecule to establish a stable conformation at its target while 9 compounds showed higer than the optimal range. The Flexibility is calculated as (nRot) divided by (nRig). Flexibility values represent the degree of molecular flexibility of each compound. Compounds with higher flexibility values tend to have greater degrees of freedom in their molecular structures, allowing them to adopt a wider range of conformations. Compounds with lower flexibility values may have more rigid molecular structures, which can impact their interactions with biological targets and their overall pharmacological properties. The flexibility of a compound can influence its bioavailability, metabolism, and potential therapeutic effects. The topological polar surface area (TPSA) optimal range is 0-140, in which

17 compounds are under the optimal range and 9 compounds exceed the ideal range. The logarithm of aqueous solubility (logS) ideal value ranges from -4 to 0.5 log mol/L. 11 compounds out of 26 are under the optimal range. The logarithm of the n-octanol/water distribution coefficient (LogP) ideal value ranges from 0 to 3 log mol/L. Of 31 compounds, only 5 compounds are under the ideal range. The logarithm of the n-octanol/water distribution coefficients (LogD7.4) at pH=7.4 optimal value ranges from 1 to 3 log mol/L. Only 8 compounds are under the ideal range.

Compounds with molecular weights closer to the optimal range for drug-like properties are generally more desirable for drug development due to their favourable pharmacokinetic profiles. However, other factors such as potency, specificity, and safety profiles also play significant roles in determining the suitability of a compound for drug development.

3.4.5. Medicinal chemistry

Medicinal Chemistry properties are summarized in Table 20 and 21.

In *L. coromandelica*, the QED score (quantitative estimate of drug-likeness) of 21 compounds is lesser than 0.67(<0.67), and only 5 compounds are greater than 0.67 (>0.67). The Synthetic accessibility score (SAscore) of 21 compounds has a low SAscore, i.e., lesser than 6 (<6). The number of sp3 hybridized carbons/total carbon count (Fsp3) of 15 compounds is greater than 0.42 (>0.42), while 5 compounds have (Fsp3) lower than 0.42 (<0.42). Pan assay interference compounds (PAINS) of 26 compounds have zero (0) alerts, and only 5 compounds have one (1) alert. Medicinal chemistry evolution in 2018 (MCE-18) of 9 compounds is greater than 45 (>45), and 10 compounds have (MCE-18) lower than 45 (<45). The natural product-likeness score (NPscore) of all 31 compounds ranges from -5 to 5, which is the ideal range. 10 compounds were accepted by the Lipinski Rule, while 5 compounds were rejected. 9 compounds were accepted by the Pfizer Rule, while 11 compounds were rejected. 2 compounds were accepted by the GSK Rule, while 18 compounds were rejected. 8 compounds were accepted in Golden Triangle, while 9 compounds were rejected.

Table 20: Prediction of medicinal chemistry characteristics of compounds identified from *Lannea coromandelica* using ADMETlab 2.0 webserver (https://admetmesh.scbdd.com/service/evaluation/cal).

Compound	Medicinal chemistry									
	QED	SA score	Fsp3	PAINS	MCE-18	NP Score	Lipinski Rule	Pfizer Rule	GSK Rule	Golden Triangle
Caryophyllene	0.445	4.590	0.867	0	51.571	3.678	-	Accepted	-	-
Phenol, 3,5-bis(1,1-dimethylethyl)-	0.680	2.097	0.571	0	12.000	0.060	Accepted	Rejected	Rejected	Accepted
Diethyl Phthalate	-	-	0.333	0	7.000	-0.393	Accepted	Accepted	Accepted	Accepted
Phenol, 2,4-bis(1,1-dimethylethyl)-5-methyl-	0.691	2.328	0.6	0	13.000	0.353	Accepted	Rejected	Rejected	Accepted
Pentadecanoic acid	0.453	-	-	0	-	0.408	-	Accepted	Rejected	-
Oxirane, tetradecyl-	0.307	-	1.000	0	8.500	0.652	Accepted	Rejected	Rejected	Accepted
cis-9-Hexadecenal	0.237	2.245	0.812	0	0.0	1.167	Accepted	Rejected	Rejected	Accepted
Phytol	-	-	-	0	0.0	1.044	-	-	-	-
9-Eicosene, (E)-	0.2	1.732	0.9	0	0.0	0.645	Accepted	Rejected	Rejected	Rejected
1-Hexadecanol	0.401	1.536	1.000	0		0.442	0.000	Accepted	Rejected	Accepted
Bis(2-ethylhexyl) phthalate	0.343	3.007	0.667	0	18.0	0.091	Accepted	Rejected	Rejected	Rejected
Phenol, 2,4-bis(1,1-dimethylethyl)-	0.68	2.015	0.571	0	12.0	-0.064	Accepted	Rejected	Accepted	Rejected
4-tert-Butylcalix[4]arene	0.135	4.599	0.455	0	91.375	0.057	Accepted	Rejected	Rejected	Accepted
Hesperetin	0.789	2.912	0.188	0	57.789	1.713	-	-	-	-
Nantenine	0.840	-	-	0	-	1.385	-	Rejected	-	-
7-O-Methylquercetin-3-O-galactoside-6''-rhamnoside	0.100	5.386	0.559	1	153.340	1.768	Rejected	Accepted	Rejected	Rejected
Kaempferol	-	2.375	-	0	-	1.546	-	-	-	-
Quercetin-3-O-rutinoside	0.140	4.783	0.444	1	122.949	2.015	-	-	Rejected	Rejected
Beta-Carotene	0.244	3.693	0.450	0	-	1.127	Rejected	Rejected	Rejected	Rejected
gamma-Carotene	0.162	3.859	-	0	-	1.701	-	-	-	-
Kaempferol 7-neohesperidoside	0.159	-	-	0	-	2.148	-	-	-	-
Kaempferol-3-O-rutinoside	0.159	4.680	-	0	-	1.945	-	-	Rejected	-

zeta-Carotene	0.120	-	-	0	-	1.225	-	-	-	-
[Gallocatechin-(4alpha->8)]2-catechin	0.109	5.557	0.200	1	200.000	1.416	Rejected	Accepted	Rejected	Rejected
Diatoxanthin	0.227	-	-	0	-	1.758	-	-	-	-
Zeaxanthin	0.257	-	-	0	50.069	1.300	Rejected	Rejected	Rejected	Rejected
Lutein	-	4.960	-	0	-	2.115	-	-	-	-
Paclitaxel	0.130	5.916	0.447	0	175.882	1.871	Rejected	Accepted	Rejected	Rejected
Chlorogenic acid	0.234	3.871	0.375	1	-	2.246	-	-	-	-
Luteolin-6-C-glucoside	-	4.060	0.286	1	91.000	2.027	-	Accepted	Rejected	Accepted
Linoleic Acid	0.318	-	0.722	0	0.000	1.187	Accepted	Accepted	Rejected	-

QED: Quantitative estimate of druglikeness. > 0.67: favorable drug likeness property; ≤ 0.67: unfavorable drug likeness property. **SAscore**: Synthetic accessibility score. ≥ 6: high SAscore, difficult to synthesize; < 6: low SAscore, easy to synthesize. **Fsp^3**: the number of sp3 hybridized carbons/total carbon count. ≥ 0.42: high solubility; ＜0.42: poor solubility. **PAINS**: Pan assay interference compounds. Zero alert means the molecule having no interference toward the biological assays. **MCE-18**: Medicinal chemistry evolution in 2018. ≥ 45: possess drug like qualities; ＜45: lacks drug like qualities. **NPscore**: The natural product-likeness score. A score of -5.0 to 5.0 indicates a greater likelihood that the molecule is a natural product. **Lipinski Rule** (molecular weight ≤500, logP ≤5, hydrogen bond acceptor ≤10, and hydrogen donors ≤5): <2 violation means high absorption and permeability; ≥2 violations mean a poor absorption and permeability. **Pfizer Rule**: High log P (>3 log mol/L) and a low TPSA (<75 Å^2) are probably toxic. **GSK Rule**: Compound satisfying the parameters of MW ≤400 and logP ≤4 may have a more favorable ADMET profile and accepted. Violation of these parameters is considered as unfavorable ADMET profile and rejected. **GoldenTriangle**: Compound possesses 200 ≤MW ≤50; -2 ≤ logD ≤5 may have a more favourable ADMET profile and accepted. Violation of these limits measured as unfavorable ADMET profile and rejected.

Table 21: Prediction of medicinal chemistry characteristics of compounds identified from *Trevesia palmata* using ADMETlab webserver (https://admetmesh.scbdd.com/service/evaluation/cal).

Compounds	Medicinal chemistry									
	QED	SA score	Fsp3	PAINS	MCE-18	NP score	Lipinski Rule	Pfizer Rule	GSK Rule	Golden Triangle
Icariin	0.140	4.912	0.485	0	122.694	1.959	Rejected	Accepted	Rejected	Rejected
Apigenin-6-C-glucoside-7-O-glucoside	0.142	4.717	0.444	0	119.436	1.714	Rejected	Accepted	Rejected	Rejected
Kaempferol 3-O-sophoroside	0.133	4.684	0.444	0	119.436	1.858	Rejected	Accepted	Rejected	Rejected
Kaempferol -3-O-rutinoside	0.159	4.680	0.444	0	119.436	1.945	Rejected	Accepted	Rejected	Rejected
Kaempferol 4'-methyl ether 3-(4Rha-rhamnosylrutinoside)	0.11	5.274	0.559	0	149.774	1.775	Rejected	Accepted	Rejected	Rejected
7,9-Di-tert-butyl-1-oxaspiro(4,5)deca-6,9-diene-2,8-dione	0.635	3.796	0.647	0	42.071	0.842	Accepted	Rejected	Accepted	Accepted
Quercetin 3-O-[2"-O-(6"'-O-p-coumaroyl)-b-D-glucopyranosyl]-a-L-rhamnopyranoside	0.062	5.045	0.333	1	140.083	1.906	Rejected	Accepted	Rejected	Rejected
gamma.-Tocopherol	0.370	3.786	0.786	0	53.040	1.571	Accepted	Rejected	Rejected	Rejected
dl-.alpha.-Tocopherol	0.359	3.780	0.793	0	56.077	1.500	Accepted	Rejected	Rejected	Rejected
Asiaticoside	0.097	6.502	0.938	0	173.419	2.605	Rejected	Accepted	Rejected	Rejected
Bacoside A3	0.102	7.872	0.957	0	248.217	2.379	Rejected	Accepted	Rejected	Rejected
Hederacoside C	0.051	7.256	0.949	0	217.043	2.197	Rejected	Accepted	Rejected	Rejected
alpha.-Amyrin	0.389	4.695	0.933	0	99.517	3.255	Accepted	Rejected	Rejected	Rejected
Neophytadiene	0.313	3.426	0.800	0	4.000	1.365	Accepted	Rejected	Rejected	Rejected
Phytol	0.392	3.291	0.900	0	4.000	1.532	Accepted	Rejected	Rejected	Rejected

alpha-Hederin	0.155	5.779	0.927	0	149.013	2.989	Rejected	Accepted	Rejected	Rejected
Zeaxanthin	0.257	4.577	0.450	0	50.069	1.300	Rejected	Rejected	Rejected	Rejected
Lutein	0.203	4.960	0.450	0	50.069	2.115	Rejected	Rejected	Rejected	Rejected
zeta-Carotene	0.120	3.480	0.450	0	0.000	1.225	Rejected	Rejected	Rejected	Rejected
Linolenic acid	0.348	2.589	0.611	0	0.000	1.358	Accepted	Rejected	Accepted	Rejected
Linoleic Acid	0.318	2.292	0.722	0	0.000	1.187	Accepted	Rejected	Rejected	Accepted
Oxyacanthine	0.271	5.740	0.351	0	129.480	1.893	Rejected	Rejected	Rejected	Rejected
Honokiol	0.795	2.442	0.111	0	12.00	0.879	Accepted	Rejected	Rejected	Accepted
Beta-Sitosterol	0.436	4.388	0.931	0	68.464	2.681	Accepted	Rejected	Rejected	Rejected
Thalsimine	0.232	5.694	0.342	0	127.706	1.893	Rejected	Accepted	Rejected	Rejected
Isofraxidin	0.78	2.276	0.182	0	12.0	1.395	Accepted	Accepted	Accepted	Accepted

QED: Quantitative estimate of druglikeness. > 0.67: favorable drug likeness property; ≤ 0.67: unfavorable drug likeness property. **SAscore**: Synthetic accessibility score. ≥ 6: high SAscore, difficult to synthesize; < 6: low SAscore, easy to synthesize. **Fsp^3**: the number of sp3 hybridized carbons/total carbon count. ≥ 0.42: high solubility; ＜0.42: poor solubility. **PAINS**: Pan assay interference compounds. Zero alert means the molecule having no interference toward the biological assays. **MCE-18**: Medicinal chemistry evolution in 2018. ≥ 45: possess drug like qualities; ＜45: lacks drug like qualities. **NPscore**: The natural product-likeness score. A score of -5.0 to 5.0 indicates a greater likelihood that the molecule is a natural product. **Lipinski Rule** (molecular weight ≤500, logP ≤5, hydrogen bond acceptor ≤10, and hydrogen donors ≤5): <2 violation means high absorption and permeability; ≥2 violations mean a poor

absorption and permeability. **Pfizer Rule**: High log P (>3 log mol/L) and a low TPSA (<75 $Å^2$) are probably toxic. **GSK Rule**: Compound satisfying the parameters of MW ≤400 and logP ≤4 may have a more favorable ADMET profile and accepted. Violation of these parameters is considered as unfavorable ADMET profile and rejected. **GoldenTriangle**: Compound possesses 200 ≤MW ≤50; -2 ≤ logD ≤5 may have a more favourable ADMET profile and accepted. Violation of these limits measured as unfavorable ADMET profile and rejected.

In *T. palmata*, the QED score (quantitative estimate of drug-likeness) of 24 compounds is lesser than 0.67(<0.67), and only 2 compounds are greater than 0.67 (>0.67). The Synthetic accessibility score (SAscore) of 23 compounds has a low SAscore, i.e., lesser than 6 (<6). The number of sp3 hybridized carbons/total carbon count (Fsp3) of 22 compounds is greater than 0.42 (>0.42), while 4 compounds have (Fsp3) lower than 0.42 (<0.42). Pan assay interference compounds (PAINS) of 25 compounds have zero (0) alerts, and only 1 compound have one (1) alert. Medicinal chemistry evolution in 2018 (MCE-18) of 18 compounds is greater than 45 (>45), and 8 compounds have (MCE-18) lower than 45 (<45). The natural product-likeness score (NPscore) of all 31 compounds ranges from -5 to 5, which is the ideal range. 12 compounds were accepted by the Lipinski Rule, while 14 compounds were rejected. 12 compounds were accepted by the Pfizer Rule, while 14 compounds were rejected. 2 compounds were accepted by the GSK Rule, while 24 compounds were rejected. 5 compounds were accepted in Golden Triangle, while 21 compounds were rejected.

Compounds with higher QED scores are more likely to exhibit drug-like properties. Lower SA scores indicate compounds that are easier to synthesize. A higher Fsp3 value suggests a more saturated and potentially drug-like compound. Absence of PAINS substructures (PAINS = 0) are desirable as it reduces the likelihood of compound interference in assays. Higher MCE-18 values indicate greater molecular complexity, often desirable in drug development. Compounds accepted by Lipinski's Rule of Five, Pfizer Rule, and GSK Rule are more likely to have favorable pharmacokinetic properties. Compounds with natural product likeness (NP score) closer to 3 are more similar to natural products. Compounds accepted by Lipinski's Rule and other pharmaceutical rules are more likely to be progressed in drug development. Rejection by these rules may indicate potential challenges in drug development or undesirable properties.

3.4.6. Pharmacokinetics; Absorption, Distribution, and Excretion

Pharmacokinetic properties are summarized in Table 22 and Table 23.

In *L. coromandelica* (Table 22), Colon adenocarcinoma cell lines permeability (Caco-2) of 13 compounds are greater than -5.15 cm/s (>-5.15 cm/s), while 18 compounds are lower than -5.15 cm/s (<-5.15 cm/s). Madin−Darby Canine Kidney cells permeability (MDCK) of 11 compounds is lesser than 2×10^{-6} cm/s (< 2 ×10-6 cm/s), 20 compounds with (MDCK) ranging from 2-20 $\times10^{-6}$ cm/s, and no compound with MDCK greater than 20×10^{-6} cm/s (>20×10^{-6} cm/s). Out of 31 compounds, the permeability glycoprotein-substrate (Pgp-substrate) of 18 compounds ranges from 0.0-0.1 and 11 compounds have Pgp-substrate that ranges from 0.9-1.0. The permeability glycoprotein-inhibitor (Pgp-inhibitor) of 12 compounds ranges from 0.0-0.3, while 10 compounds have a Pgp-inhibitor greater than 0.3 (>0.3). The Human intestinal absorption (HIA) of 12 compounds ranges from 0.0-0.3, and 9 compounds with a value ranging from 0.7-1.0. The human oral bioavailability 20% (F20%) of 18 compounds ranges from 0.0-0.3, 2 compounds with values ranging from 0.3-07, and 8 compounds with values ranging from 0.7-1.0. The human oral bioavailability 30% (F30%) of 3 compounds ranges from 0.0-0.3, 2 compounds with values ranging from 0.3-0.7, and 15 compounds with values ranging from 0.7-1.0. The Plasma Protein Binding (PPB) of 19 compounds is lesser than 90% (<90%), and 12 compounds with (PPB) greater than 90% (>90%). Volume distribution (VD) of 26 compounds ranges from 0.4-20 L/kg. Blood-Brain Barrier penetration (BBB) of 25 compounds ranges from 0.0-0.3, 2 compounds with a value ranging from 0.3-0.7, and 4 compounds with a value ranging from 0.7-1.0. The fraction unbound in plasma (FU) of 13 compounds is greater than 5% (>5%), and 14 compounds with (FU) lesser than 5% (<5%). The clearance of a drug (CL) of 15 compounds is less than 5 mL/min/kg, 14 compounds with (CL) ranging from 5-15 mL/min/kg, and 2 compounds with (CL) greater than (>15 mL/min/kg). The half-life of a drug (T1/2) of 10 compounds ranges from 0.0-0.3, 13 compounds with (T1/2) ranging from 0.3-0.7, and 8 compounds with (T1/2) ranging from 0.7-1.0.

Table 22: Prediction of absorption, distribution and excretion properties of compounds identified from *Lannea coromandelica* using ADMETlab 2.0 webserver (https://admetmesh.scbdd.com/service/evaluation/cal).

Compound	Absorption							Distribution				Excretion	
	Caco-2 Permeability	MDCK Permeability	Pgp-inhibitor	Pgp-substrate	HIA	$F_{20\%}$	$F_{30\%}$	PPB (%)	VD	BBB Penetration	Fu (%)	CL	$T_{1/2}$
Caryophyllene	-4.679	0.034	0.003 ---	0.034 ---	0.003 ---	0.048 ---	0.011 ---	86.24	1.469	0.745 ++	11.12	15.503	0.083
Phenol, 3,5-bis(1,1-dimethylethyl)-	-5.107	8e-06	0.158 --	0.008 ---	0.546 +	0.998 +++	0.994 +++	96.63	4.514	0.578 +	6.812	7.521	0.348
Diethyl Phthalate	-4.385	3.7e-05	0.03 ---	0.0 ---	0.002 ---	0.98 +++	0.992 +++	69.264	1.316	0.115 --	9.509	12.247	0.357
Phenol, 2,4-bis(1,1-dimethylethyl)-5-methyl-	-5.318	1e-05	0.334 -	0.006 ---	0.935 +++	0.998 +++	0.997 +++	98.84	5.222	0.411 -	4.207	6.339	0.263
Pentadecanoic acid	-4.996	2.7e-05	0.017 ---	0.0 ---	0.005 ---	0.7 +	0.989 +++	98.652	0.514	0.094 ---	1.117	2.343	0.670
Oxirane, tetradecyl-	-4.735	1.7e-05	0.006 ---	0.0 ---	0.002 ---	0.281 --	0.959 +++	97.662	1.620	0.133 --	1.687	4.314	0.098
cis-9-Hexadecenal	-4.671	1.3e-05	0.002 ---	0.003 ---	0.005 ---	0.863 ++	0.917 +++	93.27	3.331	0.953 +++	2.531	4.447	0.199
Phytol	-4.338	1.1e-05	0.034 ---	0.001 ---	0.002 ---	0.687 +	0.357 -	97.641	3.722	0.227 --	2.400	8.161	0.073
9-Eicosene, (E)-	-4.794	7e-06	0.0	0.002	0.003	0.122	0.96	98.68	4.69	0.064	1.60	4.713	0.046

			---	---	---	--	1 +++		3	---	0		
1-Hexadecanol	-4.728	1.6e-05	0.001 ---	0.002 ---	0.004 ---	0.156 --	0.992 +++	97.405	2.697	0.129 --	1.643	5.716	0.147
Bis(2-ethylhexyl) phthalate	-4.694	1.6e-05	0.995 +++	0.003 ---	0.001 ---	0.981 +++	0.961 +++	99.61	1.427	0.015 ---	1.107	6.965	0.13
Phenol, 2,4-bis(1,1-dimethylethyl)-	-5.048	1.1e-05	0.585 ++	0.007 ---	0.727 ++	0.989 +++	0.989 +++	98.43	4.896	0.294 --	4.953	6.3	0.324
4-tert-Butylcalix[4]arene	-6.851	7.3e-06	0.0 ---	0.017 ---	0.998 +++	0.999 +++	1.0 +++	103.955	1.797	0.027 ---	0.972	5.329	0.185
Hesperetin	-4.878	7.7e-06	0.006 ---	0.003 ---	0.014 ---	0.067 ---	0.98 +++	95.305	0.673	0.035 ---	6.130	15.680	0.73
Nantenine	-4.832	3.4e-05	0.187 --	0.822 ++	0.002 ---	0.003	0.052 ---	88.285	1.947	0.977 +++	6.371	13.457	0.254
7-O-Methylquercetin-3-O-galactoside-6"-rhamnoside	-6.325	0.000128	0.002 ---	0.994 +++	0.98 +++	0.038 ---	0.999 +++	75.97	0.603	0.163 --	26.81	0.924	0.268
Kaempferol	-4.974	9.1e-06	0.004 ---	0.011 ---	0.008 ---	0.856 ++	0.993 +++	97.861	0.522	0.009 ---	4.412	6.868	0.905
Quercetin-3-O-rutinoside	-6.336	3e-05	0.002 ---	0.978 +++	0.925 +++	0.234 --	0.999 +++	83.811	0.754	0.111 --	20.86	1.349	0.524
Beta-Carotene	-6.003	7.8e-06	1.0 +++	0.437 -	0.117 --	0.011 ---	0.318 -	101.535	7.328	0.0 ---	2.130	0.229	0.076
gamma-Carotene	-5.880	1-e05	0.999 +++	0.572 +	0.033 ---	0.008 ---	0.182 --	101.548	7.343	0.001 ---	3.554	0.107	0.100

Kaempferol 7-neohesperidoside	-6.327	5.6e-05	0.002 ---	0.978 +++	0.9 ++	0.046 ---	0.999 +++	83.062	0.688	0.121 --	10.33	1.194	0.380
Kaempferol-3-O-rutinoside	-6.277	3.1e-05	0.002 ---	0.977 +++	0.879 ++	0.162 --	0.999 +++	83.480	0.750	0.128 --	19.79	1.218	0.388
zeta-Carotene	-5.340	9e-06	0.977 +++	0.608 +	0.01 ---	0.248 --	0.929 +++	95.841	10.296	0.001 ---	3.468	0.530	0.030
[Gallocatechin-(4alpha->8)]2-catechin	-7.193	2e-06	0.0025 ---	0.0 ---	0.999 +++	0.985 +++	1.0 +++	77.76	0.33	0.0 ---	26.28	10.888	0.474
Diatoxanthin	-6.033	2.1e-05	0.999 +++	0.89 ++	0.054 ---	0.016 ---	0.032 ---	101.056	5.698		1.117	1.205	0.067
Zeaxanthin	-5.949	2.2e-05	0.999 +++	0.906 +++	0.118 --	0.005 ---	0.011 ---	99.083	4.942	0.011 ---	2.565	1.078	0.210
Lutein	-5.567	2.1 e-05	0.999 +++	0.892 ++	0.389 -	0.01 ---	0.009 ---	99.596	4.559	0.008 ---	2.431	1.066	0.13
Paclitaxel	-5.446	5.6e-05	0.999 +++	0.999 +++	0.868 ++	0.989 +++	0.98 +++	97.969	1.718	---	5.028	4.761	0.006
Chlorogenic acid	-6.127	9.9e-05	0.0 ---	0.558 +	0.873 ++	0.822 ++	0.996 +++	67.186	0.351	0.59 +	34.068	3.251	0.928
Luteolin-6-C-glucoside	-6.140	1.3e-05	0.002 ---	0.741 ++	0.936 +++	0.984 +++	1.0 +++	89.398	0.910	0.027 ---	13.446	3.640	0.718
Linoleic Acid	-4.733	1.9e-05	0.0 ---	0.002 ---	0.01 ---	0.009 ---	0.549 +	98.391	0.626	0.196 --	1.619	3.327	0.628

For the classification endpoints, the prediction probability values are transformed into six symbols: 0-0.1 (- - -), 0.1-0.3 (- -), 0.3-0.5 (-), 0.5-0.7 (+), 0.7-0.9 (++), and 0.9-1.0 (+++).

Caco-2 permeability: Colon adenocarcinoma cell lines-2 permeability. >-5.15 cm/s: highly permeable to the human intestinal epithelium. **Pgp-substrate**: Permeability glycoprotein-substrate. 0.0: no pharmacokinetic implications for Pgp substrates; 0.1–0.3: low pharmacokinetic implications for Pgp substrates and non-substrates of p-glycoprotein; 0.3–0.7: medium pharmacokinetic implications for Pgp substrates; 0.7–1.0: high pharmacokinetic implications for Pgp substrates. **HIA**: Human intestinal absorption. 0.0-0.3: high human intestinal absorption; 0.3-0.7: medium human intestinal absorption; 0.7-1.0: poor human intestinal absorption.

MDCK Permeability: Madin−Darby Canine Kidney cells. >2 $\times 10^{-6}$ cm/s: excellent permeability; 2-20 $\times$ 10^{-6} cm/s: medium permeability; < 2 $\times 10^{-6}$ cm/s: low permeability. **Pgp-inhibitor**: Permeability glycoprotein-inhibitor. 0.0-0.3: non-inhibitors of p-glycoprotein; >0.3: inhibitors of p-glycoprotein.

$F_{20\%}$: The human oral bioavailability 20%. 0.0–0.3: very high bioavailability; 0.3–0.7: medium bioavailability; 0.7–1.0: very low bioavailability**; $F_{30\%}$**: The human oral bioavailability 30%. 0.0–0.3: very high bioavailability; 0.3–0.7: medium bioavailability; 0.7–1.0: very low bioavailability

PPB: Plasma Protein Binding. ≤ 90%: excellent oral bioavailability and high therapeutic index; > 90%: poor oral bioavailability and low therapeutic index. **VD**: Volume distribution. 0.04-20 L/kg: excellent degree of tissue absorption and quantity of dispersion in body fluids; > 20 L/kg: poor degree of tissue absorption and quantity of dispersion in body fluids. **BBB Penetration**: Blood-Brain Barrier penetration. 0.0-0.3 cm/s excellent in passing through BBB to reach the target; 0.3-0.7 cm/s medium capability in passing through BBB to reach the target; 0.7-1.0 cm/s poor in passing through BBB to reach the target. **Fu**: The fraction unbound in plasma. ≥ 5%: not bound

to blood protein (unbound - efficiently it can traverse cellular membranes or diffuse); < 5%: bound to blood protein (bound - less efficiently it can traverse cellular membranes or diffuse). **CL**: The clearance of a drug. >15 mL/min/kg: high clearance; 5-15 mL/min/kg: moderate clearance; <5 mL/min/kg: low clearance**.** $\mathbf{T_{1/2}}$: The half-life of a drug involves clearance and volume of distribution. 0.0-0.3 shorter time for a chemical to be eliminated by the body; 0.3-0.7: Moderate time for a chemical to be eliminated by the body; 0.7-1.0: longer time for a chemical to be eliminated by the body**.**

Table 23: Prediction of absorption, distribution and excretion properties of compounds identified from *Trevesia palmata* using ADMETlab webserver (https://admetmesh.scbdd.com/service/evaluation/cal).

Compounds	**Absorption**							**Distribution**				**Excretion**	
	Caco-2 Permeability	**Pgp-inhibitor**	**HIA**	**MDCK Permeability**	**Pgp-substrate**	**$F_{20\%}$**	**$F_{30\%}$**	**PPB (%)**	**VD**	**BBB Penetration**	**Fu (%)**	**CL**	**$T_{1/2}$**
Icariin	-6.178	0.023 ---	0.998 ++	7.7e-05	0.883 +++	0.016 ---	0.992 +++	64.816	0.772	0.161 --	24.984	1.757	0.109
Apigenin-6-C-glucoside-7-O-glucoside	-6.334	0.95 +++	0.978 +++	0.00012	0.95 +++	0.917 +++	1.0 +++	70.566	0.643	0.422 -	28.58	1.207	0.269
Kaempferol 3-O-sophoroside	-6.353	0.001 ---	0.941 +++	7.3e-05	0.945 +++	0.912 +++	0.999 +++	79.854	0.183	0.274 --	9.586	0.593	0.032
Kaempferol-3-O-rutinoside	-6.277	0.002 ---	0.879 +++	3.1e-05	0.977 +++	0.162 --	0.999 +++	83.47	0.75	0.128 --	19.79	1.218	0.388
Kaempferol 4'-methyl ether 3-(4Rha-rhamnosylrutinoside)	-6.288	0.001 ---	0.965 +++	0.00013	0.994 +++	0.04 ---	0.999	83.807	1.002	0.194 --	5.039	10.340	0.779

							+++						
7,9-Di-tert-butyl-1-oxaspiro(4,5)deca-6,9-diene-2,8-dione	-4.646	0.966 +++	0.024 ---	1.8e-05	0.0 ---	0.01 ---	0.014 ---	91.868	1.007	0.083 ---	15.545	4.681	0.694
Quercetin 3-O-[2"-O-(6'"-O-p-coumaroyl)-b-D-glucopyranosyl]-a-L-rhamnopyranoside	-6.388	---	++	1.6e-05	+++	+++	+++	95.704	0.701	---	6.796	1.953	1.953
gamma.-Tocopherol	-4.855	0.05 ---	0.003 ---	7.6e-06	0.0 ---	0.954 +++	0.956 +++	100.603	5.329	0.838 ++	1.846	8.243	0.029
dl-.alpha.-Tocopherol	-4.776	0.023 ---	0.003 ---	7.1e-06	0.0 ---	0.964 +++	0.959 +++	101.236	6.837	0.813 ++	1.988	8.280	0.022
Asiaticoside	-6.173	0.324 -	0.997 +++	0.00028	0.071 ---	0.971 +++	0.999 +++	79.704	0.088	0.101 --	9.630	0.660	0.020
Bacoside A3	-5.931	0.989 +++	0.992 +++	0.0002	0.089 ---	0.999 +++	0.993 +++	68.909	0.009	0.077 ---	10.450	0.469	0.028
Hederacoside C	-6.089	0.953 +++	1.0 +++	0.00043	0.031 ---	0.99 +++	1.0 +++	63.170	-0.372	0.1 ---	13.740	-0.047	0.010
alpha.-Amyrin	-4.953	0.181 --	0.008 ---	6.8e-06	0.0 ---	0.434 -	0.913 +++	99.703	1.831	0.762 ++	1.813	17.973	0.008
Neophytadiene	-4.628	0.154 --	0.002 ---	5.4e-06	0.0 ---	0.004 ---	0.359 -	98.552	3.743	0.513 +	1.666	5.580	0.043
Phytol	-4.338	0.034 ---	0.002 ---	1.1e-05	0.001 ---	0.687 +	0.357 -	97.641	3.722	0.227 --	2.400	8.161	0.073
alpha-Hederin	-5.530	0.024 ---	0.837 ++	2.4e-05	0.001 ---	0.394 -	0.689 +	93.935	0.624	0.062 ---	6.893	1.025	0.028

Zeaxanthin	-5.949	0.999 +++	0.118 --	2.2e-05	0.906 +++	0.005 ---	0.011 ---	99.083	4.942	0.011 ---	2.565	1.078	0.210
Lutein	-5.567	0.999 +++	0.389 -	2.1e-05	0.892 ++	0.01 ---	0.009 ---	99.596	4.559	0.008 ---	2.431	1.066	0.134
zeta-Carotene	-5.340	0.977 +++	0.01 ---	9e-06	0.608 +	0.248 --	0.929 +++	95.841	10.296	0.001 ---	3.468	0.530	0.030
Linoleic Acid	-4.733	0.0 ---	0.01 ---	1.9e-05	0.002 ---	0.009 ---	0.549 +	98.391	0.626	0.196 --	1.619	3.327	0.628
Linolenic acid	-4.631	0.0 ---	0.007 ---	5.3e-06	0.002 ---	0.003 ---	0.849 ++	97.119	0.594	0.295 --	2.336	4.877	0.710
Oxyacanthine	-5.583	0.999 +++	0.006 ---	2.1e-05	0.055 ---	0.024 ---	0.941 +++	80.982	0.993	0.201 --	13.057	9.354	0.295
Honokiol	-4.644	0.863 ++	0.006 ---	2.7e-05	0.0 ---	0.894 ++	0.984 +++	101.06	0.453	0.093 ---	0.692	10.826	0.709
Beta-Sitosterol	-4.756	0.341 -	0.004 ---	8.6e-06	0.001 ---	0.01 ---	0.233 --	98.314	1.963	0.84 ++	1.485	16.686	0.013
Thalsimine	-5.611	0.999 +++	0.97 +++	2.7e-05	0.013 ---	0.007 ---	0.673 +	82.774	0.517	0.132 ---	6.416	7.281	0.122
Isofraxidin	-4.964	0.975 +++	0.004 ---	7.5e-06	0.0 ---	0.05 ---	0.909 +++	96.337	2.280	0.17 --	1.282	16.713	0.029

For the classification endpoints, the prediction probability values are transformed into six symbols: 0-0.1 (- - -), 0.1-0.3 (- -), 0.3-0.5 (-), 0.5-0.7 (+), 0.7-0.9 (++), and 0.9-1.0 (+++).

Caco-2 permeability: Colon adenocarcinoma cell lines -2 permeability. >-5.15 cm/s: highly permeable to the human intestinal epithelium. **Pgp-substrate**: Permeability glycoprotein-substrate. 0.0: no pharmacokinetic implications for Pgp substrates; 0.1–0.3: low pharmacokinetic implications for Pgp substrates and non-substrates of p-glycoprotein; 0.3–0.7: medium pharmacokinetic implications for Pgp substrates; 0.7–1.0: high pharmacokinetic implications for Pgp substrates. **HIA**: Human intestinal absorption. 0.0-0.3: high human intestinal absorption; 0.3-0.7: medium human intestinal absorption; 0.7-1.0: poor human intestinal absorption. **MDCK Permeability**: Madin−Darby Canine Kidney cells. >2 $\times 10^{-6}$ cm/s: excellent permeability; 2-20 $\times$ 10^{-6} cm/s: medium permeability; < 2 $\times 10^{-6}$ cm/s: low permeability. **Pgp-inhibitor**: Permeability glycoprotein-inhibitor. 0.0-0.3: non-inhibitors of p-glycoprotein; >0.3: inhibitors of p-glycoprotein. $\mathbf{F_{20\%}}$: The human oral bioavailability 20%. 0.0–0.3: very high bioavailability; 0.3–0.7: medium bioavailability; 0.7–1.0: very low bioavailability**;** $\mathbf{F_{30\%}}$: The human oral bioavailability 30%. 0.0–0.3: very high bioavailability; 0.3–0.7: medium bioavailability; 0.7–1.0: very low bioavailability.

PPB: Plasma Protein Binding. ≤ 90%: excellent oral bioavailability and high therapeutic index; > 90%: poor oral bioavailability and low therapeutic index. **VD**: Volume distribution. 0.04-20 L/kg: excellent degree of tissue absorption and quantity of dispersion in body fluids; > 20 L/kg: poor degree of tissue absorption and quantity of dispersion in body fluids. BBB Penetration: Blood-Brain Barrier penetration. 0.0-0.3 cm/s excellent in passing through BBB to reach the target; 0.3-0.7 cm/s medium capability in passing through BBB to reach the target; 0.7-1.0 cm/s poor in passing through BBB to reach the target. Fu: The fraction unbound in plasma. ≥ 5%: not bound to blood protein (unbound - efficiently it can traverse cellular membranes or diffuse); < 5%: bound to blood protein (bound - less

efficiently it can traverse cellular membranes or diffuse). CL: The clearance of a drug. >15 mL/min/kg: high clearance; 5-15 mL/min/kg: moderate clearance; <5 mL/min/kg: low clearance. T1/2: The half-life of a drug involves clearance and volume of distribution. 0.0-0.3 shorter time for a chemical to be eliminated by the body; 0.3-0.7: Moderate time for a chemical to be eliminated by the body; 0.7-1.0: longer time for a chemical to be eliminated by the body.

In *T. palmata* (Table 23), Colon adenocarcinoma cell lines permeability (Caco-2) of 15 compounds are greater than -5.15 cm/s (>-5.15 cm/s), while 11 compounds are lower than -5.15 cm/s (<-5.15 cm/s). Madin−Darby Canine Kidney cells permeability (MDCK) of 10 compounds is lesser than 2×10^{-6} cm/s (< 2 ×10-6 cm/s), 16 compounds with (MDCK) ranging from 2-20 $\times10^{-6}$ cm/s, and no compound with MDCK greater than 20×10^{-6} cm/s (>20×10^{-6} cm/s). Out of 26 compounds, the permeability glycoprotein-substrate (Pgp-substrate) of 17 compounds ranges from 0.0-0.1 and 11 compounds have Pgp-substrate that ranges from 0.9-1.0. The permeability glycoprotein-inhibitor (Pgp-inhibitor) of 12 compounds ranges from 0.0-0.3, while 10 compounds have a Pgp-inhibitor greater than 0.3 (>0.3). The Human intestinal absorption (HIA) of 12 compounds ranges from 0.0-0.3, and 9 compounds with a value ranging from 0.7-1.0. The human oral bioavailability 20% (F20%) of 14 compounds ranges from 0.0-0.3, 2 compounds with values ranging from 0.3-07, and 6 compounds with values ranging from 0.7-1.0. The human oral bioavailability 30% (F30%) of 3 compounds ranges from 0.0-0.3, 2 compounds with values ranging from 0.3-0.7, and 17 compounds with values ranging from 0.7-1.0. The Plasma Protein Binding (PPB) of 9 compounds is lesser than 90% (<90%), and 17 compounds with (PPB) greater than 90% (>90%). Volume distribution (VD) of 22 compounds ranges from 0.4-20 L/kg. Blood-Brain Barrier penetration (BBB) of 20 compounds ranges from 0.0-0.3, 2 compounds with a value ranging from 0.3-0.7, and 6 compounds with a value ranging from 0.7-1.0. The fraction unbound in plasma (FU) of 12 compounds is greater than 5% (>5%), and 14 compounds with (FU) lesser than 5% (<5%). The clearance of a drug (CL) of 11 compounds is less than 5 mL/min/kg, 13 compounds with (CL) ranging from 5-15 mL/min/kg, and 2 compounds with (CL) greater than (>15 mL/min/kg). The half-life of a drug (T1/2) of 19 compounds ranges from 0.0-0.3, 4 compounds with (T1/2) ranging from 0.3-0.7, and 3 compounds with (T1/2) ranging from 0.7-1.0.

Absorption

Caco-2 Permeability: Predicts permeability across the human intestinal epithelium. Values > -5.15 cm/s indicate high permeability. MDCK Permeability: Predicts permeability based on Madin-Darby Canine Kidney cells. Values > 2 × 10^-6 cm/s

suggest excellent permeability. Pgp-inhibitor: Indicates whether the compound inhibits P-glycoprotein, a transporter protein. Values > 0.3 suggest inhibition. Pgp-substrate: Indicates if the compound is a substrate for P-glycoprotein. Higher values suggest higher likelihood of being a substrate. HIA: Predicts human intestinal absorption. Lower values indicate better absorption.

Distribution

F20% and F30%: Predicts oral bioavailability at 20% and 30% doses, respectively. PPB (%): Predicts plasma protein binding. Higher values indicate higher binding affinity. VD: Volume distribution, indicating the degree of dispersion in body fluids. Higher values suggest better tissue absorption. BBB Penetration: Indicates the ability to penetrate the blood-brain barrier. Lower values suggest better penetration. Fu (%): Fraction unbound in plasma. Higher values suggest better cellular membrane penetration.

Excretion

CL: Clearance of the drug from the body. Higher values indicate faster clearance.

T1/2: Half-life of the drug, indicating the time taken for half of the drug to be eliminated from the body.

Each compound is classified based on the prediction probability values into six symbols: -, - -, -, +, ++, and +++. The symbols represent the likelihood or extent of the property being present or exhibited by the compound. Understanding these predictions helps in assessing the pharmacokinetic properties of the compounds, which are crucial for drug development, including absorption into the body, distribution within tissues, and elimination from the body.

3.4.7. Toxicological properties

Toxicological properties are summarized in Table 24 and 25.

In *L. coromandelica* (Table 24), the human ether-a-go-go related gene (hERG) blockers of 23 compounds range from 0.0-0.3, 3 compounds range from 0.3-0.7, and 5 compounds range from 0.7-1.0. The human hepatotoxicity (H-HT) of 25

compounds ranges from 0.0-0.3, and 3 compounds range from 0.7-1.0. The Drug-induced liver injury (DILI) of 15 compounds ranges from 0.0-0.3, 2 compounds range from 0.3-0.7, and 16 compounds range from 0.7-1.0. AMES toxicity of 18 compounds ranges from 0.0-0.3, 4 compounds range from 0.3-0.7, and 9 compounds range from 0.7-1.0. Rat oral acute toxicity of 27 compounds range from 0.0-0.3, 1 compound range from 0.3-0.7, and 2 compound range from 0.7-1.0. FDAMDD of 17 compounds range from 0.0-0.3, 2 compounds range from 0.3-0.7, and 12 compounds range from 0.7-1.0. Skin sensitization of 6 compounds ranges from 0.0-0.3, 3 compounds range from 0.3-0.7, and 22 compounds range from 0.7-1.0. The Carcinogenicity of 22 compounds ranges from 0.0-0.3, 3 compounds range from 0.3-0.7 and 6 compounds ranges from 0.7 to 1. The eye corrosion (EC) potential of a compound of 21 compounds ranges from 0.0-0.3, and 10 compounds range from 0.7-.0. The Eye irritation (EI) potential of a compound of 15 compounds range from 0.0-0.3, 1 compound range from 0.3-7.0, and 15 compounds range from 0.7-1.0. Respiratory toxicity of 14 compounds ranges from 0.0-0.3, 5 compounds range from 0.3-0.7, and 12 compounds range from 0.7-1.0.

Table 24: Prediction of toxicological properties of compounds identified from *Lannea coromandelica* using ADMETlab 2.0 webserver (https://admetmesh.scbdd.com/service/evaluation/cal).

Compounds	Toxicity										
	hERG Blockers	H-HT	DILI	AMES Toxicity	Rat Oral Acute Toxicity	FDAMDD	Skin Sensitization	Carcinogenecity	Eye Corrosion	Eye Irritation	Respiratory Toxicity
Caryophyllene	0.019 ---	0.201 --	0.225 --	0.055 ---	0.093 ---	0.591 +	0.533 +	0.112 --	0.009 ---	0.383 -	0.812 ++
Phenol, 3,5-bis(1,1-dimethylethyl)-	0.031 ---	0.089 ---	0.037 ---	0.002 ---	0.08 ---	0.908 +++	0.754 ++	0.024 ---	0.967 +++	0.983 +++	0.522 +
Diethyl Phthalate	0.136 --		0.404 -	0.013 ---	0.003 ---	0.004 ---	0.267 --	0.035 ---	0.046 ---	0.992 +++	
Phenol, 2,4-bis(1,1-dimethylethyl)-5-methyl-	0.016 ---	0.04 ---	0.044 ---	0.01 ---	0.094 ---	0.916 +++	0.49 -	0.03 ---	0.962 +++	0.978 +++	0.811 ++
Pentadecanoic acid	0.047 ---	0.028 ---	0.043 ---	0.005 ---	0.033 ---	0.015 ---	0.869 ++	0.07 ---	0.978 +++	0.981 +++	0.873 ++
Oxirane, tetradecyl-	0.263 --	0.037 ---	0.279 --	0.019 ---	0.023 ---	0.052 ---	0.964 +++	0.095 ---	0.99 +++	0.991 +++	0.716 ++
cis-9-Hexadecenal	0.23 --	0.009 ---	0.026 ---	0.025 ---	0.011 ---	0.029 ---	0.981 +++	0.24 --	0.995 +++	0.96 +++	0.935 +++
Phytol	0.013 ---	0.098 ---	0.051 ---	0.002 ---	0.008 ---	0.026 ---	0.96 +++	0.106 --	0.837 ++	0.951 +++	0.059 ---
9-Eicosene, (E)-	0.178 --	0.004 ---	0.054 ---	0.006 ---	0.019 ---	0.032 ---	0.969 +++	0.042 ---	0.995 +++	0.934 +++	0.085 ---
1-Hexadecanol	0.043 --	0.043 ---	0.043 ---	0.006 ---	0.021 ---	0.013 ---	0.953 +++	0.043 ---	0.993 +++	0.934 +++	0.934 +
Bis(2-ethylhexyl) phthalate	0.204 --	0.019 ---	0.05 ---	0.004 ---	0.002 ---	0.078 ---	0.943 +++	0.557 +	0.06 ---	0.968 +++	0.105 --

Phenol, 2,4-bis(1,1-dimethylethyl)-	0.011 ---	0.041 ---	0.04 ---	0.009 ---	0.146 --	0.744 ++	0.739 ++	0.034 ---	0.983 +++	0.986 +++	0.699 +
4-tert-Butylcalix[4]arene	0.179 --	0.166 --	0.151 --	0.013 ---	0.051 ---	0.989 +++	0.976 +++	0.003 ---	0.003 ---	0.941 ++	0.033 ---
Hesperetin	0.049 ---	0.112 --	0.895 ++	0.174 --	0.711 ++	0.58 +	0.925 +++				
Nantenine	0.709 ++				0.589 +		0.142 --	0.618 +	0.003 ---	0.008 ---	0.922 +++
7-O-Methylquercetin-3-O-galactoside-6"-rhamnoside	0.006 ---	0.084 ---	0.983 +++	0.657 +	0.03 ---	0.006 ---	0.01 ---	0.088 ---	0.003 ---	0.005 ---	0.01 ---
Kaempferol	0.07 ---	0.098 ---			0.156 --	0.109 --	0.856 ++	0.097 ---	0.009 ---	0.929 +++	0.09 ---
Quercetin-3-O-rutinoside	0.017 ---	0.092 ---	0.982 +++	0.805 ++	0.05 ---	0.014 ---	0.036 ---	0.064 ---	0.003 ---	0.01 ---	0.015 ---
Beta-Carotene	0.853 ++	0.281 --	0.009 ---	0.128 --	0.132 --	0.874 ++	0.988 +++	0.035 ---	0.003 ---	0.229 --	0.313 -
gamma-Carotene	0.867 ++	0.737 ++	0.003 ---	0.19 --	0.179 --	0.918 +++	0.994 +++	0.034 ---	0.003 ---	0.253 --	0.19 --
Kaempferol 7-neohesperidoside	0.011 ---	0.098 ---	0.983 +++	0.79 ++	0.053 ---	0.003 ---	0.02 ---	0.492 -	0.003 ---	0.006 ---	0.015 ---
Kaempferol-3-O-rutinoside	0.023 ---	0.061 ---	0.98 +++	0.78 ++	0.055 ---	0.007 ---	0.02 ---	0.147 --	0.003 ---	0.008 ---	0.014 ---
zeta-Carotene	0.9 ++	0.99 +++	0.002 ---	0.256 --	0.081 ---	0.949 +++	0.994 +++	0.059 ---	0.003 ---	0.098 ---	0.084 ---
[Gallocatechin-(4alpha->8)]2-catechin	0.011 ---	0.076 ---	0.899 ++	0.09 ---	0.174 --	0.842 ++	0.981 ++	0.005 ---	0.003 ---	0.928 +++	0.004 ---
Diatoxanthin	0.612 +							0.052 ---	0.003 ---	0.002 --	
Zeaxanthin		0.189 --	0.001 ---	0.206 --	0.132 --	0.954 +++	0.983 +++	0.047 ---	0.003 ---	0.012 ---	
Lutein	0.627 +	0.157 --	0.001 ---	0.359 -	0.193 --	0.986 +++	0.971 +++	0.044 ---	0.003 ---	0.01 ---	0.357 -

Paclitaxel	0.07 ---	0.978 +++	0.989 +++	0.016 ---	0.997 +++	0.144 --	0.028 ---	0.063 ---	0.003 ---	0.004 ---	0.324 -
Chlorogenic acid	0.014 ---	0.122 --	0.037 ---	0.026 ---	0.028 ---	0.039 ---	0.156 --	0.059 ---	0.059 ---	0.003 ---	0.02 ---
Luteolin-6-C-glucoside	0.078 ---	0.107 --	0.962 +++	0.732 ++	0.05 ---	0.013 ---	0.513 +	0.033 ---	0.003 ---	0.089 ---	0.036 ---
Linoleic Acid	0.009 ---	0.013 ---	0.009 ---	0.013 ---	0.01 ---	0.017 ---	0.961 +++	0.153 --	0.984 +++	0.98 +++	0.712 ++

For the classification endpoints, the prediction probability values are transformed into six symbols: 0-0.1 (- - -), 0.1-0.3 (- -), 0.3-0.5 (-), 0.5-0.7 (+), 0.7- 0.9 (++), and 0.9-1.0 (+++).

hERG blockers: The human ether-a-go-go related gene blockers. The interchange of the cardiac action potential and resting potential is tightly regulated by the human ether-a-go-go related gene. 0.0-0.3: non-blockade of heart; 0.3-0.7: medium blockade of heart; 0.7-1.0: strong blockade of heart. **H-HT**: The human hepatotoxicity. 0.0-0.3: non-hepatotoxic; 0.3-0.7: mildly hepatotoxic; 0.7-1.0: strongly hepatotoxic. **DILI**: Drug-induced liver injury. 0.0-0.3: non liver injury; 0.3-0.7: mild liver injury; 0.7-1.0: severe liver injury. **AMES toxicity**: The Ames test for mutagenicity. 0.0-0.3: non-mutagenic; 0.3-0.7: mild-mutagenic; 0.7-1.0: highly mutagenic. **Rat oral acute toxicity**: Determination of acute toxicity in mammals (e.g. rats or mice). 0.0-0.3: low toxicity (>500 mg/kg, Class I); 0.3-0.7: intermediate toxicity (=500 mg/kg, Class II); 0.7-1.0: high toxicity (<500 mg/kg, Class III). **FDAMDD**: The maximum recommended daily dose provides an estimate of the toxic dose threshold of chemicals in humans. 0.0-0.3: MDD is non-toxic (>0.011 mmol/kg/bw/day); 0.3-0.7: MDD is mildly toxic; 0.7-1.0: MMD is highly toxic (≤ 0.011 mmol/kg/bw/day). **Skin sensitization**: A compound can induce allergic contact dermatitis is an important safety concern. 0.0-0.3: non- sensitizer; 0.3-0.7: mild-sensitizer; 0.7-1.0: severe sensitizer. **Carcinogenicity**: The ability of a compound to damage the genome or disrupt cellular metabolic processes are

known as carcinogen. 0.0-0.3: non-carcinogen; 0.3-0.7: mild carcinogen; 0.7-1.0: severe carcinogen. **EI/EC**: Assessment of the eye irritation/corrosion potential of a compound. 0.0-0.3: non-corrosives/non-irritants; 0.3-0.7: slightly corrosives/ slightly irritants; 0.7-1.0: corrosives/irritants. **Respiratory toxicity**: Accessing drug-induced respiratory toxicity. 0.0-0.3: non-respiratory toxicant; 0.3-0.7: medium respiratory toxicant; 0.7-1.0 severe respiratory toxicant.

Table 25: Prediction of toxicological properties of compounds identified from *Trevesia palmata* using ADMETlab webserver (https://admetmesh.scbdd.com/service/evaluation/cal).

Compounds	**Toxicity**										
	hERG Blockers	**H-HT**	**DILI**	**AMES Toxicity**	**Rat Oral Acute Toxicity**	**FDA MDD**	**Skin Sensitization**	**Carcinogencity**	**Eye Corrosion**	**Eye Irritation**	**Respiratory Toxicity**
Icariin	0.013 ---	0.584 +	0.985 +++	0.729 ++	0.054 ---	0.006 ---	0.016 ---	0.293 --	0.003 ---	0.003 ---	0.016 ---
Apigenin-6-C-glucoside-7-O-glucoside	0.037 ---	0.097 ---	0.958 +++	0.427 -	0.069 ---	0.002 ---	0.017 ---	0.063 ---	0.003 ---	0.004 ---	0.012 ---
Kaempferol 3-O-sophoroside	0.025 ---	0.102 --	0.982 +++	0.674 +	0.068 ---	0.002 ---	0.019 ---	0.07 ---	0.003 ---	0.006 ---	0.008 ---
Kaempferol-3-O-rutinoside	0.023 ---	0.061 ---	0.98 +++	0.78 ++	0.055 ---	0.007 ---	0.02 ---	0.147 --	0.003 ---	0.008 ---	0.014 ---
Kaempferol 4'-methyl ether 3-(4Rha-rhamnosylrutinoside)	0.023 ---	0.068 ---	0.982 +++	0.668 +	0.031 ---	0.006 ---	0.006 ---	0.131 --	0.003 ---	0.004 ---	0.01 ---
7,9-Di-tert-butyl-1-oxaspiro(4,5)deca-6,9-diene-2,8-dione	0.04 ---	0.414 -	0.199 --	0.049 ---	0.706 ++	0.767 ++	0.551 +	0.906 +++	0.047 ---	0.143 --	0.839 ++

Quercetin 3-O-[2"-O-(6"'-O-p-coumaroyl)-b-D-glucopyranosyl]-a-L-rhamnopyranoside	---	--	+++	++	---	---	--	--	---	---	---
gamma.-Tocopherol	0.021 ---	0.181 --	0.029 ---	0.04 ---	0.036 ---	0.07 ---	0.954 +++	0.029 ---	0.01 ---	0.45 -	0.34 -
dl-.alpha.-Tocopherol	0.01 ---	0.175 --	0.031 ---	0.028 ---	0.066 ---	0.02 ---	0.951 +++	0.024 ---	0.004 ---	0.381 -	0.285 --
Asiaticoside	0.002 ---	0.168 --	0.019 ---	0.081 ---	0.523 +	0.032 ---	0.0 ---	0.025 ---	0.003 ---	0.001 ---	0.026 ---
Bacoside A3	0.004 ---	0.195 --	0.019 ---	0.122 --	0.931 +++	0.045 ---	0.011 ---	0.011 ---	0.003 ---	0.001 ---	0.093 ---
Hederacoside C	0.001 ---	0.145 --	0.009 ---	0.074 ---	0.305 -	0.011 ---	0.0 ---	0.021 ---	0.003 ---	0.001 ---	0.013 ---
alpha.-Amyrin	0.003 ---	0.133 --	0.012 ---	0.011 ---	0.243 --	0.662 +	0.027 ---	0.017 ---	0.003 ---	0.271 --	0.967 +++
Neophytadiene	0.008 ---	0.055 ---	0.856 ++	0.013 ---	0.0 ---	0.08 ---	0.965 +++	0.082 +++	0.977 +++	0.938 +++	0.904 +++
Phytol	0.013 ---	0.098 ---	0.051 ---	0.002 ---	0.008 ---	0.026 ---	0.96 +++	0.106 --	0.837 ++	0.951 +++	0.059 ---
alpha-Hederin	0.001 ---	0.195 --	0.009 ---	0.121 --	0.133 --	0.188 --	0.002 ---	0.039 ---	0.003 ---	0.003 ---	0.791 ++
Zeaxanthin	0.842 ++	0.189 --	0.001 ---	0.206 --	0.132 --	0.954 +++	0.983 +++	0.047 ---	0.003 ---	0.012 ---	0.662 +
Lutein	0.627 +	0.157 --	0.001 ---	0.359 -	0.193 --	0.986 +++	0.971 +++	0.044 ---	0.003 ---	0.01 ---	0.357 -
zeta-Carotene	0.9 ++	0.99 +++	0.002 ---	0.256 --	0.081 ---	0.949 +++	0.994 +++	0.059 ---	0.003 ---	0.098 ---	0.084 ---
Linoleic Acid	0.009 ---	0.013 ---	0.009 ---	0.013 ---	0.01 ---	0.017 ---	0.961 +++	0.153 --	0.984 +++	0.98 +++	0.712 ++
Linolenic acid	0.001 ---	0.006 ---	0.007 ---	0.113 --	0.005 ---	0.017 ---	0.965 +++	0.106 --	0.987 +++	0.987 +++	0.674 +
Oxyacanthine	0.974 +++	0.024 ---	0.25 --	0.091 ---	0.196 --	0.96 +++	0.861 ++	0.037 ---	0.003 ---	0.004 ---	0.5 -

Honokiol	0.01 ---	0.022 ---	0.039 ---	0.273 --	0.093 ---	0.599 +++	0.945 ++	0.482 -	0.007 ---	0.931 +++	0.066 ---
Beta-Sitosterol	0.049 ---	0.16 --	0.203 --	0.026 ---	0.018 ---	0.73 ++	0.133 --	0.047 ---	0.003 ---	0.01 ---	0.536 +
Thalsimine	0.972 +++	0.039 ---	0.741 ++	0.067 ---	0.476 -	0.962 +++	0.674 +	0.026 ---	0.003 ---	0.004 ---	0.742 ++
Isofraxidin	0.006 ---	0.667 +	0.903 +++	0.164 --	0.406 -	0.055 ---	0.56 +	0.644 +	0.023 ---	0.299 --	0.173 --

For the classification endpoints, the prediction probability values are transformed into six symbols: 0-0.1 (- - -), 0.1-0.3 (- -), 0.3-0.5 (-), 0.5-0.7 (+), 0.7- 0.9 (++), and 0.9-1.0 (+++).

hERG blockers: The human ether-a-go-go related gene blockers. The interchange of the cardiac action potential and resting potential is tightly regulated by the human ether-a-go-go related gene. 0.0-0.3: non-blockade of heart; 0.3-0.7: medium blockade of heart; 0.7-1.0: strong blockade of heart. **H-HT**: The human hepatotoxicity. 0.0-0.3: non-hepatotoxic; 0.3-0.7: mildly hepatotoxic; 0.7-1.0: strongly hepatotoxic. **DILI**: Drug-induced liver injury. 0.0-0.3: non liver injury; 0.3-0.7: mild liver injury; 0.7-1.0: severe liver injury. **AMES toxicity**: The Ames test for mutagenicity. 0.0-0.3: non-mutagenic; 0.3-0.7: mild-mutagenic; 0.7-1.0: highly mutagenic. **Rat oral acute toxicity**: Determination of acute toxicity in mammals (e.g. rats or mice). 0.0-0.3: low toxicity (>500

mg/kg, Class I); 0.3-0.7: intermediate toxicity (=500 mg/kg, Class II); 0.7-1.0: high toxicity (<500 mg/kg, Class III). FDAMDD: The maximum recommended daily dose provides an estimate of the toxic dose threshold of chemicals in humans. 0.0-0.3: MDD is non-toxic (>0.011 mmol/kg/bw/day); 0.3-0.7: MDD is mildly toxic; 0.7-1.0: MMD is highly toxic (≤ 0.011 mmol/kg/bw/day).

Skin sensitization: A compound can induce allergic contact dermatitis is an important safety concern. 0.0-0.3: non- sensitizer; 0.3-0.7: mild-sensitizer; 0.7-1.0: severe sensitizer. Carcinogenicity: The ability of a compound to damage the genome or disrupt cellular metabolic processes are known as carcinogen. 0.0-0.3: non-carcinogen; 0.3-0.7: mild carcinogen; 0.7-1.0: severe carcinogen. EI/EC: Assessment of the eye irritation/corrosion potential of a compound. 0.0-0.3: non-corrosives/non-irritants; 0.3-0.7: slightly corrosives/ slightly irritants; 0.7-1.0: corrosives/irritants. Respiratory toxicity: Accessing drug-induced respiratory toxicity. 0.0-0.3: non-respiratory toxicant; 0.3-0.7: medium respiratory toxicant; 0.7-1.0 severe respiratory toxicant.

In *T. palmata* (Table 25), the human ether-a-go-go related gene (hERG) blockers of 21 compounds range from 0.0-0.3, 1 compound range from 0.3-0.7, and 4 compounds range from 0.7-1.0. The human hepatotoxicity (H-HT) of 22 compounds ranges from 0.0-0.3, 3 compounds range from 0.3-0.7 and 1 compounds range from 0.7-1.0. The Drug-induced liver injury (DILI) of 17 compounds ranges from 0.0-0.3 and 9 compounds range from 0.7-1.0. AMES toxicity of 19 compounds ranges from 0.0-0.3, 4 compounds range from 0.3-0.7, and 3 compounds range from 0.7-1.0. Rat oral acute toxicity of 20 compounds range from 0.0-0.3, 4 compounds range from 0.3-0.7, and 2 compounds range from 0.7-1.0. FDAMDD of 17 compounds range from 0.0-0.3, 1 compound range from 0.3-0.7 and 7 compounds range from 0.7-1.0. Skin sensitization of 12 compounds ranges from 0.0-0.3, 3 compounds range from 0.3-0.7 and 11 compounds range from 0.7-1.0. The Carcinogenicity of 22 compounds ranges from 0.0-0.3, 2 compounds range from 0.3-0.7 and 2 compounds ranges from 0.7 to 1. The eye corrosion (EC) potential of a compound of 22 compounds ranges from 0.0-0.3 and 4 compounds range from 0.7-1.0. The Eye irritation (EI) potential of a compound of 19 compounds range from 0.0-0.3, 2 compounds range from 0.3-

7.0 and 5 compounds range from 0.7-1.0. Respiratory toxicity of 14 compounds ranges from 0.0-0.3, 6 compounds range from 0.3-0.7 and 6 compounds range from 0.7-1.0.

Each compound is classified based on the prediction probability values into six symbols: -, - -, -, +, ++, and +++. These symbols represent the likelihood or severity of the toxicological property being present or exhibited by the compound.

Understanding these predictions helps in assessing the potential toxicological risks associated with the compounds, which is crucial for evaluating their safety profiles in various applications, including pharmaceuticals, cosmetics, and agrochemicals.

3.4.8. Toxicophore Rules and Environmental Toxicity Characteristics

Toxicophore Rules and Environmental Toxicity Characteristics are summarized in Table 26 for *L. coromandelica* and Table 27 for *T. palmata*.

In *L. coromandelica* (Table 26), the Acute Toxicity Rule (AcTR) of all the compounds has 0 alerts. The Genotoxic Carcinogenicity Rule (GCR) of 28 compounds has 0 alerts, and 3 compounds have greater than or equal to 1 alert (≥1 alert). The Non-Genotoxic Carcinogenicity Rule (NGCR) of 28 compounds has 0 alerts and 3 compounds have 1 alert (1 alert). Skin Sensitization Rule (SSR) of 17 compounds has 0 alerts and 14 compounds have greater than or equal to 1 alert (≥1 alert). The Aquatic Toxicity Rule (AqTR) of 14 compounds has 0 alerts, and 17 compounds have greater than or equal to 1 alert (≥1 alert). The Non-Biodegradable Rule (NBR) of 16 compounds has 0 alerts and 15 compounds have greater than or equal to 1 alert (≥1 alert). The Sure ChEMBL Rule (SCR) of 20 compounds has 0 alerts and 11 compounds have greater than or equal to 1 alert (≥1 alert). The FAF-Drugs4 Rule (FAF-D4R) of 9 compounds has 0 alerts, and 22 compounds have greater than or equal to 1 alert (≥1 alert). The Bio-Concentration Factor of 31 compounds are less than 2000 (<2000). The Growth inhibition concentration 50 percent to Tetrahymena pyriformis (mg/L, 48 h) (IGC50 TP) of all 31 compounds ranges from 1-10 (mg/L). Lethal concentration 50 percent to Fathead minnow (mg/L, 96 h) (LC50 FM) of all the 31 compounds ranges from 1-10 (mg/L). Lethal

concentration 50 percent to Daphnia magna (mg/L, 48 h) (LC50 DM) of all 31 compounds ranges from 1-10 (mg/L).

In *T. palmata* (Table 27), the Acute Toxicity Rule (AcTR) of all 26 compounds has 0 alerts. The Genotoxic Carcinogenicity Rule (GCR) of 20 compounds has 0 alerts, and 6 compounds have greater than or equal to 1 alert (≥1 alert). The Non-Genotoxic Carcinogenicity Rule (NGCR) of 23 compounds has 0 alerts and 3 compounds have 1 alert (1 alert). Skin Sensitization Rule (SSR) of 7 compounds has 0 alerts and 19 compounds have greater than or equal to 1 alert (≥1 alert). The Aquatic Toxicity Rule (AqTR) of 10 compounds has 0 alerts, and 15 compounds have greater than or equal to 1 alert (≥1 alert). The Non-Biodegradable Rule (NBR) of 14 compounds has 0 alerts and 11 compounds have greater than or equal to 1 alert (≥1 alert). The Sure ChEMBL Rule (SCR) of 22 compounds has 0 alerts and 3 compounds have greater than or equal to 1 alert (≥1 alert). The FAF-Drugs4 Rule (FAF-D4R) of 10 compounds has 0 alerts, and 15 compounds have greater than or equal to 1 alert (≥1 alert). The Bio-Concentration Factor of 26 compounds are less than 2000 (<2000). The Growth inhibition concentration 50 percent to Tetrahymena pyriformis (mg/L, 48 h) (IGC50 TP) of all 26 compounds ranges from 1-10 (mg/L). Lethal concentration 50 percent to Fathead minnow (mg/L, 96 h) (LC50 FM) of all the 26 compounds ranges from 1-10 (mg/L). Lethal concentration 50 percent to Daphnia magna (mg/L, 48 h) (LC50 DM) of all 26 compounds ranges from 1-10 (mg/L).

Testing toxicophore rules and predicting environmental toxicity are both critical aspects of assessing the safety and potential risks associated with chemical compounds. Toxicophore Rules helps in the identification of Potential Toxicity. Toxicophores are structural features or functional groups within molecules that are associated with toxicity. By testing toxicophore rules, researchers can identify these specific patterns in chemical structures that may contribute to toxicity. Predicting toxicophores also helps in assessing the potential risk associated with a compound even before extensive experimental testing. By recognizing these structural features, scientists can prioritize compounds for further investigation or avoid synthesizing those with known toxicophores altogether. In the drug discovery process, identifying toxicophores early on, allows medicinal chemists to modify compound structures to

mitigate toxicity risks while retaining desired pharmacological properties. Understanding toxicophores also aids in regulatory compliance by providing insights into potential hazards associated with chemical compounds. This information is crucial for regulatory agencies to evaluate the safety of pharmaceuticals, agrochemicals, and other industrial chemicals.

Predicting environmental toxicity helps in assessing the potential impact of chemical compounds on ecosystems and non-target organisms. This includes aquatic life, soil organisms, plants, and wildlife. Regulatory bodies worldwide require environmental toxicity data as part of chemical safety assessments for registration and approval. Understanding the potential ecological risks associated with chemical compounds is essential for compliance with environmental regulations. Predicting environmental toxicity allows for proactive risk management strategies to be implemented, such as modifying chemical formulations or usage practices to minimize adverse environmental effects. As society moves towards more sustainable practices, evaluating environmental toxicity helps in the development of environmentally friendly products and processes. It enables industries to innovate responsibly while minimizing their ecological footprint. Environmental toxicity assessments also indirectly protect public health by safeguarding ecosystems and the services they provide, such as clean water, air, and food resources.

In brief, testing toxicophore rules and predicting environmental toxicity are integral parts of chemical risk assessment, ensuring the safety of both human health and the environment. These approaches contribute to informed decision-making in various industries, regulatory frameworks, and research endeavours.

Table 26: Prediction of toxicophore rules and environmental toxicity characteristics of compounds identified from *Lannea coromandelica* using ADMETlab 2.0 webserver (https://admetmesh.scbdd.com/service/evaluation/cal)

Compounds	Uniprot ID	Toxicophore Rules								Environmental toxicity (mg/L)			
		AcTR (Alerts)	GCR (Alerts)	NGCR (Alerts)	SSR (Alerts)	AqTR (Alerts)	NBR (Alerts)	SCR (Alerts)	FAF-Drugs4 (Alerts)	BCF (mg/L)	IGC_{50} TP (mg/L)	LC_{50} FM (mg/L)	LC_{50} DM (mg/L)
Caryophyllene	5281515	0	5	1	2	2	2	2	1	3.207	4.373	4.951	5.791
Phenol, 3,5-bis(1,1-dimethylethyl)-	70825	0	0	0	0	0	1	0	1	2.599	4.695	5.251	5.325
Diethyl Phthalate	6781	0	0	0	0	0	0	0	0	0.578	3.585	4.210	4.050
Phenol, 2,4-bis(1,1-dimethylethyl)-5-methyl-	10346	0	0	0	0	0	1	1	1	2.809	4.946	5.581	5.661
Pentadecanoic acid	13849	0	0	0	0	0	0	0	0	0.988	5.023	5.259	4.241
Oxirane, tetradecyl-	23741	0	0	0	0	1	0	0	0	2.330	5.489	5.571	5.355
cis-9-Hexadecenal	5364643	0	0	0	2	0	0	1	1	2.805	5.080	5.526	5.278
Phytol	5280435	0	1	0	1	0	0	0	0	2.868	4.969	5.465	5.218
9-Eicosene, (E)-	5365037	0	0	0	0	1	0	0	0	2.041	5.746	5.882	5.862
1-Hexadecanol	2682	0	0	0	0	1	0	0	0	2.311	5.451	5.946	4.635
Bis(2-ethylhexyl) phthalate	8343	0	0	0	0	0	0	0	0	1.180	5.589	2.313	5.994
Phenol, 2,4-bis(1,1-dimethylethyl)-	7311	0	0	0	0	0	1	1	1	2.554	4.869	5.474	5.536
4-tert-Butylcalix[4]arene	335377	0	0	0	0	0	1	0	1	2.859	6.806	8.102	6.759
1,2-	33934	0	0	0	0	0	0	0	0	1.159	5.497	5.652	5.159

Benzenedicarboxylic Acid, Diisooctyl Ester													
Hesperetin	72281	0	0	0	1	0	1	0	1	1.029	4.857	6.342	6.390
Nantenine	197001	0	3	1	1	0	0	0	1	2.769	4.120	6.236	6.868
7-O-Methylquercetin-3-O-galactoside-6''-rhamnoside	56995003	0	0	0	7	2	2	0	3	1.095	4.023	5.418	5.763
Kaempferol	5280863	0	0	0	4	0	1	0	1	0.986	4.386	5.223	5.205
Quercetin-3-O-rutinoside	5280805	0	0	0	8	2	2	0	2	0.938	3.968	4.920	5.517
Beta-Carotene	5280489	0	0	0	0	1	0	2	1	1.472	5.641	7.267	6.531
gamma-Carotene	5280791	0	0	0	0	1	0	2	1	1.755	5.662	7.298	6.722
Kaempferol 7-neohesperidoside	5483905	0	0	0	3	2	2	0	1	0.883	4.041	5.040	5.285
Kaempferol-3-O-rutinoside	5318767	0	0	0	4	2	2	0	1	0.888	4.020	4.918	5.457
zeta-Carotene	5280788	0	0	0	0	1	0	2	1	2.228	5.406	7.058	6.376
[Gallocatechin-(4alpha->8)]2-catechin	14890508	0	0	0	9	2	1	1	2	0.221	4.679	7.075	6.421
Diatoxanthin	6440986	0	0	0	0	1	0	3	4	1.504	5.705	7.236	6.069
Zeaxanthin	5280899	0	0	0	0	1	0	2	1	1.628	5.368	6.906	6.209
Lutein	5281243	0	0	0	0	1	0	2	1	2.052	5.582	7.757	7.089
Paclitaxel	36314	0	0	0	3	0	2	0	0	0.586	4.828	7.387	6.179
Chlorogenic acid	1794427	0	1	1	8	4	1	0	3	0.220		3.622	4.856
Luteolin-6-C-glucoside	114776	0	0	0	7	3	2	0	2	0.846	4.097	4.867	5.602
Linoleic Acid	5280450	0	0	0	0	0	0	0	0	0.898	4.453	5.113	4.266

AcTR: Acute toxicity rule. 0 alerts: non-acute oral toxicant; ≥1 alerts: acute oral toxicant; **GCR**: Genotoxic carcinogenicity rule. 0 alerts: non-carcinogen/non-mutagen through genotoxic mechanisms; ≥1 alerts: carcinogen/mutagen through genotoxic mechanisms. **NGCR**: Non-genotoxic carcinogenicity rule. 0 alerts: non-carcinogen through non-genotoxic mechanisms; ≥1 alerts: carcinogen through non-genotoxic mechanisms. **SSR**: Skin sensitization rule. 0 alerts: non-skin irritant; ≥1 alerts: skin irritant; **AqTR**: Aquatic toxicity rule. 0 alerts: non-aquatic toxicant; ≥1 alerts: aquatic toxicant; **NBR**: Non-biodegradable rule. 0 alerts: biodegradable; ≥1alerts: non-biodegradable; **SCR**: Sure ChEMBL rule. 0 alerts: MedChem friendly status; ≥1 alerts: MedChem unfriendly status. **FAF-D4R**: FAF-Drugs4 Rule. Zero alerts are thought to be non-harmful chemicals.

BCF: Bio-Concentration factor. Assessment of a particular molecule's secondary poisoning potential for human's health through the food chain. A compound is termed non-bioaccumulative and non-ecotoxic, if its BCF value < 2000, bioaccummulative and ecotoxic if its BCF value is > 2000 and very bioaccummulative and extremely ecotoxic if its value is > 5000. **IGC_{50} TP**: Growth inhibition concentration 50 percent to *Tetrahymena pyriformis* (mg/L, 48 h); **LC_{50} FM**: Lethal concentration 50 percent to *Fathead minnow* (mg/L, 96 h)**; LC_{50} DM**: Lethal concentration 50 percent to *Daphnia magna* (mg/L, 48 h), <0.1 Very highly toxic, 0.1–1 Highly toxic, >1–10 Moderately toxic, >10–100 Slightly toxic, >100 Practically nontoxic.

Table 27: Prediction of toxicological properties of compounds identified from *Trevesia palmata* using ADMETlab webserver (https://admetmesh.scbdd.com/service/eva luation/cal).

Compounds	**Uniprot ID**	**Toxicophore Rules**								**Environmental toxicity (mg/L)**			
		AcTR (Alerts)	**GCR (Alerts)**	**NGCR (Alerts)**	**SSR (Alerts)**	**AqTR (Alerts)**	**NBR (Alerts)**	**SCR (Alerts)**	**FAF-Drug4 rule**	**BCF (mg/L)**	**IGC_{50} TP (mg/L)**	**LC_{50} FM (mg/L)**	**LC_{50} DM (mg/L)**
Icariin	5318997	0	0	0	2	2	1	0	1	1.059	3.957	5.858	5.895
Apigenin-6-C-glucoside-7-O-glucoside	4636593	0	0	0	2	3	1	0	1	0.662	3.852	3.855	5.361
Kaempferol 3-O-sophoroside	5282155	0	0	0	4	2	2	0	1	0.760	3.684	4.511	5.045
Kaempferol-3-O-rutinoside	5318767	0	0	0	4	2	2	0	0	0.888	4.020	4.918	5.457
Kaempferol 4'-methyl ether 3-(4Rha-rhamnosylrutinoside)	44257995	0	0	0	4	2	2	0	1	1.137	4.043	5.254	5.760
7,9-Di-tert-butyl-1-oxaspiro(4,5)deca-6,9-diene-2,8-dione	545303	0	1	0	1	4	2	0	1	0.616	3.174	4.006	3.889
Quercetin 3-O-[2"-O-(6"'-O-p-coumaroyl)-b-D-glucopyranosyl]-a-L-rhamnopyranoside	10169367	0	1	1	11								
gamma.-Tocopherol	92729	0	0	0	2	0	0	0	1	2.345	5.546	5.247	6.278
dl-.alpha.-Tocopherol	2116	0	0	0	2	0	0	0	1	2.548	5.486	5.816	6.369
Asiaticoside	11954171	0	0	0	1	2	1	0	0	1.089	5.718	5.718	5.718

Bacoside A3	91827005	0	0	0	2	2	1	0	1	1.717	4.588	6.446	5.692
Hederacoside C	11491905	0	0	0	1	2	1	0	0	4.794	4.794	5.530	5.862
alpha.-Amyrin	131752025	0	0	0	0	1	0	0	0	3.271	5.455	6.821	6.691
Phytol	5280435	0	1	0	1	0	0	0	0	2.868	4.969	5.465	5.218
Neophytadiene	10446	0	0	0	0	1	0	1	2	2.658	5.338	6.167	5.745
alpha-Hederin	73296	0	0	0	1	2	1	0	0	0.991	4.742	5.625	5.741
Zeaxanthin	5280899	0	0	0	0	1	0	2	1	1.628	5.368	6.906	6.209
Lutein	5281243	0	0	0	0	1	0	2	1	2.052	5.582	7.757	7.089
zeta-Carotene	5280788	0	0	0	1	0	2	0	1	2.228	5.406	7.058	6.376
Isopropyl Tetradecanoate	8042	0	0	0	0	0	0	0	0	2.437	4.683	4.683	4.683
Linoleic Acid	5280450	0	0	0	0	0	0	0	0	0.898	5.113	5.113	4.266
Linolenic acid	5280934	0	0	0	0	0	0	0	0	0.512	3.625	4.821	4.084
Oxyacanthine	442333	0	3	1	1	0	0	0	1	1.753	5.332	7.609	7.454
Honokiol	72303	0	0	0	1	0	0	0	2	1.958	5.112	5.873	5.627
Beta-Sitosterol	222284	0	0	0	0	1	0	0	0	2.963	4.984	5.365	6.231
Thalsimine	362568	0	3	1	1	0	0	0	0	2.088	5.354	8.311	7.494
Isofraxidin	5318565	0	1	0	4	0	0	0	2	0.841	2.803	3.298	4.793

AcTR: Acute toxicity rule. 0 alerts: non-acute oral toxicant; ≥1 alerts: acute oral toxicant. **GCR**: Genotoxic carcinogenicity rule. 0 alerts: non-carcinogen/non-mutagen through genotoxic mechanisms; ≥1 alerts: carcinogen/mutagen through genotoxic mechanisms. **NGCR**: Non-genotoxic carcinogenicity rule. 0 alerts: non-carcinogen through non-genotoxic mechanisms; ≥1 alerts: carcinogen through non-genotoxic mechanisms. **SSR**: Skin sensitization rule. 0 alerts: non-skin irritant; ≥1 alerts: skin irritant. **AqTR**: Aquatic toxicity rule.

0 alerts: non-aquatic toxicant; ≥1 alerts: aquatic toxicant. **NBR**: Non-biodegradable rule. 0 alerts: biodegradable; ≥1alerts: non-biodegradable. **SCR**: Sure ChEMBL rule. 0 alerts: MedChem friendly status; ≥1 alerts: MedChem unfriendly status. **FAF-D4R**: FAF-Drugs4 Rule. Zero alerts are thought to be non-harmful chemicals.

BCF: Bio-Concentration factor. Assessment of a particular molecule's secondary poisoning potential for human's health through the food chain. A compound is termed non-bioaccumulative and non-ecotoxic, if its BCF value < 2000, bioaccummulative and ecotoxic if its BCF value is > 2000 and very bioaccummulative and extremely ecotoxic if its value is > 5000. **IGC_{50} TP**: Growth inhibition concentration 50 percent to *Tetrahymena pyriformis* (mg/L, 48 h); **LC_{50} FM**: Lethal concentration 50 percent to *Fathead minnow* (mg/L, 96 h); **LC_{50} DM**: Lethal concentration 50 percent to *Daphnia magna* (mg/L, 48 h), <0.1 Very highly toxic, 0.1–1 Highly toxic, >1–10 Moderately toxic, >10–100 Slightly toxic, >100 Practically nontoxic.

3.5. DISCUSSION

This experiment outlines the analysis of phytocompounds from two plant sources, *Lannea coromandelica* and *Trevesia palmata*, focusing on their metabolic interactions, repeated dose toxicity, reproductive toxicity, and predicted biological activities using various computational tools such as QSAR Tool Software, ADMETLab 2.0, and PASS Online.

SAR analysis typically precedes molecular docking in the drug discovery process. SAR analysis guides the design and optimization of lead compounds based on their structure-activity relationships, while molecular docking is used to predict and rationalize ligand-receptor binding interactions, often in the context of lead optimization and virtual screening (Temml and Kutil, 2021). ADMET analysis is typically conducted after lead optimization to evaluate pharmacokinetic and safety properties of candidate compounds. However, these processes are often iterative and can influence each other throughout the drug discovery pipeline (Duraan-Iturbide et al., 2020).

The metabolic interactions of *Lannea coromandelica* and *Trevesia palmata* chemicals with CYP enzymes is critical for determining their potential toxicity after repeated exposure and reproductive health implications. Metabolic interactions data presents the interaction of identified compounds from both plants with cytochrome P450 (CYP) enzymes. These interactions can influence the metabolism and bioavailability of the compounds, impacting their toxicity and pharmacokinetics (Minerdi et al., 2023). Repeated dose toxicity result provides NOAEL values, representing the highest dose of a substance that causes no adverse effects when administered repeatedly, were determined for the compounds (Sewell et al., 2022). The classification of compounds as toxic or non-toxic based on their NOAEL values provides insights into their potential for causing adverse effects upon repeated exposure. The data also evaluates the reproductive toxicity of the compounds, considering their potential effects on fertility, foetal development and reproductive organs. Compounds are classified as toxic or non-toxic to reproductive organs based on their NOAEL values (Monnot et al., 2021). PASS Online predicts the potential

biological activities of the compounds based on their chemical structures. The probability of activity (Pa) and inactivity (Pi) are provided for various activities such as anti-ulcerative, antioxidant, anti-inflammatory, anti-protozoal, and antineoplastic effects. Compounds with Pa values greater than 0.7 are considered to have significant potential for the respective biological activity. The analysis indicates the potential pharmacological effects of the compounds, aiding in the identification of lead compounds for further investigation in pharmaceutical, cosmetic, and other industries (Reza et al., 2021). The data underscores the diverse biological activities exhibited by the identified phytocompounds from *Lannea coromandelica* and *Trevesia palmata*, ranging from antioxidant and anti-inflammatory effects to antineoplastic and anti-ulcerative properties. Understanding the metabolic interactions, repeated dose toxicity, and reproductive toxicity of these compounds is crucial for assessing their safety and potential therapeutic applications. Computational tools such as QSAR, ADMETLab and PASS Online provide valuable insights into the biological properties of phytocompounds, offering a cost-effective and efficient approach for preliminary screening and prioritization of compounds for further experimental validation.

Molecular docking is a versatile and powerful computational tool that accelerates drug discovery and design by providing valuable insights into ligand-receptor interactions, guiding lead optimization, and facilitating the identification of novel drug candidates with therapeutic potential (Agu et al., 2023). The results of molecular docking studies evaluating the binding affinities of various ligands derived from *Lannea coromandelica* and *Trevesia palmata* against four important receptors involved in inflammatory pathways: COX-2, iNOS, TNF-α, and IL-6. *Lannea coromandelica* ligands like Paclitaxel, Quercetin-3-O-rutinoside and Kaempferol 7-neohesperidoside exhibit strong binding affinities to the COX-2 receptor. *Trevesia palmata* ligands like Quercetin 3-O-[2"-O-(6'"-O-p-coumaroyl)-b-D-glucopyranosyl]-a-L-rhamnopyranoside and Kaempferol-3-O-rutinoside show strong binding affinities. These findings suggest that certain compounds from both plants have the potential to modulate COX-2 activity, which is significant in inflammatory processes. *Lannea coromandelica* ligands such as Quercetin-3-O-rutinoside and

Paclitaxel demonstrate strong binding affinities to the iNOS receptor. *Trevesia palmata* ligands like Kaempferol-3-O-rutinoside and Quercetin 3-O-[2"-O-(6"'-O-p-coumaroyl)-b-D-glucopyranosyl]-a-L-rhamnopyranoside exhibit strong binding affinities to iNOS receptor. These ligands show potential in modulating iNOS activity, which is crucial in inflammation and immune response regulation. Compounds like 4-tert-Butylcalix[4]arene and Paclitaxel from *Lannea coromandelica* demonstrate strong binding affinities to TNF-α. On the other hand, ligands such as Asiaticoside, alpha.-Amyrin and Oxyacanthine from *Trevesia palmata* exhibit strong binding affinities to TNF-α. The ligands from both plants show potential in modulating TNF-α activity, which is central to inflammation and immune response. Ligand Kaempferol-3-O-rutinoside present in both the plants shows strong binding affinity to IL-6 receptor. In addition, ligand Asiaticoside also present in *Trevesia palmata* exhibit strong binding affinities as well. These compounds have potential in modulating IL-6 activity, which is implicated in various inflammatory conditions.

Compounds like Paclitaxel, Quercetin-3-O-rutinoside, and Kaempferol derivatives consistently show strong binding affinities across multiple receptors, indicating their potential efficacy in modulating inflammatory pathways. Ligands with moderately negative values also demonstrate significant interactions with the receptors, suggesting potential therapeutic relevance, albeit slightly weaker than strong binders. Compounds with less negative values exhibit weaker binding affinities and may have less significant interactions with the receptors. These findings provide valuable insights for drug discovery and development efforts targeting inflammatory pathways, indicating potential lead compounds for further investigation and development into anti-inflammatory agents. In summary, the molecular docking studies provide promising candidates from *Lannea coromandelica* and *Trevesia palmata* for further exploration as potential anti-inflammatory agents targeting COX-2, iNOS, TNF-α, and IL-6 receptors. However, further experimental validation and optimization are necessary to confirm their therapeutic potential.

Physicochemical properties refer to the physical and chemical characteristics of a compound that influence its behaviour in biological systems. These properties

include molecular weight, solubility, lipophilicity (logP), polarity, hydrogen bonding capacity, pKa (acid dissociation constant), and stereochemistry. Understanding the physicochemical properties of a drug candidate is crucial for drug design and development. For example, optimal solubility and lipophilicity are important for drug absorption, distribution, metabolism, and excretion (ADME), while appropriate pKa values affect drug ionization and bioavailability (Volak et al., 2023). Medicinal chemistry is a multidisciplinary field that combines principles of organic chemistry, biochemistry, pharmacology, and computational chemistry to design, synthesize, and optimize drug candidates. Medicinal chemists aim to develop small molecules or biologics with specific pharmacological properties, such as potency, selectivity, efficacy, and safety. They optimize lead compounds through structure-activity relationship (SAR) studies, molecular modelling, and synthetic chemistry techniques (Zamberlan et al., 2023). Pharmacokinetics (PK) is the study of the absorption, distribution, metabolism, and excretion (ADME) of drugs in the body, as well as the time course of drug concentrations in plasma and tissues. PK parameters, such as bioavailability, half-life, clearance, volume of distribution, and drug-drug interactions, influence the efficacy and safety of drugs. Understanding PK properties is essential for optimizing dosing regimens, predicting drug exposure, and minimizing the risk of adverse effects (Curry and Whelpton, 2022). Toxicological properties refer to the potential adverse effects of drugs or chemicals on biological systems, including cells, tissues, organs, and organisms (Sukhanova et al., 2018). Toxicity assessments evaluate the safety profile of drug candidates by studying their acute, subacute, sub-chronic, and chronic effects in preclinical models. Common toxicity endpoints include cytotoxicity, genotoxicity, cardiotoxicity, hepatotoxicity, nephrotoxicity, neurotoxicity, and immunotoxicity (Panghal and Flora, 2022). Toxicology studies inform risk assessment, dose selection, and regulatory approval of drugs by identifying potential safety concerns and establishing acceptable exposure limits. In drug discovery and development, an integrated approach that considers physicochemical properties, medicinal chemistry optimization, pharmacokinetics, and toxicological properties is essential for identifying and advancing promising drug candidates with favourable efficacy and safety profiles (Pognan et al., 2023). The results presented in the physicochemical properties, medicinal chemistry,

pharmacokinetics, and toxicological properties sections provide a comprehensive overview of the characteristics of phytochemicals derived from *L. coromandelica* and *T. palmata*. In physicochemical properties analysis most compounds fall within the optimal range required for molecular weight, indicating suitability for drug-like properties (Table 18 and 19). Majority of compounds are within optimal ranges for Hydrogen bond acceptors and donors, except for a few outliers. Some compounds exceed the optimal range for rotatable bonds and rings, which may affect molecular flexibility. Several compounds deviate from ideal values required for topological polar surface area (TPSA), solubility, and distribution coefficients, potentially impacting pharmacokinetic properties. In medicinal chemistry analysis, majority of compounds have lower QED score and Synthetic accessibility scores, suggesting challenges in drug-likeness and synthesis (Table 18 and 19). Many compounds are rejected by Lipinski's Rule, Pfizer Rule, and GSK Rule, indicating potential difficulties in drug development (Table 20 and 21). Most compounds fall within the ideal range of natural product-likeness score, indicating similarity to natural products. Overall, the medicinal chemistry properties suggest varying degrees of suitability for drug development among the compounds (Table 20 and 21). In pharmacokinetics analysis, compounds exhibit diverse pharmacokinetic profiles, with some showing favourable characteristics for oral bioavailability, permeability, and distribution, while others may have limitations. Understanding these parameters is crucial for predicting the compounds' behaviour in the body and optimizing their therapeutic efficacy (Table 22 amd 23). In toxicological properties evaluation, toxicity prediction models assess various endpoints, including acute toxicity, genotoxicity, hepatotoxicity, and environmental toxicity. The results highlight potential risks associated with the compounds, such as cytotoxicity, genotoxicity, and environmental hazards. Identifying compounds with favourable toxicological profiles is essential for ensuring their safety in pharmaceutical, cosmetic, and agrochemical applications. In toxicophore rules and environmental toxicity characteristic analysis, testing toxicophore rules helps identify structural features associated with toxicity, guiding compound optimization and regulatory compliance (Table 24 and 25). Predicting environmental toxicity aids in assessing the ecological risks posed by the compounds, facilitating sustainable product development and environmental

stewardship (Singh et al., 2021). Overall, the comprehensive characterization of phytochemical properties and their implications for drug development, pharmacokinetics, and toxicity assessment provides valuable insights for further research and development efforts. Understanding these properties is essential for selecting promising candidates for drug discovery and ensuring their safety and efficacy in clinical applications.

The computational analysis provides a comprehensive understanding of the phytochemicals derived from *Lannea coromandelica* and *Trevesia palmata*, offering valuable insights into their potential as drug candidates. Compounds with favourable physicochemical, medicinal chemistry, pharmacokinetic, and toxicological profiles are more likely to be prioritized for further experimental validation and development as potential therapeutics. Moreover, understanding the environmental toxicity characteristics ensures responsible development and usage of these compounds, minimizing ecological impacts. Therefore, the computational analysis serves as a valuable tool in drug discovery and development, facilitating the identification of promising phytochemicals with desirable properties for various therapeutic applications while ensuring safety and sustainability. Additional research, including in vitro and in vivo toxicity evaluations, is required to completely characterise the safety profile of these drugs and determine any potential dangers associated with their use.

3.6. SUMMARY

- This experiment outlines the analysis of phytocompounds from two plant sources, Lannea coromandelica and Trevesia palmata, focusing on their metabolic interactions, repeated dose toxicity, reproductive toxicity, and predicted biological activities using various computational tools such as QSAR Tool Software, ADMETLab 2.0, and PASS Online.
- Compounds with less negative values exhibit weaker binding affinities and may have less significant interactions with the receptors.

- In summary, the molecular docking studies provide promising candidates from Lannea coromandelica and Trevesia palmata for further exploration as potential anti-inflammatory agents targeting COX-2, iNOS, TNF-α, and IL-6 receptors.
- Understanding the physicochemical properties of a drug candidate is crucial for drug design and development.
- In drug discovery and development, an integrated approach that considers physicochemical properties, medicinal chemistry optimization, pharmacokinetics, and toxicological properties is essential for identifying and advancing promising drug candidates with favourable efficacy and safety

3.7. CONCLUSION

The comprehensive analysis presented in the study facilitates the identification of lead compounds with desirable pharmacological profiles, contributing to drug discovery and development efforts in various therapeutic areas. In summary, the integration of computational predictions with experimental data enhances our understanding of the pharmacological potential and safety profile of phytocompounds, paving the way for the development of novel therapeutics and natural products.

VIII. REFERENCES

Kar, S., & Leszczynski, J. (2022). Computational approaches in assessments of mixture toxicity. Current Opinion in Toxicology, 29, 31-35.

Hussein, R. A., & El-Anssary, A. A. (2019). Plants secondary metabolites: the key drivers of the pharmacological actions of medicinal plants. Herbal medicine, 1(3).

Nisa, N., Dinata, R., Arati, C., Abdelgani-Baraka, G. A., Bhanushree, B., Bidanchi, R. M., ... & Gurusubramanian, G. (2023). Computational toxicology and food safety assessment of Parkia timoriana phytoconstituents using quantitative structure-activity relationship (QSAR) modeling approaches. Indian Journal of Biochemistry and Biophysics (IJBB), 60(12), 896-918.

van Wyk, A. S., & Prinsloo, G. (2020). Health, safety and quality concerns of plant-based traditional medicines and herbal remedies. South African Journal of Botany, 133, 54-62.

Van Norman, G. A. (2019). Limitations of animal studies for predicting toxicity in clinical trials: is it time to rethink our current approach? JACC: Basic to Translational Science, 4(7), 845-854.

Pognan, F., Beilmann, M., Boonen, H., Czich, A., Dear, G., Hewitt, P., ... & Newham, P. (2023). The evolving role of investigative toxicology in the pharmaceutical industry. Nature reviews drug discovery, 22(4), 317-335.

Kar, S., & Leszczynski, J. (2019). Exploration of computational approaches to predict the toxicity of chemical mixtures. Toxics, 7(1), 15.

Dinata, R., Nisa, N., Arati, C., Rasmita, B., Uditraj, C., Siddhartha, R., Bhanushree, B., Saeed-Ahmed, L., Manikandan, B., Bidanchi, R. M., Abinash, G., Pori, B., Khushboo, M., Roy, V. K. & Gurusubramanian, G. (2024). Repurposing immune boosting and anti-viral efficacy of Parkia bioactive entities as multi-target directed therapeutic approach for SARS-CoV-2: exploration of lead drugs by drug likeness, molecular docking and molecular dynamics simulation methods. Journal of Biomolecular Structure and Dynamics, 42(1), 43-81.

Ranjith Kumar, M., Ashwin Karthick, N., Bhuvaneswari, S. & Udaya Prakash, N. K. (2019). In silico evaluation of multispecies toxicity of natural compounds. Drug and Chemical Toxicology, 44(5), 480-486.

Kumar, K. K., Yugandhar, P., Devi, B. U., Kumar, T. S., Savithramma, N., & Neeraja, P. (2019). Applications of in silico methods to analyze the toxicity and estrogen receptor-mediated properties of plant-derived phytochemicals. Food and Chemical Toxicology, 125, 361-369.

Barba-Ostria, C., Carrera-Pacheco, S. E., Gonzalez-Pastor, R., Heredia-Moya, J., Mayorga-Ramos, A., Rodríguez-Pólit, C., Zuniga-Miranda, J., Arias-Almeida, B. & Guamán, L. P. (2022). Evaluation of biological activity of natural compounds: Current trends and methods. Molecules, 27(14), 4490.

Bokhtia, R. M., Panda, S. S., Girgis, A. S., Samir, N., Said, M. F., Abdelnaser, A., ... & Ghanim, A. M. (2023). New NSAID conjugates as potent and selective COX-2 inhibitors: Synthesis, molecular modeling and biological investigation. Molecules, 28(4), 1945.

Kulesza, A., Paczek, L., & Burdzinska, A. (2023). The role of COX-2 and PGE2 in the regulation of immunomodulation and other functions of mesenchymal stromal cells. Biomedicines, 11(2), 445.

Zarghi, A., & Arfaei, S. (2011). Selective COX-2 inhibitors: a review of their structure-activity relationships. Iranian journal of pharmaceutical research: IJPR, 10(4), 655.

Szweda, M., Rychlik, A., Babińska, I., & Pomianowski, A. (2020). Cyclooxygenase-2 as a biomarker with diagnostic, therapeutic, prognostic, and predictive relevance in small animal oncology. Journal of veterinary research, 64(1), 151-160.

Jang, D. I., Lee, A. H., Shin, H. Y., Song, H. R., Park, J. H., Kang, T. B., ... & Yang, S. H. (2021). The role of tumor necrosis factor alpha (TNF-α) in autoimmune disease and current TNF-α inhibitors in therapeutics. International journal of molecular sciences, 22(5), 2719.

Tanaka, T., Narazaki, M., & Kishimoto, T. (2014). IL-6 in inflammation, immunity, and disease. Cold Spring Harbor perspectives in biology, 6(10), a016295.

Aliyu, M., Zohora, F. T., Anka, A. U., Ali, K., Maleknia, S., Saffarioun, M., & Azizi, G. (2022). Interleukin-6 cytokine: An overview of the immune regulation, immune dysregulation, and therapeutic approach. International Immunopharmacology, 111, 109130.

Forstermann, U., & Sessa, W. C. (2012). Nitric oxide synthases: regulation and function. European heart journal, 33(7), 829-837.

Agu, P. C., Afiukwa, C. A., Orji, O. U., Ezeh, E. M., Ofoke, I. H., Ogbu, C. O., Ugwuja, E.I. & Aja, P. M. (2023). Molecular docking as a tool for the discovery of molecular targets of nutraceuticals in diseases management. Scientific Reports, 13(1), 13398.

Giordano, D., Biancaniello, C., Argenio, M. A., & Facchiano, A. (2022). Drug design by pharmacophore and virtual screening approach. Pharmaceuticals, 15(5), 646.

Vazquez, J., Lopez, M., Gibert, E., Herrero, E. & Luque, F. J. (2020). Merging ligand-based and structure-based methods in drug discovery: An overview of combined virtual screening approaches. Molecules, 25(20), 4723.

Xiong, G., Wu, Z., Yi, J., Fu, L., Yang, Z., Hsieh, C., Yin, M., Zeng, X., Wu, C., Lu, A., Chen, X. & Cao, D. (2021). ADMETlab 2.0: an integrated online platform for accurate and comprehensive predictions of ADMET properties. Nucleic acids research, 49(W1), W5-W14.

Gajendran, M., Loganathan, P., Jimenez, G., Catinella, A. P., Ng, N., Umapathy, C., Ziade, N. & Hashash, J. G. (2019). A comprehensive review and update on ulcerative colitis. Disease-a-month, 65(12), 100851.

Gandhi, G. R., Mohana, T., Athesh, K., Hillary, V. E., Vasconcelos, A. B. S., de Franca, M. N. F., ... & Xu, B. (2023). Anti-inflammatory natural products modulate interleukins and their related signaling markers in inflammatory bowel disease: a systematic review. Journal of pharmaceutical analysis.

Spisni, E., Valerii, M. C., De Fazio, L., Cavazza, E., Borsetti, F., Sgromo, A., Candela, M., Centanni, M., Rizello, F. & Strillacci, A. (2015). Cyclooxygenase-2 silencing for the treatment of colitis: a combined in vivo

strategy based on RNA interference and engineered Escherichia coli. Molecular Therapy, 23(2), 278-289.
Peyrin-Biroulet, L., Sandborn, W. J., Panaccione, R., Domènech, E., Pouillon, L., Siegmund, B., Danese, S. & Ghosh, S. (2021). Tumour necrosis factor inhibitors in inflammatory bowel disease: the story continues. Therapeutic Advances in Gastroenterology, 14, 17562848211059954.
Cao, Q., Lin, Y., Yue, C., Wang, Y., Quan, F., Cui, X., Bi, R., Tang, X., Yang, Y., Wang, C., Li, X. & Gao, X. (2021). IL-6 deficiency promotes colitis by recruiting Ly6Chi monocytes into inflamed colon tissues in a CCL2-CCR2-dependent manner. European Journal of Pharmacology, 904, 174165.
Soufli, I., Toumi, R., Rafa, H., & Touil-Boukoffa, C. (2016). Overview of cytokines and nitric oxide involvement in immuno-pathogenesis of inflammatory bowel diseases. World journal of gastrointestinal pharmacology and therapeutics, 7(3), 353.
Temml, V., & Kutil, Z. (2021). Structure-based molecular modeling in SAR analysis and lead optimization. Computational and Structural Biotechnology Journal, 19, 1431-1444.
Duraan-Iturbide, N. A., Diaz-Eufracio, B. I., & Medina-Franco, J. L. (2020). In silico ADME/Tox profiling of natural products: A focus on BIOFACQUIM. ACS omega, 5(26), 16076-16084.
Minerdi, D., Savoi, S., & Sabbatini, P. (2023). Role of Cytochrome P450 Enzyme in Plant Microorganisms' Communication: A Focus on Grapevine. International Journal of Molecular Sciences, 24(5), 4695.
Sewell, F., Corvaro, M., Andrus, A., Burke, J., Daston, G., Delaney, B., Domoradzki, J., Forlini, C., Green, M.L., Hofmann, T., Jackel, S. & Lewis, R. (2022). Recommendations on dose level selection for repeat dose toxicity studies. Archives of Toxicology, 96(7), 1921-1934.
Monnot, A. D., Kovochich, M., Bandara, S. B., Wilsey, J. T., Christian, W. V., Eichenbaum, G., Perkins, L.E., Hasgall, P., Taneja, M., Connor, K., Sague, J., & Unice, K. (2021). A hazard evaluation of the reproductive/developmental toxicity of cobalt in medical devices. Regulatory Toxicology and Pharmacology, 123, 104932.
Reza, A. A., Haque, M. A., Sarker, J., Nasrin, M. S., Rahman, M. M., Tareq, A. M., Khan, Z., Rashid, M., Sadik, M.G., Tsukahara, T. & Alam, A. K. (2021). Antiproliferative and antioxidant potentials of bioactive edible vegetable fraction of Achyranthes ferruginea Roxb. in cancer cell line. Food Science & Nutrition, 9(7), 3777-3805.
Agu, P. C., Afiukwa, C. A., Orji, O. U., Ezeh, E. M., Ofoke, I. H., Ogbu, C. O., Ugwuja, E.I. & Aja, P. M. (2023). Molecular docking as a tool for the discovery of molecular targets of nutraceuticals in diseases management. Scientific Reports, 13(1), 13398.
Volak, L. P., Duevel, H. M., Humphreys, S., Nettleton, D., Phipps, C., Pike, A., Rynn, C., Scott-Stevens, P., Zhang, D. & Zientek, M. (2023). Industry perspective on the pharmacokinetic and absorption, distribution, metabolism, and excretion characterization of heterobifunctional protein degraders. Drug Metabolism and Disposition, 51(7), 792-803.

Zamberlan, F., Castagnolo, D., Sarkar, P., & Schultz, D. (2023). Looking back and moving forward in medicinal chemistry. Nature Communications, 14.

Curry, S. H., & Whelpton, R. (2022). Drug disposition and pharmacokinetics: principles and applications for medicine, toxicology and biotechnology. John Wiley & Sons.

Sukhanova, A., Bozrova, S., Sokolov, P., Berestovoy, M., Karaulov, A., & Nabiev, I. (2018). Dependence of nanoparticle toxicity on their physical and chemical properties. Nanoscale research letters, 13, 1-21.

Panghal, A., & Flora, S. J. S. (2022). Toxicity evaluation of nanomedicine. In Recent Advances in Therapeutic Drug Monitoring and Clinical Toxicology (pp. 323-345). Cham: Springer International Publishing.

Pognan, F., Beilmann, M., Boonen, H., Czich, A., Dear, G., Hewitt, P., Mow, T., Oinonen, T., Roth, A., Steger-Hartmann, T., Valentin, J.P., & Newham, P. (2023). The evolving role of investigative toxicology in the pharmaceutical industry. Nature reviews drug discovery, 22(4), 317-335.

Singh, A. K., Bilal, M., Iqbal, H. M., & Raj, A. (2021). Trends in predictive biodegradation for sustainable mitigation of environmental pollutants: Recent progress and future outlook. Science of The Total Environment, 770, 144561.

Chapter 4

Acute and Sub-acute toxicity of *Lannea coromandelica* and *Trevesia palmata* on rats

4.1. INTRODUCTION

4.1.1. Acute Toxicity

Acute toxicity testing in rats is a crucial component of preclinical drug and chemical safety assessment. It involves the administration of a single, high dose of a substance to laboratory rats to evaluate its potential harmful effects within a short period, typically within 24 to 72 hours. This type of testing provides essential information on the immediate adverse effects of a substance, helping to establish safe dosage levels and assess potential risks to human health (Niyomchan et al., 2023).

Acute toxicity testing serves as an initial screening step to identify substances that may cause severe adverse effects at high doses. By assessing acute toxicity, researchers can prioritize further testing and development efforts for substances with acceptable safety profiles. Understanding the lethal dose (LD50) or the dose at which adverse effects occur in 50% of the test animals allows researchers to establish safe dosage levels for subsequent studies or human use. This information is crucial for determining appropriate dosing regimens in clinical trials or setting exposure limits in occupational or environmental settings (Erhirhie et al., 2018). Regulatory agencies worldwide require acute toxicity data as part of the safety evaluation process for pharmaceuticals, agrochemicals, industrial chemicals, and consumer products. Compliance with these regulatory requirements is essential for obtaining approval for the sale and use of these substances (Strickland et al., 2023).

Acute toxicity data contribute to the overall risk assessment of a substance by providing insight into its potential hazards and helping to estimate the level of risk posed to human health or the environment. This information guides decision-making regarding the management and regulation of hazardous substances (Zhang et al., 2023). Comparing the acute toxicity of different substances allows researchers to prioritize resources and focus further testing efforts on compounds with lower toxicity profiles. It also helps identify structural or functional similarities between toxicants, aiding in the development of predictive toxicology models (Pognan et al., 2023; Cavasotto and Scardino, 2022; Schuijt et al., 2021). Therefore, conducting acute toxicity testing in rats is essential for evaluating the immediate adverse effects of substances, establishing safe dosage levels, ensuring regulatory compliance,

assessing risks to human health, and guiding further toxicological evaluations. This type of testing plays a critical role in safeguarding public health and environmental safety throughout the development and use of various chemicals and pharmaceuticals.

4.1.2. Sub-Acute Toxicity

Sub-acute toxicity testing in rats is an essential component of preclinical safety assessment conducted after acute toxicity evaluation. Unlike acute toxicity, which assesses the immediate adverse effects of a single high dose over a short period, sub-acute toxicity testing involves repeated exposure to lower doses of a substance over several weeks. This extended duration allows for the evaluation of potential cumulative or delayed toxic effects that may not be evident in acute toxicity studies (Niyomchan et al., 2023).

While acute toxicity testing provides valuable information on immediate adverse effects, sub-acute toxicity studies help identify toxic effects that may manifest over time with repeated exposure to lower doses. Some substances may accumulate in tissues or organs, leading to toxicity that becomes apparent only after prolonged exposure (Ugwah-Oguejiofor et al., 2019). Sub-acute toxicity testing also enables the assessment of cumulative effects that result from repeated exposure to a substance over an extended period. This type of testing is particularly important for substances intended for chronic use in humans, such as pharmaceuticals or consumer products, where long-term exposure is common (Nouioura et al., 2023). This toxicity study also helps identify specific target organs or systems affected by the test substance. By examining histopathological changes and functional alterations in various organs following repeated exposure, researchers can better understand the mechanisms of toxicity and potential organ-specific risks (Ugwah-Oguejiofor et al., 2019). Some adverse effects observed in acute toxicity studies may be reversible upon cessation of exposure. Sub-acute toxicity testing allows researchers to determine whether toxic effects persist, resolve, or worsen after discontinuation of exposure, providing critical information on the reversibility of toxicity (Porwal et al., 2017). Regulatory agencies often require sub-acute toxicity data as part of the safety assessment process for

chemicals, pharmaceuticals, and consumer products. These studies provide essential information for risk assessment and regulatory decision-making, ensuring the safety of human health and the environment (Strickland et al., 2023). Sub-acute toxicity studies also help establish dose-response relationships by evaluating the effects of varying doses of the test substance over time. This information is valuable for determining safe exposure levels and setting dose recommendations for subsequent studies or human use (Alelign et al., 2020). Therefore, conducting sub-acute toxicity testing in rats is crucial for identifying delayed or cumulative toxic effects, assessing target organ toxicity, evaluating the reversibility of adverse effects, ensuring regulatory compliance, and establishing dose-response relationships. These studies provide comprehensive safety data that contribute to informed risk assessment and decision-making throughout the development and regulatory approval process of chemicals, pharmaceuticals, and consumer products.

4.1.2. Why Acute and Sub-Acute Testing Analysis Is Important?

Performing in-vivo acute and sub-acute toxicity testing on methanolic extracts of *Lannea coromandelica* and *Trevesia palmata* after computational analysis of phytocompounds is essential for several reasons. First being the reason for validation of computational analysis results. Computational analysis provides insights into the potential bioactive compounds present in the plant extracts. However, in-vivo toxicity testing confirms whether these compounds indeed possess therapeutic potential without causing harmful effects in living organisms. It helps validate the computational predictions by assessing the actual physiological response to the plant extracts (Frangiamone et al., 2024). Secondly, for comprehensive safety evaluation. In-vivo toxicity testing allows for a comprehensive evaluation of the safety profile of the plant extracts. While computational analysis can identify potential bioactive compounds, it does not account for potential interactions, metabolites, or unforeseen toxic effects that may occur in living organisms. Acute and sub-acute toxicity testing provide valuable data on the overall safety and tolerability of the extracts (Jitareanu et al., 2022). Thirdly, the identification of safe doses. Toxicity testing helps determine the safe dosage range of the plant extracts for potential therapeutic use. By

evaluating the effects of different doses on animals over various durations, researchers can establish dose-response relationships and identify the maximum tolerated dose without causing significant adverse effects. This information is crucial for determining appropriate dosing regimens in human studies (Ugwah-Oguejiofor et al., 2019). Toxicity testing is also important for fulfilling the regulatory agencies which often require in-vivo toxicity data as part of the safety assessment process for herbal medicines or natural products. Acute and sub-acute toxicity testing in animals provides essential information for regulatory submissions and ensures compliance with safety standards and guidelines before human trials or commercialization (Strickland et al., 2023). In-vivo toxicity testing provides insights into the absorption, distribution, metabolism, and excretion (ADME) of the bioactive compounds present in the plant extracts. It helps elucidate their pharmacokinetic profiles and pharmacodynamic effects in living organisms, which are crucial for understanding their mechanisms of action and potential therapeutic applications. In-vivo toxicity testing also allows for the early identification of potential toxic effects or adverse reactions associated with the plant extracts. By assessing acute and sub-acute toxicity, researchers can identify and mitigate risks before advancing to more costly and time-consuming clinical trials or commercialization efforts (Jitareanu et al., 2022).

Overall, performing in-vivo acute and sub-acute toxicity testing complements computational analysis by providing crucial data on the safety, efficacy, and pharmacological properties of methanolic extracts of *Lannea coromandelica* and *Trevesia palmata*. It ensures a comprehensive understanding of the potential therapeutic benefits and risks associated with these plant extracts, ultimately guiding their development and regulatory approval for medicinal use.

4.2. REVIEW OF LITERATURE

4.2.1. Acute Toxicity Studies

Several studies have evaluated the acute toxicity of *Lannea coromandelica* (Islam et al., 2022; Sobeh et al., 2018; Imam et al., 2014) and *Trevesia palmata* (Rahman et al., 2014; Victoria et al., 2019; Sayeed et al., 2014) extracts in rats. These studies typically involve administering a single high dose of the extract and observing the animals for signs of toxicity or mortality over a short period, usually 24 to 72 hours. Results from these studies have indicated that acute administration of methanolic extracts of *Lannea coromandelica* and *Trevesia palmata* generally does not cause significant adverse effects or mortality in rats at moderate to high doses. However, dose-dependent effects such as changes in behaviour, clinical signs, and biochemical parameters have been reported.

4.2.2. Sub-acute Toxicity Studies

Sub-acute toxicity studies involve administering the plant extracts to rats daily for a longer duration, typically ranging from 14 to 28 days, to assess potential cumulative toxic effects. Studies investigating the sub-acute toxicity of *Lannea coromandelica* (Ha et al., 2024; Gandhidasan et al., 1991) and *Trevesia palmata* (Victoria et al., 2019) extracts have reported varying results depending on the dose, duration of exposure, and endpoints evaluated. While some studies have demonstrated no significant adverse effects on general health, organ morphology, or biochemical parameters, others have reported mild to moderate toxicity, including alterations in haematological parameters, liver enzymes, and histopathological changes in vital organs.

4.2.3. Mechanistic Insights of the Study

Some studies have aimed to elucidate the mechanisms underlying the observed acute and sub-acute toxicity of *Lannea coromandelica* (Srinivasa Rao et al., 2014) and *Trevesia palmata* (Ha et al., 2024) extracts in rats. These investigations often involve assessing oxidative stress markers, inflammatory cytokines, and apoptotic pathways to understand the underlying pathophysiological mechanisms (Dimitrov et al., 2023; Anwar et al., 2022). Some studies have suggested that *L. coromandelica* and *T.*

palmata extracts may induce oxidative stress in various tissues. Elevated levels of reactive oxygen species (ROS) and lipid peroxidation products have been reported following administration of the extracts. This oxidative stress can lead to cellular damage and dysfunction, contributing to the observed toxicity (Manoharan et al., 2023; Belmehdi et al., 2023; Alam et al., 2017; Kumar and Jain, 2015; Srinivasa Rao et al., 2014; Rahman et al., 2014).

Liver toxicity is a common concern associated with the consumption of herbal extracts. Studies have shown that *L. coromandelica* and *T. palmata* extracts can induce hepatotoxic effects in animal models, including hepatocyte necrosis, inflammation, and altered liver function tests. Hepatotoxicity may result from direct toxic effects of the extracts on liver cells or from secondary mechanisms such as oxidative stress and inflammation (Srinivasa Rao et al., 2014; Pugazenthi et al., 2016; Ha et al., 2024; Deresa and Diriba, 2023; Belmehdi et al., 2023; Muhseen et al., 2020).

Overall, these mechanistic studies highlight the complex interplay of oxidative stress and organ-specific toxicity in the observed acute and sub-acute toxicity of both *L. coromandelica* and *T. palamata*. Further research is needed to fully elucidate these mechanisms and their relevance to human health, as well as to identify potential strategies for mitigating the adverse effects of *L. coromandelica* and *T. palmata* extracts. Additionally, studies may explore the pharmacokinetics and tissue distribution of bioactive compounds present in the extracts to correlate their levels with observed toxic effects (Shakya et al., 2020).

4.2.4. Limitations and Future Directions

Despite the wealth of studies on acute and sub-acute toxicity, there are still gaps in our understanding of the safety profile of *Lannea coromandelica* and *Trevesia palmata* extracts. Many studies lack standardized protocols, sample sizes, and control groups, making it challenging to compare results across studies. Future research should focus on elucidating the dose-response relationships, identifying specific toxic constituents, and conducting long-term toxicity studies to assess the chronic effects of repeated exposure to these plant extracts.

However, acute and sub-acute toxicity studies of *Lannea coromandelica* and *Trevesia palmata* in rats provide valuable insights into their safety profile, further research is needed to fully understand the potential risks associated with their use and to establish safe therapeutic doses for human consumption.

4.3. MATERIALS AND METHODS

4.3.1. Toxicity Studies

Acute and sub-acute toxicity tests were performed based on the OECD (Organisation for Economic Co-operation and Development) - Guidelines 425 and 407 (OECD, 2008a, 2008b).

4.3.2. Acute toxicity (LD50 test)

The oral acute toxicity research was carried out in accordance with OECD guideline No. 425 for the acute toxicity class method (ATC) protocol, with minimal changes. Male rats were divided into treatment groups (5 animals per group). Prior to the treatment, the animals were weighed and marked, and they were not permitted to eat or drink for the night. The control group got distilled water, whereas the treated groups received a single dose of 2000 and 5000 mg/kg body weight of the freshly made methanolic leaf extracts of *Lannea coromandelica* and *Trevesia palmata*, respectively. Signs of acute toxicity and the number of deaths per dosage within 24 hours of delivery were observed and recorded, followed by once a day for 14 days to determine the oral median lethal dose, LD50 (Lorke, 1983). Daily records were kept of water and feed consumption, as well as body weight (OECD, 2008a). At the end of the observation time, all animals were anaesthetized with ketamine and xylazine (25 and 10 mg/kg, respectively). Blood samples were taken via heart puncture for later haematological and biochemical analysis, while organs were removed, weighed, and preserved in Bouin's fixative for histological study.

4.3.3. Sub-acute toxicity

Each plant was separated into four experimental groups of five animals each (males). Three different doses of Lannea coromandelica and Trevesia palmata (200, 400, and 800 mg/kg) were given orally (gavage) to each group daily for 28 days. The control group was given simply distilled water and maintained under the same conditions. The doses were chosen using the OECD Guideline 407 (Repeated Dose 28-Day Oral Toxicity Study in Rodents) (OECD, 2008b). During therapy, daily body weight, food and drink consumption, and potential toxicity indicators were monitored and documented. A clinical examination was performed once every day. After 28 days of observation, all animals were starved overnight and anaesthetized with ketamine and xylazine at 25 and 10 mg/kg, respectively. Blood samples were collected via heart puncture for further haematological and biochemical investigation. After drawing blood, the important organs (heart, lung, kidney, liver, and spleen) and reproductive organs (testis and epididymis) were weighed.

4.3.4. Haematological analysis

Haematological assays were done on all surviving animals at the conclusion of the trial, on the 15th day for acute toxicity and the 29th day for sub-acute toxicity. Animals were sacrificed, and their blood was collected in tubes.

The hematologic parameters were assessed for white blood cell (WBC), red blood cell (RBC), haemoglobin (Hb), hematocrit, mean corpuscular volume (MCV), mean corpuscular haemoglobin (MCH), and mean corpuscular haemoglobin concentration (MCHC).

4.3.5. Serum Biochemical Analysis

The biochemical assay was performed on all surviving animals at the end of the experiment. The blood was collected into tubes and centrifuged at 3500 rpm for 30 minutes. Serum from each sample was collected and kept at -80ºC until analysis. Serum alanine aminotransferase (ALT), aspartate aminotransferase (AST), alkaline phosphatase (ALP), total protein, globulin (Glo), albumin (Alb), urea, blood urea

nitrogen (BUN), creatinine, triglycerides, total cholesterol, and calcium activity were measured using a coral clinical diagnostic kit.

4.3.5. Histological Analysis

The liver and kidney organs were fixed using Bouin's fixative, embedded in paraffin, sectioned at 5 µm, stained with hematoxylin and eosin, and studied under light microscopy (Martey et al., 2010). The histological analysis intended to determine the organs' tissue integrity. The characteristics studied included degeneration, necrosis, apoptosis, leukocyte infiltration, congestion, blood extravasation, and fibrosis (Cunha et al., 2009).

4.3.6. Statistical analysis

Data is provided as mean ± SEM. One-way ANOVA was used to compare and analyse data. p-values < 0.05 were considered significant.

4.4. RESULTS

4.4.1. Body weight, Rectal temperature, food and water consumption

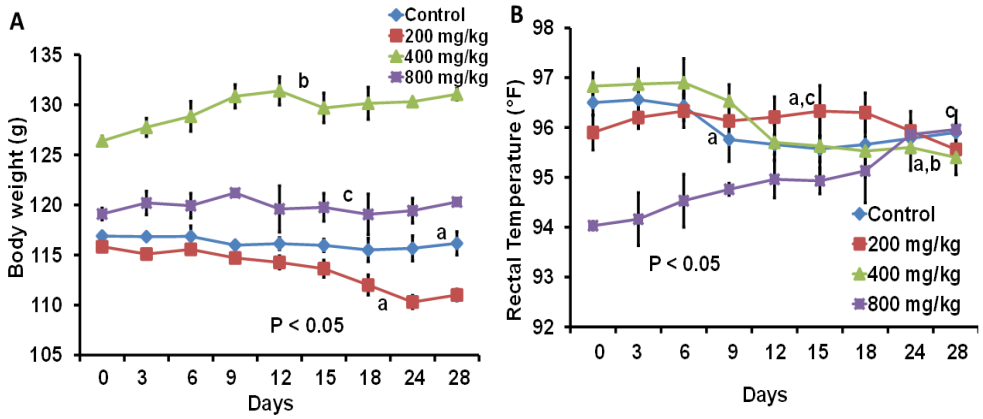

Figure 19: The effect of methanolic extract of *Lannea coromandelica* leaves on body weight (A) and rectal temperature (B) of the repeated exposure of Wistar rats.

Significant change was observed in the animal's body weight (Figure 19:A) and rectal temperature (Figure 19:B) during the study in *Lannea coromandelica* treated group (Figure 19). Administration of the *Lannea coromandelica* leaf extract (LCLE)

affected the food intake and water consumption greatly. Significant changes were found in the relative organ weight or liver and right kidney in higher dose (800 mg/kg) when compared to the control group. Kidney (l) and Testis (l) showed no significant changes of control when compared with 400 mg/kg but showed significant changes at higher dose (800 mg/kg) and at lower dose (200 mg/kg).

Table 28: Effect of methanolic extract of *Lannea coromandelica* leaves on relative body weight of Wistar rats in sub- acute toxicity study.

Relative organ weight (g)	**Treatment group (n=5)**				**$F_{(3,19)}$ value**	**P value**
	Control	**800 mg/kg**	**400 mg/kg**	**200 mg/kg**		
Liver	2.803 ± 0.006a	4.450 ± 0.008b	2.450 ± 0.006a	2.909 ± 0.004a	119460	NS
Kidney (r)	0.276 ± 0.006a	0.455 ± 0.006b	0.279 ± 0.004a	0.335 ± 0.008a	15581	<0.0001
Kidney (l)	0.282 ± 0.003a	0.444 ± 0.006b	0.260 ± 0.005a	0.337 ± 0.003c	28381	<0.0001
Testis (r)	0.910 ± 0.006a	1.061 ± 0.002b	0.946 ± 0.004a	0.928 ± 0.004a	451.66	<0.0001
Testis (l)	0.938 ± 0.004a	0.988 ± 0.004b	0.936 ± 0.003a	0.928 ± 0.006c	162.96	<0.0001

Values are expressed as mean ± SEM, n = 5 animals/group.

p<0.05 (ANOVA) is considered significantly different. NS: Non-significant. Different letters in the column mean significantly different among the groups.

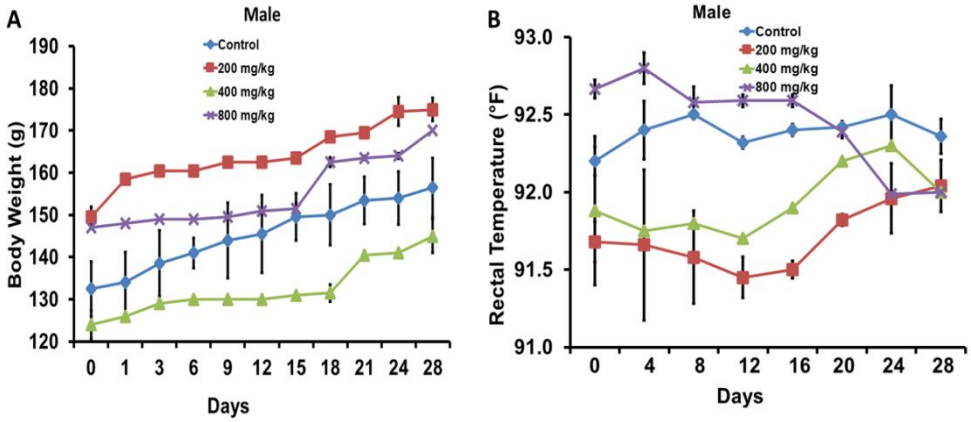

Figure 20: The effect of methanolic extract of *Trevesia palmata* leaves on body weight (A) and rectal temperature (B) of the repeated exposure of Wistar rats.

Significant increase in the body weight (Figure 20:A) and non-significant changes in rectal temperature (Figure 20:B) were observed in the *T. palmata* treated groups (Figure 20). Final body weights of experimental rats were significantly ($p < 0.05$) higher than their pooled initial weights in all the experimental groups (Table 29). Significant changes were noted for the higher dose (800 mg/kg) initial and final body weights and absolute weight of the kidney. No significant changes were observed for absolute weight of liver and testis and relative weight of liver, kidney and testis (Table 29).

Table 29: Effect of methanolic extract of *T. palmata* leaf treatment for 28 days on body weight (g), absolute (g) and relative (g/100 g) weights of organs in sub-acute toxicity study of male Wistar rats.

Parameters	**Experimental group**				**$F_{(3,19)}$ value**	***p* value**
	Control	**800 mg/kg**	**400 mg/kg**	**200 mg/kg**		
Initial body weight (g)	132.500 ± 6.490a	149.500 ± 2.460b	124.000 ± 3.350a	147.000 ± 0.000a,b	9.861	<0.05

Final body weight (g)	156.500 ± 6.93a	175.000 ± 2.680b	180.730 ± 4.030a	171.570 ± 0.00a,b	10.295	<0.05
Liver (g)	3.730 ± 0.130a	3.980 ± 0.150a	3.480 ± 0.11a	3.470 ± 0.15a	3.255	NS
Liver (g/100 g)	2.380 ± 0.110a	2.280 ± 0.11a	2.400 ± 0.12a	2.040 ± 0.15a	1.785	NS
Kidney (g)	0.610 ± 0.160a	1.400 ± 0.130b	0.450 ± 0.110a	0.460 ± 0.180a	12.541	<0.05
Kidney (g/100g)	0.390 ± 0.010a	0.800 ± 0.020a	0.310 ± 0.010a	0.270 ± 0.010a	2.797	NS
Testis (g)	0.990 ± 0.140a	1.160 ± 0.110a	0.980 ± 0.150a	1.230 ± 0.210a	0.5901	NS
Testis (g/100g)	0.630 ± 0.110a	0.660 ± 0.150a	0.680 ± 0.110a	0.720 ± 0.110a	0.08919	NS

Values are expressed as mean ± SEM, n = 5 animals/group.

p<0.05 (ANOVA) shows significant differences. Different letters in the columns indicate significant differences between groups. Same letter indicates no significant changes. NS: Non-significant.

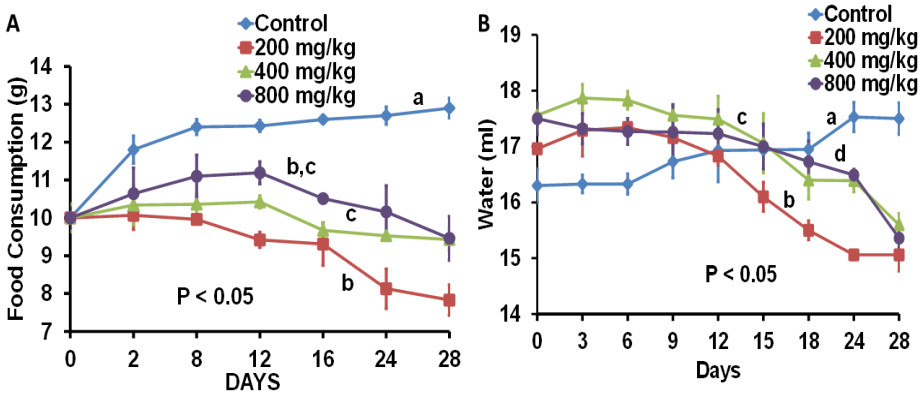

Figure 21: The effect of methanolic extract of *Lannea coromandelica* leaves on the food (A) and water (B) consumption of the exposed Wistar rats.

In *Lannea coromandelica* treated groups significant increase in the food consumption (A) and significant decrease in the water consumption (B) was observed when compared with the control group (Figure 21).

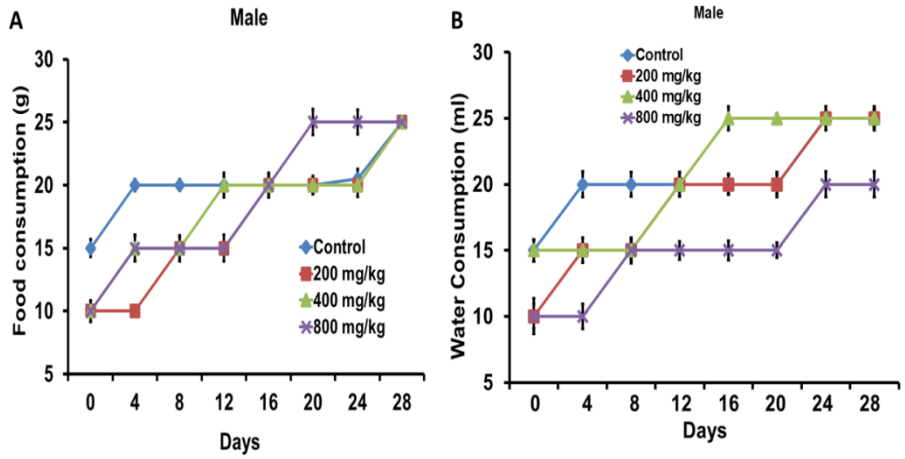

Figure 22: The effect of methanolic extract of *Trevesia palmata* leaves on the food (A) and water (B) consumption of the exposed Wistar rats.

In *T. palmata* treated groups significant increase in the food (Figure 22:A) and water consumption (Figure 22:B) was observed when compared with the control groups (Figure 22).

4.4.2. Clinical signs and symptoms

Table 30 represents observations on the behavioural responses and general appearance of rats treated with single dose of *Lannea coromandelica* (*L. coromandelica*) and *Trevesia palmata* (*T. palmata*) in acute and repeated dose in sub-acute toxicity studies.

In Table 30 of *L. coromandelica* acute toxicity study, Control group shows no changes in skin or eye colour. Normal food intake, general physique, no occurrence of diarrhoea, coma, tremors, or death were observed. At both 2000 mg/kg and 5000 mg/kg doses no changes in skin or eye colour were observed with normal food intake, general physique and absence of diarrhoea, coma and tremors. No mortality was found. In sub-acute toxicity study, doses 200 mg/kg a showed no changes in skin or eye colour with normal food intake. General physique remained normal with no

occurrence of diarrhoea, coma and tremors, but there was a 17 % mortality rate. At a dose of 400 mg/kg, no changes in skin or eye colour with effect on food intake was observed. General physique slightly became weak but no occurrence of diarrhoea, coma, tremors, but there was a 17 % mortality rate. At a dose of 800 mg/kg, no changes in skin or eye colour with effect on food intake was observed. General physique became weak but but no occurrence of diarrhoea, coma and tremors was observed. Mortality rate of 33 % was recorded.

In *T. palmata* acute toxicity study, Control group shows no changes in skin or eye colour. Normal food intake, general physique, no occurrence of diarrhoea, coma, tremors, or death were observed. At both 2000 mg/kg and 5000 mg/kg doses no changes in skin or eye colour were observed with normal food intake, general physique and absence of diarrhoea, coma and tremors. No mortality was found. In sub-acute toxicity study, doses 200 and 400 mg/kg showed no changes in skin or eye colour with normal food intake. General physique remained normal with no occurrence of diarrhoea, coma and tremors, but there was a 17 % mortality rate at dose 200 mg/kg and 33 % mortality rate at dose 400 mg/kg. At a dose of 800 mg/kg, no changes in skin or eye colour with effect on food intake was observed. General physique became weak but no occurrence of diarrhoea, coma and tremors. Mortality rate of 50 % was recorded (Table 30).

Table 30: Behavioral responses and general appearance of rat treated with single and repeated dose of *Lannea coromandelica* (*L. coromandelica*) and *Trevesia palmata* (*T. palmata*) in acute and sub-acute toxicity study.

Observation	*Lannea coromandelica* (*L. coromandelica*)							*Trevesia palmata* (*T. palmata*)						
	Acute toxicity			Sub-acute toxicity				Acute toxicity			Sub-acute toxicity			
	Control	2000 mg/kg	5000 mg/kg	Control	200 mg/kg	400 mg/kg	800 mg/kg	Control	2000 mg/kg	5000 mg/kg	Control	200 mg/kg	400 mg/kg	800 mg/kg
Change in skin colour	No effect	No effect	No effect	No effect	No effect	No effect	No effect	No effect	No effect	No effect	No effect	No effect	No effect	No effect
Eye colour change	No effect	No effect	No effect	No effect	No effect	No effect	No effect	No effect	No effect	No effect	No effect	No effect	No effect	No effect
Food intake	Normal	Normal	Normal	Normal	Effect	Effect	Effect	Normal	Normal	Normal	Normal	Normal	Normal	Effect
General physique	Normal	Normal	Normal	Normal	Normal	Weakness	Weakness	Normal	Normal	Normal	Normal	Normal	Normal	Weakness
Diarrhoea	Not present	Not present	Not present	Not present	Not present	Not present	Not present	Not present	Not present	Not present	Not present	Not present	Not present	Not present
Coma	Not present	Not present	Not present	Not present	Not present	Not present	Not present	Not present	Not present	Not present	Not present	Not present	Not present	Not present
Tremor	Not present	Not present	Not present	Not present	Not present	Not present	Not present	Not present	Not present	Not present	Not present	Not present	Not present	Not present
Death	Alive	Alive	Alive	Alive	17 %	17 %	33 %	Alive	Alive	Alive	Alive	17 %	33 %	50 %

4.4.3. Haematological and biochemical analysis

Table 29 presents the biochemical and haematological parameters measured in rats exposed to different doses of *Lannea coromandelica* (*L. coromandelica*) and *Trevesia palmata* (*T. palmata*) in both acute and sub-acute toxicity studies.

L. coromandelica acute toxicity study shows AST (Aspartate Aminotransferase) with no significant difference observed between control and treated groups. ALT (Alanine Aminotransferase), creatinine, urea and BUN showed significant increase at 5000 mg/kg compared to control and 2000 mg/kg. ALP (Alkaline Phosphatase) showed no significant difference at lower doses but decreased at higher dose (5000 mg/kg).

Haematological parameters revealed that WBC, haemoglobin, and MCHC (Mean Corpuscular Haemoglobin Concentration) showed no significant differences. RBC results were significantly decreased at all doses compared to control. Hematocrit, MCV (Mean Corpuscular Volume) and MCH (Mean Corpuscular Haemoglobin) data reveals significant increase at higher dose (5000 mg/kg).

Sub-acute toxicity study in *L. coromandelica* interprets that AST, ALT, ALP, Creatinine, Urea and BUN showed similar patterns observed as in acute toxicity, with significant increases at higher doses. Haematological parameters for sub-acute toxicity shows that WBC and RBC was significantly decreased at all doses compared to control. Hematocrit, haemoglobin (Hb) and MCHC showed no significant difference. MCV and MCH reveals significant increase at higher dose (800 mg/kg). No significant differences were observed for MCHC.

In *T. palmata* acute toxicity study, AST levels show a decreasing trend with increasing doses, but the changes are not statistically significant. ALT levels increase significantly at the highest dose compared to control, indicating potential liver damage. ALP levels show a decreasing trend with increasing doses, and the decrease is statistically non-significant at the highest dose compared to control, suggesting no effect on liver function. For renal function test creatinine levels show an increasing trend with increasing doses, but the changes are not statistically significant except for a significant decrease at the lowest dose compared to control. Urea levels increase

significantly at the highest dose compared to control, indicating possibility for kidney dysfunction. BUN levels show increase in higher dose non-significantly when compared to control, further suggesting no adverse effects on renal function.

In sub-acute toxicity study of *T. palmata*, a significant decrease at the highest dose compared to control was observed. ALT, creatinine and urea showed similar observations to the acute toxicity study observation. ALP decreased significantly at the highest dose compared to control, suggesting a possible adverse effect on liver function. BUN increased significantly at the highest dose when compared to the control group, signifying possible kidney dysfunction.

For acute toxicity study of *T. palmata*, haematological parameters reveal that WBC, RBC, haemoglobin (Hb) and MCHC levels show a decreasing trend with increasing doses, but the changes are not statistically significant when compared to control. Hematocrit levels increase significantly at the highest dose compared to control, indicating potential dehydration or haemoconcentration. MCV levels increase significantly at the highest dose compared to control, indicating potential macrocytic anaemia. MCH levels increase significantly at the highest dose compared to control, suggesting altered erythropoiesis or haemoglobin synthesis. In sub-acute study of *T. palmata*, haematological study suggests that WBC, RBC, Hb, MCV, MCH and MCHC levels showed no significant changes when compared to the control group. Hematocrit level showed similar observations with that of acute toxicity.

Overall, the data suggests that *T. palmata* administration may lead to liver and kidney dysfunction, as evidenced by alterations in liver enzymes and renal function markers. Additionally, there are notable effects on haematological parameters, indicating potential adverse effects on blood composition and erythropoiesis.

Table 31: Biochemical estimation from blood serum and haematological parameters of rats at different dose level in acute and sub- acute toxicity study.

	Parameters	Acute toxicity					Sub-acute					
		Control	2000 mg/kg	5000 mg/kg	$F_{(2,14)}$	P value	Control	200 mg/kg	400 mg/kg	800 mg/kg	$F_{(3,19)}$	P value
L. coromandelica	AST (U/L)	47.00 ± 1.33a	43.00 ± 1.18a	45.00 ± 1.39a	2.36	NS	49.00 ± 2.00a	45.20 ± 1.88a	43.00 ± 1.83a,b	36.00 ± 2.31b	7.36	<0.05
	ALT (U/L)	43.00 ± 1.09a	44.76 ± 1.10a	52.00 ± 1.03b	19.73	<0.001	45.20 ± 1.66a	48.00 ± 1.84a	57.80 ± 1.91b	58.40 ± 2.63b	10.89	<0.001
	ALP (K.A. Units)	130.89 ± 1.17a	128.32 ± 1.12a,b	125.21 ± 1.30b	5.62	<0.05	135.73 ± 2.84a	128.30 ± 2.16a,b	126.75 ± 2.11b	118.05 ± 1.73c	10.43	<0.001
	Creatinine (mg %)	0.80 ± 0.11a	0.90 ± 0.10a	1.40 ± 0.08b	10.88	<0.01	0.65 ± 0.11a	0.90 ± 0.10a	0.89 ± 0.06a	1.40 ± 0.08b	12.39	<0.001
	Urea (mg/dl)	28.80 ± 1.15a	30.76 ± 1.11a	39.32 ± 1.21b	23.37	<0.0001	30.88 ± 1.22a	33.95 ± 1.04a	39.74 ± 1.36b	45.59 ± 1.18c	29.06	<0.0001
	BUN (mg/dl)	13.34 ± 1.15a	14.36 ± 1.11a,b	18.36 ± 1.21b	5.10	<0.05	14.42 ± 1.22a	15.85 ± 1.01a	18.56 ± 1.16a,b	21.29 ± 1.18b	7.030	<0.05
	Hematological parameters											
	WBC ($10^3/mm^3$)	4.48 ± 1.93a	5.25 ± 0.66a	5.33 ± 0.93a	0.13	NS	4.18 ± 0.66a	3.99 ± 0.54a	3.16 ± 0.32a	1.16 ± 0.33a	8.13	<0.05
	RBC ($10^6/mm^3$)	7.76 ± 1.30a	6.34 ± 1.66a	4.22 ± 1.17a	1.64	NS	7.33 ± 1.28a	6.32 ± 0.45a	4.33 ± 1.41a	3.38 ± 0.36a	3.30	<0.05
	Hematocrit (%)	41.00	43.00	47.00	5.84	<0.05	43.50	42.00	46.50	47.00	2.58	NS

		± 1.32a	± 1.26a,b	± 1.21b			± 1.35a	± 1.95a	± 1.22a	± 1.35a		
	Hemoglobin (g/dL)	13.72 ± 1.06a	14.33 ± 1.13a	15.61 ± 1.13a	0.76	NS	14.51 ± 1.48a	14.03 ± 1.27a	15.50 ± 1.83a	15.66 ± 1.54a	0.26	NS
	MCV (fL)	52.84 ± 3.33a	67.82 ± 3.51a	111.37 ± 5.11b	56.00	<0.0001	59.35 ± 3.11a	66.46 ± 3.66a	107.39 ± 4.38b	139.05 ± 4.95c	83.18	<0.0001
	MCH (pg)	17.68 ± 1.80a	22.60 ± 1.95a	36.99 ± 1.85b	28.87	<0.0001	19.80 ± 1.35a	22.20 ± 2.00a	35.80 ± 2.52b	46.33 ± 1.96c	38.38	<0.0001
	MCHC (g/dL)	33.46 ± 0.65a	33.33 ± 0.89a	33.21 ± 1.01a	0.02	NS	33.36 ± 0.23a	33.40 ± 0.31a	33.33 ± 0.41a	33.32 ± 0.35a	0.01	NS
T. palmata	**AST (U/ml)**	46.00 ± 1.45a	44.00 ± 1.40a	41.00 ± 1.33a	3.26	NS	49.00 ± 2.23a	47.89 ± 2.11a	45.00 ± 1.91a	35.56 ± 1.66b	9.42	<0.001
	ALT (U/ml)	41.00 ± 2.05a	48.00 ± 1.85a	57.00 ± 2.22b	15.38	<0.001	45.33 ± 1.22a	46.13 ± 1.04a	47.09 ± 1.42a	59.92 ± 1.83b	12.17	<0.001
	ALP (K.A. Units)	139.32 ± 1.06a	136.11 ± 1.13a	137.35 ± 1.11a	2.17	NS	136.33 ± 1.89a	138.39 ± 2.33a	133.36 ± 1.35a	125.09 ± 1.44b	10.60	<0.001
	Creatinine (mg %)	0.70 ± 0.12a	1.10 ± 0.16a	1.20 ± 0.12a	3.86	NS	0.60 ± 0.11a	0.70 ± 0.41a	0.90 ± 0.14a	1.20 ± 0.45a	0.70	NS
	Urea (mg/dl)	29.34 ± 1.85a	27.09 ± 1.98a	36.98 ± 1.87b	7.44	<0.05	30.33 ± 1.11a	31.39 ± 1.39a,b	35.85 ± 1.25b	41.66 ± 1.44c	15.64	<0.0001
	BUN (mg/dl)	13.70 ± 1.83a	12.65 ± 1.98a	17.27 ± 1.87a	1.62	NS	14.16 ± 1.01a	14.66 ± 1.33a	16.74 ± 1.25a,b	19.46 ± 1.11b	4.17	<0.05
	Hematological parameters											
	WBC (10^3/mm^3)	3.17 ±	2.21 ±	2.25 ±	0.85	NS	4.33 ±	4.74 ±	3.88 ±	3.85 ±	0.13	NS

		0.36a	0.86a	0.42a			1.18a	1.08a	1.31a	1.11a		
	RBC (10^6/mm^3)	7.38 ± 0.41a	7.16 ± 0.95a	6.34 ± 0.17a	0.82	NS	8.18 ± 1.33	7.98 ± 0.41a	8.26 ± 0.17a	8.19 ± 1.43a	0.12	NS
	Hematocrit (%)	41.00 ± 1.28a	38.00 ± 1.36a	47.00 ± 1.19b	12.85	<0.05	43.00 ± 1.31a	44.00 ± 1.23a,b	41.00 ± 1.41a	38.00 ± 1.22a,c	4.18	<0.05
	Hemoglobin (g/dl)	13.77 ± 1.11a	12.66 ± 1.18a	15.62 ± 1.15a	1.70	NS	14.33 ± 0.89a	14.68 ± 0.45a	13.65 ± 0.11a	12.69 ± 0.21a	0.37	NS
	MCV (fL)	55.56 ± 3.22a	53.07 ± 2.89a	74.13 ± 4.31b	10.66	<0.01	52.57 ± 3.63a	55.14 ± 3.13a	49.64 ± 3.97a	46.40 ± 4.01a	1.03	NS
	MCH (pg)	18.66 ± 1.15a	17.68 ± 1.12a	24.64 ± 1.10b	11.18	<0.01	17.52 ± 0.89a	18.40 ± 1.15a	16.53 ± 1.13a	15.49 ± 1.26a	1.17	NS
	MCHC (g/dL)	33.59 ± 0.21a	33.32 ± 0.28a	33.23 ± 0.22a	0.62	NS	33.33 ± 0.23a	33.36 ± 0.21a	33.29 ± 0.25a	33.39 ± 0.27a	0.03	NS

Data are presented as mean ± standard error mean (n = 5 rats/treatment). Statistical comparison was performed using one-way ANOVA followed by Tukey's post hoc tests for all pair-wise multiple comparisons. Different letters column wise indicate that treatment groups are significantly different at $p < 0.05$ and with similar letters indicate that treatment groups are not statistically significant at $p > 0.05$. NS – non significant.

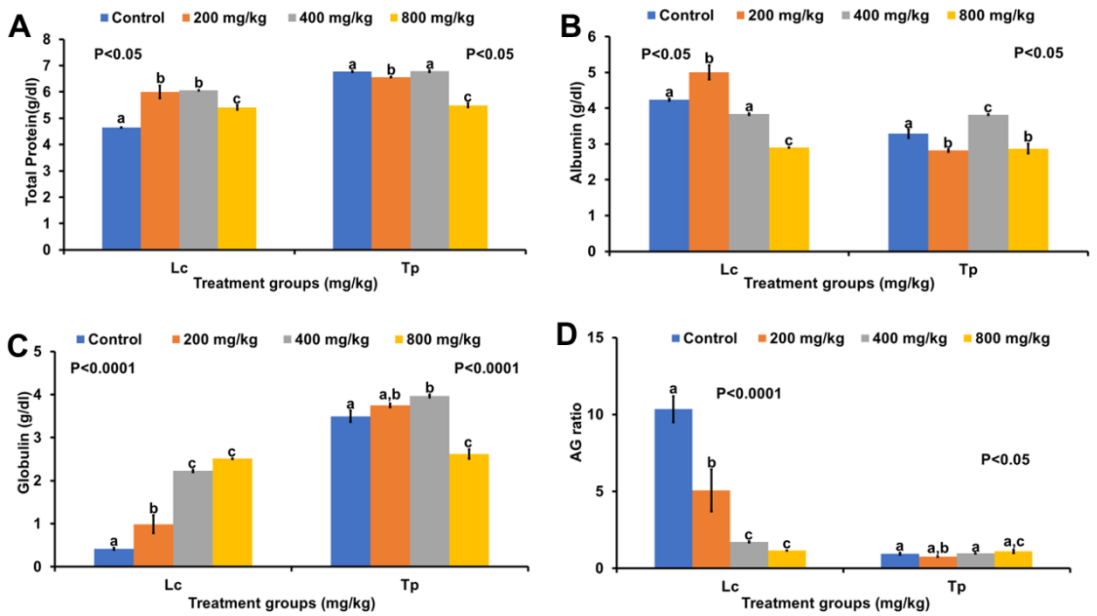

Figure 23: The effect of LCLE and TPLE on the total protein (A), albumin (B), globulin (C) and albumin globulin (AG) ratio (D) in rats. Lc – *Lannea coromandelica*. Tp – *Trevesia palmata*. P<0.05 shows significant differences. Different letters in the bar graph indicates significant differences within the columns and similar letter mean no significant difference.

In LCLE, significant increase in the total protein content with higher dose was observed with increase in the dose when compared to the control group suggesting that the extract may have beneficial effects on protein metabolism and overall protein status in the body (Figure 23:A). In TPLE, no significant changes were observed in the total protein content between control and 400 mg/kg but a significant decrease with increase in the dose was observed which suggest a dose-dependent effect on protein levels within the body (Figure 23:A). In LCLE, the significant increase in albumin observed in the 200 mg/kg group compared to the control group in the LCLE study suggests that this particular dosage of the extract may have a positive effect on albumin levels (Figure 23:B). On the other hand, a significant decrease with lowest albumin content was observed for TPLE at the highest dose (800 mg/kg) which could indicate several potential health implications. LCLE showed a significant increase in the globulin content with increase in the dose which may indicate modulation of immune function, inflammation, or liver activity suggesting

several potential implications (Figure 23:C). On the contrary, TPLE show significant increase in the globulin content till 400 mg/kg but then suddenly drops back with a significant decrease at the highest dose (800 mg/kg) suggesting complex interactions between the extract and the immune system or other physiological processes (Figure 23:C). The albumin globulin (AG) ratio of LCLE shows a significant decrease with the increase in dose indicating alterations in serum protein levels and suggests potential effects on immune function, inflammation, liver health, or toxicity (Figure 23:D). TPLE AG ratio shows that there is no significant changes in the level when compared with the control group but at 200 mg/kg and 800 mg/kg group there was a significant changes which may suggest dose-dependent or threshold effects on serum protein composition (Figure 23:D).

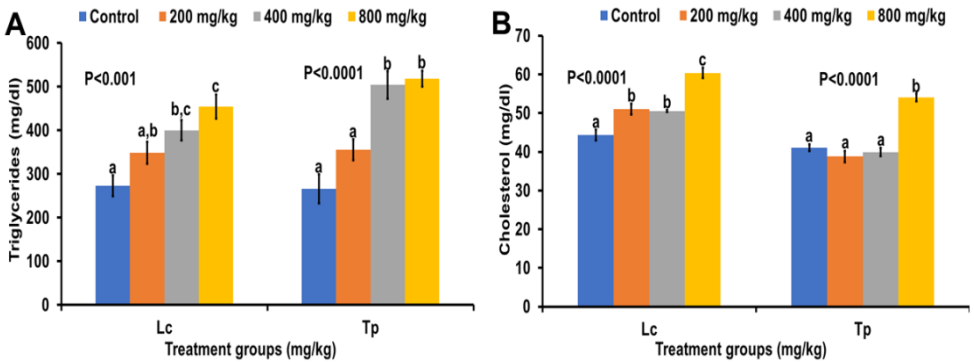

Figure 24: The effect of LCLE and TPLE on the triglycerides (A) and cholesterol level (B) in rats. Lc – *Lannea coromandelica*. Tp – *Trevesia palmata*. P<0.05 shows significant differences. Different letters in the bar graph indicates significant differences within the columns and similar letter mean no significant difference.

The triglyceride analysis of both the plants showed significant increase with the increase in the dose indicating potential adverse metabolic effects or disturbances in lipid metabolism induced by the extracts (Figure 24:A). Cholesterol level in LCLE shows significant increase with the increase in dose suggesting potential adverse effects on lipid metabolism and cardiovascular health (Figure 24:B). TPLE on the other hand, shows a non-significant difference between control, 200 mg/kg and 400 mg/kg groups with a significantly extreme alteration in the highest dose (800 mg/kg) (Figure 18:B). The non-significant differences in cholesterol levels at lower doses of

TPLE, followed by a significant alteration at the highest dose, suggest a dose-dependent response and raise concerns about potential adverse effects or toxicity of TPLE on cholesterol metabolism, particularly at higher concentrations.

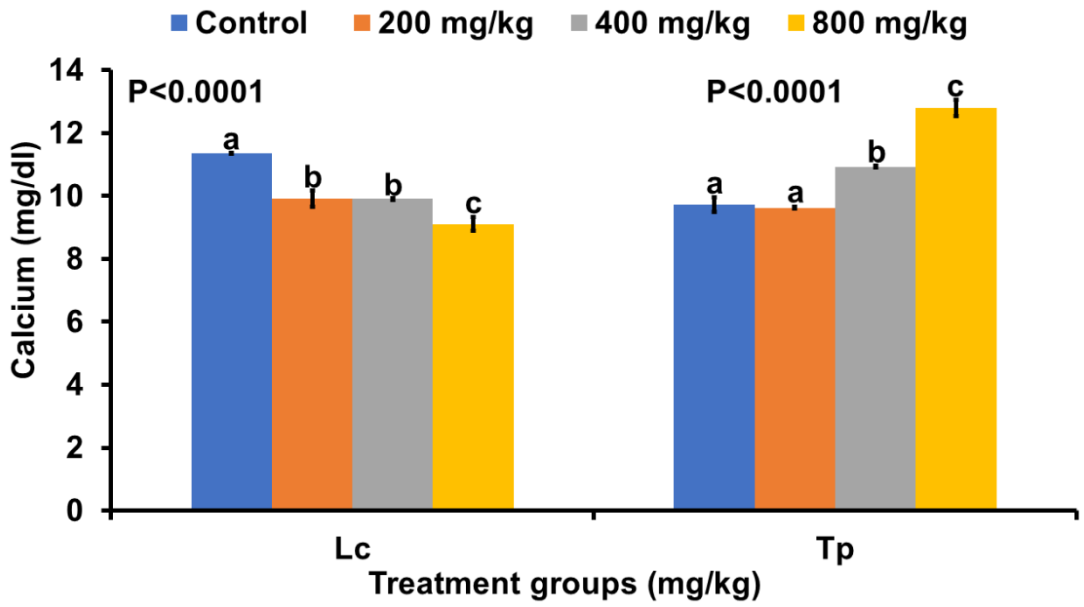

Figure 25: The effect of LCLE and TPLE on the calcium content in rats. Lc – *Lannea coromandelica*. Tp – *Trevesia palmata*. P<0.05 shows significant differences. Different letters in the bar graph indicates significant differences within the columns and similar letter mean no significant difference.

The graph of *L. coromandelica* indicates that there is a significant decrease with the increase in dose suggesting dose-dependent effect, potential impact on the bone health, alterations in mineral balance and toxicological considerations (Figure 25:Lc). On the contrary, the bar graph of *T. palmata* shows a significant increase in the calcium content indicating dose-dependent response, potential benefits for bone health, mineral absorption enhancement and safety considerations (Figure 25:Tp).

4.4.4. Histological analysis

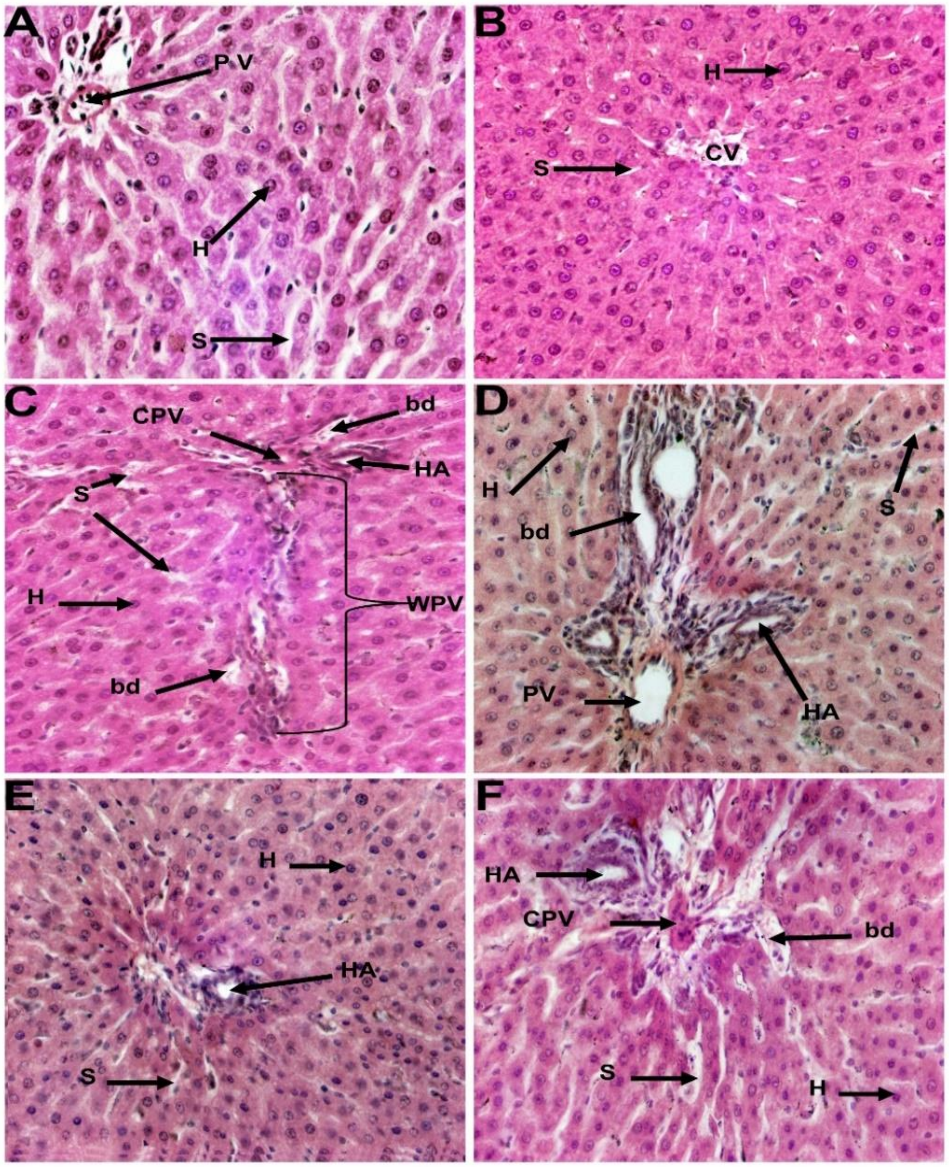

Figure 26: 40X magnification photomicrograph of sections of male livers in control and treated groups. A-C shows *LCLE* Control group, 2000 mg/kg and 5000 mg/kg methanolic plant extract treated group. D-E showed *TPLE* extract treated groups. D-Control group, E- 2000 mg/kg treated group and F– 5000 mg/kg treated group. The livers section at 5000 mg/kg of both the plants extract showed congested portal vein (CPV), infiltration of hepatic artery (HA), slightly dilated sinusoids (S), and some proliferation of bile duct (bd). 2000 mg/kg liver sections were similar to the control with normal hepatocytes (H), central vein (CV) and sinusoids (S).

The histological analysis of liver sections provides valuable insights into the effects of *L. coromandelica* and *T. palmata* extracts on liver morphology and potential pathological changes.

In LCLE treatment, the liver section from the control group (Figure 26:A) appears normal, with well-preserved hepatocytes (H), central vein (CV), and sinusoids (S). There are no apparent signs of tissue damage or pathological changes. In the liver sections of 2000 mg/kg LCLE treated Group (Figure 26:B), similar morphology to the control group, indicating no significant alterations in liver architecture or histology at this dose was observed. 5000 mg/kg LCLE Treated Group (Figure 26:C) reveal congested portal veins (CPV), infiltration of the hepatic artery (HA), slightly dilated sinusoids (S), and some proliferation of bile ducts (bd). These findings suggest that the higher dose of the extract may induce pathological changes in the liver, including vascular congestion and bile duct proliferation.

In the liver section from the Control group (Figure 26:D) of TPLE treated animals appear normal, with intact hepatocytes (H), central vein (CV), and sinusoids (S), similar to the control group of *L. coromandelica* extract-treated animals. In 2000 mg/kg treated Group (Figure 26:E) liver section from TPLE show no significant deviations from the control group, suggesting that this dose does not induce noticeable changes in liver histology. 5000 mg/kg treated group (Figure 26:F) liver section exhibit similar pathological changes as observed in the 5000 mg/kg group of LCLE-treated animals, including congested portal veins (CPV), infiltration of the hepatic artery (HA), slightly dilated sinusoids (S), and some proliferation of bile ducts (bd). These findings indicate that the higher dose of *T. palmata* extract may also lead to liver damage and pathological alterations.

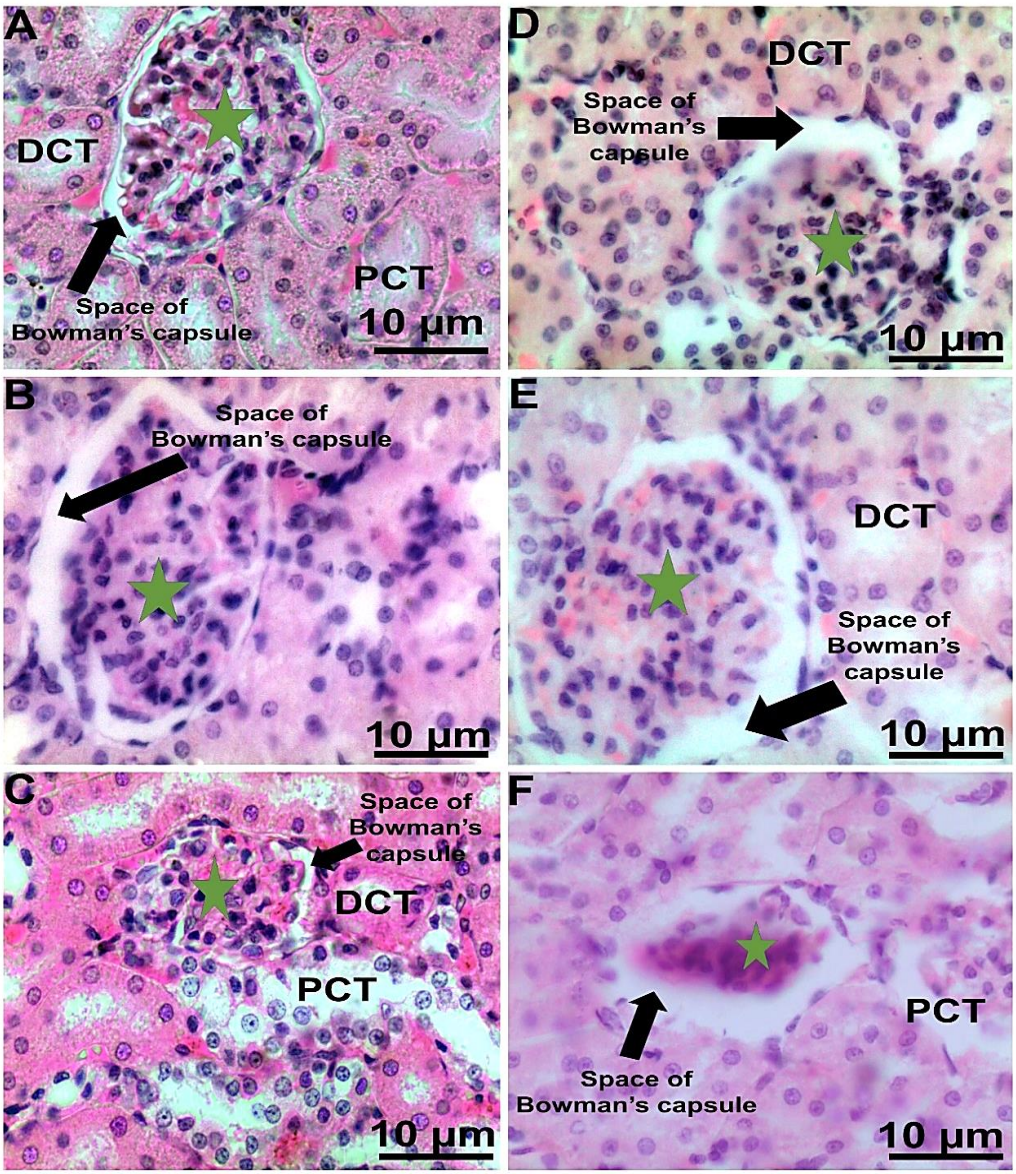

Figure 27: Photomicrographs of cortex of kidney from Control group (A and D) showing normal glomerulus (green star), having capillaries lined by endothelium and mesangial cells, enclosed by visceral layer and parietal layers of Bowman's capsule having urinary space in between. Proximal convoluted tubule (PCT) and distal convoluted tubule (DCT) was also seen with simple cuboidal epithelium. In 2000 mg/kg dose treatment both LCLE (B) and TPLE (E) treatment similar structures of glomerulus (green star), space of bowman's capsule and DCT were observed. In 5000 mg/kg dose treatment of LCLE (C), compressed space of bowman's capsule around glomerulus (green star) can be found with enlarged PCT. Whereas in 5000

mg/kg treated TPLE the glomerulus (green star) was compressed with enlarged space of bowman’s capsule. H & E, X40.

This histology image depicts sections of the kidney cortex from different treatment groups (Control, LCLE at 2000 mg/kg dose, TPLE at 2000 mg/kg dose, LCLE at 5000 mg/kg dose, and TPLE at 5000 mg/kg dose) stained with Hematoxylin and Eosin (H&E) at a magnification of 40x. In the control group (Figure 27:A and D), the glomerulus (highlighted with a green star) appears normal. The glomerulus is surrounded by Bowman's capsule, which has both visceral and parietal layers with a urinary space in between. Both proximal convoluted tubules (PCT) and distal convoluted tubules (DCT) are visible, characterized by simple cuboidal epithelium. In the 2000 mg/kg dose treatment groups (LCLE and TPLE, Figure 27:B and E), the structures of the glomerulus, Bowman's capsule, and DCT remain similar to the control group. However, in the 5000 mg/kg dose treatment groups (LCLE and TPLE, Figure 27:C and F), there are noticeable changes. In the LCLE-treated group (Figure 27:C), the space of Bowman's capsule around the glomerulus appears compressed, and the PCT appears enlarged. In contrast, in the TPLE-treated group (Figure 27:F), the glomerulus itself appears compressed, with an enlarged space of Bowman's capsule. These changes in the kidney cortex histology suggest that high doses of LCLE and TPLE treatments may lead to structural alterations in the glomerulus and Bowman's capsule, potentially indicating renal pathology or dysfunction.

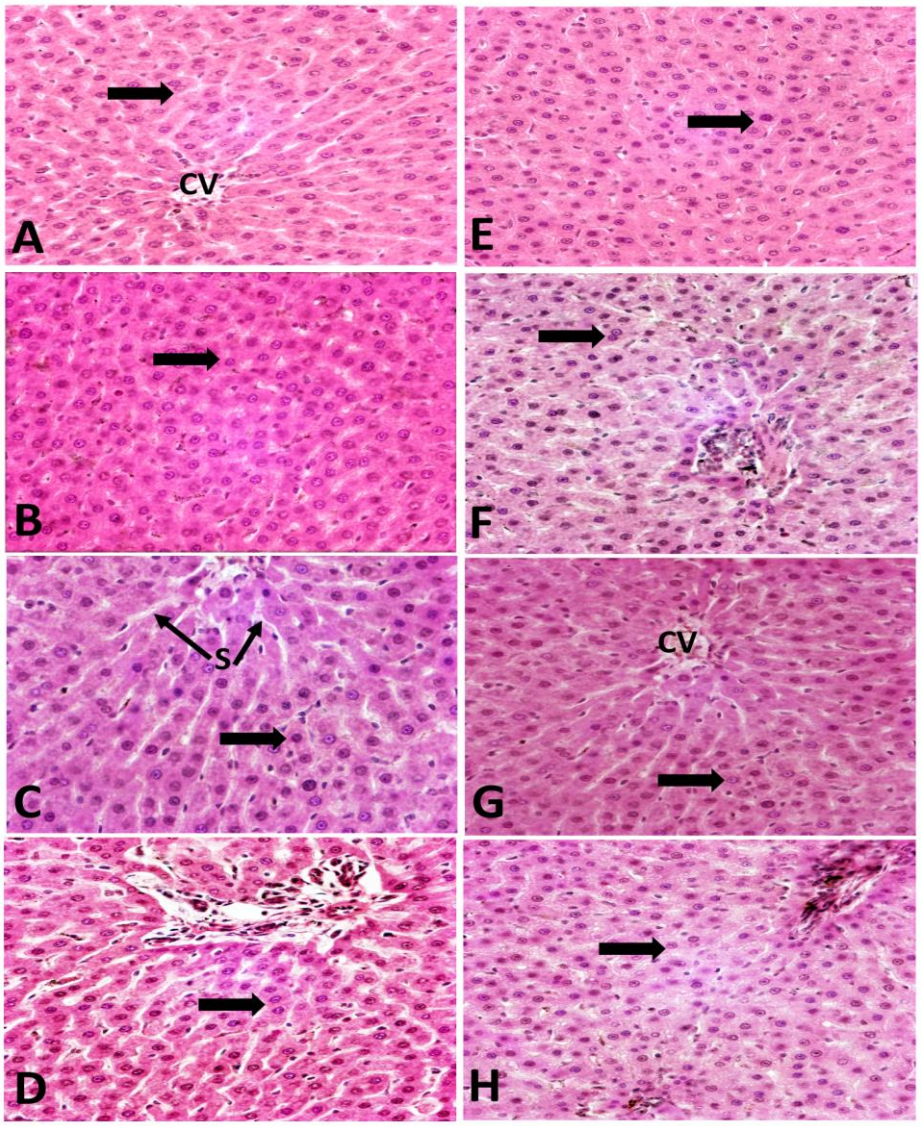

Figure 28: 40X magnification photomicrograph of sections of male livers in control and treated groups. A-D shows LCLE Control group, 200 mg/kg, 400 mg/kg and 800 mg/kg plant extract treated group. D-E showed TPLE extract treated groups. E- Control group, F- 200 mg/kg treated group, G- 400 mg/kg and H- 800 mg/kg treated group. The control groups (A and E) showed normal hepatocytes (arrow) in both the plants and central vein in LCLE. The liver section of 200 mg/kg and 400 mg/kg of both the plants extract showed normal hepatocytes and sinusoids as well. Congested portal vein (CPV) was observed in LCLE 800 mg/kg and infiltration of sinusoids were observed in TPLE 800 mg/kg treated rat liver.

This histology image presents sections of male liver tissue from different treatment groups, including control and various doses of two different plant extracts: LCLE (Figure 28 A-D) and TPLE (Figure E-H). The sections are stained and viewed at a magnification of 40x. In the control groups (Figure 28 A and E), both from the LCLE and TPLE treatments, normal hepatocytes (highlighted with arrows) and central veins are observed. The hepatocytes appear to be arranged in a typical hepatic lobule pattern around the central vein, indicating normal liver architecture. In the LCLE-treated groups at doses of 200 mg/kg and 400 mg/kg (Figure B and C), as well as in the TPLE-treated groups at similar doses (Figure 28 F and G), normal hepatocytes and sinusoids are still observed, indicating that these doses do not significantly affect liver tissue morphology. However, in the LCLE-treated group at a dose of 800 mg/kg (Figure D), congested portal veins (CPV) are observed, indicating possible vascular congestion in the portal system. In the TPLE-treated group at the same dose (Figure 28 H), infiltration of sinusoids is observed, which may suggest an inflammatory response or tissue damage within the liver. These histological findings suggest that while lower doses of both LCLE and TPLE do not cause significant changes in liver tissue morphology, higher doses lead to observable alterations indicative of liver injury or pathology.

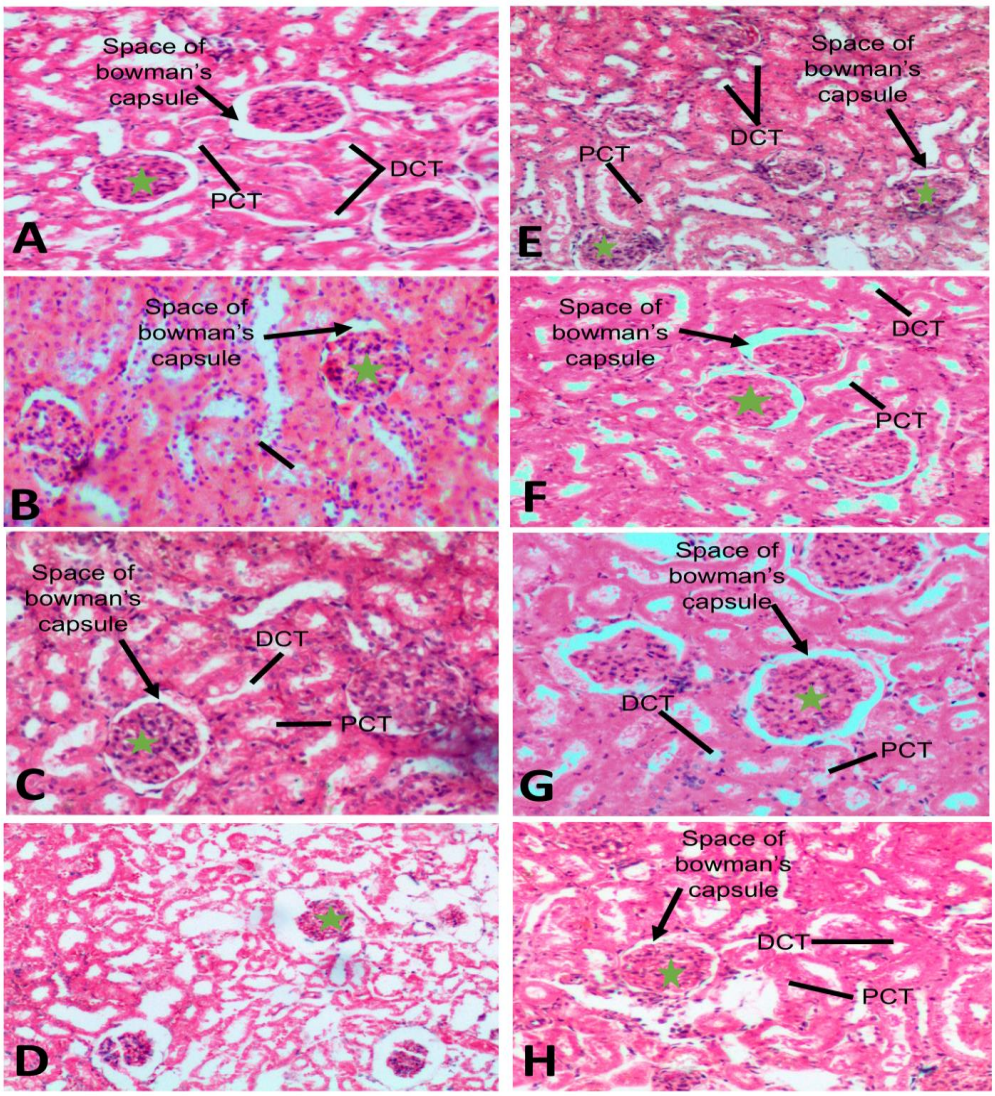

Figure 29: Photomicrographs of kidney histology. A-D *Lannea coromandelica* treated groups and E-H *Trevesia palmata* treated groups. Control group (A and E) showing normal glomerulus (green star), having capillaries lined by endothelium and mesangial cells, enclosed by visceral layer and parietal layers of Bowman's capsule having urinary space in between. Proximal convoluted tubule (PCT) and distal convoluted tubule (DCT) was also seen with simple cuboidal epithelium. In both 200 mg/kg (B and F) and 400 mg/kg (C and G) dose treatment of both LCLE (B) and TPLE (E) treatment similar structures of glomerulus (green star), space of bowman's capsule, PCT and DCT were observed. In 800 mg/kg (D) dose treatment of LCLE, lumen atrophy was observed. In TPLE treated 800 mg/kg dose, slight enlargement of the tubule was observed near the glomerulus. H & E, X10.

This histology data presents photomicrographs of kidney tissue sections from different treatment groups, focusing on the effects of *Lannea coromandelica* (LCLE) and Trevesia palmata (TPLE) treatments at varying doses. The sections are stained with Hematoxylin and Eosin (H&E) and viewed at a magnification of 10x.

In the control groups (Figure 29:A and E), which represent untreated kidneys, normal histological features of the kidney are observed. The glomerulus (highlighted with a green star) appears intact, with capillaries lined by endothelial cells and mesangial cells. The glomerulus is enclosed by both visceral and parietal layers of Bowman's capsule, with a urinary space in between. Proximal convoluted tubules (PCT) and distal convoluted tubules (DCT) are visible, characterized by simple cuboidal epithelium. In the groups treated with 200 mg/kg and 400 mg/kg doses of both LCLE (Figure 29:B and C) and TPLE (Figure 29:F and G), similar structures of the glomerulus, Bowman's capsule, PCT, and DCT are observed compared to the control groups. There are no significant histological alterations noted in these treatment groups, suggesting that these doses do not cause observable changes in kidney tissue morphology. However, in the group treated with 800 mg/kg dose of LCLE (Figure 29:D), lumen atrophy is observed, indicating a reduction in the size of the tubular lumens. This could suggest a possible adverse effect on kidney function or structural integrity at this higher dose of LCLE. In contrast, in the group treated with 800 mg/kg dose of TPLE (Figure 29:H), slight enlargement of the tubule near the glomerulus is observed. This enlargement could be indicative of tubular dilation or mild renal tubular injury associated with the higher dose of TPLE treatment.

Overall, these histological findings suggest that while lower doses of both LCLE and TPLE do not cause significant changes in kidney tissue morphology, higher doses may lead to adverse effects such as lumen atrophy or tubular enlargement, indicating potential renal toxicity.

4.5. DISCUSSION

Body weight, rectal temperature, food and water consumption are crucial parameters monitored during toxicity testing for several reasons. Changes in body weight and rectal temperature can serve as early indicators of physiological distress or systemic toxicity. Significant alterations in body weight may indicate changes in metabolism, nutrient absorption, or overall health status. Similarly, changes in rectal temperature can reflect changes in thermoregulation, which may occur in response to stress, inflammation, or metabolic disturbances caused by toxic substances (Ouchi et al., 2021; Rivas et al., 2013), whereas the Hippocratic screening provides a broad estimate of pharmacological and toxicological nature (Lucio et al., 2000). In this experiment LCLE-treated groups exhibited significant changes in body weight and rectal temperature, suggesting potential systemic effects of the extract on metabolism and thermoregulation. TPLE-treated groups showed significant increases in body weight but non-significant changes in rectal temperature, indicating potential differences in metabolic responses compared to LCLE treatment. Toxic substances can affect metabolism and energy balance, leading to changes in body weight. Increased or decreased food intake and water consumption can reflect alterations in metabolic processes, appetite regulation, or gastrointestinal function induced by toxicants. Monitoring these parameters allows for the assessment of metabolic effects and potential alterations in nutrient utilization or absorption (Wolfart et al., 2023). LCLE treatment led to significant increases in food consumption but decreases in water consumption, while TPLE treatment resulted in significant increases in both food and water consumption. These alterations may indicate differential effects on appetite and fluid balance induced by the two plant extracts. Alterations in food and water consumption can also provide insights into the functioning of specific organs, such as the liver and kidneys (Mitra et al., 2022; Matovic et al., 2015). In this experiment significant changes in the relative organ weights of the liver and kidney were observed in the higher dose (800 mg/kg) LCLE-treated group, suggesting potential organ-specific effects or toxicity at this dose. TPLE treatment showed significant changes in kidney weight at the highest dose, indicating potential renal effects. Changes in food intake may indicate alterations in liver function, as the liver

plays a crucial role in nutrient metabolism and synthesis of bile acids involved in digestion (Xie et al., 2021). Similarly, changes in water consumption can reflect alterations in kidney function, as the kidneys are responsible for maintaining fluid balance and excreting waste products (Popkin et al., 2010). Toxic substances can induce alterations in behaviour, including changes in feeding and drinking behaviour. Monitoring food and water consumption allows for the detection of potential behavioural changes induced by toxicants, such as alterations in appetite, feeding patterns, or thirst perception (Goma and Mahrous, 2013).

Changes in body weight, rectal temperature, food, and water consumption can manifest as clinical signs of toxicity, including alterations in growth rate, hypothermia or hyperthermia, anorexia, polydipsia, or polyuria. In this experiment, acute and sub-acute toxicity studies revealed dose-dependent effects of both LCLE and TPLE treatments on behavioural responses, with mortality rates increasing at higher doses. This indicates potential toxicity associated with elevated doses of both extracts. These clinical signs provide valuable information regarding the severity and progression of toxicity and can guide further investigation into potential underlying mechanisms of toxicity. Overall, monitoring body weight, rectal temperature, food, and water consumption during toxicity testing is essential for assessing overall health status, metabolic effects, organ function, and behavioural changes induced by toxic substances. These parameters serve as sensitive indicators of toxicity and provide valuable insights into the potential adverse effects of test compounds on physiological processes and organismal health (Hines, 2018).

The analysis of biochemical and haematological parameters is integral to toxicity testing, providing valuable information about organ function, systemic effects, mechanisms of toxicity, and dose-response relationships. These parameters serve as sensitive indicators of toxicity and play a crucial role in the safety assessment of pharmaceuticals, chemicals, environmental contaminants, and other substances (Olayode et al., 2020). In this experiment, LCLE treatment led to alterations in liver enzymes and renal function markers, suggesting potential hepatotoxic and nephrotoxic effects, especially at higher doses. TPLE treatment also induced significant changes in liver enzymes and renal function markers, indicating potential

liver and kidney dysfunction. Both extracts showed significant alterations in haematological parameters, suggesting potential effects on blood composition and erythropoiesis.

Protein and lipid metabolism tests are integral components of toxicity testing, providing valuable information about organ function, metabolic effects, nutritional status, and dose-response relationships. These tests help assess the impact of toxicants on key metabolic pathways and facilitate the identification of potential adverse effects on health and metabolic homeostasis (Parasuraman, 2011; Bedia, 2022). In this experiment, LCLE treatment led to significant increases in total protein and albumin content, potentially indicating beneficial effects on protein metabolism. TPLE treatment showed dose-dependent effects on total protein levels, with significant decreases observed at higher doses, suggesting potential adverse effects on protein metabolism. Both the extracts induce significant increase in the triglyceride levels, indicating potential disturbances in lipid metabolism.

The assessment of mineral content in rat toxicity testing is integral to evaluating the effects of toxicants on nutritional status, bone health, electrolyte balance, metabolic function, organ function, and overall health. Monitoring mineral levels provides valuable insights into the mechanisms of toxicity, identifies potential health risks associated with toxicant exposure, and guides the development of preventive and therapeutic interventions to mitigate toxic effects (Kesari and Noel, 2022; Noguchi et al., 2011). LCLE treatment led to significant decreases in calcium content, suggesting potential adverse effects on bone health and mineral balance. TPLE treatment, in contrast, led to significant increases in calcium content, indicating potential benefits for bone health and mineral absorption.

Liver and kidney histology analysis is indispensable in toxicity testing, providing critical insights into organ damage, mechanisms of toxicity, dose-response relationships, and predictive biomarkers for human toxicity. By integrating histopathological findings with other toxicological endpoints, researchers can comprehensively evaluate the safety profile of test compounds and inform risk assessment and regulatory decision-making processes (Ekasari et al., 2022). Both LCLE and TPLE treatments induced histological alterations in the liver, including

congestion, sinusoidal dilation, and bile duct proliferation, especially at higher doses, suggesting potential liver damage or pathology. Also, higher doses of both LCLE and TPLE treatments induced histological changes in the kidneys, including lumen atrophy and tubular enlargement, indicating potential renal toxicity. Overall, the interpretation of these results suggests that both LCLE and TPLE treatments have complex effects on various physiological parameters, organ function, and histology in rats. While lower doses may not induce significant changes, higher doses of both extracts may lead to adverse effects on liver, kidney, and metabolic parameters, highlighting the importance of dose optimization and further safety assessments before considering their therapeutic use. Additionally, the observed histological changes underscore the need for further investigation into the mechanisms and potential long-term consequences of extract administration.

4.6. SUMMARY

- Effect on Physiological Parameters: Changes in body weight, rectal temperature, food intake, and water consumption were observed in response to both LCLE and TPLE treatments.
- LCLE treatment led to significant alterations in body weight and rectal temperature, indicating potential systemic effects on metabolism and thermoregulation.
- Histological Changes: Both LCLE and TPLE treatments induced histological alterations in the liver and kidneys, including congestion, sinusoidal dilation, bile duct proliferation, lumen atrophy, and tubular enlargement.
- Overall, the findings highlight the complex effects of LCLE and TPLE extracts on various physiological parameters, organ function, and histology in rats.
- While lower doses may not induce significant changes, higher doses of both extracts may lead to adverse effects on liver, kidney, and metabolic parameters.

4.7. CONCLUSION

In conclusion, the findings from the study demonstrate that both *Lannea coromandelica* (LCLE) and *Trevesia palmata* (TPLE) extracts exert complex effects on physiological parameters, organ function, biochemical profiles, and histological characteristics in rats. While lower doses of the extracts may not induce significant changes, higher doses result in notable alterations indicative of potential adverse effects, particularly on liver, kidney, and metabolic parameters. The observed changes in body weight, rectal temperature, organ weights, biochemical markers, and histological features highlight the need for careful dose optimization and further safety evaluations before considering the therapeutic use of these extracts. These results underscore the importance of comprehensive toxicity testing to assess the potential risks and benefits associated with the administration of natural extracts for therapeutic purposes. Further research is warranted to elucidate the underlying mechanisms and long-term consequences of extract administration, ensuring the safety and efficacy of these botanical remedies.

4.8. REFERENCES

Alam, M. B., Kwon, K. R., Lee, S. H., & Lee, S. H. (2017). Lannea coromandelica (houtt.) merr. induces heme oxygenase 1 (HO-1) expression and reduces oxidative stress via the p38/c-jun n-terminal kinase–nuclear factor erythroid 2-related factor 2 (p38/JNK–Nrf2)-mediated antioxidant pathway. International journal of molecular sciences, 18(2), 266.

Alelign, T., Chalchisa, D., Fekadu, N., Solomon, D., Sisay, T., Debella, A., & Petros, B. (2020). Evaluation of acute and sub-acute toxicity of selected traditional antiurolithiatic medicinal plant extracts in Wistar albino rats. Toxicology Reports, 7, 1356-1365.

Anwar, F., Saleem, U., Ismail, T., Mirza, M. U., & Ahmad, S. (2022). Acute oral, subacute, and developmental toxicity profiling of naphthalene 2-yl, 2-chloro, 5-nitrobenzoate: Assessment based on stress response, toxicity, and adverse outcome pathways. Frontiers in pharmacology, 12, 810704.

Bedia, C. (2022). Metabolomics in environmental toxicology: Applications and challenges. Trends in Environmental Analytical Chemistry, 34, e00161.

Belmehdi, O., Taha, D., Abrini, J., Ming, L. C., Khalid, A., Abdalla, A. N., Algarni, A.S., Hermansyah, A. & Bouyahya, A. (2023). Anticancer properties and mechanism insights of α-hederin. Biomedicine & Pharmacotherapy, 165, 115205.

Belmehdi, O., Taha, D., Abrini, J., Ming, L. C., Khalid, A., Abdalla, A. N., ... & Bouyahya, A. (2023). Anticancer properties and mechanism insights of α-hederin. Biomedicine & Pharmacotherapy, 165, 115205.

Cavasotto, C. N., & Scardino, V. (2022). Machine learning toxicity prediction: Latest advances by toxicity end point. ACS omega, 7(51), 47536-47546.

Deresa, E. M., & Diriba, T. F. (2023). Phytochemicals as alternative fungicides for controlling plant diseases: A comprehensive review of their efficacy, commercial representatives, advantages, challenges for adoption, and possible solutions. Heliyon, 9(3).

Dimitrov, S., Slavchev, I., Simeonova, R., Mileva, M., Pencheva, T., Philipov, S., Georgieva, A., Tsvetanova, E., Teneva, Y., Rimpova, N., Dobrikov, G & Valcheva, V. (2023). Evaluation of Acute and Sub-Acute Toxicity, Oxidative Stress and Molecular Docking of Two Nitrofuranyl Amides as Promising Anti-Tuberculosis Agents. Biomolecules, 13(8), 1174.

Ekasari, W., Mahardiani, A., Putri, N. T., Wahyuni, T. S., & Arwati, H. (2022). Toxicological evaluation and protective effects of ethanolic leaf extract of Cassia spectabilis DC on liver and kidney function of Plasmodium berghei-infected mice. Veterinary Medicine International, 2022.

Erhirhie, E. O., Ihekwereme, C. P., & Ilodigwe, E. E. (2018). Advances in acute toxicity testing: strengths, weaknesses and regulatory acceptance. Interdisciplinary toxicology, 11(1), 5-12.

Frangiamone, M., Lazaro, A., Cimbalo, A., Font, G., & Manyes, L. (2024). In vitro and in vivo assessment of AFB1 and OTA toxic effects and the beneficial role of bioactive compounds. A systematic review. Food Chemistry, 138909.

Gandhidasan, R., Thamaraichelvan, A., & Baburaj, S. (1991). Anti-inflammatory action of Lannea coromandelica by HRBC membrane stabilization.

Goma, A., & Mahrous, U. E. (2013). Changes in behavior and learning ability of rats intoxicated with lead. International Journal of Animal and Veterinary Sciences, 7(12), 1096-1102.

Ha, H. A., Al-Sadoon, M. K., Saravanan, M., & Jhanani, G. K. (2024). Antibacterial, antidiabetic, acute toxicity, antioxidant, and nephroproductive competence of extracts of Lannea coromandelica fruit through in-vitro and in-vivo animal model investigation. Environmental Research, 242, 117767.

Hines, M. T. (2018). Clinical approach to commonly encountered problems. Equine internal medicine, 232.

Imam, M. Z., & Moniruzzaman, M. (2014). Antinociceptive effect of ethanol extract of leaves of Lannea coromandelica. Journal of ethnopharmacology, 154(1), 109-115.

Islam, F., Mitra, S., Nafady, M. H., Rahman, M. T., Tirth, V., Akter, A., Emran, T.B., Mohamed, A.A.R., Algahtani, A. & El-Kholy, S. S. (2022). Neuropharmacological and antidiabetic potential of lannea coromandelica (houtt.) merr. Leaves extract: an experimental analysis. Evidence-Based Complementary and Alternative Medicine, 2022.

Jitareanu, A., Trifan, A., Vieriu, M., Caba, I. C., Mârțu, I., & Agoroaei, L. (2022). Current trends in toxicity assessment of herbal medicines: A narrative review. Processes, 11(1), 83.

Kesari, A., & Noel, J. Y. (2022). Nutritional assessment. Treasure Island (FL): StatPearls Publishing.

Kumar, T., & Jain, V. (2015). Appraisal of total phenol, flavonoid contents, and antioxidant potential of folkloric Lannea coromandelica using in vitro and in vivo assays. Scientifica, 2015.

Lucio, E. D. A., Rosalen, P. L., Sharapin, N., & Souza Brito, A. R. M. (2000). Avaliação toxicológica aguda e screening hipocrático da epiisopilosina, alcalóide secundário de Pilocarpus microphyllus Stapf. Revista Brasileira de Farmacognosia, 9, 23-35.

Manoharan, A. L., Jagadeesan, G., Nataraj, G., Muniyandi, K., Guruswami, G., Arunachalam, K., & Thangaraj, P. (2023). Efficacy of Trevesia palmata (Roxb. ex Lindl.) Vis. Extract on MG 63 cell lines and arthritis-induced animal models. Journal of Ethnopharmacology, 300, 115742.

Matovic, V., Buha, A., Dukic-Cosic, D., & Bulat, Z. (2015). Insight into the oxidative stress induced by lead and/or cadmium in blood, liver and kidneys. Food and Chemical Toxicology, 78, 130-140.

Mitra, S., Chakraborty, A. J., Tareq, A. M., Emran, T. B., Nainu, F., Khusro, A., ... & Simal-Gandara, J. (2022). Impact of heavy metals on the environment and human health: Novel therapeutic insights to counter the toxicity. Journal of King Saud University-Science, 34(3), 101865.

Muhseen, Z. T., Hameed, A. R., Al-Hasani, H. M., ul Qamar, M. T., & Li, G. (2020). Promising terpenes as SARS-CoV-2 spike receptor-binding domain (RBD) attachment inhibitors to the human ACE2 receptor: Integrated computational approach. Journal of molecular liquids, 320, 114493.

Niyomchan, A., Chatgat, W., Chatawatee, B., Keereekoch, T., Issuriya, A., Jaisamut, P., Chusri, S. & Kunworarath, N. (2023). Safety evaluation of the polyherbal formulation NawaTab: acute and subacute oral toxicity studies in rats. Evidence-Based Complementary and Alternative Medicine, 2023.

Noguchi, C., Miyata, H., Sato, Y., Iwaki, Y., & Okuyama, S. (2011). Evaluation of bone toxicity in various bones of aged rats. Journal of toxicologic pathology, 24(1), 41-48.

Nouioura, G., Tourabi, M., Tahraoui, A., El-Yagoubi, K., Maache, S., Elfatemi, H., Lyoussi, B. & houssine Derwich, E. (2023). Assessment of the acute and subacute toxicity of the aqueous extract of Moroccan Ferula communis fruit in a mouse model. Saudi Pharmaceutical Journal, 31(8), 101701.

Olayode, O. A., Daniyan, M. O., & Olayiwola, G. (2020). Biochemical, hematological and histopathological evaluation of the toxicity potential of the leaf extract of Stachytarpheta cayennensis in rats. Journal of traditional and complementary medicine, 10(6), 544-554.

Ouchi, Y., Chowdhury, V. S., Cockrem, J. F., & Bungo, T. (2021). Effects of thermal conditioning on changes in hepatic and muscular tissue associated with reduced heat production and body temperature in young chickens. Frontiers in Veterinary Science, 7, 610319.

Parasuraman, S. (2011). Toxicological screening. Journal of pharmacology & pharmacotherapeutics, 2(2), 74.

Pognan, F., Beilmann, M., Boonen, H., Czich, A., Dear, G., Hewitt, P., Mow, T., Oinonen, T., Roth, A., Steger-Hartmann, T., Valentin, J.P. & Newham, P. (2023). The

evolving role of investigative toxicology in the pharmaceutical industry. Nature reviews drug discovery, 22(4), 317-335.

Popkin, B. M., D'Anci, K. E., & Rosenberg, I. H. (2010). Water, hydration, and health. Nutrition reviews, 68(8), 439-458.

Porwal, M., Khan, N. A., & Maheshwari, K. K. (2017). Evaluation of acute and subacute oral toxicity induced by ethanolic extract of Marsdenia tenacissima leaves in experimental rats. Scientia Pharmaceutica, 85(3), 29.

Pugazenthi, P., & Dominic Amalraj, A. (2016). Hepato-reno protective effect of lannea coromandelica on cadmium chloride induced oxidative damage in rats. Asian Journal of Innovative Research, 1(1), 29-34.

Rahman, K. H., Nandi, J. K., Sultana, S., Rahman, S., Hossan, S., & Rahmatullah, M. (2014). Phytochemical screening, antihyperglycemic and analgesic activity studies with methanol extract of Trevesia palmata leaves. World Journal of Pharmacy and Pharmaceutical Sciences, 3(10), 91-101.

Rivas, C. A. B., Castillo, A. A., Martínez, H. S., Zapata, E. P., Hernandez, J. B., & Tasse, Y. M. (2013). Acute oral toxicity of Azadirachta indica (Neem Tree). Revista Cubana de Plantas Medicinales, 18(3), 502-507.

Sayeed, M. A., Faruk, M., Chowdhury, A. I., & Rusti, A. (2014). Thrombolytic and Anti-arthritic Activities of Methanolic Extract of Trevesia palmata. J. Sci. Technol, 5(9), 119-124.

Schuijt, L. M., Peng, F. J., van den Berg, S. J., Dingemans, M. M. & Van den Brink, P. J. (2021). (Eco) toxicological tests for assessing impacts of chemical stress to aquatic ecosystems: facts, challenges, and future. Science of the total environment, 795, 148776.

Shakya, A., Chaudhary, S. K., Bhat, H. R., & Ghosh, S. K. (2020). Acute and sub-chronic toxicity studies of Benincasa hispida (Thunb.) cogniaux fruit extract in rodents. Regulatory Toxicology and Pharmacology, 118, 104785.

Sobeh, M., Mahmoud, M. F., Hasan, R. A., Abdelfattah, M. A., Sabry, O. M., Ghareeb, M. A., El-Shazly, A.M. & Wink, M. (2018). Tannin-rich extracts from Lannea stuhlmannii and Lannea humilis (Anacardiaceae) exhibit hepatoprotective activities in vivo via enhancement of the anti-apoptotic protein Bcl-2. Scientific reports, 8(1), 9343.

Srinivasa Rao, V., Wilkin Einstein, J., & Das, K. (2014). Hepatoprotective and antioxidant activity of Lannea coromandelica Linn. on thioacetamide induced hepatotoxicity in rats. International letters of natural sciences, 3.

Strickland, J., Haugabrooks, E., Allen, D. G., Balottin, L. B., Hirabayashi, Y., Kleinstreuer, N. C., Kojima, H., Nishizawa, C., Prieto, P., Ratzlaff, D.E., Jeong, J. & Casey, W. (2023). International regulatory uses of acute systemic toxicity data and

integration of new approach methodologies. Critical Reviews in Toxicology, 53(7), 385-411.

Ugwah-Oguejiofor, C. J., Okoli, C. O., Ugwah, M. O., Umaru, M. L., Ogbulie, C. S., Mshelia, H. E., Umar, M. & Njan, A. A. (2019). Acute and sub-acute toxicity of aqueous extract of aerial parts of Caralluma dalzielii NE Brown in mice and rats. Heliyon, 5(1).

Victoria, S., RIPANS, A., Sailo, N., Lahlenmawia, H., Shantabi, L., & Selesih, A. (2019). Effect of trevesia palmata on some biochemical and haematological parameters. International Journal of Engineering Applied Sciences and Technology, 4(3), 610-614. ISSN No. 2455-2143.

Wolfart, J. C., Theodoro, J. L., Silva, F. C., de Oliveira, C. M. R., Ferreira, N. G., & Bittencourt Guimarães, A. T. (2023). Metabolic consequences of the water we drink: a study based on field evidence and animal model experimentation. Toxics, 11(4), 315.

Xie, C., Huang, W., Young, R. L., Jones, K. L., Horowitz, M., Rayner, C. K., & Wu, T. (2021). Role of bile acids in the regulation of food intake, and their dysregulation in metabolic disease. Nutrients, 13(4), 1104.

Zhang, S., Han, Y., Peng, J., Chen, Y., Zhan, L., & Li, J. (2023). Human health risk assessment for contaminated sites: A retrospective review. Environment International, 171, 107700.

Chapter 5

Modulatory, anti-inflammatory and antioxidant effects of phytocompounds isolated from Lannea coromandelica and Trevesia palmata in trinitrobenzene sulphonic acid (TNBS) induced ulcerative colitis rat model

5.1. INTRODUCTION

Inflammatory bowel disease (IBD), characterized by chronic inflammation of the gastrointestinal tract, encompasses various conditions, including Crohn's disease and ulcerative colitis (UC). UC, specifically, involves inflammation and ulceration of the colon and rectum, leading to debilitating symptoms such as abdominal pain, diarrhea, rectal bleeding, and weight loss. Despite advancements in treatment options, the management of UC remains challenging, often necessitating long-term pharmacotherapy with potential side effects and limited efficacy in inducing and maintaining remission (McDowell et al., 2023).

In recent years, there has been growing interest in exploring the therapeutic potential of natural compounds derived from medicinal plants, particularly in the context of inflammatory conditions like UC (Duan et al., 2021). *Lannea coromandelica* (LC) and *Trevesia palmata* (TP) are two such botanical sources that have garnered attention for their diverse pharmacological properties, including modulatory, anti-inflammatory, and antioxidant effects.

L. coromandelica and *T. palmata* are rich reservoirs of bioactive phytocompounds, including flavonoids, phenolics, alkaloids, terpenoids, and tannins, which exhibit a wide range of biological activities. Several studies have reported the anti-inflammatory and antioxidant properties of extracts derived from LC and TP in various experimental models (Islam et al., 2022; Hussain et al., 2021; Thao et al., 2018; Rahman et al., 2014 and De Tommasi et al., 2000). However, the specific effects of isolated phytocompounds from these plants in the context of UC remain relatively underexplored.

Trinitrobenzene sulphonic acid (TNBS)-induced colitis in rats is a well-established experimental model that closely mimics the pathological features of human UC, making it a valuable tool for studying the efficacy and mechanisms of potential therapeutic agents. By inducing mucosal damage, inflammation, and oxidative stress in the colon, TNBS administration recapitulates key aspects of UC pathogenesis and

provides a platform for evaluating the therapeutic potential of novel interventions (Antoniou et al., 2016).

In this context, the present study aims to investigate the modulatory, anti-inflammatory, and antioxidant effects of phytocompounds isolated from *Lannea coromandelica* leaf extract (LCLE) and *Trevesia palmata* leaf extract (TPLE) in a TNBS-induced UC rat model. Through comprehensive evaluation of biochemical, histological, and molecular parameters, we seek to elucidate the mechanisms underlying the potential protective effects of these phytocompounds against UC-associated inflammation and tissue damage. Understanding the therapeutic implications of LCLE and TPLE-derived phytocompounds in UC may pave the way for the development of novel botanical-based therapies with improved efficacy and safety profiles for the management of this challenging condition.

5.1.1. Reactive Oxygen species in Inflammatory Bowel Disease

Oxidative stress and inflammation are closely intertwined pathophysiological processes implicated in the development of numerous chronic diseases (Biswas SK., 2016). Reactive oxygen species (ROS), generated during normal cellular metabolism, play key roles in signal transduction, gene expression, and immune regulation. However, excessive ROS production can lead to oxidative damage to biomolecules such as DNA, proteins, and lipids, contributing to various pathological conditions including cancer, atherosclerosis, neurodegenerative diseases, and inflammation (Jomova et al., 2023; Biswas, 2016).

Inflammatory bowel disease (IBD), encompassing conditions like ulcerative colitis (UC) and Crohn's disease, is characterized by dysregulated immune responses and environmental factors interacting with genetic predispositions. In the context of UC, increased production of ROS in the intestinal mucosa, primarily by neutrophils and macrophages, contributes to tissue damage and inflammation (Hitoshi et al., 2018).

Phagocytic cells utilize ROS to combat invading microbes, but dysregulated ROS production in UC patients can exacerbate tissue damage. ROS, including superoxide, hydrogen peroxide, hydroxyl radicals, and hypochlorous acid, can directly damage

cellular components and activate proinflammatory pathways. Additionally, interactions between platelets and neutrophils, as well as the activation of tissue macrophages, further contribute to ROS production and inflammation in UC (Ashique et al., 2023).

Various antioxidant defense mechanisms, such as superoxide dismutase (SOD), catalase, glutathione peroxidase, and non-enzymatic antioxidants, normally counteract ROS-induced damage. However, UC patients often exhibit depleted antioxidant reserves and dysregulated immune responses, leading to chronic oxidative stress and inflammation in the colon (Jarmakiewicz-Czaja; Rajput et al., 2021).

Studies utilizing TNBS-induced ulcerative colitis rat models have shown elevated ROS levels and inflammatory markers in UC, providing insights into the pathogenesis of the disease. Furthermore, modulation of ROS production and antioxidant pathways has emerged as a potential therapeutic strategy for UC management (Hambardikar and Mandlik, 2022).

The medicinal plants *Lannea coromandelica* and *Trevesia palmata* have been investigated for their antioxidant and anti-inflammatory properties in the context of UC. These plants contain bioactive compounds such as phenolics and flavonoids, which have been associated with antioxidant and anti-inflammatory effects. Studies have demonstrated the potential of these plant extracts in mitigating oxidative stress and inflammation in UC rat models, suggesting their therapeutic utility in managing UC (Islam et al., 2022; Hussain et al., 2021; Thao et al., 2018; Rahma et al., 2014 and De Tommasi et al., 2000).

In conclusion, oxidative stress and inflammation play pivotal roles in the pathogenesis of UC, and targeting ROS-mediated pathways may offer novel therapeutic approaches for UC management. The antioxidant and anti-inflammatory properties of medicinal plants like *L. coromandelica* and *T. palmata* highlight their potential as natural remedies for UC, warranting further investigation into their efficacy and mechanisms of action in preclinical and clinical studies.

5.1.2. Antioxidant and Anti-inflammatory Effects of plants containing phenolic and Flavonoid compounds

The literature discusses the therapeutic potential of antioxidants derived from plants in treating oxidative stress-related diseases and reducing the formation of free radicals. Phenolics and flavonoids present in medicinal herbs exhibit antioxidant and anti-inflammatory effects, which can help mitigate cell damage and tissue inflammation (Al-Khayri et al., 2022; Tungmunnithum et al., 2018). For instance, proinflammatory substances like TNF-α and nitric oxide (NO) can cause irreversible harm to cell membranes when they interact with free radicals, leading to cell death and tissue damage, highlighting the importance of antioxidants in controlling inflammation (Garcia-Sanchez et al., 2020).

Emerging research suggests that antioxidants can prevent the generation or spread of free radicals, thereby minimizing oxidative stress and boosting immune system function, potentially prolonging healthy lifespan (Chaudhary et a., 2023). Polyphenols, a type of antioxidant, have shown efficacy in treating experimental colitis by acting as antioxidants, immunosuppressants, and improving intestinal flora (Asakura and Kitahora, 2018).

Medicinal plants are rich sources of bioactive compounds such as alkaloids, flavonoids, terpenoids, and phenolic compounds, which possess various therapeutic properties including antibacterial, anti-inflammatory, anti-cancer, and antioxidant effects (Roy et al., 2022). *Lannea coromandelica*, for example, contains a wide range of secondary metabolites and bioactive phytocompounds associated with medicinal properties, including diuretic, cardiovascular, antiepileptic, antibacterial, anticonvulsant, anti-cancer, anti-diabetic, and anti-asthmatic effects.

L. coromandelica has been traditionally used for its anti-inflammatory, antimicrobial, hypotensive, wound-healing, and aphrodisiac properties, along with its efficacy in treating conditions such as ulcerative stomatitis, dyspepsia, general weakness, gout, cholera, diarrhoea, dysentery, sore eyes, leprosy, sprains, bruises, elephantiasis, snakebite, stomach ache, and vaginal problems (Swathi and Lakshman, 2022).

T. palmata also exhibits antioxidant and anti-inflammatory effects, among other biological activities. Its methanolic leaf extract shows promise for diagnosing diseases due to its broad-spectrum antibacterial properties, strong antioxidant effects, cytotoxicity, and membrane stability (Manoharan et al., 2023).

Studies have demonstrated the autoprotective and anti-inflammatory benefits of several phytocompounds, particularly flavonoids, on the oesophagus and stomach which is abundantly present in both the plant extract (Panche et al., 2016). Therefore, this current research aims to compare the anti-inflammatory effects of flavonoid compounds derived from LCLC and TPLE to sulfasalazine, a medication commonly used to treat inflammatory bowel disease, aims to explore their potential therapeutic role in inflammatory bowel disease using an animal model induced by 2,4,6-trinitrobenzene sulfonic acid in rat model.

5.2. REVIEW OF LITERATURE

Ulcerative colitis (UC) is a chronic inflammatory condition affecting the colon, characterized by oxido-nitrosative stress, pro-inflammatory cytokine secretion, and apoptosis. Although the introduction of cutting-edge drugs has revolutionized UC treatment, current medications still exhibit low net remission rates and durability, highlighting the need for further pharmacological research and innovative clinical trial design. Animal models play a crucial role in understanding complex diseases like UC, although no single model can fully represent the diverse manifestations of the human disease (Guo and Wang 2023; Lasa et al., 2022 and Ungaro et al., 2019).

The etiology of UC is multifactorial, involving genetics, immunity, infection, and environmental factors. The cornerstones of therapeutic treatment for UC include immunosuppressants, adrenal glucocorticoids, and aminosalicylic drugs, but these medications may have adverse effects. Hence, research focusing on the potential therapeutic effects of amino acid supplementation for UC is gaining attention (Ungaro et al., 2019).

The concept of an "IBD integrom" aims to understand the pathogenesis of inflammatory bowel disease (IBD) by integrating genetic information, environmental

stimuli, gut microbial diversity, and intestinal immune reactivity (Fiocchi, 2015). Animal models, such as those induced by 2,4,6-trinitrobenzene sulfonic acid (TNBS), provide valuable insights into UC pathogenesis and allow the study of cytokine release patterns and the development of immunotherapy (Au et al., 2023; Goyal et al., 2014).

Oxidative stress (OS), characterized by an imbalance between reactive oxygen species (ROS) and antioxidant mechanisms, plays a significant role in UC pathophysiology (Tian et al., 2017). OS damages the gastrointestinal mucosa, triggering an inflammatory response, and disrupting cellular homeostasis. Strategies aimed at boosting antioxidant defences or inhibiting oxidizing enzymes may mitigate OS and positively impact disease progression (Sahoo et al., 2023).

Animal models of IBD, including genetically altered models, have facilitated the study of IBD pathogenesis and the development of novel treatments (Mizoguchi et al., 2020). Histological assessment of endoscopic biopsies or resection specimens is crucial for diagnosing and distinguishing between UC and Crohn's disease. Integration of histological scoring into routine clinical practice may enhance IBD treatment outcomes in the future (Fabian and Bajer, 2022).

Overall, animal models of IBD are essential for understanding histological alterations in the gastrointestinal tract and developing novel therapeutics to improve patient outcomes.

5.2.1. Use of dimethylsulfoxide as vehicle in in-vivo experiment

An organosulfur chemical dimethylsulfoxide (DMSO) has the formula $(CH_3)_2SO$. The German chemical industry made the discovery of DMSO in the nineteenth century. DMSO has two nonpolar domains and a highly polar group, making it soluble in both aqueous solutions and organic solutions (Huang et al., 2020). Additionally, DMSO is easily absorbed by both animals and people via the skin and oral routes. It also facilitates the dermal and oral absorption of many other compounds.

DMSO solutions in water with higher concentrations absorb more quickly than those with lower concentrations (Sullivan Jr and Gad, 2023). Similarly, it has recently been demonstrated that DMSO have immunomodulatory effects, such as immunological stimulation and anti-inflammatory effects in the innate immunity, in contradiction to this conventional utilisation. Furthermore, DMSO influences adaptive immunity by controlling the expression of transcription factors in immune cells (Huang et al., 2020).

5.2.2. Role of Myeloperoxidase in ulcerative colitis

Most immune cells drawn to the inflammatory bowel are neutrophils, which are short-lived immune cells that releases azurophilic granules containing the enzyme myeloperoxidase (MPO) (Arnhold, 2020). In the past, serum and faecal MPO levels have been shown to correlate with disease severity in IBD patients. Several researches have also proven that daily intravenous administration of MPO inhibitors significantly slowed colitis progression by reversing clinical markers such as body weight loss and disease activity index, reducing serum peroxidation, maintaining colon length, and significantly reducing histoarchitectural damage caused by colitis (Derkacz et al., 2018; Hansberry et al., 2017). Additionally, it was established that MPO inhibition reduced neutrophil migration to the gut, indicating that MPO may contribute to the maintenance of the inflammatory cell by attracting additional cells to the inflamed gut (Li et al., 2021).

Mutual verifications have also been performed through experiments in which it was shown that MPO is not only a significant clinical measure of disease severity but may also be a key factor in maintaining host-tissue damage and inflammation (Chami et al., 2021).

5.2.3. Role of Calprotectin, LTB4, PG-E2, FAD-linked Sulfhydryl Augmenter of Liver Regeneration and Interleukin 10 in Inflammation

Faecal calprotectin (FC), a protein released during intestinal inflammation, reflects increased neutrophil migration to the colon. FC is resistant to degradation and stable in faeces, making it a valuable non-invasive marker for neutrophil flow to the colon.

In ulcerative colitis (UC), higher FC levels indicate disease activity, while lower levels may suggest other inflammatory conditions or indicate inflammation resolution.

Leukotriene B4 (LTB4) plays a significant role in inflammation, acting as a chemoattractant primarily produced by myeloid cells. LTB4-BLT1 signaling facilitates the recruitment of neutrophils, macrophages, and lymphocytes to inflamed sites, contributing to inflammation in conditions like ulcerative colitis. Elevated LTB4 levels in inflamed mucosa are associated with increased 5-lipoxygenase activity and decreased LTB4 omega-hydroxylase activity.

Prostaglandin E2 (PGE2) affects inflammation by promoting wound healing, enhancing epithelial integrity, and modulating cytokine expression. Elevated PGE2 synthesis during inflammation can exacerbate inflammatory responses, but selective COX2 inhibitors may reduce relapse rates in inflammatory bowel disease (IBD). PGE2 also activates EGFR, suggesting potential therapeutic targets for IBD treatment.

Augmenter of liver regeneration (ALR) is a sulfhydryl oxidase enzyme expressed in mammalian tissues, exhibiting cellular defence and pro-survival properties. ALR protects against apoptosis and promotes cell survival and regeneration in various tissues, including the colon. Transcription of the ALR gene is regulated by multiple factors, and ALR plays a crucial role in mitochondrial function and oxidative stress regulation.

Interleukin-10 (IL-10) is an anti-inflammatory cytokine that regulates immune cell function and expression of pro-inflammatory molecules. IL-10 targeting has shown promise in treating inflammatory bowel disease (IBD), with abnormalities in the IL-10 pathway linked to severe colitis. IL-10 inhibits dendritic cell maturation and suppresses inflammatory cytokine expression, contributing to immune regulation and inflammation control in IBD.

5.2.4. Role of herbal natural compounds in modulation of ulcerative colitis

The modulatory effects of phytocompounds from *Lannea coromandelica* and *Trevesia palmata* on oxido-nitrosative stress, inflammation, transcription factors, and apoptosis in TNBS-induced ulcerative colitis in rats can be a multifaceted topic with significant implications for both traditional and modern medicine. *L. coromandelica* and *T. palmata* are medicinal plants known for their rich content of bioactive compounds such as phenols, flavonoids, and terpenoids. These compounds have been traditionally used for their therapeutic properties, including anti-inflammatory and antioxidant effects ((Swathi and Lakshman, 2022; Manoharan et al., 2023).

TNBS-induced ulcerative colitis in rats serves as a model to simulate human inflammatory bowel disease (IBD) (Antoniou et al., 2016). Oxido-nitrosative stress, characterized by an imbalance between reactive oxygen species (ROS) and reactive nitrogen species (RNS), plays a crucial role in the pathogenesis of UC (Sadar et al., 2016). Phytocompounds from *Lannea coromandelica* and *Trevesia palmata* may attenuate this stress by scavenging free radicals and restoring antioxidant balance, thus reducing tissue damage and inflammation in the colon.

Transcription factors such as NF-κB and AP-1 are key regulators of inflammatory gene expression. In UC, these factors are often overactivated, leading to the upregulation of pro-inflammatory cytokines and chemokines (Liu et al., 2017). Phytocompounds derived from both the plants may exert their anti-inflammatory effects by modulating the activity of these transcription factors, thereby suppressing the production of inflammatory mediators.

Apoptosis, or programmed cell death, is dysregulated in UC, leading to excessive loss of epithelial cells and impaired tissue repair (Wan et al., 2022). Phytocompounds may promote cell survival and tissue regeneration by inhibiting apoptotic pathways and enhancing the proliferation of colonic epithelial cells.

The findings from studies on the modulatory effects of phytocompounds from *Lannea coromandelica* and *Trevesia palmata* in TNBS-induced UC hold promise for the development of novel therapeutic interventions for IBD. These natural agents

offer a potentially safer and more sustainable alternative to conventional drugs, with fewer side effects and broader therapeutic benefits.

In conclusion, the investigation of the modulatory effects of phytocompounds from *Lannea coromandelica* and *Trevesia palmata* on oxido-nitrosative stress, inflammation, transcription factors, and apoptosis in TNBS-induced ulcerative colitis in rats may represent a significant advancement in our understanding of the therapeutic potential of natural compounds in the management of inflammatory bowel diseases.

5.3. METHODS

5.3.1. Materials

2,4,6 Trinitrobenzene sulfonic acid (TNBS) was purchased from TCI and rat ELISA Kits from Bioassay Technology Laboratory was purchased from Hind Biotech, Kolkata, West Bengal. Sulfasalazine, DMSO, polyurethane catheter and ethanol was purchased from the local store.

5.3.2. Animal Care and Handling

The animal care and handling (CPCSEA Registration No. 1999/GO/ReBi/S/18/CPCSEA, valid from 16/02/2018 to 15/02/2023) was carried out in accordance with the rules allowed by Mizoram University's Institutional Animal Ethics Committee in Aizawl, India (Permit No. MZU-IAEC/2018/11). Three-month-old male/female Wistar albino rats weighing 150 to 180 g were selected from an inbred colony maintained under controlled conditions of temperature (23 ± 2º C), humidity (50 ± 5%), and light (12 hours of light and dark, respectively). The animals were given sterile food and drink. Throughout the experiment, five animals were confined in a polypropylene cage with bedding made from locally sourced wood powder. All efforts were made to alleviate the suffering and misery of male Wistar albino rats.

5.3.3. Induction of colitis and drug treatment schedule

Colitis was induced according to the procedure described elsewhere (Li et al., 2011). Briefly, rats were slightly anaesthetized with ether following a 24 h fast, and then TNBS dissolved in 50 % ethanol were instilled into the colon of the animals (150 mg/kg in a volume of 0.25 mL) using a medical-grade polyurethane catheter for enteral feeding (external diameter 2 mm) inserted 8 cm into the anus. Control group were made for comparison with TNBS/ethanol instillation: rats in the sham group received an enema of physiological saline instead of the TNBS solution. Rats were randomly divided into following 10 groups as follows (Table 32 and 33):

5.3.4. Body weight, organ indices, food and water intake and rectal temperature

Body weight (g), food consumption (g) and water consumption (mL) were computed everyday between 08:00 h and 11:00 h for 7 days all throughout the experiment. The absolute organ weight of colon tissue samples was recorded.

Table 32: Induction of ulcerative colitis using experimental rat model of trinitrobenzene sulphonic acid (TNBS) - *Lannea coromandelica* bioactive compounds

Group no.	Animal group	Treatment	Dose	Route of Administration	No. of Animals	Days of Treatment		
						0 day	1-7th days	8th day
I	Sham control	Dimethyl sulfoxide (DMSO) (1 %)	1 ml	p.o.	5	-	√	Blood sample were collected and animals were sacrificed for bio-chemical, molecular and histo-pathological examination
II	TNBS induced control	DMSO (1%)	1 mL	p.o	5	-	√	
		Trinitrobenzensulfonic acid (TNBS)	150 mg/kg	intrarectally		√	-	
III	TNBS induced and Sulfasalazine treated	Sulfasalazine in DMSO (1%)	1 mL	p.o	5	-	√	
		Trinitrobenzensulfonic acid (TNBS)	150 mg/kg	intrarectally		√	-	
IV	TNBS induced and Lannea coromandelica (Lc) bioactive compounds (10 mg/kg)	10 mg/kg Lc leaf extract in DMSO (1%)	1 mL	p.o	5	-	√	
		Trinitrobenzensulfonic acid (TNBS)	150 mg/kg	intrarectally		√	-	
V	TNBS induced and Lannea coromandelica bioactive compounds (20 mg/kg) treated	20 mg/kg Lc leaf extract in DMSO (1%)	1 mL	p.o	5	-	√	
		Trinitrobenzensulfonic acid (TNBS)	150 mg/kg	intrarectally		√	-	

Table 33: Induction of ulcerative colitis using experimental rat model of trinitrobenzene sulphonic acid (TNBS) - *Trevesia palmata* bioactive compounds

Group no.	Animal group	Treatment	Dose	Route of Administration	No. of Animals	Days of Treatment		
						0 day	1-7th days	8th day
I	Sham control	Dimethyl sulfoxide (DMSO) (1 %)	1 mL	p.o.	5	-	√	Blood sample were collected and animals were sacrificed for bio-chemical, molecular and histo-pathological examination
II	TNBS induced control	DMSO (1%)	1 mL	p.o	5	-	√	
		Trinitrobenzensulfonic acid (TNBS)	150 mg/kg	intrarectally		√	-	
III	TNBS induced and Sulfasalazine treated	Sulfasalazine in DMSO (1%)	1 mL	p.o	5	-	√	
		Trinitrobenzensulfonic acid (TNBS)	150 mg/kg	intrarectally		√	-	
IV	TNBS induced and *Trevesia palmata* (Tp) bioactive compounds (10 mg/kg)	10 mg/kg Tp leaf extract in DMSO (1%)	1 mL	p.o	5	-	√	
		Trinitrobenzensulfonic acid (TNBS)	150 mg/kg	intrarectally		√	-	
V	TNBS induced and Trevesia palmata (Tp) bioactive compounds (20 mg/kg) treated	20 mg/kg Tp leaf extract in DMSO (1%)	1 mL	p.o	5	-	√	
		Trinitrobenzensulfonic acid (TNBS)	150 mg/kg	intrarectally		√	-	

5.3.5. Assessment of Disease activity index, colonic damage, ulcer area and ulcer index

5.3.5.1. Disease activity index (DAI)

Disease activity index (DAI) was based on body weight loss, stool consistency and blood in stools. Body weight loss, stool consistency and blood in stools were recorded daily for the study. Briefly, scores were assigned for each item to calculate DAI as follows:

Scoring system for loss in body weight was as follows: no weight loss = 0; weight loss of 1% to 5% = 1; weight loss of 6% to 10% = 2; weight loss of 11% to 20% = 3; and weight loss 20% and above = 4.

Scoring levels for stool consistency was as follows: normally formed pellets = 0; pasty and semiformed pellets = 2; and liquid stools = 4.

Occult bleeding was scored as stated: negative hemoccult = 0; positive hemoccult = 2; and visible blood/gross bleeding from the rectum = 4.

The scoring parameters were added together resulting in a total score ranging from 0 to 12 divided by 3.

Body weight of rat was measured daily from the start of the experiment to the termination day. All animals were monitored daily for the duration of the study to assess DAI changes in response to treatment (Yang et al., 2014).

5.3.5.2. Morphological Evaluation

The removed colons were excised free of adherent adipose tissue, rinsed with ice-cold saline and dissected longitudinally. It was examined visually immediately and the macroscopic scoring of the colonic damage was assessed using the criteria shown in Table 34, on a scale of 0–5 as previously described by Morris et al., 1989.

Table 34. Criteria for scoring of macroscopic damage.

Score	Macroscopic Morphology
0	No damage.
1	Localized hyperemia, but no ulcers.
2	Linear ulcers with no significant inflammation*.
3	Linear ulcer with inflammation at one site.
4	Two or more sites of ulceration and/or inflammation.
5	Two or more major sites of inflammation and ulceration or one major site of inflammation and ulceration extending >1 cm along the length of the colon.

*Inflammation was defined as regions of hyperemia and bowel wall thickening.

The ulcer area and ulcer index were assessed according to Dengiz and Gursan's method. The ulcer index was calculated by using the following formula (Kandhare et al., 2013; Kumar et al., 2014; Rachmilewitz et a., 1989):

$$\textbf{Ulcer index (UI) = Total area of ulcer (mm}^2\textbf{)/Total area of colon (mm}^2\textbf{)}$$

and the inhibition rate was calculated by using the formula:

$$\textbf{\% Inhibition} = [(UI_{control} - UI_{treated}/UI_{control})] \textbf{ X 100}$$

5.3.6. Sample collection

After 24 hours of final treatment, all animals were sacrificed with an intraperitoneal injection of Ketamine (90 mg/kg body weight) and Xylazine (10 mg/kg body weight). Serum was obtained after centrifugation of whole blood at 1000 × g at room temperature for 10 minutes. Colon tissues were obtained after removing the adhering connective tissues of each animal and kept immediately at -20°C. The tissue was fixed in Bouin's fixative, which contained 75% saturated picric acid, 25% formaldehyde, and 5% glacial acetic acid, for at least 24 hours before being

transferred to 70% ethanol for further testing. All dissection techniques were carried out under aseptic conditions.

Total protein lysate was prepared by weighing colon pieces. The tissue fragments were homogenized in an ice-cold suspension buffer containing 50 mM Tris-Hydrochloric acid, pH 8.0; 150 mM Sodium Chloride (NaCl); 0.1% Sodium Dodecyl Sulphate (SDS); 1 g/ml Aprotinin; 1 mM Phenylmethylsulfonyl fluoride (PMSF) and 1mM Ethylenediaminetetraacetic acid (EDTA) disodium salt dehydrate (cat# E5134; Sigma-Aldrich, St. Louis, MO, USA) to yield 10% homogenate (w/v). The supernatants were centrifuged at 10000 × g at 4 °C for 10 minutes and kept at -20 °C for western blot analysis. Tissues were homogenized with the above-mentioned SDS-free buffer for the enzyme assay.

5.3.6. ELISA assays

Determination of Nitric oxide content (NO), myeloperoxidase (MPO), Calprotectin (CALP), Interleukin-6 (IL-6), Interleukin-1 (IL-1), Leukotriene-B4 (LT-B4), FAD-Linked sulfhydryl oxidase ALR, Prostaglandin E2 (PG-E2), Total Antioxidant (T-AOC) and Interleukin-10 (IL-10) was done using ELISA kits (Bioassay Technology Laboratory Rat ELISA kit) as per manufacturer's protocol.

5.3.7. Measurement of Lipid Peroxidation

The malondialdehyde (MDA) level in the colon was determined using the approach previously published by Ohkawa et al., 1979, with slight modifications (Aboul-Soud et al., 2011). Briefly, 75 µl of colon lysates were combined with the equivalent amount of 10% Trichloroacetic acid. Freshly made 0.2% Thiobarbituric acid was then added at a 1:2 ratio and heated for 45 minutes. The solutions were allowed to cool before the optical densities were measured at 532 nm against a blank, and the MDA concentration was expressed as nM/mg protein. A mixture devoid of colon protein lysate served as a blank.

5.3.8. Assessment of GSH, SOD, CAT, GPx

Superoxide dismutase (SOD) assay. The previously published approach was used in the superoxide dismutase assay (Kakkar et al., 1984). To prepare the mixture, add 50 µl of 10% tissue homogenate, 600 µl of 52 mM sodium pyrophosphate buffer (pH 8.3), 50 µl of 186 µM phenazine methosulphate (PMS), and 150 µl of 300 µM Nitroblue tetrazolium (NBT). To begin the reaction, add 100 µl of 750µMml NADH and incubate at 30°C. After 90 seconds of incubation, the reaction was stopped by adding 500 µl glacial acetic acid. 2 ml of n-butanol were added, vortexed and left to stand for ten minutes. The mixture was centrifuged at 10000 × g for 10 minutes at room temperature, then the supernatant was collected. Colour intensity was measured at 560 nm.

Glutathione reduced (GSH) assay. A previously established principle and method were used for the Glutathione reduction assay (Rahman et al., 2006). Briefly, A mixture with 2.0 M Pyrophosphate buffer (pH 7.4), 0.2 M of 5,5′-dithio-bis-[2-nitrobenzoic acid], and 50 µl of 10% tissue homogenate. The experiment was based on the rate of TNB-chromophore production following the reaction of DTNB with intracellular GSH concentration. The TNB complex has a maximum absorbance of 412 nm. The TNB complex production rate was thought to be related to the GSH level of the tissue samples, with GSH concentration represented as U/mg protein. The reaction mixture free of tissue homogenate served as a blank.

Catalase assay. A previously published approach was used to determine Catalase activity (Sinha, 1972). The assay mixture consisted of 1 ml of PBS (pH 7), 100 µl of testis tissue lysate, and 400 µl of 2 M hydrogen peroxide (H_2O_2). After 1 minute, the reaction was stopped by adding 2.0 ml of dichromate-acetic acid reagent (5% potassium dichromate and glacial acetic acid in a 1:3 ratio). Absorbance was measured at 570 nm with a spectrophotometer. The activity was measured as U/mg of H_2O_2 consumed per minute per mg of protein (H_2O_2/min/mg protein). A mixture devoid of tissue homogenate was used as a blank.

Glutathione Peroxidase (GPx) assay. Sazuka et al.'s (1985) approach was used to determine GPx activity. To prepare the mixture, 100 µl of homogenate was combined with 200 µl of EDTA, sodium azide, GSH, H2O2, and 400 µl buffer. The reaction mixture was incubated at 37ºC for 10 minutes before adding 10% trichloroacetic acid (TCA). After centrifugation, the supernatant was collected and mixed with 3 ml disodium hydrogen phosphate and 1000 µl of 5,5'-dithio-bis(2-nitrobenzoic acid) (DTNB). A spectrophotometer was used to measure the absorbance of the sample/s in comparison to the blank at 412 nm. The activity was calculated as micromoles GSH per milligram protein.

5.3.9. Histopathological examination of gastric lesions and measurement

Hematoxylin and eosin staining (H&E)

Colon tissues were fixed in Bouin's fixative for 24 h in Bouin's fixative. The fixed specimen was processed through the conventional paraffin embedding technique, sectioned at 5µm and stained with hematoxylin and eosin (Bancroft and Gamble, 2002), for histopathological studies. Microscopic scoring was assessed using the criteria illustrated in table 2 (Fabia et al., 1993).

Table 35. The variables used for microscopic scoring.

Variables	Severity of changes			
	0	1	2	3
Ulceration	No ulcer	Erosion or single ulceration not exceeding lamina muscularis mucosa	Multifocal ulcerations not exceeding the submucosa	Ulcerations exceeding the submucosa
Mucus cell depletion	Preserved mucus cell	Mild depletion in a few cell	Moderate depletion (less than 50% complete disappearance of cells)	Severe depletion or complete disappearance of cells mucosa
Cyrpt abcesses	No abcesses	1–3 abscesses/slide	4–9 abscesses/slide	10 or more abscesses/slide
Inflammatory cysts	No cysts	1–3 cysts/slide	4–9 cysts/slide	10 or more cysts/slide
Mucosal atrophy	Normal thickness	Mild atrophy (less than 10%)	Moderate atrophy (10–50%)	Severe atrophy (>50%)
Edema (submucosa)	Normal thickness	Mild edema (submucosal expansion less than 10%)	Moderate edema (submucosal expansion, 10–100%)	Severe edema (submucosal expansion, >100%)
Inflammatory cell infiltration	No inflammatory cell infiltration	Mild inflammatory cell infiltration	Moderate (distributed but not dense) inflammatory cell infiltration	Dense inflammatory cell infiltration
Vascular dilatation	Normal blood vessels	Mild dilatation of single blood vessel	Moderate dilatation of several blood vessels	Severe dilatation of several blood vessels

5.3.10. Western blotting

Western blot analysis was performed on colon protein lysates, as previously described (Jeremy et al., 2017). Briefly, the total protein concentration of each lysate was determined using Bradford techniques (Bradford, 1976). Proteins (50 µg) were

electrophoresed using 10% sodium dodecyl sulfate-polyacrylamide gel electrophoresis (SDS-PAGE) at 150 V. The resolved proteins were transferred to a polyvinylidene difluoride (PVDF) membrane using the Medox-Bio Mini SemiDry Blotting MX-1295-01 device for 20-30 minutes. Membranes were then blocked for at least 1 hour at room temperature in a blocking solution containing 0.05% Tween 20 in Phosphate-buffered saline (PBS) and 10% non-fat skimmed milk (Cat# GRM1254-500G HiMedia Laboratory Private Limited, Mumbai, India). The membranes were next probed with BCL-2 (1:2000, Mouse polyclonal antibody, Cat#sc-7382, Santa Cruz Biotechnology, INC., Dallas, USA), BAX (1:1000, Mouse polyclonal IgG, Cat#sc-7480, Santa Cruz Biotechnology INC. Dallas, USA), Anti-Active Caspase-3 (1:1000, Mouse monoclonal antibody, Cat# E-AB-22115, Elabscience), Tumour Necrosis Factor Alpha (TNF-α) (1:1000, Rabbit polyclonal IgG, Cat# BS-2081R, BIOSS), Interleukin-6 (IL-6) (1:1000, Rabbit monoclonal IgG, BIOSS), Nuclear Factor Kappa B p65 (NFkB p65) (1:2000, Mouse monoclonal IgG, Cat# E-AB-22066, Elabscience), NOX2 (NADPH OXIDASE 2), also called CYBB (CYTOCHROME b (-245) (1:1000, Rabbit Polyclonal antibody, Cat# E-AB-60387, Elabscience) and Peroxisome Proliferator Activated Receptor gamma (PPARG) (1:1000, Rabbit polyclonal IgG, Elabscience) for overnight inside humidified chamber at 4 °C. Membranes probed with rabbit raised primary antibody were incubated with Horse-radish Peroxidase (HRP) conjugated goat-anti-rabbit secondary IgG antibody (1:4000, Cat#E-AB-1003, Elabscience), and membranes probed with mouse raised primary antibody were incubated with HRP conjugated goat-anti-mouse secondary IgG antibody (1:4000, Cat#E-AB-1001, Elabscience) for 3 hours with constant agitation at room temperature. The membranes were rinsed four times with PBST before being immersed in Enhanced Chemiluminescence (ECL) solutions (Cat #1705061, BioRad, Hercules, CA, USA) according to the manufacturer's instructions and developed on X-ray film in a dark room. The band intensities were quantified using ImageJ software. A probe was created for β-Tubulin (1:1500, Rabbit monoclonal IgG, Cat#E-AB-20070, Elabscience), which served as a loading control for all antibodies utilised in this investigation.

5.3.11. Statistical analysis

All data were expressed as mean ± standard error of the mean (SEM). Comparison and analysis were performed using one way ANOVA. The P values <0.05 were considered significant.

5.4. RESULTS

5.4.1. Therapeutic efficacy of LCLE and TPLE on TNBS-induced alteration in body weight, food consumption, water consumption, colon weight to length ratio, ulcer area, ulcer index, disease activity index and macroscopic scores.

The given results pertain to the effect of different treatments on the body weight of rats in the context of ulcerative colitis (Figure 30 A and Figure 16 A). In LCLE treatment TNBS treatment led to a significant decrease in the body weight of rats compared to the control group. Sulfasalazine (SPS) treatment resulted in a significant increase in the body weight of rats compared to TNBS-treated groups. LCLE treatment showed a significant increase in body weight compared to both TNBS and SPS treated groups (Figure 30 A). TPLE treatment showed similar trend to LCLE treatment, where TNBS treatment led to a significant decrease in body weight compared to the control group. On the other hand, both SPS and TPLE treatment groups showed a significant increase in body weight compared to TNBS-treated groups. Within TPLE treatment groups, the lower dose (10 mg/kg) did not show a significant difference compared to SPS treatment. However, the higher dose (20 mg/kg) of TPLE resulted in a significant increase in body weight compared to the SPS-treated group (Figure 31 A). The significant decrease in body weight observed in TNBS-treated rats indicates the adverse effects of this treatment on the overall health and well-being of the animals, possibly due to the induction of ulcerative colitis. The significant increase in body weight in the SPS-treated groups suggests that sulfasalazine might have a protective or therapeutic effect against the development of ulcerative colitis, allowing the rats to maintain or gain weight. The even greater increase in body weight in both LCLE and TPLE treated groups compared to TNBS and SPS treated groups indicates that these treatments might be

more effective in ameliorating the negative effects of ulcerative colitis on body weight regulation. The dose-dependent effect observed in TPLE treatment, where the higher dose led to a greater increase in body weight compared to the lower dose and SPS treatment, suggests that the efficacy of this treatment might be influenced by dosage.

The provided results describe the impact of various treatments on the food consumption rate in rats undergoing ulcerative colitis treatment. Both LCLE treatment (Figure 30 B) and TPLE treatment showed similar trend in the food consumption rate of rats. TNBS treatment led to a significant decrease in food consumption compared to the control group. This decreases, likely reflects the negative impact of TNBS on the rats' appetite and ability to consume food, possibly due to the development of ulcerative colitis. Sulfasalazine (SPS), LCLE and TPLE treatment groups showed a significant increase in food consumption compared to the TNBS-treated groups. This suggests that both SPS and plant extracts' treatment might have protective or therapeutic effects against the loss of appetite associated with ulcerative colitis, allowing the rats to consume food more readily. Additionally, there were no significant differences in food consumption between the SPS-treated groups and either the LCLE-treated groups or the lower dose TPLE-treated groups indicating similar efficacy in promoting food intake. However, the higher-dose TPLE treatment group showed a significant increase in food consumption compared to the SPS-treated group, suggesting a potential dose-dependent effect of TPLE on food consumption. This suggests that the effectiveness of SPS in promoting food consumption is comparable to that of the plant extracts (LCLE and TPLE).

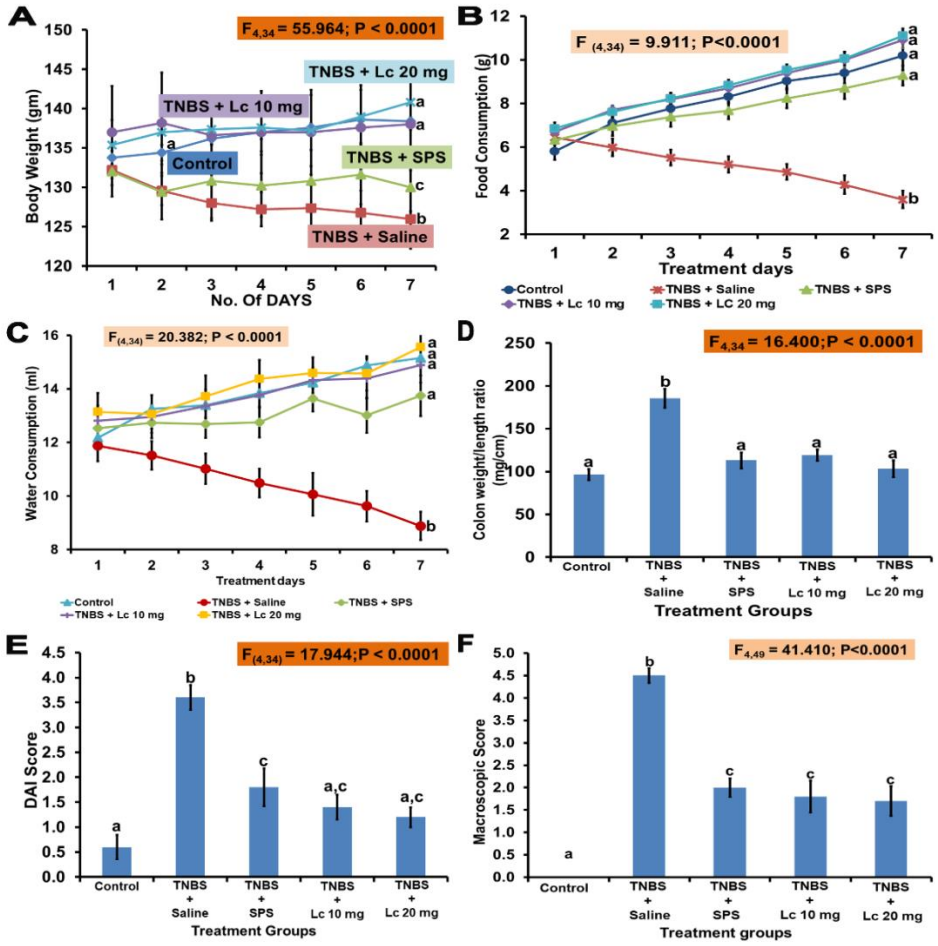

Figure 30: Systemic treatment with *L. coromandelica* is able to ameliorate the clinical signs of TNBS-induced colitis. The initial body weight (A), Food consumption (B), Water consumption (C), colon weight/length ratio (D), DAI Score (E), and macroscopic score (F), in TNBS-induced in rat. Datas are represented as mean ± SEM. Statistical comparison was performed using one-way ANOVA followed by Tukey's multiple comparison tests. The bar graph with a different letter means statistically significant difference at $p < 0.05$ and similar letters are not significant. Lc – Lannea coromandelica. TNBS – Trinitrobenzenesulfonic acid. SPS – Sulfasalazine.

The provided results discuss the impact of various treatments on the water consumption rate in rats undergoing treatment for ulcerative colitis (Figure 30 C and Figure 31 C). Both LCLE treatment (Figure 30 C) and TPLE treatment (Figure 31 C)

showed similar inclination in water consumption rate of the rats. The TNBS-treated group exhibited a significant decrease in water consumption rate compared to the control group. This decrease may indicate a reduction in the rats' thirst or water intake due to the effects of TNBS, possibly related to the development of ulcerative colitis. In contrast, the SPS, LCLE, and TPLE treated groups all showed a significant increase in water consumption rate compared to the TNBS-treated group. This suggests that these treatments are effective in promoting hydration or increasing the rats' thirst response, potentially counteracting the reduced water intake associated with ulcerative colitis. Importantly, there were no significant differences in water consumption rate between the SPS-treated group and either the LCLE-treated group or the TPLE-treated group suggesting similar efficacy in promoting water intake.

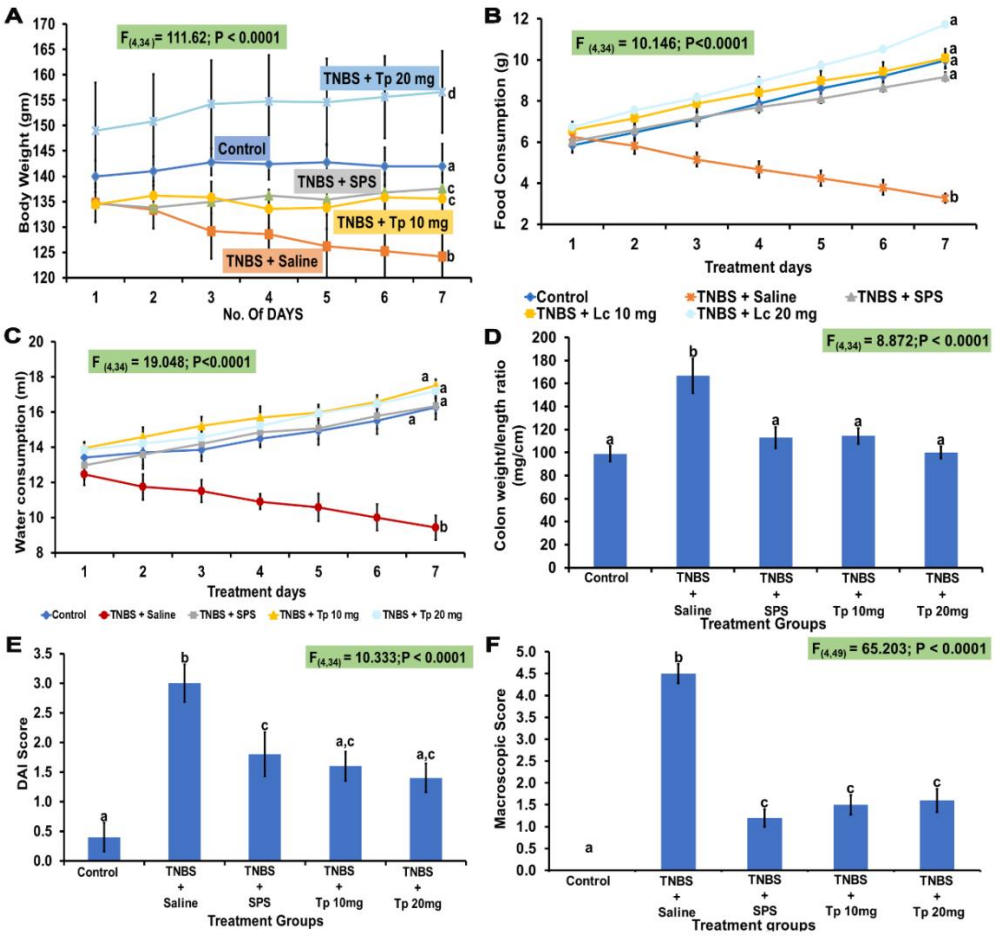

Figure 31: Systemic treatment with *T. palmata* is able to ameliorate the clinical signs of TNBS-induced colitis. The initial body weight (A), Food consumption (B), Water

consumption (C), colon weight/length ratio (D), DAI Score (E), and macroscopic score (F), in TNBS-induced in rat. Data are represented as mean ± SEM. Statistical comparison was performed using one-way ANOVA followed by Tukey's multiple comparison tests. The bar graph with a different letter means statistically significant difference at $p < 0.05$ and similar letters are not significant. Lc – *Lannea coromandelica*. TNBS – Trinitrobenzenesulfonic acid. SPS – Sulfasalazine.

The provided results describe the impact of various treatments on the colon weight to length ratio in rats undergoing treatment for ulcerative colitis. Both LCLE Treatment (Figure 30 D) and TPLE treatment (Figure 31 D) showed similar effects on the colon weight to length ratio of rats. The TNBS-treated group exhibited a significant increase in the colon weight to length ratio compared to the control group. This increase suggests that TNBS treatment led to an increase in the relative weight of the colon compared to its length, which could indicate inflammation, edema, or other pathological changes associated with ulcerative colitis. In contrast, the SPS, LCLE, and TPLE treated groups all showed a significant decrease in the colon weight to length ratio compared to the TNBS-treated group. This suggests that these treatments were effective in reducing the relative weight of the colon compared to its length, potentially indicating a reduction in inflammation or other pathological changes associated with ulcerative colitis. Importantly, there were no significant differences in the colon weight to length ratio between the SPS-treated group and either the LCLE-treated group or the TPLE-treated group. This suggests that the efficacy of SPS in reducing colon weight to length ratio is comparable to that of the plant extracts (LCLE and TPLE).

Table 36: Effect of LCLE on TNBS-induced alterations in ulcer area, ulcer index, and % inhibition in rats.

Treatment	Ulcer area (mm2)	Ulcer Index	% inhibition
Control	0.00 ± 0.00a	0.00 ± 0.00a	-
TNBS + Saline	38.56 ± 2.38b	81.42 ± 4.21b	-
TNBS + SPS	13.40 ± 2.18c	13.71 ± 4.11c	83.16
TNBS + Lc 10mg/kg	18.30 ± 4.62c	19.33 ± 3.11c	76.26
TNBS + Lc 20mg/kg	14.61 ± 3.11c	8.61 ± 2.52a,c	89.43

Data are expressed as mean ± S.E.M. (n = 5) and analyzed by one-way ANOVA followed by Tukey's multiple range test. $P < 0.05$ is significantly different.

This table (Table 36) presents the effects of LCLE on TNBS-induced alterations in ulcer area, ulcer index, and percent inhibition in rats.

Ulcer area (mm^2): Ulcer area refers to the size of ulcers present in the colon, measured in square millimeters (mm^2). In the control group, there were no ulcers observed, indicated by a value of 0.00 ± 0.00 mm^2. TNBS (trinitrobenzene sulfonic acid) administration resulted in significant ulcer formation, with ulcer areas of 38.56 ± 2.38 mm^2 in the TNBS + Saline group. Treatment with SPS (sulfasalazine), LCLE at doses of 10 mg/kg, and LCLE at doses of 20 mg/kg resulted in reductions in ulcer area compared to the TNBS + Saline group. The ulcer areas were 13.40 ± 2.18 mm^2, 18.30 ± 4.62 mm^2, and 14.61 ± 3.11 mm^2, respectively.

Ulcer Index: The ulcer index is a scoring system used to quantify the severity of ulceration. Similar to ulcer area, the control group showed an index of 0.00 ± 0.00. TNBS administration significantly increased the ulcer index, with values of 81.42 ± 4.21 in the TNBS + Saline group. Treatment with SPS, LCLE at doses of 10 mg/kg,

and LCLE at doses of 20 mg/kg resulted in reductions in ulcer index compared to the TNBS + Saline group. The ulcer indexes were 13.71 ± 4.11, 19.33 ± 3.11, and 8.61 ± 2.52, respectively.

% Inhibition: Percent inhibition represents the extent to which the treatment inhibits or reduces ulcer formation compared to the TNBS treated group. In this table, only the TNBS + SPS group and the two LCLE treatment groups are compared for percent inhibition. SPS treatment resulted in a percent inhibition of 83.16%, indicating a significant reduction in ulcer formation compared to the TNBS + Saline group. LCLE treatment at doses of 10 mg/kg and 20 mg/kg resulted in percent inhibitions of 76.26% and 89.43%, respectively, indicating significant reductions in ulcer formation compared to the TNBS + Saline group.

Overall, the results suggest that treatment with SPS and LCLE at both 10 mg/kg and 20 mg/kg doses effectively reduces ulcer area and ulcer index in TNBS-induced ulcerative colitis in rats. Additionally, LCLE treatment at 20 mg/kg shows the highest percentage inhibition, indicating its potential as a therapeutic agent for ulcerative colitis.

Table 37: Effect of TPLE on TNBS-induced alterations in ulcer area, ulcer index, and % inhibition in rats.

Treatment	**Ulcer area (mm2)**	**Ulcer Index**	**% inhibition**
Control	0.00 ± 0.00a	0.00 ± 0.00a	-
TNBS + Saline	36.84 ± 2.11b	80.63 ± 3.55b	-
TNBS + SPS	15.62 ± 3.12c	16.61 ± 3.12c	79.40
TNBS + Tp 10mg/kg	10.63 ± 2.12c	11.85 ± 2.13a,c	85.30
TNBS + Tp 20mg/kg	9.18 ± 1.16c	10.32 ± 2.16a	87.20

Data are expressed as mean ± S.E.M. (n = 5) and analyzed by one-way ANOVA followed by Tukey's multiple range test. $P < 0.05$ is significantly different.

Table 37 presents the effects of LCLE on TNBS-induced alterations in ulcer area, ulcer index, and percent inhibition in rats.

Ulcer Area (mm^2): This column shows the mean ulcer area in square millimeters (mm^2) observed in the rats under each treatment condition. Ulcer area is a measure of the size of ulcers formed in the colon. Lower values indicate a reduction in ulcer size and potentially less severe ulceration. In this experiment, TPLE higher dose (20 mg/kg) showed the lowest value 9.18 ± 1.16 mm^2.

Ulcer Index: The ulcer index provides a score indicating the severity of ulceration in the colon. Lower values suggest less severe ulceration. In this table TPLE 20 mg/kg showed the lowest ulcer index with the value 10.32 ± 2.16.

% Inhibition: This column represents the percentage of inhibition of ulcer formation compared to the TNBS + Saline group. It indicates the extent to which the treatment inhibits or reduces ulcer formation in comparison to the TNBS-induced group given saline. In this table comparison was made among three groups including SPS, TPLE lower dose (10 mg/kg) and TPLE higher dose (20 mg/kg) treated groups. TPLE treated group with higher dose showed the highest % inhibition value 87.20 among the three groups.

In brief, the table provides insights into the effects of TPLE at different doses on TNBS-induced alterations in ulcer area, ulcer index, and percent inhibition in rats. It demonstrates the potential of TPLE treatment in reducing ulcer formation and inflammation associated with ulcerative colitis, with higher doses potentially resulting in greater efficacy compared to the TNBS + Saline group. Additionally, the comparison with the TNBS + SPS group provides a reference for the effectiveness of TPLE treatment relative to a known treatment option.

The Disease Activity Index (DAI) is a commonly used measure in preclinical studies of inflammatory bowel disease (IBD), such as ulcerative colitis in rats. It typically includes parameters like weight loss, stool consistency, and rectal bleeding. The graph of DAI score of LCLE treatment (Figure 30 E) showed significant increase of

TNBS group when compared to control group suggesting that TNBS induction effectively induced colitis-like symptoms in the rats. This increase likely indicates weight loss, diarrhea, and possibly rectal bleeding in the TNBS-treated rats compared to the control group. SPS treated group and LCLE treated groups showed significant decrease in the score when compared to TNBS treated group. The significant decrease in DAI scores observed in both the SPS and LCLE treated groups compared to the TNBS group indicates that both SPS and LCLE treatments were effective in ameliorating the symptoms of colitis induced by TNBS. This decrease suggests improvements in weight loss, stool consistency, and possibly a reduction in rectal bleeding in the treated groups compared to the TNBS group. Additionally, the LCLE treated groups showed no significant changes compared with both SPS treated group and control. Interpret this result. The lack of significant changes in DAI scores in the LCLE treated groups compared to both the SPS treated group and the control group suggests that LCLE treatment was as effective as SPS in reducing the symptoms of colitis induced by TNBS. Additionally, the lack of significant changes compared to the control group indicates that LCLE treatment potentially normalized the DAI scores, bringing them back to baseline levels observed in healthy rats.

The graph of DAI score of TPLE treatment (Figure 31 E) showed similar score to that of LCLE treatment where TNBS group significantly increased when compared to control group indicates that TNBS induction effectively induced colitis-like symptoms in the rats like weight loss, diarrhea, and possibly rectal bleeding. SPS treated group and TPLE treated groups showed significant decrease in the score when compared to TNBS treated group indicating that both SPS and TPLE treatments effectively mitigated the symptoms of colitis induced by TNBS. Additionally, the TPLE treated groups showed no significant changes compared with to SPS treated group. The lack of significant changes in DAI scores in the LCLE treated groups compared to the SPS treated group indicates that LCLE treatment was as effective as SPS in reducing the symptoms of colitis induced by TNBS. This suggests that both treatments achieved similar levels of improvement in colitis symptoms.

The macroscopic scoring data provides valuable insights into the overall appearance and severity of colitis symptoms in rats treated with different agents. The macroscopic scoring data shows that in both LCLE (Figure 30 F) and TPLE (Figure 31 F) treatment, TNBS showed significant increase in the score when compared to control group indicating that TNBS induction resulted in a notable exacerbation of colitis-like symptoms. This increase likely reflects heightened inflammation, ulceration, and tissue damage induced by TNBS administration compared to untreated rats. The significant decrease in the macroscopic score observed in both the SPS and plant extract treatment groups compared to the TNBS group suggests that these treatments effectively attenuated the severity of colitis symptoms induced by TNBS. This reduction likely indicates improvements in parameters such as inflammation, ulceration, and tissue damage due to the therapeutic effects of SPS and the plant extracts. SPS and plant extract treatment showed no significant changes when compared to SPS treated group suggesting that these treatments achieved similar levels of efficacy in reducing colitis symptoms. This indicates that SPS, LCLE, and TPLE treatments are equally effective in mitigating the severity of colitis symptoms in this experimental model.

5.4.2. The effects of *Lannea coromandelica* and *Trevesia palmata* on the myeloperoxidase (MPO), Calprotectin (CALP), Interleukin-6 (IL-6), Interleukin-1 (IL-1), Leukotriene-B4 (LT-B4), FAD-Linked sulfhydryl oxidase ALR, Prostaglandin E2 (PG-E2), Total Antioxidant (T-AOC) and Interleukin-10 (IL-10) activity in TNBS induced colitis

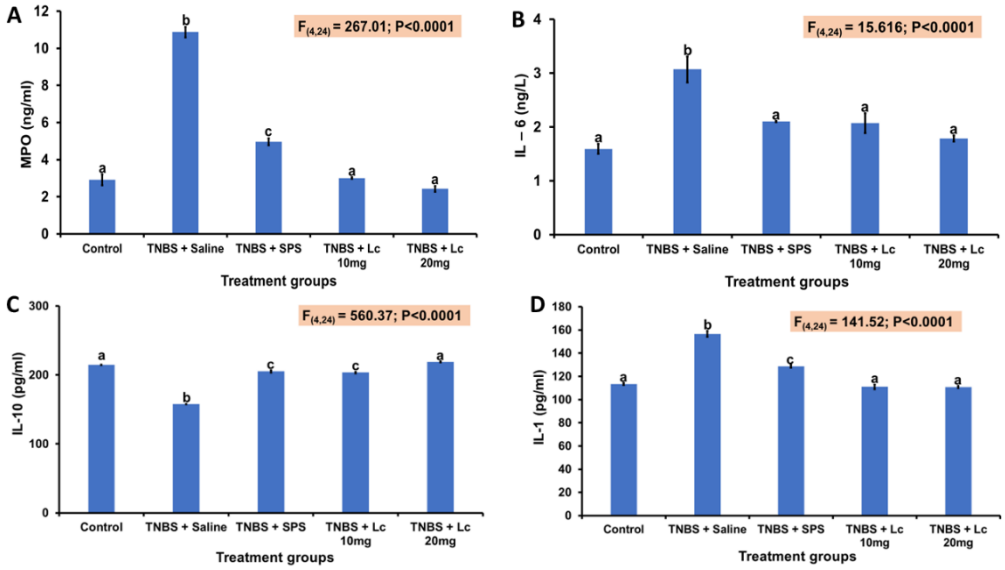

Figure 32: Modulatory effects of *Lannea coromandelica* methanolic extract treatment on inflammation in the colon of TNBS induced rats. *L. coromandelica* decreased the activity of Myeloperoxidase (MPO) (A), reducing the production of IL-6 (B), IL-1 (D) and significantly increasing the IL-10 (C) levels. The data indicates that the protective effect of *L. coromandelica* in the inflamed Colon was correlated with the repression of pro-inflammatory cytokines. n = 5

Figure 32 illustrates the modulatory effects of *Lannea coromandelica* methanolic extract treatment on inflammation in the colon of rats induced with TNBS (trinitrobenzene sulfonic acid), a commonly used model for inducing colitis. The figure provides insights into various inflammatory markers measured in the colon tissue of rats subjected to different treatments.

Myeloperoxidase (MPO) Activity (Figure 32 A): Myeloperoxidase is an enzyme found predominantly in neutrophils and is indicative of neutrophil infiltration, a hallmark of inflammation. The data suggests that treatment with Lannea

coromandelica methanolic extract led to a decrease in MPO activity in the colon tissue compared to untreated TNBS-induced rats. This indicates a reduction in neutrophil infiltration and, by extension, inflammation in the colon.

Levels of Pro-inflammatory Cytokines IL-6 (Figure 32 B) and IL-1 (Figure 32 D): Interleukin-6 (IL-6) and interleukin-1 (IL-1) are pro-inflammatory cytokines involved in the regulation of immune responses and inflammation. The data suggests that treatment with *Lannea coromandelica* methanolic extract resulted in a reduction in the levels of IL-6 and IL-1 in the colon tissue compared to untreated TNBS-induced rats. This indicates a suppression of pro-inflammatory responses and inflammation in the colon.

Level of Anti-inflammatory Cytokine IL-10 (Figure 32 C): Interleukin-10 (IL-10) is an anti-inflammatory cytokine that plays a crucial role in regulating immune responses and suppressing inflammation. The data suggests that treatment with *Lannea coromandelica* methanolic extract led to a significant increase in the levels of IL-10 in the colon tissue compared to untreated TNBS-induced rats. This indicates an enhancement of anti-inflammatory responses in the colon.

Overall, the data presented in Figure 32 suggests that treatment with *Lannea coromandelica* methanolic extract exerted protective effects against inflammation in the colon of TNBS-induced rats. This protective effect is associated with a decrease in neutrophil infiltration (as indicated by reduced MPO activity) and a suppression of pro-inflammatory cytokines (IL-6 and IL-1) along with an enhancement of the anti-inflammatory cytokine IL-10. These findings support the notion that *Lannea coromandelica* methanolic extract possesses anti-inflammatory properties and may hold therapeutic potential for conditions associated with colon inflammation, such as ulcerative colitis.

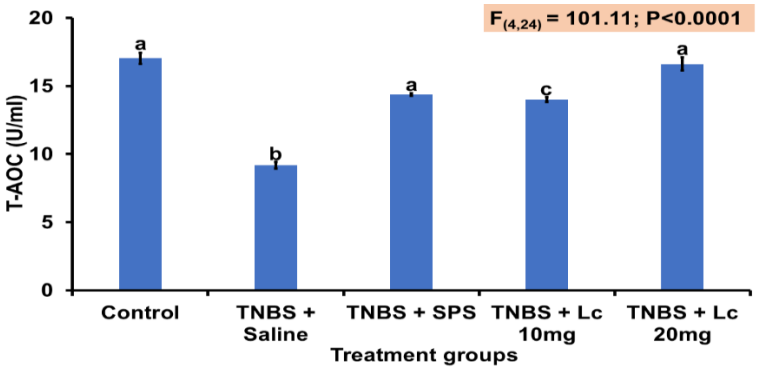

Figure 33: Modulatory effects of *Lannea coromandelica* methanolic extract treatment on inflammation in the colon of TNBS induced rats. The total antioxidant activity with potent anti-inflammatory properties may be responsible for the protective effect of *L. coromandelica*. n = 5

Figure 33 illustrates the modulatory effects of *Lannea coromandelica* methanolic extract treatment on inflammation in the colon of rats induced with TNBS (trinitrobenzene sulfonic acid), a model for inducing colitis. The figure focuses on the total antioxidant activity of *Lannea coromandelica* methanolic extract and its potential role in exerting anti-inflammatory effects.

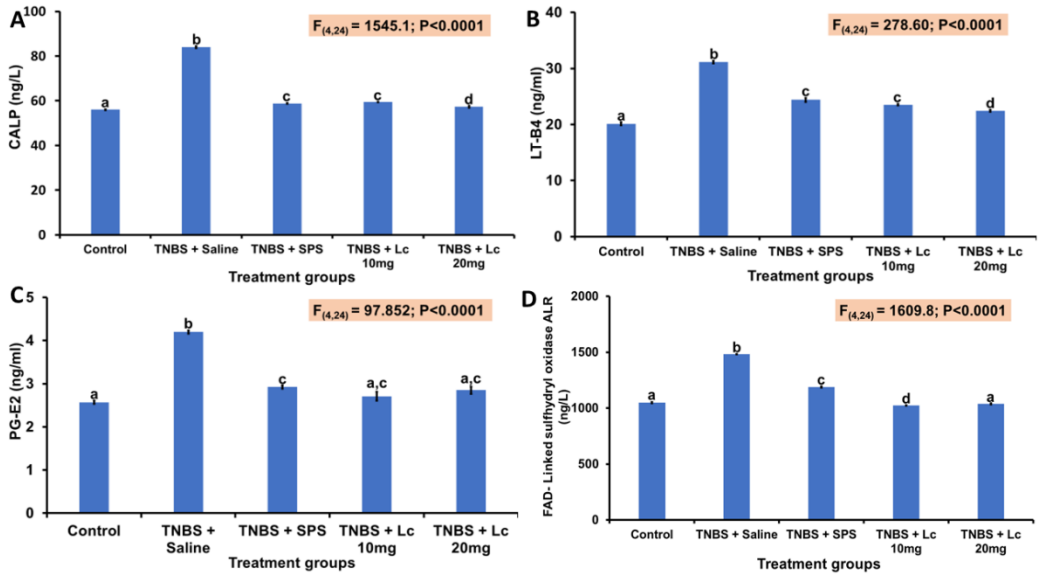

Figure 34: Modulatory effects of *Lannea coromandelica* methanolic extract treatment on inflammation in the colon of TNBS induced rats. *L. coromandelica* decreased the

levels of CALP (A), LT-B4 (B), PG-E2 (C) and FAD-Linked sulfhydryl oxidase ALR (D) levels. n = 5

Figure 34 presents the modulatory effects of *Lannea coromandelica* methanolic extract treatment on inflammation in the colon of rats induced with TNBS (trinitrobenzene sulfonic acid), a model for inducing colitis. The figure focuses on various inflammatory markers measured in the colon tissue of rats subjected to different treatments.

CALP Levels (Figure 34 A): CALP (calprotectin) is a protein complex that is released by activated neutrophils and is used as a marker of inflammation in the gastrointestinal tract. The data suggests that treatment with *Lannea coromandelica* methanolic extract led to a decrease in CALP levels in the colon tissue of TNBS-induced rats compared to untreated rats. This decrease indicates a reduction in neutrophil activation and inflammation in the colon.

LT-B4 Levels (Figure 34 B): Leukotriene B4 (LT-B4) is a pro-inflammatory lipid mediator involved in the inflammatory response. The data suggests that treatment with *Lannea coromandelica* methanolic extract resulted in a decrease in LT-B4 levels in the colon tissue of TNBS-induced rats compared to untreated rats. This decrease indicates a suppression of the inflammatory cascade mediated by LT-B4.

PG-E2 Levels (Figure 34 C): Prostaglandin E2 (PG-E2) is a pro-inflammatory lipid mediator that plays a role in inflammation and pain. The data suggests that treatment with *Lannea coromandelica* methanolic extract led to a decrease in PG-E2 levels in the colon tissue of TNBS-induced rats compared to untreated rats. This decrease indicates a reduction in inflammation and associated symptoms.

FAD-Linked Sulfhydryl Oxidase ALR Levels (Figure 34 D): FAD-linked sulfhydryl oxidase ALR (augmenter of liver regeneration) is an enzyme involved in redox regulation and inflammation. The data suggests that treatment with *Lannea coromandelica* methanolic extract resulted in a decrease in ALR levels in the colon tissue of TNBS-induced rats compared to untreated rats. This decrease indicates a modulation of redox processes and a reduction in inflammation in the colon.

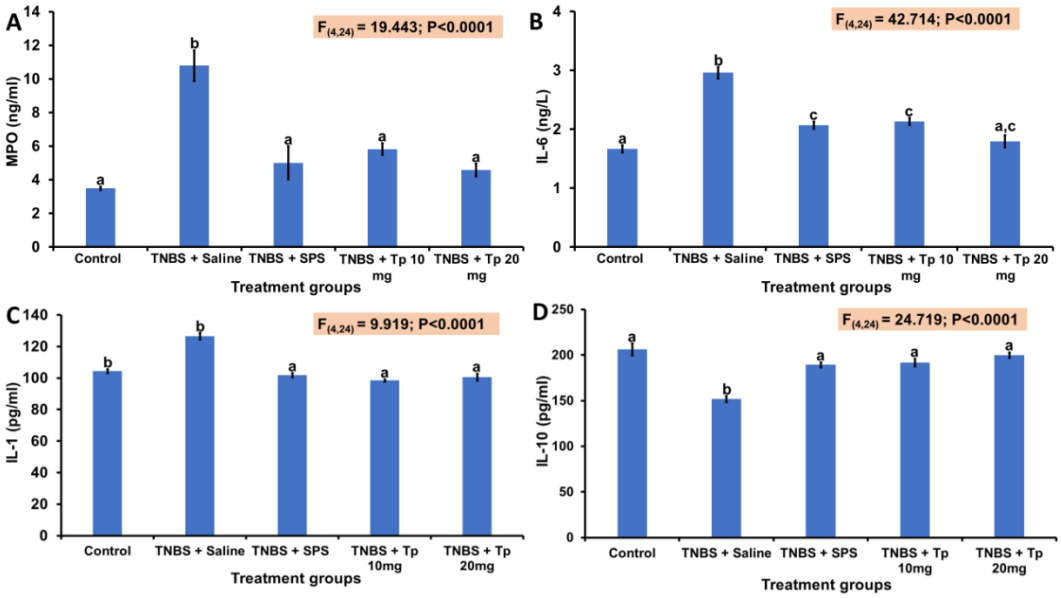

Figure 35: Modulatory effects of *Trevesia palmata* methanolic extract treatment on inflammation in the colon of TNBS induced rats. *T. palmata* decreased the activity of Myeloperoxidase (MPO) (A), reducing the production of IL-6 (B) and IL-1 (C) levels. The IL-10 (D) levels were increased significantly in the *T. palmata* extract treatment groups. The data indicates that the protective effect of T. palmata in the inflamed Colon was correlated with the repression of pro-inflammatory cytokines. n = 5

Figure 35 illustrates the modulatory effects of *Trevesia palmata* methanolic extract treatment on inflammation in the colon of rats induced with TNBS (trinitrobenzene sulfonic acid), a model for inducing colitis. The figure focuses on various inflammatory markers measured in the colon tissue of rats subjected to different treatments.

Myeloperoxidase (MPO) Activity (Figure 35 A): Myeloperoxidase is an enzyme found predominantly in neutrophils and is indicative of neutrophil infiltration, a hallmark of inflammation. The data suggests that treatment with *Trevesia palmata* methanolic extract led to a decrease in MPO activity in the colon tissue of TNBS-

induced rats compared to untreated rats. This decrease indicates a reduction in neutrophil infiltration and, by extension, inflammation in the colon.

Levels of Pro-inflammatory Cytokines IL-6 (Figure 35 B) and IL-1 (Figure 35 C): Interleukin-6 (IL-6) and interleukin-1 (IL-1) are pro-inflammatory cytokines involved in the regulation of immune responses and inflammation. The data suggests that treatment with *Trevesia palmata* methanolic extract resulted in a decrease in the levels of IL-6 and IL-1 in the colon tissue of TNBS-induced rats compared to untreated rats. This indicates a suppression of pro-inflammatory responses and inflammation in the colon.

Level of Anti-inflammatory Cytokine IL-10 (Figure 35 D): Interleukin-10 (IL-10) is an anti-inflammatory cytokine that plays a crucial role in regulating immune responses and suppressing inflammation. The data suggests that treatment with *Trevesia palmata* methanolic extract led to a significant increase in the levels of IL-10 in the colon tissue of TNBS-induced rats compared to untreated rats. This indicates an enhancement of anti-inflammatory responses in the colon.

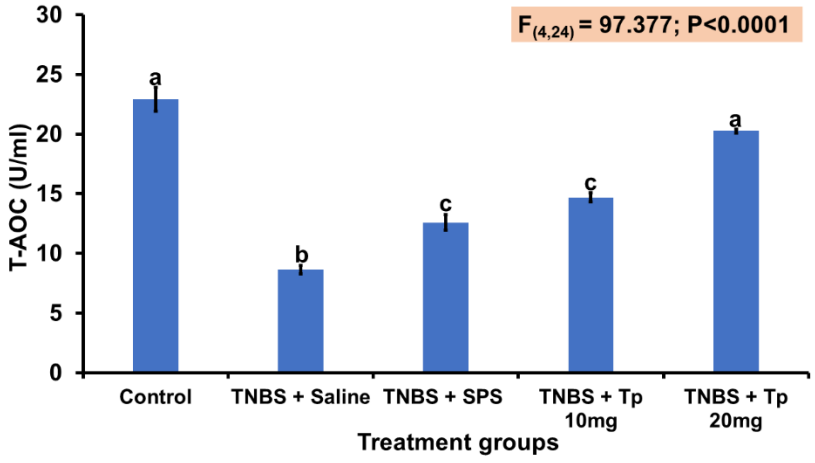

Figure 36: Modulatory effects of *Trevesia palmata* methanolic extract treatment on inflammation in the colon of TNBS induced rats. The total antioxidant activity with potent anti-inflammatory properties may be responsible for the protective effect of *T. palmata*. n = 5

Figure 36 illustrates the modulatory effects of *Trevesia palmata* methanolic extract treatment on inflammation in the colon of rats induced with TNBS (trinitrobenzene sulfonic acid), a model for inducing colitis. The figure highlights the total antioxidant activity of *Trevesia palmata* methanolic extract and its potential role in exerting anti-inflammatory effects.

Total Antioxidant Activity: Antioxidants are compounds that neutralize harmful free radicals in the body, thereby reducing oxidative stress and inflammation. The data suggests that treatment with *Trevesia palmata* methanolic extract led to an increase in total antioxidant activity in the colon tissue of TNBS-induced rats compared to untreated rats. This increase in antioxidant activity indicates the ability of *Trevesia palmata* methanolic extract to scavenge free radicals and reduce oxidative stress in the colon tissue, which is often associated with inflammation.

Potent Anti-inflammatory Properties: The figure suggests that the observed increase in total antioxidant activity may be responsible for the protective effect of *Trevesia palmata* methanolic extract against inflammation in the colon.

By scavenging free radicals and reducing oxidative stress, the extract likely suppresses inflammatory processes and mitigates tissue damage in the colon of TNBS-induced rats. Additionally, the anti-inflammatory properties of antioxidants may contribute to the overall reduction in inflammation observed in the treated rats.

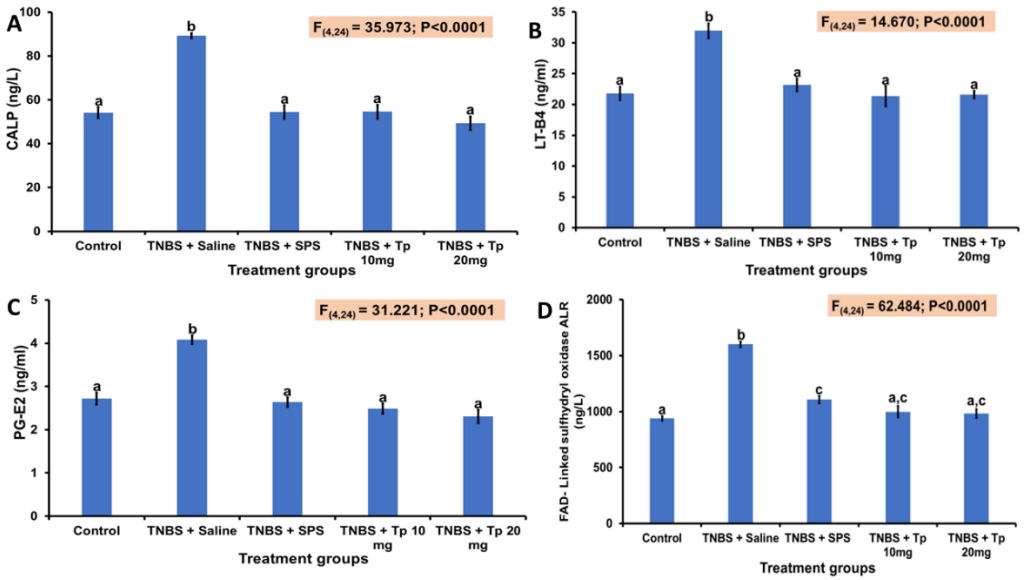

Figure 37: Modulatory effects of *Trevesia palmata* methanolic extract treatment on inflammation in the colon of TNBS induced rats. *T. palmata* reduced the production of CALP (A), LT-B4 (B), PG-E2 (C) and FAD-Linked sulfhydryl oxidase ALR (D) levels. n = 5

Figure 37 presents the modulatory effects of *Trevesia palmata* methanolic extract treatment on inflammation in the colon of rats induced with TNBS (trinitrobenzene sulfonic acid), a model for inducing colitis. The figure focuses on various inflammatory markers measured in the colon tissue of rats subjected to different treatments.

CALP Levels (Figure 37 A): CALP (calprotectin) is a protein complex released by activated neutrophils and is used as a marker of inflammation in the gastrointestinal tract. The data suggests that treatment with *Trevesia palmata* methanolic extract led to a decrease in CALP levels in the colon tissue of TNBS-induced rats compared to untreated rats. This decrease indicates a reduction in neutrophil activation and inflammation in the colon.

LT-B4 Levels (Figure 37 B): Leukotriene B4 (LT-B4) is a pro-inflammatory lipid mediator involved in the inflammatory response. The data suggests that treatment with *Trevesia palmata* methanolic extract resulted in a decrease in LT-B4 levels in

the colon tissue of TNBS-induced rats compared to untreated rats. This decrease indicates a suppression of the inflammatory cascade mediated by LT-B4.

PG-E2 Levels (Figure 37 C): Prostaglandin E2 (PG-E2) is a pro-inflammatory lipid mediator that plays a role in inflammation and pain. The data suggests that treatment with *Trevesia palmata* methanolic extract led to a decrease in PG-E2 levels in the colon tissue of TNBS-induced rats compared to untreated rats. This decrease indicates a reduction in inflammation and associated symptoms.

FAD-Linked Sulfhydryl Oxidase ALR Levels (Figure 37 D): FAD-linked sulfhydryl oxidase ALR (augmenter of liver regeneration) is an enzyme involved in redox regulation and inflammation. The data suggests that treatment with *Trevesia palmata* methanolic extract resulted in a decrease in ALR levels in the colon tissue of TNBS-induced rats compared to untreated rats. This decrease indicates a modulation of redox processes and a reduction in inflammation in the colon.

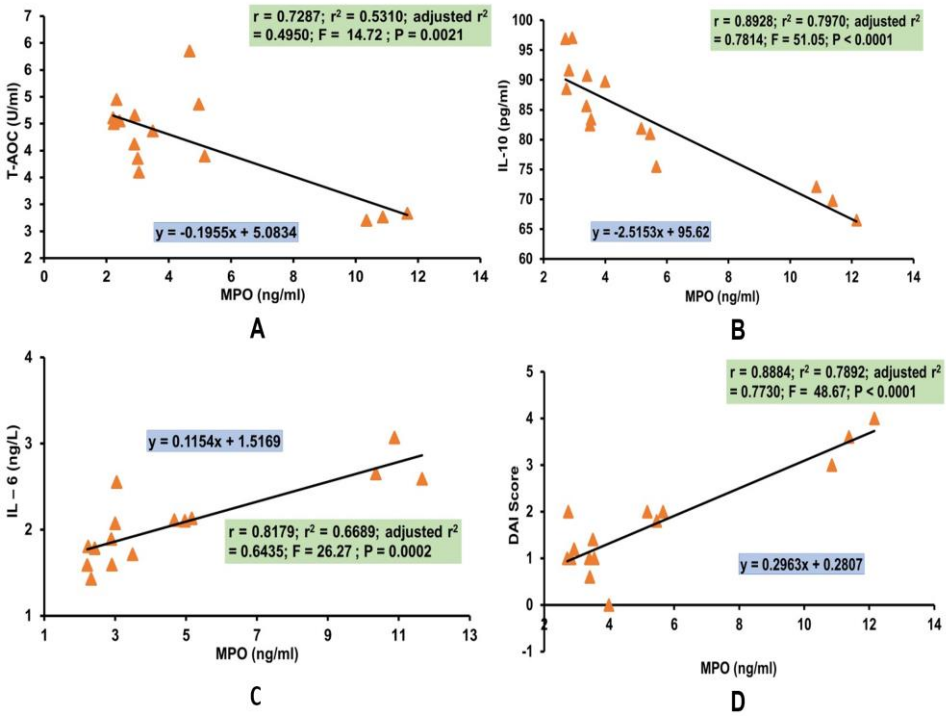

Figure 38: Correlation regression in *Lannea coromandelica* treated groups. This figure shows that there is negative correlation between MPO and antioxidant marker (T-AOC) ($P<0.05$) (figure A), and also between MPO and anti-inflammatory

biomarker (IL-10, (B)) (P<0.0001). Figure (C) shows positive correlation between MPO and pro inflammatory cytokine (IL-6) (P<0.05). (D) shows positive correlationship between the disease activity index (DAI) and MPO (P<0.0001). n=5. TAOC- Total Antioxidant. IL-10: Interleukin-10. MPO: Myeloperoxidase. IL-6: Interleukin – 6. DAI – Disease Activity Index.

Figure 38 presents correlation regression analyses conducted within *Lannea coromandelica* treated groups, focusing on various biomarkers and disease activity index in the context of TNBS-induced colitis.

Negative Correlation between MPO and Antioxidant Marker (T-AOC) (Figure 38 A): The negative correlation between MPO (Myeloperoxidase), a marker of neutrophil infiltration and inflammation, and the antioxidant marker T-AOC (Total Antioxidant Capacity) suggests an inverse relationship between neutrophil activity and antioxidant capacity. This finding indicates that higher levels of neutrophil activity, as indicated by elevated MPO levels, are associated with lower antioxidant capacity, implying increased oxidative stress and inflammation.

Negative Correlation between MPO and Anti-inflammatory Biomarker (IL-10) (Figure 38 B): The negative correlation between MPO and the anti-inflammatory cytokine IL-10 suggests an inverse relationship between neutrophil activity and the presence of anti-inflammatory responses. This finding indicates that higher levels of neutrophil activity, as indicated by elevated MPO levels, are associated with reduced levels of IL-10, implying a diminished anti-inflammatory response.

Positive Correlation between MPO and Pro-inflammatory Cytokine (IL-6) (Figure 38 C): The positive correlation between MPO and the pro-inflammatory cytokine IL-6 suggests a direct relationship between neutrophil activity and the production of IL-6. This finding indicates that higher levels of neutrophil activity, as indicated by elevated MPO levels, are associated with increased levels of IL-6, implying heightened inflammation.

Positive Correlation between Disease Activity Index (DAI) and MPO (Figure 38 D): The positive correlation between Disease Activity Index (DAI), a measure of

colitis severity, and MPO suggests a direct relationship between disease severity and neutrophil infiltration. This finding indicates that higher DAI scores, indicative of more severe colitis symptoms, are associated with increased neutrophil activity, as reflected by elevated MPO levels.

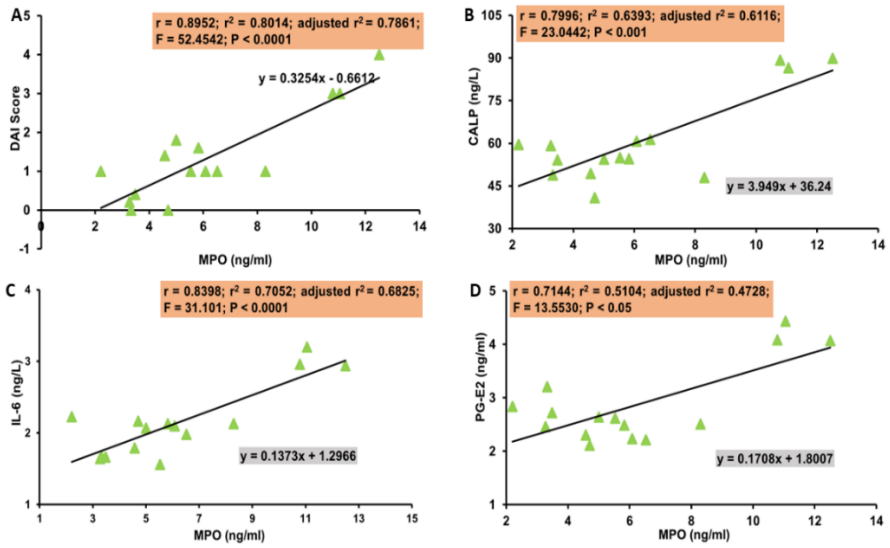

Figure 39: Correlation regression of *Trevesia palmata* treated groups. This figure shows that there is positive correlation between MPO and disease activity index (DAI) ($P<0.05$) (figure A), between MPO and calprotectin (CALP, (B)) ($P<0.0001$). Figure (C) and (D) also shows positive correlation between MPO and pro inflammatory cytokine (IL-6) ($P<0.05$) and between MPO and PG-E2 ($P<0.0001$). n=5. DAI -Disease Activity Index. MPO: Myeloperoxidase. IL-6: Interleukin – 6. CALP - Calprotectin. PG-E2 – Prostaglandin E2.

Figure 39 presents correlation regression analyses conducted within *Trevesia palmata* treated groups, focusing on various biomarkers in the context of TNBS-induced colitis.

Positive Correlation between MPO and Disease Activity Index (DAI) (Figure 39 A): The positive correlation between Myeloperoxidase (MPO), an enzyme associated with neutrophil activity and inflammation, and Disease Activity Index (DAI) suggests a direct relationship between neutrophil infiltration and the severity of

colitis symptoms. This finding indicates that higher levels of MPO, indicative of increased neutrophil activity, are associated with more severe colitis symptoms, as reflected by higher DAI scores.

Positive Correlation between MPO and Calprotectin (CALP) (Figure 39 B): The positive correlation between MPO and Calprotectin (CALP), a marker of inflammation produced by neutrophils, suggests a direct relationship between neutrophil activity and the presence of inflammation in the colon. This finding indicates that higher levels of MPO are associated with elevated levels of CALP, reflecting increased neutrophil infiltration and inflammation in the colon.

Positive Correlation between MPO and Pro-inflammatory Cytokine (IL-6) (Figure 39 C): The positive correlation between MPO and the pro-inflammatory cytokine IL-6 suggests a direct relationship between neutrophil activity and the production of IL-6. This finding indicates that higher levels of MPO, indicative of increased neutrophil activity, are associated with elevated levels of IL-6, implying heightened inflammation.

Positive Correlation between MPO and Prostaglandin E2 (PG-E2) (Figure 39 D): The positive correlation between MPO and Prostaglandin E2 (PG-E2), a pro-inflammatory mediator, suggests a direct relationship between neutrophil activity and the production of PG-E2. This finding indicates that higher levels of MPO are associated with elevated levels of PG-E2, reflecting increased inflammation in the colon.

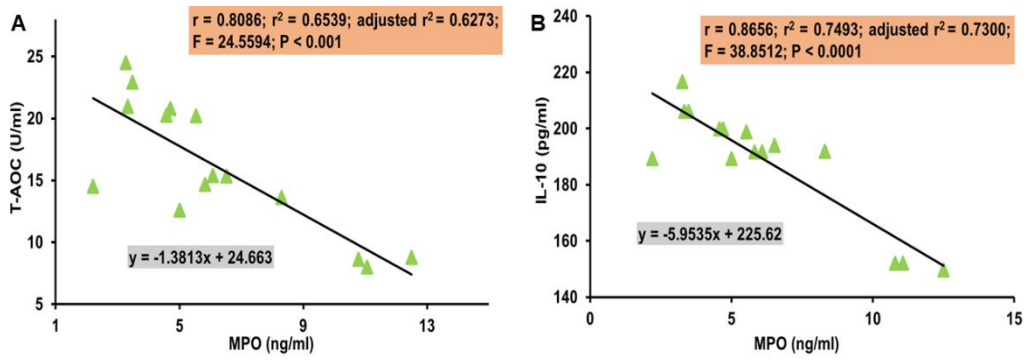

Figure 40: Correlation regression of *Trevesia palmata* treated groups. This figure shows that there is negative correlation between MPO and antioxidant marker (T-AOC) ($P<0.05$) (figure A), and also between MPO and anti-inflammatory biomarker (IL-10, (B)) ($P<0.0001$). n=5. TAOC- Total Antioxidant. IL-10: Interleukin-10. MPO: Myeloperoxidase.

Figure 40 illustrates correlation regression analyses conducted within *Trevesia palmata* treated groups, focusing on various biomarkers in the context of TNBS-induced colitis.

Negative Correlation between MPO and Antioxidant Marker (T-AOC) (Figure 40 A): The negative correlation between Myeloperoxidase (MPO), an enzyme associated with neutrophil activity and inflammation, and the antioxidant marker T-AOC (Total Antioxidant Capacity) suggests an inverse relationship between neutrophil activity and antioxidant capacity. This finding implies that higher levels of MPO, indicative of increased neutrophil activity and inflammation, are associated with lower antioxidant capacity, implying elevated oxidative stress.

Negative Correlation between MPO and Anti-inflammatory Biomarker (IL-10) (Figure 40 B): The negative correlation between MPO and the anti-inflammatory cytokine IL-10 suggests an inverse relationship between neutrophil activity and the presence of anti-inflammatory responses. This finding indicates that higher levels of MPO, indicative of increased neutrophil activity and inflammation, are associated with reduced levels of IL-10, implying a diminished anti-inflammatory response.

5.4.3. Therapeutic efficacy of LCLE and TPLE on TNBS-induced alteration in oxidative stress and improved the antioxidant status in experimental rats

Figure 41 depicts the effects of *Lannea coromandelica* extracts on oxidative stress markers and antioxidant enzymes in a study involving TNBS-induced colitis in rats.

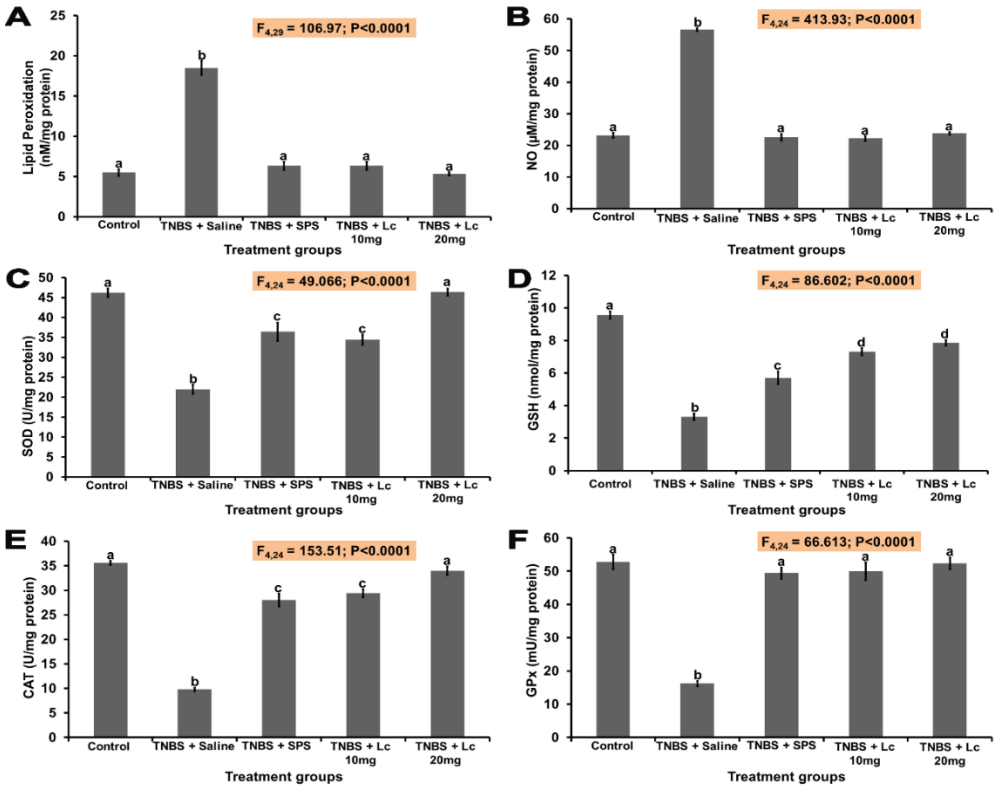

Figure 41: *Lannea coromandelica* extracts reduced the oxidative stress markers (Lipid peroxidation and Nitric oxide) and increased the antioxidant enzymes of SOD (C), GSH (D), CAT (E) and GPx (F) both in low and higher dose. Data are represented as Mean ± SEM (n = 5). Statistical comparison was performed using one-way ANOVA followed by Tukey's multiple comparison tests. The bar graph with a different letter means statistically significant difference at $p < 0.05$ and similar letters are not significant.

Lipid Peroxidation (Figure 41 A) and Nitric Oxide (NO) (Figure 41 B): *Lannea coromandelica* extracts significantly reduced the levels of lipid peroxidation and nitric oxide in the colon tissue of rats with TNBS-induced colitis. This reduction indicates a decrease in oxidative damage and nitrosative stress, which are associated with inflammation and tissue damage in colitis.

Antioxidant Enzymes: *Lannea coromandelica* extracts increased the activity of several antioxidant enzymes including Superoxide Dismutase (SOD) (Figure 41 C), Glutathione (GSH) (Figure 41 D), Catalase (CAT) (Figure 41 E), Glutathione Peroxidase (GPx) (Figure 41 F), These antioxidant enzymes play crucial roles in neutralizing reactive oxygen species (ROS) and protecting cells from oxidative damage. The increase in antioxidant enzyme activity suggests an enhancement of the antioxidant defense system in the colon tissue, which may help mitigate oxidative stress and inflammation associated with colitis.

The effects of *Lannea coromandelica* extracts on oxidative stress markers and antioxidant enzymes were observed at both low and higher doses, indicating a dose-dependent response. This suggests that *Lannea coromandelica* extracts exert beneficial effects on oxidative stress and antioxidant status in a dose-dependent manner (Figure 41).

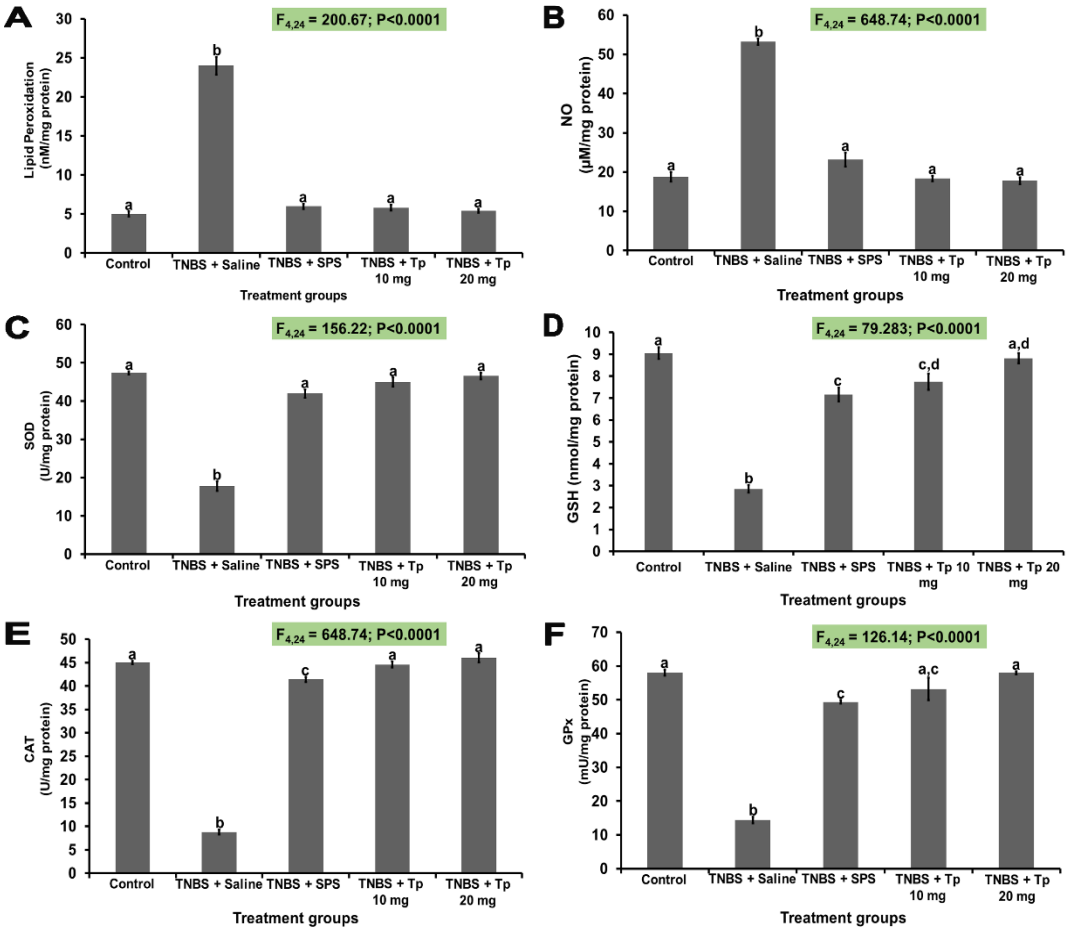

Figure 42: *Trevesia palmata* extracts reduced the oxidative stress markers (Lipid peroxidation (A) and Nitric oxide (B)) and increased the antioxidant enzymes of SOD (C), GSH (D), CAT (E) and GPx (F). Data are represented as Mean ± SEM (n = 5). Statistical comparison was performed using one-way ANOVA followed by Tukey's multiple comparison tests. The bar graph with a different letter means statistically significant difference at $p < 0.05$ and similar letters are not significant.

Figure 42 illustrates the effects of *Trevesia palmata* extracts on oxidative stress markers and antioxidant enzymes in a study involving TNBS-induced colitis in rats. Here's a breakdown of the findings:

Lipid Peroxidation (Figure 42 A) and Nitric Oxide (NO) (Figure 42 B): *Trevesia palmata* extracts significantly reduced the levels of lipid peroxidation and nitric oxide in the colon tissue of rats with TNBS-induced colitis. This reduction indicates

a decrease in oxidative damage and nitrosative stress, which are associated with inflammation and tissue damage in colitis.

Antioxidant Enzymes: *Trevesia palmata* extracts increased the activity of several antioxidant enzymes including Superoxide Dismutase (SOD) (Figure 42 C), Glutathione (GSH) (Figure 42 D), Catalase (CAT) (Figure 42 E), Glutathione Peroxidase (GPx) (Figure 42 F). These antioxidant enzymes play crucial roles in neutralizing reactive oxygen species (ROS) and protecting cells from oxidative damage. The increase in antioxidant enzyme activity suggests an enhancement of the antioxidant defense system in the colon tissue, which may help mitigate oxidative stress and inflammation associated with colitis.

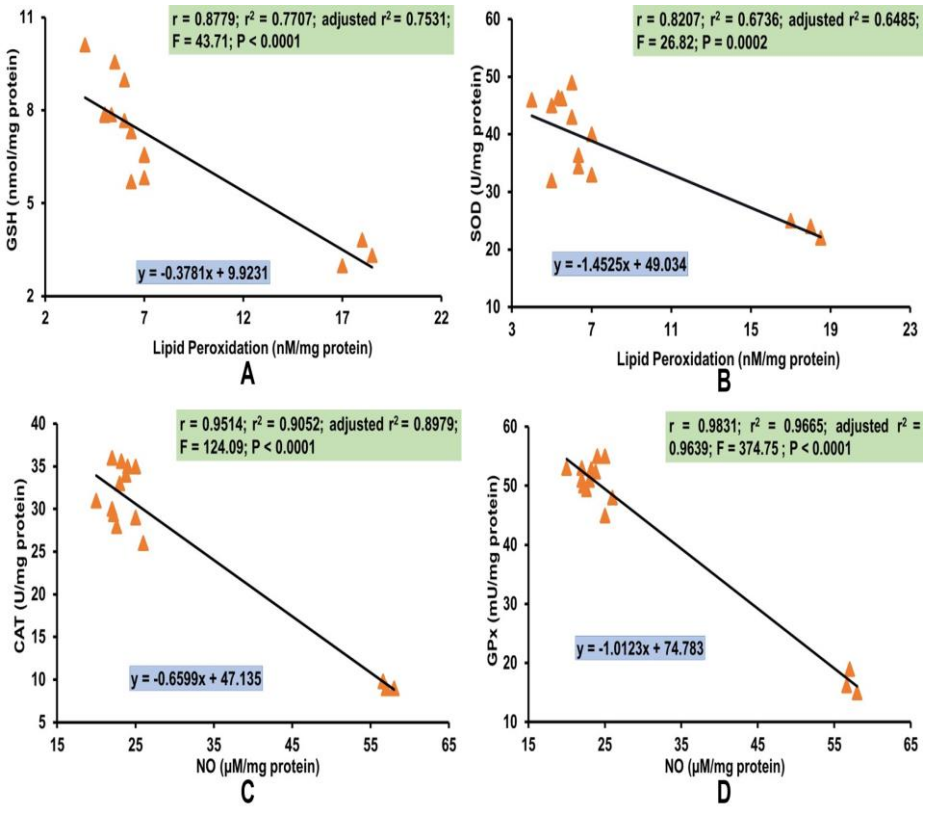

Figure 43: Linear regression analysis for the main oxidative parameters significantly altered between groups (n = 5) when treated with *Lannea coromandelica* leaf extract. This figure shows that there is negative correlation between LPO and antioxidant

enzyme, GSH (A) and SOD (B) at $P<0.05$. Also, there was a negative impact between NO and CAT (C) and between NO and GPx ($P<0.0001$). n=5. LPO: Lipid Peroxidation; GSH: Glutathione; SOD: Superoxide Dismutase; CAT; Catalase; GPx: Glutathione Peroxidase; NO: Nitric oxide.

Figure 43 presents linear regression analyses for the main oxidative parameters significantly altered between groups treated with *Lannea coromandelica* leaf extract in a study involving TNBS-induced colitis in rats.

Negative Correlation between Lipid Peroxidation (LPO) and Antioxidant Enzymes: There is a negative correlation between LPO and the antioxidant enzymes including Glutathione (GSH) (Figure 43 A), Superoxide Dismutase (SOD) (Figure 43 B). These negative correlations suggest that higher levels of lipid peroxidation are associated with lower levels of GSH and SOD activity. Lipid peroxidation reflects oxidative damage to cell membranes, and the negative correlation with antioxidant enzymes indicates a potential role of these enzymes in mitigating lipid peroxidation and oxidative stress.

Negative Correlation between Nitric Oxide (NO) and Antioxidant Enzymes: There is a negative correlation between NO and the antioxidant enzymes including Catalase (CAT) (Figure 43 C), Glutathione Peroxidase (GPx) (Figure 43 D). These negative correlations suggest that higher levels of NO are associated with lower activity of CAT and GPx. Nitric oxide is a signaling molecule involved in inflammation, and its negative correlation with antioxidant enzymes indicates a potential role of these enzymes in modulating nitrosative stress and inflammation.

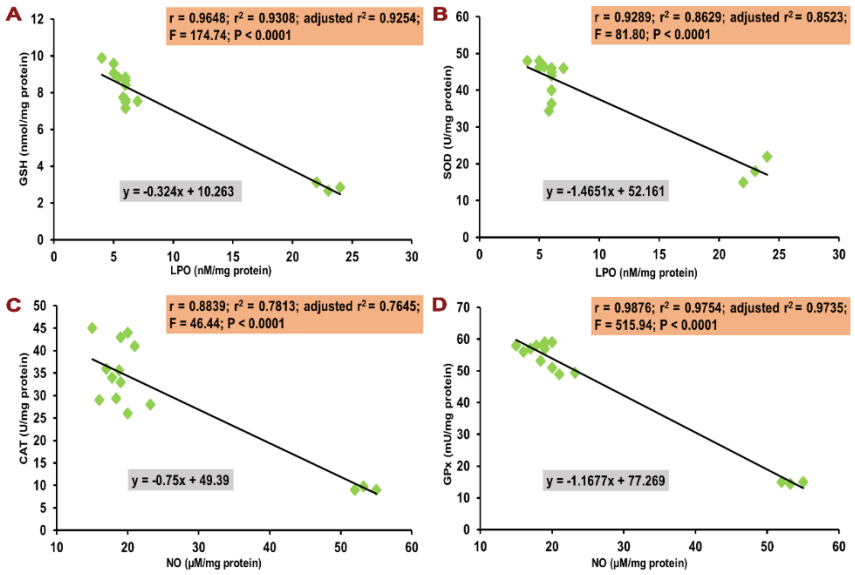

Figure 44: Linear regression analysis for the main oxidative parameters significantly altered between groups (n = 5) when treated with *Trevesia palmata* leaf extract. This figure shows that there is negative correlation between LPO and antioxidant enzyme, GSH (A) and SOD (B) at P<0.05. Also, there was a negative impact between NO and CAT (C) and between NO and GPx (P<0.0001). n=5. LPO: Lipid Peroxidation; GSH: Glutathione; SOD: Superoxide Dismutase; CAT; Catalase; GPx: Glutathione Peroxidase; NO: Nitric oxide.

Figure 44 presents linear regression analyses for the main oxidative parameters significantly altered between groups treated with *Trevesia palmata* leaf extract in a study involving TNBS-induced colitis in rats. Here's an interpretation of the findings:

Negative Correlation between Lipid Peroxidation (LPO) and Antioxidant Enzymes: There is a negative correlation between LPO and the antioxidant enzymes including Glutathione (GSH) (Figure 44 A), Superoxide Dismutase (SOD) (Figure Figure 44 B). These negative correlations suggest that higher levels of lipid peroxidation are associated with lower levels of GSH and SOD activity. Lipid peroxidation reflects oxidative damage to cell membranes, and the negative correlation with antioxidant enzymes indicates a potential role of these enzymes in mitigating lipid peroxidation and oxidative stress.

Negative Correlation between Nitric Oxide (NO) and Antioxidant Enzymes: There is a negative correlation between NO and the antioxidant enzymes including Catalase (CAT) (Figure 44 C), Glutathione Peroxidase (GPx) (Figure 44 D). These negative correlations suggest that higher levels of NO are associated with lower activity of CAT and GPx. Nitric oxide is a signaling molecule involved in inflammation, and its negative correlation with antioxidant enzymes indicates a potential role of these enzymes in modulating nitrosative stress and inflammation.

5.4.4. Therapeutic efficacy of *Lannea coromandelica* leaf extract (LCLE) and *Trevesia palmata* leaf extract (TPLE) by altering the histological status of the colon

Figure 45 provides photomicrographs of colon sections stained with hematoxylin and eosin (H&E) from five experimental groups in rats, along with corresponding histopathological scores. Control group (Figure 30 A), shows the colon section from the control rat, displaying intact epithelial and mucosal layers (ML). Histopathological assessment likely reveals minimal to no damage, reflected in a low histopathological score (%). TNBS-Induced group (Figure 45 B) shows the colon section from the TNBS-induced rat, exhibiting extensive hemorrhage (H), inflammatory cell (IC) infiltration, edema (E), and complete destruction of ML architecture. Histopathological assessment likely reveals significant damage, characterized by loss of epithelium, crypt damage, depletion of goblet cells, and infiltration of inflammatory cells, reflected in a high histopathological score (%). TNBS + SPS Group (Figure 45 C) depicts the colon section from the TNBS + SPS (Sulfasalazine) post-treated rat, showing IC infiltration and E, but with intact ML. Histopathological assessment likely reveals moderate damage, but with some preservation of ML architecture, resulting in a lower histopathological score (%) compared to the TNBS-induced group. TNBS + Lc 10mg (Figure 45 D) and TNBS + Lc 20mg (Figure 45 E) groups display colon sections from TNBS + Lc (*Lannea coromandelica*) post-treated rats, showing submucosa and mucosa layers with a normal aspect similar to the control group (Figure 45 A). Histopathological assessment likely reveals minimal damage, with restoration of epithelial and mucosal

layers, resulting in low histopathological scores (%), comparable to the control group. Histopathological Score (%) (Figure 45 F, G, H & I) likely show quantified histopathological scores for each experimental group, representing various parameters such as loss of epithelium, crypt damage, depletion of goblet cells, and infiltration of inflammatory cells. The histopathological scores provide a quantitative measure of the severity of colonic damage and inflammation, with higher scores indicating more significant tissue injury and inflammation.

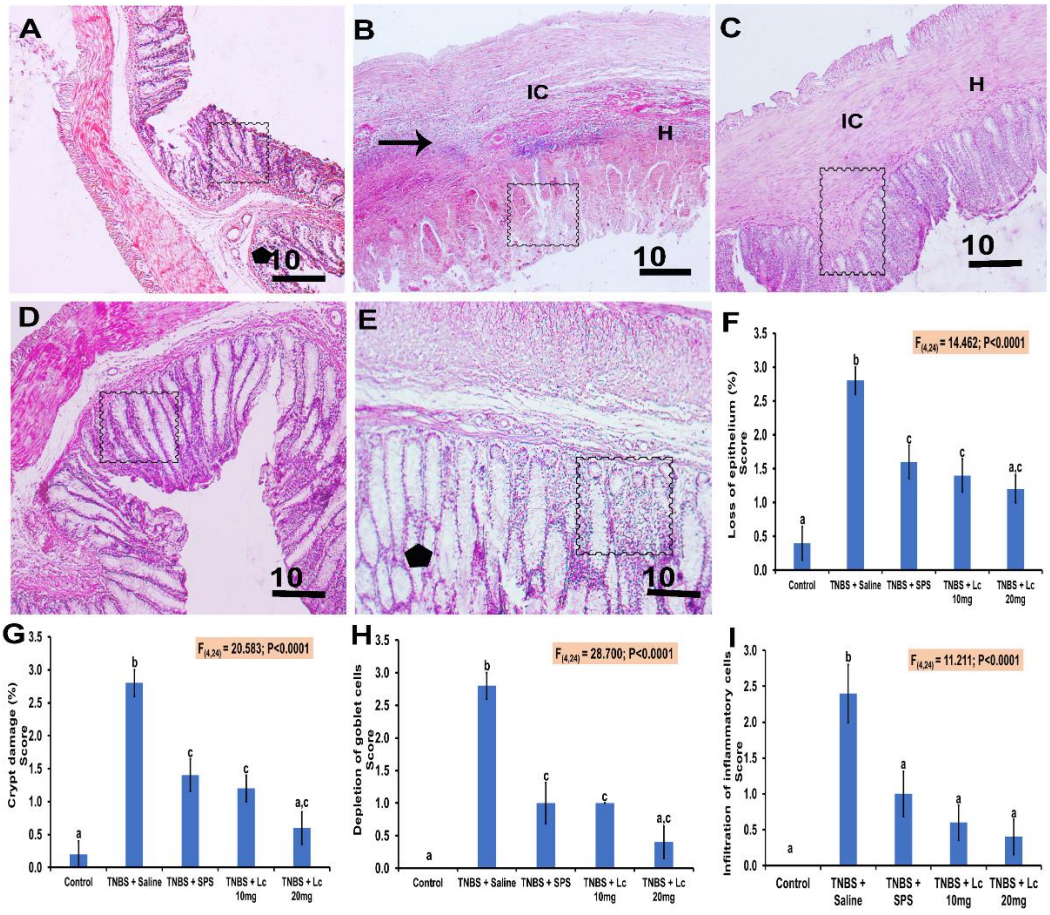

Figure 45: Photomicrographs of sections of colons from five experimental groups in rats stained with H&E (X10 magnification). Colon microscopic image of (A) Control rat with intact epithelial and mucosal layer (ML);(B) TNBS induced rat with extensive hemorrhage (H), including inflammatory cell (IC) infiltration, edema (E), and the complete destruction of ML architecture; (C) TNBS + SPS, post-treated rat with IC infiltration and E, but with intact ML; (D) TNBS + Lc 10mg and (E) TNBS

+ Lc 20mg post-treated rat showed submucosa and mucosa layer of normal aspect similar to the control group. (F, G, H & I) Histopathological score (%) showing loss of epithelium, crypt damage, depletion of goblet cells and infiltration of inflammatory cells.

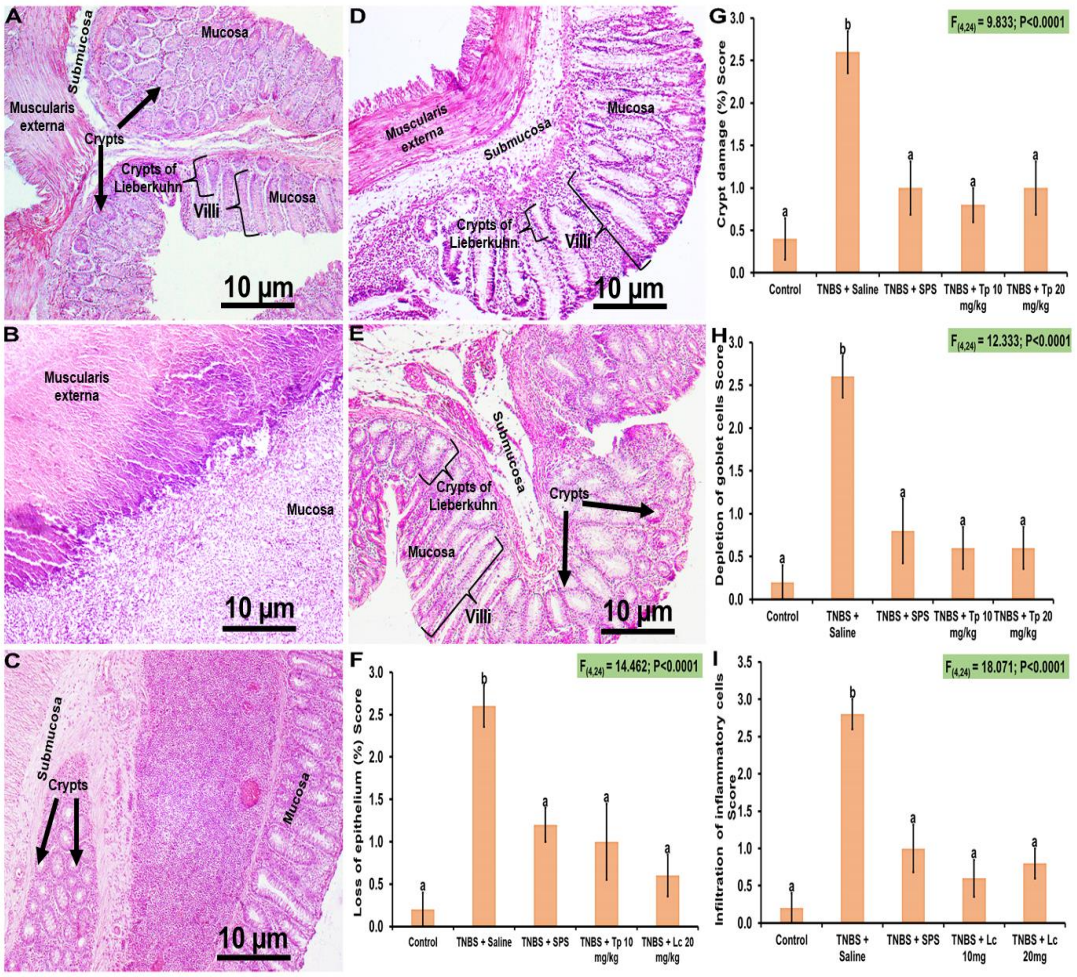

Figure 46: Photomicrographs of sections of colons from five experimental groups in rats stained with H&E (X10 magnification). Colon microscopic image of (A) Control rat with intact epithelial and mucosal layer (ML);(B) TNBS induced rat with extensive hemorrhage (H), including inflammatory cell (IC) infiltration, edema (IE), and the complete destruction of ML architecture; (C) TNBS + SPS, post-treated rat with IC infiltration and E, but with intact ML; (D) TNBS + Tp 10mg and (E) TNBS

+ Tp 20mg post-treated rat showed submucosa and mucosa layer of normal aspect similar to the control group. Submucosa is largely unremarkable.

Figure 46 provides photomicrographs of colon sections stained with hematoxylin and eosin (H&E) from five experimental groups in rats, along with corresponding histopathological descriptions. Control group (Figure 46 A) shows the colon section from the control rat, displaying intact epithelial and mucosal layers (ML). The description likely indicates minimal to no damage to the colon tissue. TNBS-Induced group (Figure 46 B) displays the colon section from the TNBS-induced rat, characterized by extensive hemorrhage (H), inflammatory cell (IC) infiltration, edema (IE), and complete destruction of ML architecture. The description suggests significant damage to the colon tissue, indicative of TNBS-induced colitis. TNBS + SPS Group (Figure 46 C) depicts the colon section from the TNBS + SPS (Sulfasalazine) post-treated rat, showing IC infiltration and E, but with intact ML. The description suggests moderate damage to the colon tissue, with some preservation of ML architecture due to sulfasalazine treatment. TNBS + Tp 10mg (Figure 31 D) and TNBS + Tp 20mg Groups (Figure 46 E) show colon sections from TNBS + Tp (*Trevesia palmata*) post-treated rats, displaying submucosa and mucosa layers with a normal aspect similar to the control group (Figure 46 A). The descriptions indicate minimal damage to the colon tissue in the *Trevesia palmata*-treated groups, with restoration of submucosa and mucosa layers.

5.4.5. Therapeutic efficacy of *Lannea coromandelica* leaf extract (LCLE) and *Trevesia palmata* leaf extract (TPLE) by influencing the levels of protein content in the colon

Figure 47 illustrates the western blot analysis showing effects of *Lannea coromandelica* extract treatment on apoptotic markers in TNBS-treated rats.

Decreased Bcl-2 Expression (Figure 47 A): Bcl-2 is an anti-apoptotic protein. The figure shows that treatment with both doses of *Lannea coromandelica* (Lc 10 mg/kg and Lc 20 mg/kg) resulted in decreased expression of Bcl-2 compared to TNBS-

treated rats. This decrease suggests a downregulation of the anti-apoptotic pathway by *Lannea coromandelica* treatment.

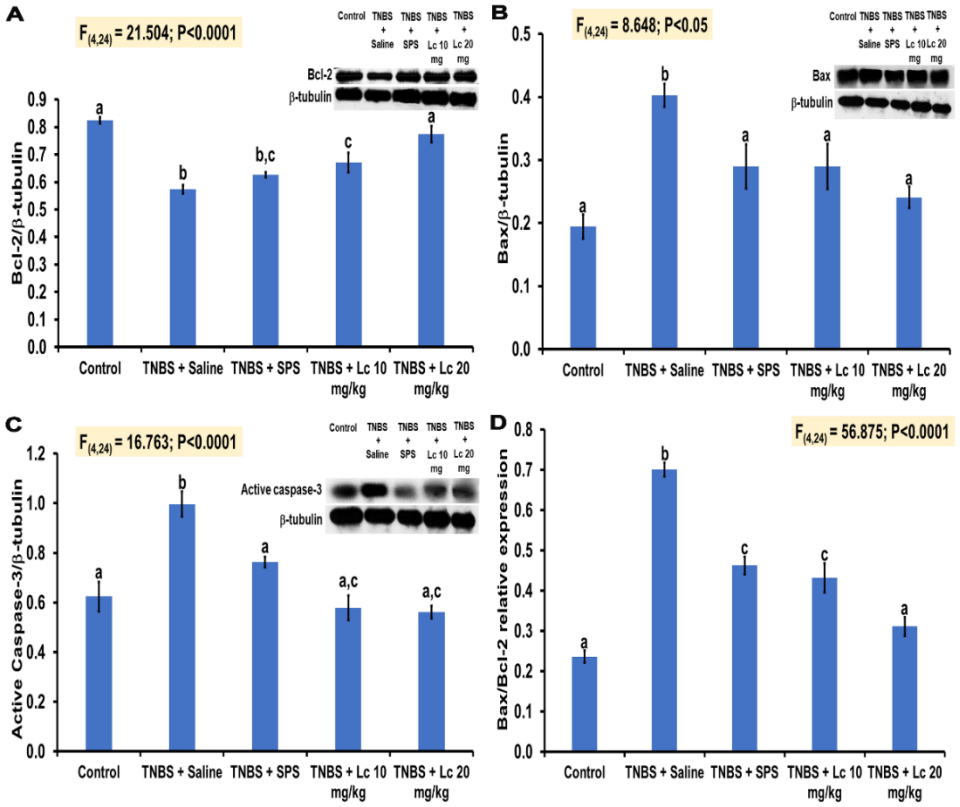

Figure 47: *Lannea coromandelica* – induced suppression of apoptotic markers in TNBS-treated rats. *Lannea coromandelica* (Lc 10 mg/kg) and *Lannea coromandelica* (Lc 20 mg/kg) decreased the high expression of Bax (B) and Active Caspase 3 (C) and decreased the Bcl-2 expression (A). The Bax/Bcl-2 ratio was also decreased by the administration of *Lannea coromandelica* (Lc 10 mg/kg) and *Lannea coromandelica* (Lc 20 mg/kg). Data are represented as Mean ± SEM (n = 5). Statistical comparison was performed using one-way ANOVA followed by Tukey's multiple comparison tests. The bar graph with a different letter means statistically significant difference at $p < 0.05$ and similar letters are not significant. TNBS: Trinitrobenzene sulfonic acid; SPS: Sulfasalazine; Lc: *L. coromandelica*.

Decreased Expression of Bax and Active Caspase 3 (Figure 47 B and C): Bax is a pro-apoptotic protein, and Active Caspase 3 is an executioner caspase involved in apoptosis. The figure demonstrates that both doses of *Lannea coromandelica* significantly decreased the expression of Bax and Active Caspase 3 compared to TNBS-treated rats. This decrease indicates suppression of the apoptotic pathway by *Lannea coromandelica* treatment.

Decreased Bax/Bcl-2 Ratio (Figure 47 D): The ratio of Bax to Bcl-2 is often used as an indicator of apoptosis susceptibility. The figure shows that *Lannea coromandelica* treatment reduced the Bax/Bcl-2 ratio compared to TNBS-treated rats. This reduction suggests a shift towards a less apoptotic-prone state in the colon tissue following *Lannea coromandelica* treatment.

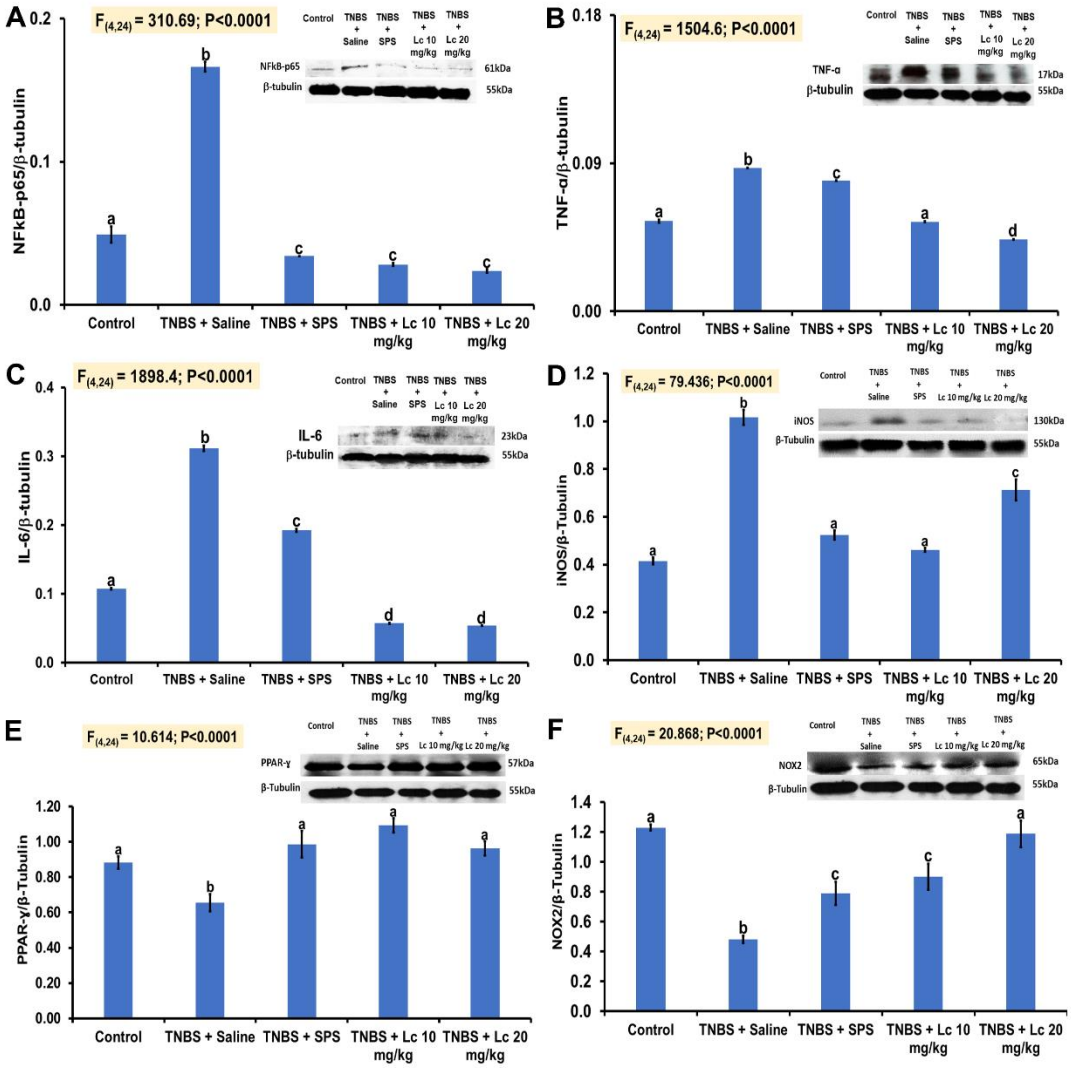

Figure 48: *Lannea coromandelica* – induced suppression of inflammatory parameter in TNBS-treated rats. *Lannea coromandelica* (Lc 10 mg/kg) and Lannea coromandelica (Lc 20 mg/kg) decreased the high expression of TNF alpha (B), IL-6 (C) and iNOS (D) expression. *Lannea coromandelica* reduced the increase in NFkB-p65 (A) phosphorylation and inducible nitric oxide synthase (iNOS) (D) protein expression in TNBS-treated rats. *Lannea coromandelica* also increased the transcription factor PPAR gamma (E) and NOX2 (F) NADPH oxidase protein expression by the administration of *Lannea coromandelica* (Lc 10 mg/kg) and *Lannea coromandelica* (Lc 20 mg/kg). Data are represented as Mean ± SEM (n = 5). Statistical comparison was performed using one-way ANOVA followed by Tukey's multiple comparison tests. The bar graph with a different letter means statistically

significant difference at $p < 0.05$ and similar letters are not significant. TNBS: Trinitrobenzene sulfonic acid; SPS: Sulfasalazine; Lc: *Lannea coromandelica*

Figure 48 illustrates the western blot analysis showing effects of *Lannea coromandelica* extract treatment on inflammatory parameters in TNBS-treated rats.

Decreased Expression of TNF alpha, IL-6, and iNOS (Figure 48 B, C, and D): TNF alpha, IL-6, and iNOS are pro-inflammatory mediators. The figure shows that treatment with both doses of *Lannea coromandelica* (Lc 10 mg/kg and Lc 20 mg/kg) resulted in decreased expression of TNF alpha, IL-6, and iNOS compared to TNBS-treated rats. This decrease suggests a suppression of the inflammatory response by *Lannea coromandelica* treatment.

Reduced NFkB-p65 Phosphorylation (Figure 48 A): NFkB-p65 is a transcription factor involved in the expression of pro-inflammatory genes. The figure demonstrates that *Lannea coromandelica* treatment reduced the phosphorylation of NFkB-p65 compared to TNBS-treated rats. This reduction suggests inhibition of the NFkB signaling pathway, which plays a central role in inflammation.

Increased Expression of PPAR gamma and NOX2 (Figure 48 E and F): PPAR gamma is a nuclear receptor that regulates inflammation and metabolism. The figure shows that *Lannea coromandelica* treatment increased the expression of PPAR gamma compared to TNBS-treated rats. NOX2 is a subunit of NADPH oxidase, which generates reactive oxygen species (ROS) involved in inflammation. The figure demonstrates that *Lannea coromandelica* treatment increased the expression of NOX2 compared to TNBS-treated rats. These increases suggest potential anti-inflammatory and antioxidant effects of *Lannea coromandelica* treatment.

5.5. DISCUSSION

UC induction led to a significant decrease in body weight and food consumption, indicating its adverse effects on the rats' overall health and well-being. Sulfasalazine (SPS) treatment resulted in a significant increase in body weight and food consumption compared to the TNBS-treated groups, suggesting its protective or therapeutic effect against UC. Both LCLE and TPLE treatments showed even greater increases in body weight and food consumption compared to TNBS and SPS-treated groups, indicating potentially enhanced efficacy in mitigating UC-induced weight loss and appetite reduction (Motavallian-Naeini et al., 2012).

UC induction led to a significant decrease in water consumption, indicating reduced thirst or water intake, possibly related to the development of UC. SPS, LCLE, and TPLE treatments all showed significant increases in water consumption compared to the TNBS-treated group, suggesting their effectiveness in promoting hydration and potentially counteracting UC-associated reduced water intake (Adamkova et al., 2022). TNBS induction resulted in a significant increase in the colon weight to length ratio, indicating inflammation or other pathological changes associated with UC which is in correlation to previous studies (Mandlik et al., 2021). SPS, LCLE, and TPLE treatments all showed significant decreases in the colon weight to length ratio compared to the TNBS-treated group, suggesting their effectiveness in reducing inflammation or other pathological changes associated with UC (Figure 30 and 31 D). SPS and LCLE treatments at both 10 mg/kg and 20 mg/kg doses effectively reduced ulcer area and ulcer index in TNBS-induced UC in rats. LCLE treatment at 20 mg/kg showed the highest percentage inhibition, indicating its potential as a therapeutic agent for UC. SPS and both LCLE and TPLE treatments effectively decreased DAI scores compared to the TNBS group, suggesting improvements in weight loss, stool consistency, and possibly rectal bleeding. The lack of significant changes in DAI scores in the LCLE and TPLE treated groups compared to the SPS treated group indicates comparable effectiveness in reducing UC symptoms. SPS, LCLE, and TPLE treatments effectively attenuated the severity of colitis symptoms induced by TNBS, as evidenced by significant decreases in macroscopic scores

compared to the TNBS group. SPS, LCLE, and TPLE treatments achieved similar levels of efficacy in reducing colitis symptoms, as indicated by no significant differences in macroscopic scores between these treatment groups.

Overall, these findings suggest that SPS, LCLE, and TPLE treatments hold promise as therapeutic options for UC, with potential efficacy in reducing weight loss, improving food and water intake, reducing inflammation, and ameliorating other symptoms associated with UC.

The provided data elucidates the effects of *Lannea coromandelica* and *Trevesia palmata* methanolic extracts on various inflammatory markers in the context of TNBS-induced colitis, shedding light on their potential as therapeutic agents for inflammatory bowel diseases like ulcerative colitis (UC). Treatment with *Lannea coromandelica* led to decreased MPO activity, indicating reduced neutrophil infiltration and inflammation in the colon. The plant extract suppressed levels of IL-6 and IL-1, indicating a dampened pro-inflammatory response in the colon tissue. *Lannea coromandelica* treatment also significantly increased IL-10 levels, suggesting an enhancement of anti-inflammatory responses.

Overall, these findings suggest that *Lannea coromandelica* extract exerts protective effects against inflammation by modulating various inflammatory markers, making it a potential therapeutic candidate for UC.

Similar to *Lannea coromandelica*, *Trevesia palmata* treatment reduced MPO activity, indicating decreased neutrophil infiltration and inflammation. *Trevesia palmata* treatment resulted in decreased levels of IL-6 and IL-1, indicating suppression of pro-inflammatory responses. Treatment with *Trevesia palmata* significantly increased IL-10 levels, suggesting augmentation of anti-inflammatory responses. Moreover, *Trevesia palmata* extract increased total antioxidant activity, indicating its ability to scavenge free radicals and reduce oxidative stress, which is often associated with inflammation in UC. Overall, these findings highlight the anti-inflammatory properties of *Trevesia palmata* extract, making it a potential therapeutic agent for UC.

Both *Lannea coromandelica* and *Trevesia palmata* extracts exhibited negative correlations between MPO activity and antioxidant markers, implying that increased neutrophil activity is associated with reduced antioxidant capacity and elevated oxidative stress.

Higher MPO activity was associated with reduced levels of IL-10, indicating a diminished anti-inflammatory response in the presence of heightened neutrophil activity (Khan et al., 2018). Increased MPO activity correlated positively with higher levels of pro-inflammatory cytokines and mediators, indicating a direct association between neutrophil activity and inflammation severity (Lockhart et al., 2022). These correlation analyses further support the notion that neutrophil activity plays a crucial role in modulating inflammatory responses in UC and that antioxidant and anti-inflammatory interventions can potentially mitigate inflammation and oxidative stress associated with the disease (Sahoo et al., 2023). In conclusion, both *Lannea coromandelica* and *Trevesia palmata* extracts demonstrate promising anti-inflammatory effects in TNBS-induced colitis, suggesting their potential as therapeutic agents for UC. These extracts modulate various inflammatory markers, including neutrophil activity, pro-inflammatory cytokines, and anti-inflammatory responses, while also enhancing antioxidant capacity. The correlation analyses further underscore the intricate interplay between inflammation, oxidative stress, and immune responses in UC pathogenesis.

The results outline the therapeutic efficacy of *Lannea coromandelica* leaf extract (LCLE) and *Trevesia palmata* leaf extract (TPLE) in mitigating oxidative stress, improving antioxidant status, influencing histological changes in the colon, and modulating protein expression related to apoptosis and inflammation in TNBS-induced colitis in rats. Both LCLE and TPLE significantly reduced lipid peroxidation and nitric oxide levels in the colon tissue of TNBS-induced colitis rats, indicating a decrease in oxidative damage and nitrosative stress. These extracts increased the activity of several antioxidant enzymes including Superoxide Dismutase (SOD), Glutathione (GSH), Catalase (CAT), and Glutathione Peroxidase (GPx), suggesting enhancement of the antioxidant defense system to mitigate oxidative stress and

inflammation. The observed effects were dose-dependent, indicating a potential for dose optimization in therapeutic interventions (Alam et al., 2017 and Manoharan et al., 2023).

Treatment with both LCLE and TPLE resulted in the restoration of epithelial and mucosal layers in the colon tissue of TNBS-induced colitis rats, as evidenced by histopathological assessments. LCLE and TPLE-treated groups exhibited minimal damage to the colon tissue, comparable to the control group, indicating potential therapeutic benefits in preserving colon integrity and mitigating inflammation-induced tissue damage. LCLE treatment led to decreased expression of anti-apoptotic protein Bcl-2 and pro-apoptotic proteins Bax and Active Caspase 3, suggesting a suppression of the apoptotic pathway. Both LCLE and TPLE treatment resulted in decreased expression of pro-inflammatory markers TNF alpha, IL-6, and iNOS, indicating suppression of the inflammatory response. LCLE treatment also reduced NFkB-p65 phosphorylation, suggesting inhibition of the NFkB signaling pathway involved in inflammation. Additionally, LCLE treatment increased the expression of anti-inflammatory nuclear receptor PPAR gamma and NOX2, indicating potential anti-inflammatory and antioxidant effects (Qian et al., 2022; Klimentova et al., 2021; Giridharan et al., 2018 and Liu et al., 2017).

Overall, the data suggests that both LCLE and TPLE exhibit therapeutic potential in ameliorating TNBS-induced colitis in rats by reducing oxidative stress, improving antioxidant status, preserving colon histology, and modulating protein expression related to apoptosis and inflammation. These findings highlight the promising prospects of LCLE and TPLE as natural therapeutic agents for inflammatory bowel diseases like colitis. Further research is warranted to elucidate their mechanisms of action and potential translation to clinical settings.

5.7. SUMMARY

- The findings suggest that SPS, LCLE, and TPLE treatments hold promise as therapeutic options for UC, with potential efficacy in reducing weight loss, improving food and water intake, reducing inflammation, and ameliorating other symptoms associated with UC.
- The provided data elucidates the effects of *Lannea coromandelica* and *Trevesia palmata* methanolic extracts on various inflammatory markers in the context of TNBS-induced colitis, shedding light on their potential as therapeutic agents for inflammatory bowel diseases like ulcerative colitis (UC).
- These extracts modulate various inflammatory markers, including neutrophil activity, pro-inflammatory cytokines, and anti-inflammatory responses, while also enhancing antioxidant capacity.
- The results outline the therapeutic efficacy of *Lannea coromandelica* leaf extract (LCLE) and *Trevesia palmata* leaf extract (TPLE) in mitigating oxidative stress, improving antioxidant status, influencing histological changes in the colon, and modulating protein expression related to apoptosis and inflammation in TNBS-induced colitis in rats.
- Both LCLE and TPLE significantly reduced lipid peroxidation and nitric oxide levels in the colon tissue of TNBS-induced colitis rats, indicating a decrease in oxidative damage and nitrosative stress.

5.8. CONCLUSION

In conclusion, the findings presented in the provided data highlight the potential therapeutic efficacy of SPS, Lannea coromandelica leaf extract (LCLE), and Trevesia palmata leaf extract (TPLE) as treatment options for ulcerative colitis (UC). These treatments demonstrate promising results in reducing weight loss, improving food and water intake, reducing inflammation, and ameliorating other symptoms associated with UC.

Furthermore, the data elucidates the effects of LCLE and TPLE on various inflammatory markers in the context of TNBS-induced colitis, suggesting their

potential as therapeutic agents for inflammatory bowel diseases like UC. These extracts modulate inflammatory markers such as neutrophil activity, pro-inflammatory cytokines, and anti-inflammatory responses, while also enhancing antioxidant capacity.

Moreover, both LCLE and TPLE show significant potential in mitigating oxidative stress by reducing lipid peroxidation and nitric oxide levels in the colon tissue of TNBS-induced colitis rats. This indicates a decrease in oxidative damage and nitrosative stress, which are associated with inflammation and tissue damage in colitis.

Overall, the therapeutic efficacy of LCLE and TPLE extends to influencing histological changes in the colon and modulating protein expression related to apoptosis and inflammation in TNBS-induced colitis in rats. These findings suggest the promising prospects of LCLE and TPLE as natural therapeutic agents for UC, warranting further research to elucidate their mechanisms of action and potential clinical translation.

5.9. REFERENCES

Aboul-Soud, M. A., Al-Othman, A. M., El-Desoky, G. E., Al-Othman, Z. A., Yusuf, K., Ahmad, J., & Al-Khedhairy, A. A. (2011). Hepatoprotective effects of vitamin E/selenium against malathion-induced injuries on the antioxidant status and apoptosis-related gene expression in rats. The Journal of toxicological sciences, 36(3), 285-296.

Adamkova, P., Hradicka, P., Kupcova Skalnikova, H., Cizkova, V., Vodicka, P., Farkasova Iannaccone, S., ... & Demeckova, V. (2022). Dextran Sulphate Sodium Acute Colitis Rat Model: A Suitable Tool for Advancing Our Understanding of Immune and Microbial Mechanisms in the Pathogenesis of Inflammatory Bowel Disease. Veterinary Sciences, 9(5), 238.

Alam, M. B., Kwon, K. R., Lee, S. H., & Lee, S. H. (2017). Lannea coromandelica (houtt.) merr. induces heme oxygenase 1 (HO-1) expression and reduces oxidative stress via the p38/c-jun n-terminal kinase–nuclear factor erythroid 2-related factor 2 (p38/JNK–Nrf2)-mediated antioxidant pathway. International journal of molecular sciences, 18(2), 266.

Al-Khayri, J. M., Sahana, G. R., Nagella, P., Joseph, B. V., Alessa, F. M., & Al-Mssallem, M. Q. (2022). Flavonoids as potential anti-inflammatory molecules: A review. Molecules, 27(9), 2901.

Antoniou, E., Margonis, G. A., Angelou, A., Pikouli, A., Argiri, P., Karavokyros, I., Papalois, A. & Pikoulis, E. (2016). The TNBS-induced colitis animal model: An overview. Annals of medicine and surgery, 11, 9-15.

Antoniou, E., Margonis, G. A., Angelou, A., Pikouli, A., Argiri, P., Karavokyros, I., ... & Pikoulis, E. (2016). The TNBS-induced colitis animal model: An overview. Annals of medicine and surgery, 11, 9-15.

Arnhold, J. (2020). The dual role of myeloperoxidase in immune response. International Journal of Molecular Sciences, 21(21), 8057.

Asakura, H., & Kitahora, T. (2018). Antioxidants and polyphenols in inflammatory bowel disease: ulcerative colitis and Crohn disease. In Polyphenols: prevention and treatment of human disease (pp. 279-292). Academic Press.

Asakura, H., & Kitahora, T. (2018). Antioxidants and polyphenols in inflammatory bowel disease: ulcerative colitis and Crohn disease. In Polyphenols: prevention and treatment of human disease (pp. 279-292). Academic Press.

Ashique, S., Mishra, N., Garg, A., Sibuh, B. Z., Taneja, P., Rai, G., Djearamane, S., Wong, L.S., Al-Dayan, N., Roychoudhury, S., Kesari, K.K. & Gupta, P. K. (2023). Recent updates on correlation between reactive oxygen species and synbiotics for effective management of ulcerative colitis. Frontiers in nutrition, 10.

Au, K. M., Wilson, J. E., Ting, J. P. Y., & Wang, A. Z. (2023). An injectable subcutaneous colon-specific immune niche for the treatment of ulcerative colitis. Nature Biomedical Engineering, 1-23.

Biswas, S. K. (2016). Does the interdependence between oxidative stress and inflammation explain the antioxidant paradox?. Oxidative medicine and cellular longevity, 2016.

Bradford, M. M. (1976). A rapid and sensitive method for the quantitation of microgram quantities of protein utilizing the principle of protein-dye binding. Analytical biochemistry, 72(1-2), 248-254.
c A., Khan, A., Ahmad, I., Alghamdi, S., Rajab, B. S., Babalghith, A. O., ... & Islam, M. R. (2022). Flavonoids a bioactive compound from medicinal plants and its therapeutic applications. BioMed research international, 2022.
Chami, B., Ahmad, G., Schroder, A., San Gabriel, P., & Witting, P. (2021). The role of myeloperoxidase and neutrophil extracellular traps in the pathogenesis of inflammatory bowel disease. Gastroenterology, 160(3), S5-S6.
Chaudhary, P., Janmeda, P., Docea, A. O., Yeskaliyeva, B., Abdull Razis, A. F., Modu, B., ... & Sharifi-Rad, J. (2023). Oxidative stress, free radicals and antioxidants: Potential crosstalk in the pathophysiology of human diseases. Frontiers in chemistry, 11, 1158198.
De Tommasi, N., Autore, G., Bellino, A., Pinto, A., Pizza, C., Sorrentino, R., & Venturella, P. (2000). Antiproliferative Triterpene Saponins from Trevesia p almata. Journal of natural products, 63(3), 308-314.
Derkacz, A., Olczyk, P., & Komosinska-Vassev, K. (2018). Diagnostic markers for nonspecific inflammatory bowel diseases. Disease markers, 2018.
Duan, L., Cheng, S., Li, L., Liu, Y., Wang, D., & Liu, G. (2021). Natural anti-inflammatory compounds as drug candidates for inflammatory bowel disease. Frontiers in Pharmacology, 12, 684486.
Fabian, O., & Bajer, L. (2022). Histopathological assessment of the microscopic activity in inflammatory bowel diseases: What are we looking for?. World Journal of Gastroenterology, 28(36), 5300.
Fiocchi, C. (2015). Inflammatory bowel disease pathogenesis: where are we?. Journal of gastroenterology and hepatology, 30, 12-18.
Garcia-Sanchez, A., Miranda-Díaz, A. G., & Cardona-Muñoz, E. G. (2020). The role of oxidative stress in physiopathology and pharmacological treatment with pro-and antioxidant properties in chronic diseases. Oxidative Medicine and Cellular Longevity, 2020.
Giridharan, S., & Srinivasan, M. (2018). Mechanisms of NF-κB p65 and strategies for therapeutic manipulation. Journal of inflammation research, 407-419.
Goyal, N., Rana, A., Ahlawat, A., Bijjem, K. R. V., & Kumar, P. (2014). Animal models of inflammatory bowel disease: a review. Inflammopharmacology, 22(4), 219-233.
Guo, M., & Wang, X. (2023). Pathological mechanism and targeted drugs of ulcerative colitis: A review. Medicine, 102(37), e35020.
Hambardikar, V. R., & Mandlik, D. S. (2022). Protective effect of naringin ameliorates TNBS-induced colitis in rats via improving antioxidant status and pro-inflammatory cytokines. Immunopharmacology and Immunotoxicology, 44(3), 373-386.
Hansberry, D. R., Shah, K., Agarwal, P., & Agarwal, N. (2017). Fecal myeloperoxidase as a biomarker for inflammatory bowel disease. Cureus, 9(1).
Huang, S. H., Wu, C. H., Chen, S. J., Sytwu, H. K., & Lin, G. J. (2020). Immunomodulatory effects and potential clinical applications of dimethyl sulfoxide. Immunobiology, 225(3), 151906.

Hussain, M. I., Shill, S., Barman, S. K., & Jahan, K. (2021). Assessment of preliminary phytochemical screening, cytotoxic and hypoglycemic activity of lannea coromandelica bark extract. Pharmacologyonline, 2, 89-96.
Islam, F., Mitra, S., Nafady, M. H., Rahman, M. T., Tirth, V., Akter, A., ... & El-Kholy, S. S. (2022). Neuropharmacological and antidiabetic potential of lannea coromandelica (houtt.) merr. Leaves extract: an experimental analysis. Evidence-Based Complementary and Alternative Medicine, 2022.
Jarmakiewicz-Czaja, S., Ferenc, K., & Filip, R. (2023). Antioxidants as protection against reactive oxidative stress in inflammatory bowel disease. Metabolites, 13(4), 573.
Jeremy, M., Gurusubramanian, G., & Roy, V. K. (2017). Localization pattern of visfatin (NAMPT) in d-galactose induced aged rat testis. Annals of Anatomy-Anatomischer Anzeiger, 211, 46-54.
Jomova, K., Raptova, R., Alomar, S. Y., Alwasel, S. H., Nepovimova, E., Kuca, K., & Valko, M. (2023). Reactive oxygen species, toxicity, oxidative stress, and antioxidants: Chronic diseases and aging. Archives of toxicology, 97(10), 2499-2574.
Kakkar, P., Das, B., & Viswanathan, P. N. (1984). A modified spectrophotometric assay of superoxide dismutase.
Kandhare, A. D., Ghosh, P., Ghule, A. E., Zambare, G. N., & Bodhankar, S. L. (2013). Protective effect of Phyllanthus amarus by modulation of endogenous biomarkers and DNA damage in acetic acid induced ulcerative colitis: Role of phyllanthin and hypophyllanthin. Apollo Medicine, 10(1), 87-97.
Khan, A. A., Alsahli, M. A., & Rahmani, A. H. (2018). Myeloperoxidase as an active disease biomarker: recent biochemical and pathological perspectives. Medical sciences, 6(2), 33.
Klimentova, E. A., Suchkov, I.A., Shchulkin, A. V., Glazkova, A. P., Kalinin, R. E. (2021). Expression of Apoptotic Markers Bcl-2 and Bax in the Vascular Wall. Sovrem Tekhnologii Med. 13(2):46-50.
Kumar, V. S., Rajmane, A. R., Adil, M., Kandhare, A. D., Ghosh, P., & Bodhankar, S. L. (2014). Naringin ameliorates acetic acid induced colitis through modulation of endogenous oxido-nitrosative balance and DNA damage in rats. Journal of biomedical research, 28(2), 132.
Lasa, J. S., Olivera, P. A., Danese, S., & Peyrin-Biroulet, L. (2022). Efficacy and safety of biologics and small molecule drugs for patients with moderate-to-severe ulcerative colitis: a systematic review and network meta-analysis. The Lancet Gastroenterology & Hepatology, 7(2), 161-170.
Li, G., Lin, J., Zhang, C., Gao, H., Lu, H., Gao, X., ... & Liu, Z. (2021). Microbiota metabolite butyrate constrains neutrophil functions and ameliorates mucosal inflammation in inflammatory bowel disease. Gut microbes, 13(1), 1968257.
Liu, T., Zhang, L., Joo, D., & Sun, S. C. (2017). NF-κB signaling in inflammation. Signal transduction and targeted therapy, 2(1), 1-9.
Liu, T., Zhang, L., Joo, D., & Sun, S. C. (2017). NF-κB signaling in inflammation. Signal transduction and targeted therapy, 2(1), 1-9.
Lockhart, J. S., & Sumagin, R. (2022). Non-canonical functions of myeloperoxidase in immune regulation, tissue inflammation and cancer. International journal of molecular sciences, 23(20), 12250.

Mandlik, D. S., Mandlik, S. K., & Patel, S. (2021). Protective effect of sarsasapogenin in TNBS induced ulcerative colitis in rats associated with downregulation of pro-inflammatory mediators and oxidative stress. Immunopharmacology and Immunotoxicology, 43(5), 571-583.
Manoharan, A. L., Jagadeesan, G., Nataraj, G., Muniyandi, K., Guruswami, G., Arunachalam, K., & Thangaraj, P. (2023). Efficacy of Trevesia palmata (Roxb. ex Lindl.) Vis. Extract on MG 63 cell lines and arthritis-induced animal models. Journal of Ethnopharmacology, 300, 115742.
Manoharan, A. L., Jagadeesan, G., Nataraj, G., Muniyandi, K., Guruswami, G., Arunachalam, K., & Thangaraj, P. (2023). Efficacy of Trevesia palmata (Roxb. ex Lindl.) Vis. Extract on MG 63 cell lines and arthritis-induced animal models. Journal of Ethnopharmacology, 300, 115742.
McDowell, C., Farooq, U., & Haseeb, M. Continuing Education Activity. (2023). Treasure Island (FL): StatPearls Publishing.
Mizoguchi, E., Low, D., Ezaki, Y., & Okada, T. (2020). Recent updates on the basic mechanisms and pathogenesis of inflammatory bowel diseases in experimental animal models. Intestinal research, 18(2), 151.
Motavallian-Naeini, A., Andalib, S., Rabbani, M., Mahzouni, P., Afsharipour, M., & Minaiyan, M. (2012). Validation and optimization of experimental colitis induction in rats using 2, 4, 6-trinitrobenzene sulfonic acid. Research in pharmaceutical sciences, 7(3), 159.
Ohkawa, H., Ohishi, N., & Yagi, K. (1979). Assay for lipid peroxides in animal tissues by thiobarbituric acid reaction. Analytical biochemistry, 95(2), 351-358.
Panche, A. N., Diwan, A. D., & Chandra, S. R. (2016). Flavonoids: an overview. Journal of nutritional science, 5, e47.
Qian, S., Wei, Z., Yang, W., Huang, J., Yang, Y., & Wang, J. (2022). The role of BCL-2 family proteins in regulating apoptosis and cancer therapy. Frontiers in oncology, 12, 985363.
Rachmilewitz, D., Simon, P. L., Schwartz, L. W., Griswold, D. E., Fondacaro, J. D., & Wasserman, M. A. (1989). Inflammatory mediators of experimental colitis in rats. Gastroenterology, 97(2), 326-337.
Rahman, I., Kode, A., & Biswas, S. K. (2006). Assay for quantitative determination of glutathione and glutathione disulfide levels using enzymatic recycling method. Nature protocols, 1(6), 3159-3165.
Rahman, K. H., Nandi, J. K., Sultana, S., Rahman, S., Hossan, S., & Rahmatullah, M. (2014). Phytochemical screening, antihyperglycemic and analgesic activity studies with methanol extract of Trevesia palmata leaves. World J Pharm Pharmaceut Sci, 3(10), 91-101.
Rajput, V. D., Harish, Singh, R. K., Verma, K. K., Sharma, L., Quiroz-Figueroa, F. R., Meena, M., Gour, V.S., Minkina, T., Sushkova, S. & Mandzhieva, S. (2021). Recent developments in enzymatic antioxidant defence mechanism in plants with special reference to abiotic stress. Biology, 10(4), 267.
References
Sadar, S. S., Vyawahare, N. S., & Bodhankar, S. L. (2016). Ferulic acid ameliorates TNBS-induced ulcerative colitis through modulation of cytokines, oxidative stress, iNOs, COX-2, and apoptosis in laboratory rats. EXCLI journal, 15, 482.

Sahoo, D. K., Heilmann, R. M., Paital, B., Patel, A., Yadav, V. K., Wong, D., & Jergens, A. E. (2023). Oxidative stress, hormones, and effects of natural antioxidants on intestinal inflammation in inflammatory bowel disease. Frontiers in Endocrinology, 14, 1217165.
Sahoo, D. K., Heilmann, R. M., Paital, B., Patel, A., Yadav, V. K., Wong, D., & Jergens, A. E. (2023). Oxidative stress, hormones, and effects of natural antioxidants on intestinal inflammation in inflammatory bowel disease. Frontiers in Endocrinology, 14, 1217165.
Sazuka, Y., Tanizawa, H., & Takino, Y. (1989). Effect of adriamycin on the activities of superoxide dismutase, glutathione peroxidase and catalase in tissues of mice. Japanese journal of cancer research, 80(1), 89-94.
Sinha, A. K. (1972). Colorimetric assay of catalase. Analytical biochemistry, 47(2), 389-394.
Sullivan Jr, D. W., & Gad, S. E. (2023). Dimethyl sulfoxide (DMSO). Reference Module in Biomedical Sciences, Elsevier. ISBN 9780128012383.
Swathi, S., & Lakshman, K. (2022). Photochemistry and Pharmacological Bio-Activities of Lannea coromandelica: A Review. Innovare Journal of Medical Science, 10(5).
Thao, L. T. T., Quyen, D., Vu, D. B., Tai, B. H., & Van Kiem, P. (2018). New acetylated saponins from the leaves of Trevesia palmata. Natural Product Communications, 13(4), 1934578X1801300407.
Tian, T., Wang, Z., & Zhang, J. (2017). Pathomechanisms of oxidative stress in inflammatory bowel disease and potential antioxidant therapies. Oxidative medicine and cellular longevity, 2017.
Tungmunnithum, D., Thongboonyou, A., Pholboon, A., & Yangsabai, A. (2018). Flavonoids and other phenolic compounds from medicinal plants for pharmaceutical and medical aspects: An overview. Medicines, 5(3), 93.
Ungaro, R., Colombel, J. F., Lissoos, T., & Peyrin-Biroulet, L. (2019). A treat-to-target update in ulcerative colitis: a systematic review. Official journal of the American College of Gastroenterology| ACG, 114(6), 874-883.
Wan, Y., Yang, L., Jiang, S., Qian, D., & Duan, J. (2022). Excessive apoptosis in ulcerative colitis: crosstalk between apoptosis, ROS, ER stress, and intestinal homeostasis. Inflammatory bowel diseases, 28(4), 639-648.

BRIEF BIO-DATA OF THE CANDIDATE

Name: Bidanchi R. Momin

Father's Name: Late Siljeng Ch. Marak

Mother's Name: Mrs. Angelitha R. Momin

Date of Birth: 2nd August 1993

Gender: Female

Nationality: Indian

Category: Tribal

Contact No.: 9774284489/7005475274

Email ID: bidanrema@gmail.com

Permanent Address: Upper Wadanang, Tura, West Garo Hills, Meghalaya - 794002

Address for correspondence: Chhawkhlei Women's Hostel, Mizoram University, Tanhril, Aizawl, Mizoram - 796004

Educational qualifications:

Exam passed	Board/University	Year of Passing	Subject	Division	Percentage
SSLC	Meghalaya Board of School Education	2009	General with Garo (MIL)	First	69.83 %
HSSLC	Meghalaya Board of School Education	2011	Science	Second	56 %
B.Sc.	NEHU	2014	Zoology	Second	48.87 %
M.Sc.	Mizoram University	2016	Zoology	First	62.3 %
M.Phil.	Mizoram University	2018	Zoology	Distinction	81.6 %

List of Conferences and Workshops Attended and Participated

Sl No.	Conferences and Workshops Attended and Participated	Date
1.	Participated in the "National Workshop on National Seminar on Animals Handling, Maintenance and Care", organized by Advanced level State Biotech Hub, Department of Biotechnology, Mizoram University.	26th March, 2018
2.	Participated in an oral presentation at the International Conference on Biodiversity, Environment and Human Health: Innovations and Emerging Trends (BEHIET 2018) organized by School of Life Sciences, Mizoram University, Aizawl and Association of Biotechnology and Pharmacy (ABAP), India, on the topic entitled, "Protective effects of Ellagic acid against Cadmium-induced testicular injury via steroidogenic pathway in Wistar albino rats".	12th – 14th November, 2018
3.	Participated in the "National Workshop on Bioinformatics for Zoologist" organized by Bioinformatics Infrastructure Facility (BIF), Department of Biotechnology, Mizoram University, sponsored by Department of Biotechnology (DBT), New Delhi.	26th – 31st August, 2019
4.	Participated in webinar organized by the School of Life Sciences, Mizoram University, Aizawl, India on the topic "Mending the Broken Heart: Evolution of Novel Therapeutic Approach".	18th June, 2020
5.	Participated in International E-Conference on New Frontiers in Science and Technology, organized by Research Institute of Science and Technology (RIST), Manipur, India.	9th - 11th July, 2020
6.	Participated in UGC-STRIDE Refresher course (Multidisciplinary) on "Research Methodology: Research Ethics, Methods, Skills, Writing and communication", organized by Mizoram University, Aizawl, Mizoram, India sponsored by UGC, New Delhi.	19th August – 1st September, 2020
7.	Participated in Two days Online Skill Development Program on "Data Interpretation of GCMS and LCMS", organized by Cytogene Research and Development	26th-27th March, 2022
8.	Participation in One-Week Training Program on "Instruments in Biotechnology: Theories and Practices", under Synergistic Training Program Utilizing the Science and Technology Infrastructure (STUTI), An Initiative of Department of Science & Technology (DST), Govt. of India organized by Department of Biotechnology, School of Life Sciences, Mizoram University.	30th May – 5th June, 2022

9.	Participated in an oral presentation at the International Conference on "Bioresources & Bioeconomy" (ICBB-2022) organized by Department of Botany, Nagaland University, Lumami, Nagaland, India in collaboration with Nagaland Forest Management Project, Department of Environment, Forest and Climate Change, Govt. of Nagaland, India, on the topic entitled, "Evaluation of Anti-Inflammatory Effects of Methanolic Leaf Extract of *Lannea coromandelica* on TNBS-Induced Ulcerative Colitis in Rats".	19th – 21st September, 2022
10.	Participated as a speaker giving oral presentation in the 3rd International Hybrid Conference on Traditional and Alternative Medicine organized by Conference Mind, Goa, India on the topic entitled, "The Anti-Oxidant and Anti-Inflammatory Effects of *Trevesia palmata* Methanolic Extract on TNBS-induced Ulcerative Colitis in Rats".	17th – 18th November, 2022
11.	Participated in an oral presentation at the International Conference on Environment and Sustainable Development (ICESD 2022) organized by NEHU, Tura Campus, Meghalaya, India under the aegis of Biotech KISAN Hub, North-Eastern Hill University, Tura Campus, Meghalaya, India in Collaboration with Department of Computer Application, North-Eastern Hill University, Tura Campus, Meghalaya, India, on the topic entitled, "*Lannea coromandelica* Alleviate Intestinal Inflammation, Oxidative Stress and Apoptosis Resulted in Ulcerative Colitis".	24th – 25th November, 2022
12.	Participated in the International Workshop on "Nanopore Sequencing and Data Analysis: Opportunities for Rapid Biodiversity and Biosurveillance Programs and Local Capacity Buildings", organized by Department of Zoology, Mizoram University, Aizawl, Mizoram sponsored by Global Initiative for Academic Networks, Ministry of Education, Govt. of India.	16th – 29th March, 2023
13.	Participated in "National Workshop on "The Value and Interconnections of Human, Animal, Plant and Microorganisms: Metataxonomics and Metagenomics Approach", organized by Department of Zoology, Mizoram University, Aizawl, Mizoram.	18th – 25th March, 2023
14.	Participated in International Workshop on "Computational Genomics with R: A Hands-On Course on NGS Data Analysis", organized by Department of Zoology, Mizoram University, Aizawl, Mizoram.	22nd – 29th March, 2023

List of Publications

1. Bidanchi, R. M., Roy, V. K., Sanjeev, S., Khushboo, M., & Gurusubramanian, G. (2018). Cadmium toxicity and its effect on testicular dysfunction in male rats. Science & Amp; Technology Journal, 6(1), 62-67. https://doi.org/10.22232/stj.2018.06.01.08

2. Sanjeev, S., Bidanchi, R. M., Murthy, M. K., Gurusubramanian, G., & Roy, V. K. (2019). Influence of ferulic acid consumption in ameliorating the cadmium-induced liver and renal oxidative damage in rats. Environmental Science and Pollution Research, 26(20), 20631-20653.

3. Bidanchi, R. M., Lalrindika, L., Khushboo, M., Bhanushree, B., Dinata, R., Das, M., ... & Gurusubramanian, G. (2022). Antioxidative, anti-inflammatory and anti-apoptotic action of ellagic acid against lead acetate induced testicular and hepato-renal oxidative damages and pathophysiological changes in male Long Evans rats. Environmental Pollution, 302, 119048.

4. Nisa, N., Dinata, R., Arati, C., Abdelgani-Baraka, G. A., Bhanushree, B., Bidanchi, R. M., Bose, M., Saeed, A.L., Abinash, G., Pori, B. and Lalrinzuali, S., Maurya, K., Sonar, I., Vikas, K. R., KRS, S. R., & Gurusubramanian, G. (2023). Computational toxicology and food safety assessment of Parkia timoriana phytoconstituents using quantitative structure-activity relationship (QSAR) modeling approaches. Indian Journal of Biochemistry and Biophysics (IJBB), 60(12), 896-918.

5. Dinata, R., Nisa, N., Arati, C., Rasmita, B., Uditraj, C., Siddhartha, R., ... & Gurusubramanian, G. (2024). Repurposing immune boosting and anti-viral efficacy of Parkia bioactive entities as multi-target directed therapeutic approach for SARS-CoV-2: exploration of lead drugs by drug likeness, molecular docking and molecular dynamics simulation methods. Journal of Biomolecular Structure and Dynamics, 42(1), 43-81.

6. Khushboo, M., Sanjeev, S., Murthy, M. K., Sunitadevi, M., Dinata, R., Bhanushree, B., ... & Gurusubramanian, G. (2023). Dietary phytoestrogen diosgenin interrupts metabolism, physiology, and reproduction of Swiss albino mice: Possible mode of action as an emerging environmental contaminant, endocrine disruptor and reproductive toxicant. Food and Chemical Toxicology, 176, 113798.

7. Nisa, N., Rasmita, B., Arati, C., Uditraj, C., Siddhartha, R., Dinata, R., ... & Gurusubramanian, G. (2023). Repurposing of phyto-ligand molecules from the honey bee products for Alzheimer's disease as novel inhibitors of BACE-1: Small molecule bioinformatics strategies as amyloid-based therapy. Environmental Science and Pollution Research, 30(17), 51143-51169.

8. Lalrinzuali, S., Khushboo, M., Dinata, R., Bhanushree, B., Nisa, N., Bidanchi, R. M., ... & Gurusubramanian, G. (2023). Long-term consumption of fermented pork fat-based diets differing in calorie, fat content, and fatty acid levels mediates oxidative stress, inflammation, redox imbalance, germ cell apoptosis, disruption of steroidogenesis, and testicular dysfunction in Wistar rats. Environmental Science and Pollution Research, 30(18), 52446-52471.

9. Roy, D., Arati, C., Manikandan, B., Abinash, G., Nisa, N., Bhanushree, B., ... & Gurusubramanian, G. (2023). Pharmacological and therapeutic potential of honey bee antimicrobial peptides.

Science and Technology Journal Vol. 6 Issue: 1 January 2018 ISSN: 2321-3388

Cadmium Toxicity and Its Effect on Testicular Dysfunction in Male Rats

Bidanchi R Momin[1]*, Vikas Kumar Roy[2], Sanasam Sanjeev[3], Khushboo Maurya[4] and Guruswami Gurusubramanian[5]

[1,2,3,4,5]Department of Zoology, Mizoram Central University, Aizawl-796004, Mizoram, India
E-mail: *bidanrema@gmail.com

Abstract—Cadmium (Cd) is an inorganic heavy metal which is of significant occupational concern, has been classified as human carcinogen. Administration of Cd in animals results in multiple organ tumorigenesis. Evidences indicate that the oxidative stress plays an important role in Cd carcinogenesis. Cd exposure has been related to human diseases such as cancer and studies have shown the adverse effects of different doses of cadmium chloride ($CdCl_2$) on reproductive functions in male. Studies have shown that $CdCl_2$-induced testicular and spermatozoa toxicity associated with the oxidative stress in male downregulating the apoptotic genes and up regulating gonadotropins and anti-apoptotic genes. $CdCl_2$ toxicity significantly decreases the reproductive organ weights, epididymal sperm concentration, motility and B-cell lymphoma 2 (*BCL 2*) positive anti-apoptotic cell rate, whereas it caused significant increases in level of lipid peroxidation and abnormal sperm rates. *BAX* gene expression has been detected in leydig cells, indicating that *BAX* gene is a promotor of cell death is often positively regulated by the tumour suppressor gene p53 and may also cause the formation of multinucleated giant cells which is caused by additional DNA replication of the primary spermatocytes that fail to undergo meiosis. Thus, this article reviews some of the molecular toxicity mechanism of Cd and its effect on the testis which will be helpful in anticipation and deterrence of Cd-induced testicular toxicity.

Keywords: Cadmium Chloride, Exposure, Humans, Testis, Apoptosis, Oxidative stress

INTRODUCTION

Cadmium is a commonly used chemical in agricultural and industrial operations and is released into the environment causing atmosphere, soil, and water pollution. Cadmium can accumulate in the body for up to 40 years, so it can harm human health over an extended period of time (Wang *et al.* 2016). The general population is exposed to Cd via contaminants found in drinking water and food (ATSDR, 2007). There has been a surge in Cd pollution of the environment partly due to urbanization resulting in increase in Cd exposure in human beings which is subsequently leading to higher incidence of Cd-related diseases. Administration of Cd significantly increased the relative weight of testis of rats (Wang *et al.* 2016; Adaramoye *et al.* 2016). Lipid peroxidation was significantly increased while antioxidant parameters decreased in testis of Cd-treated rats. Also, Cd-treated rats had significantly reduced sperm count, motility, sialic acid, luteinising hormone and testosterone relative to controls (Adaramoye *et al.* 2016).

Cadmium is a toxic heavy metal, which probably cause infertility by impairment in spermatogenesis (Yari *et al.* 2016). With high levels of exposure to toxic chemicals including heavy metals, released into the environment and introduced in the food chain, the health of living organisms is affected, sometimes with fatal consequences (Predes *et al.* 2016). In fact, the International Agency for Research on Cancer classified Cd as a known human carcinogen in 1993 (IARC, 1993) and Cd is ranked the 7th toxicant in the Priority List of Hazardous Substances (Priority List) of the Agency for Toxic Substances and Disease Registry (ATSDR) (ATSDR, 2007). Recent studies have demonstrated that the testis is sensitive to cadmium, but studies investigating cadmium-induced testicular injury have not yet clearly revealed the underlying mechanisms. Hematoxylin and

http://doi.org/10.22232/stj.2018.06.01.08

Environmental Pollution 302 (2022) 119048

Contents lists available at ScienceDirect

Environmental Pollution

journal homepage: www.elsevier.com/locate/envpol

Antioxidative, anti-inflammatory and anti-apoptotic action of ellagic acid against lead acetate induced testicular and hepato-renal oxidative damages and pathophysiological changes in male Long Evans rats☆

Rema Momin Bidanchi, Lalrinsanga Lalrindika, Maurya Khushboo, Baishya Bhanushree, Roy Dinata, Milirani Das, Nisekhoto Nisa, Sailo Lalrinzuali, Bose Manikandan, Laskar Saeed-Ahmed, Sanasam Sanjeev, Meesala Krishna Murthy, Vikas Kumar Roy, Guruswami Gurusubramanian*

Department of Zoology, Mizoram University, Aizawl, 796004, Mizoram, India

ARTICLE INFO

Keywords:
Lead toxicity
Ellagic acid
Oxidative stress
Antioxidant defense
Inflammation
Apoptosis

ABSTRACT

Lead (Pb), is an environmental toxicant, causes multi-organ dysfunction including reproductive impairments. This study designed to investigate the prospective antioxidative, anti-inflammatory and anti-apoptotic effects of ellagic acid (EA) on Pb-mediated testicular and hepato-renal toxicity. Four experimental groups of five male Long-Evans rats each were used: control, Pb (60 mg/kg), EA (30 mg/kg), and Pb + EA groups. All groups were given their respective treatment orally for 30 days. Pb exposure altered body and organs weight, food and water consumption, rectal temperature, Pb residue levels in tissues, liver and kidney function, sperm quality parameters, serum metabolic and hematology profiles, and impaired the oxidative/antioxidative balance in the testicular and hepato-renal tissue, as shown by the decreased antioxidant proteins (superoxide dismutase, catalase, glutathione peroxidase, and reduced glutathione) and increased the oxidative (MDA, lipid hydroperoxides, conjugated dienes, protein carbonyl, fragmented DNA and GSH:GSSG ratio) stress and inflammatory (IL-1, IL-6, TNF-α, prostaglandin, LTB4, NO, myeloperoxidase, LDH) markers. Moreover, a dysregulation in the stress response (HSP-70) and apoptotic-regulating proteins (BAX, BCL-2, and active Caspase-3) were recorded upon Pb exposure. Remarkably, EA oral administration reduced the Pb residue levels in tissues, improved the liver and kidney function, revived the spermatogenesis and sperm quality, restored redox homeostasis, suppressed the oxidative stress, inflammatory and apoptotic responses in the liver, kidney and testis tissue. Our findings point out that EA can be used as a phyto-chelator to overcome the adverse effects of Pb exposure due to its potent antioxidant, anti-inflammatory, and anti-apoptotic effects.

1. Introduction

Lead (Pb) has become a global health hazard (0.6%) because of exposure to animals and human beings with ingestion of feed and food, inhalation of industrial emissions, food chain, environment, and water resources (Ericson et al., 2016; Rehman et al., 2018). Globally, blood lead levels of 1 in 3 children (800 million) are estimated to be ≥ 5 μg/dL and over 275 million children in India suffer mild to severe effects of lead poisoning (Rees and Fuller, 2020). Pb is absorbed by the duodenum via DMT1 (divalent metal transporter 1), combined with erythrocyte protein and later dispensed to tissues and organs (García-Niño and Pedraza-Chaverri, 2014). One third of the total absorbed Pb is stored in the liver due to hepatic conjugation, followed by the kidney and finally the residual quantity is accumulated in various tissues and organs causing biomolecules (DNA, lipid, protein, RNA) injury, cell damage and cell death (Flora et al., 2006; Chen et al., 2019). Pb is multi-organ cumulative toxicants that cause oxidative damage, hemato-biochemical alterations (Al-Omair et al., 2017) and interrupts organ functions causing various metabolic disorders (Caito et al., 2017; Gandhi et al., 2017; Park et al., 2019). Inflammation and oxidative stress that play a

☆ This paper has been recommended for acceptance by Wen Chen.

* Corresponding author.
E-mail address: gurus64@yahoo.com (G. Gurusubramanian).

https://doi.org/10.1016/j.envpol.2022.119048
Received 19 November 2021; Received in revised form 14 February 2022; Accepted 21 February 2022
Available online 24 February 2022

Environmental Science and Pollution Research (2019) 26:20631–20653
https://doi.org/10.1007/s11356-019-05420-7

RESEARCH ARTICLE

Influence of ferulic acid consumption in ameliorating the cadmium-induced liver and renal oxidative damage in rats

Sanasam Sanjeev[1] · Rema Momin Bidanchi[1] · Meesala Krishna Murthy[1] · Guruswami Gurusubramanian[1] · Vikas Kumar Roy[1]

Received: 21 June 2018 / Accepted: 8 May 2019 / Published online: 18 May 2019

Abstract
The aim of this study relates to the modulatory role of ferulic acid (FA) against cadmium (Cd)-induced oxidative stress in the liver and kidney of male Wistar albino rats. Cd is an extremely toxic industrial and environmental pollutant and is well known for its varied toxic clinical manifestations. FA is a derivative of curcumin and a ubiquitous phenolic compound having a wide range of therapeutic activities. In the current study, Cd (10 mg/kg) was administered subcutaneously for 15 and 30 days to induce hepato-renal toxicity. Cd concentration was found to be significantly high in Cd-intoxicated rats (liver > kidney) while the supplementation of FA (50 mg/kg) significantly reduces the Cd concentration in liver and kidney tissues. Reduced body and organ weights and food and water consumption and increased rectal temperature were noticed in Cd-treated rats while these parameters were significantly ameliorated in FA-supplemented rats. Liver and kidney damage induced by Cd was significantly revealed by the reduction in serum total protein contents (TPC) and increased activities of serum nitric oxide (NO) levels and hepato-nephrotoxicity marker enzymes, namely aspartate transaminase (AST), alanine transaminase (ALT), alkaline phosphatase (ALP), lactic dehydrogenase (LDH), AST:ALT ratio, uric acid, urea, urea nitrogen, and creatinine, along with the increased levels of hepatic and renal oxidative stress markers, namely lipid peroxidation (MDA levels), lipid hydroperoxides (LOOH), protein carbonyl content (PCC), total oxidant status (TOS), and oxidative stress index (OSI) in liver and kidney tissues. In addition, the toxicity of Cd was also evidenced by a significant decrease in the levels of total thiols (TTH), total antioxidant concentration (TAC), enzymatic antioxidants (superoxide dismutase (SOD), catalase (CAT), and glutathione peroxidase (GPx)), and non-enzymatic antioxidants (reduced glutathione (GSH) and total free sulfhydryl groups (TSH)). Administration of FA significantly restored the serum total protein levels and activities of serum NO levels and hepatic and renal marker enzymes to normal levels in comparison with Cd-intoxicated rats. Furthermore, FA significantly reduced the oxidative stress markers and recuperated the levels of antioxidant defense in the liver and kidney as evidenced by native PAGE and spectrophotometric assays, correlation and regression analysis and multivariate analysis of variance (MANOVA), and inferring the antioxidant role of FA. Histopathological damage due to Cd intoxication in the liver and kidney is demonstrated as vasodilatation and congestion in central veins and sinusoids as well as around the glomerulus, infiltration of mixed inflammatory cells and peripheral hemorrhage, hemorrhagic and enlarged sinusoids, disorganization of the hepatic parenchyma, focal necrosis, swelling of hepatocytes, calcified tissue inside blood vessels, hepatocyte degeneration and vacuolization of liver cells, hyaline casts, degenerated glomerulus with wide space and detached basement membrane, distal tubule with wide lumen, deformed proximal tubules with detached brush border, and degeneration and hyalinization of glomerular tuft. But, FA significantly reduced the toxicity of Cd and protected the normal histological architecture of the liver and kidney tissues. Cd-intoxicated rats were associated with a significant upregulation of TNF-α, COX-2, and HSP70 proteins, whereas treatment with FA caused downregulation of the above inflammatory

Responsible editor: Philippe Garrigues

✉ Guruswami Gurusubramanian
gurus64@yahoo.com

Sanasam Sanjeev
sanasamsanjeev@gmail.com

Meesala Krishna Murthy
krishnameesala6@gmail.com

Vikas Kumar Roy
vikasroy4araria@gmail.com

[1] Department of Zoology, Mizoram Central University, Aizawl, Mizoram 796004, India

Indian Journal of Biochemistry & Biophysics
Vol. 60, December 2023, pp. 896-918
DOI: 10.56042/ijbb.v60i12.6933

Computational toxicology and food safety assessment of *Parkia timoriana* phytoconstituents using quantitative structure-activity relationship (QSAR) modeling approaches

Nisekhoto Nisa[1], Roy Dinata[1], Chettri Arati[1], Gumaa Abdelmuala Abdelgani-Baraka[1], Baishya Bhanushree[1], Rema Momin Bidanchi[1], Bose Manikandan[1], Ahmed-Laskar Saeed[1], Giri Abinash[1], Buragohain Pori[1], Sailo Lalrinzuali[1], Maurya Khushboo[1], Sonar Indira[1], Vikas Kumar Roy[1], KRS Sambasiva Rao[2]* & Guruswami Gurusubramanian[1]*

[1]Department of Zoology, Mizoram University (A Central University), Aizawl-796 004, Mizoram, India
[2]Department of Pharmacy, Mangalayatan University-Jabalpur, Jabalpur-483 001, Madhya Pradesh, India

Received 24 November 2023; revised 27 December 2023

As a lead compound, natural compounds have undergone extensive research in different enterprises. Since they might also have other adverse effects, determining their toxicity is crucial. Computational methods can circumvent the main challenges associated with assessing the toxicity of substances using *in vivo* and *in vitro* techniques, including time, money, labor, and the use of animal models. Although *Parkia timoriana* (PT) has a significant economic potential, its exploitation has yet to be thoroughly explored in terms of its toxicity and food safety. In PT seed pod extracts, 61 phytocompounds with a predominance of alkaloids, flavonoids, and terpenoids were identified using GC-MS and LC-MS/MS analysis. Utilizing the TEST, OECD QSAR toolkit, VEGA-HUB, Toxtree, and PASS tools, phytocompounds from PT were assessed for toxicity, food safety risk assessment, and biological activity. The phytochemicals were tested on multiple species, including *Daphnia magna*, *Pimephales promelas*, *Tetrahymena pyriformis*, and rats, to determine their toxicity using the QSAR-TEST tool. For aquatic and mammalian organisms, the phytocompounds from PT were shown to be hazardous in the following four hierarchical orders: i) *P. promelas*>*T. pyriformis*>*D. magna*>*R. norvegicus*, ii) *P. promelas*>*D. magna*>*T. pyriformis*>*R. norvegicus*, iii) *D. magna*> *P. promelas*>*T. pyriformis*>*R. norvegicus*, and *T. pyriformis*>*P. promelas*>*D. magna*>*R. norvegicus*. Despite being non-bioaccumulative, non-mutagenic, and non-carcinogenic in nature, the majority of phytocompounds were developmental toxins. More than half of the phytochemicals derived from PT were highly toxic (Cramer oral toxicity) and manifested negative side effects (with a lower NOAEL value).Most of the substances did not exhibit organ toxicity in the repeated dose toxicity test, were bioavailable, metabolized by cytochrome-P450 pathway, and were excreted from the body. PASS predicted that the examined phytoconstituents from PT were to demonstrate a wide range of anti-oxidant, free radical scavenger, anti-inflammatory, antiviral, anti-fungal, anti-neoplastic, antibacterial, and anti-protozoal activities. For the purpose of exploring drug discovery, additional research of the phytocompounds on *in vivo* models is advised.

Keywords: Computational toxicology, Food safety, GC-MS, LC-MS/MS, *Parkia timoriana*, Quantitative structure-activity relationship modeling, Risk assessment

Parkia timoriana (PT, Fabaceae), also known as the tree bean, is a nutritionally rich, underutilized leguminous tree that grows in northeastern India and various Southeast Asian countries. From an ethnobotanical standpoint, tree beans are significant to ethnic groups in a number of provinces of Northeast India, Burma, Bangladesh, Pakistan, China, Thailand, Malaysia, and the Gambia. Numerous ailments are treated with concoctions of bark, fruit, and leaf portions. All edible parts of this plant, from the flowers and young pods through the mature seeds, are in seasonally high demand and offer a good supply of nutrients[1]. If utilized properly, tree beans could serve as an additional source of vegetable proteins. The protein level of pods ranged from 12.1% in tender to 18.8% in mature pods, but kernels had substantially greater protein content (28.8%) than pods[1] it has been found that the pods of PT contain significant amounts of tannins, flavonoids, saponins, anthocyanins, and leuco-anthocyanins[2]. Tree bean has been found to have antioxidant, α-glucosidase and α-amylase inhibitory, antibacterial, antidiabetic, antiproliferative, antiviral, immune boosting, and insecticidal effects. It has also been used to treat liver and skin diseases, ulcer, colon cancer, leprosy, hypertension, and painful eyes[3]. In the case of PT pods, leaves, and other plant parts are eaten

*Correspondence:
Phone: +91-7630079075 (Mob); +91-9862399411 (Mob)
E-mail: krssrao@yahoo.com; gurus64@yahoo.com

Taylor & Francis

Journal of Biomolecular Structure and Dynamics

ISSN: (Print) (Online) Journal homepage: https://www.tandfonline.com/loi/tbsd20

Repurposing immune boosting and anti-viral efficacy of *Parkia* bioactive entities as multi-target directed therapeutic approach for SARS-CoV-2: exploration of lead drugs by drug likeness, molecular docking and molecular dynamics simulation methods

Roy Dinata, Nisekhoto Nisa, Chettri Arati, Borgohain Rasmita, Chetia Uditraj, Rajkonwar Siddhartha, Baishya Bhanushree, Laskar Saeed-Ahmed, Bose Manikandan, Rema Momin Bidanchi, Giri Abinash, Buragohain Pori, Maurya Khushboo, Vikas Kumar Roy & Guruswami Gurusubramanian

To cite this article: Roy Dinata, Nisekhoto Nisa, Chettri Arati, Borgohain Rasmita, Chetia Uditraj, Rajkonwar Siddhartha, Baishya Bhanushree, Laskar Saeed-Ahmed, Bose Manikandan, Rema Momin Bidanchi, Giri Abinash, Buragohain Pori, Maurya Khushboo, Vikas Kumar Roy & Guruswami Gurusubramanian (2023): Repurposing immune boosting and anti-viral efficacy of *Parkia* bioactive entities as multi-target directed therapeutic approach for SARS-CoV-2: exploration of lead drugs by drug likeness, molecular docking and molecular dynamics simulation methods, Journal of Biomolecular Structure and Dynamics, DOI: 10.1080/07391102.2023.2192797

To link to this article: https://doi.org/10.1080/07391102.2023.2192797

Dietary phytoestrogen, diosgenin interrupts metabolism, physiology and reproduction of the Swiss albino mice: possible mode of action as an emerging environmental contaminant, endocrine disruptor and reproductive toxicant

Maurya Khushboo
Mizoram University
Sanasam Sanjeev
Mizoram University
Meesala Krishna Murthy
Mizoram University
Maibam Sunitadevi
Mizoram University
Roy Dinata
Mizoram University
Baishya Bhanushree
Mizoram University
Rema Momin Bidanchi
Mizoram University
Nisekhoto Nisa
Mizoram University
Sailo Lalrinzuali
Mizoram University
Bose Manikandan
Mizoram University
Ahmed-Laskar Saeed
Mizoram University
Giri Abinash
Mizoram University
Buragohain Pori
Mizoram University
Chettri Arati
Mizoram University
Vikas Kumar Roy

Environmental Science and Pollution Research
https://doi.org/10.1007/s11356-023-25943-4

RESEARCH ARTICLE

Repurposing of phyto-ligand molecules from the honey bee products for Alzheimer's disease as novel inhibitors of BACE-1: small molecule bioinformatics strategies as amyloid-based therapy

Nisekhoto Nisa[1] · Borgohain Rasmita[1] · Chettri Arati[1] · Chetia Uditraj[1] · Rajkonwar Siddhartha[1] · Roy Dinata[1] · Baishya Bhanushree[1] · Rema Momin Bidanchi[1] · Bose Manikandan[1] · Saeed Ahmed Laskar[1] · Giri Abinash[1] · Buragohain Pori[1] · Vikas Kumar Roy[1] · Guruswami Gurusubramanian[1]

Received: 25 August 2022 / Accepted: 10 February 2023

Abstract
Alzheimer's disease (AD) is one of the neurodegenerative diseases, manifesting dementia, spatial disorientation, language, cognitive, and functional impairment, mainly affects the elderly population with a growing concern about the financial burden on society. Repurposing can improve the traditional progress of drug design applications and could speed up the identification of innovative remedies for AD. The pursuit of potent anti-BACE-1 drugs for AD treatment has become a pot boiler topic in the recent past and to instigate the design of novel improved inhibitors from the bee products. Drug-likeness characteristics (ADMET: absorption, distribution, metabolism, excretion, and toxicity), docking (AutoDock Vina), simulation (GROMACS), and free energy interaction (MM-PBSA, molecular mechanics Poisson–Boltzmann surface area) analyses were performed to identify the lead candidates from the bee products (500 bioactives from the honey, royal jelly, propolis, bee bread, bee wax, and bee venom) for Alzheimer's disease as novel inhibitors of BACE-1 (beta-site amyloid precursor protein cleaving enzyme (1) receptor using appropriate bioinformatics tools. Forty-four bioactive lead compounds were screened from the bee products through high throughput virtual screening on the basis of their pharmacokinetic and pharmacodynamics characteristics, showing favorable intestinal and oral absorption, bioavailability, blood brain barrier penetration, less skin permeability, and no inhibition of cytochrome P450 inhibitors. The docking score of the forty-four ligand molecules was found to be between −4 and −10.3 kcal/mol, respectively, exhibiting strong binding affinity to BACE1 receptor. The highest binding affinity was observed in the rutin (−10.3 kcal/mol), 3,4-dicaffeoylquinic acid (−9.5 kcal/mol), nemorosone (−9.5 kcal/mol), and luteolin (−8.9 kcal/mol). Furthermore, these compounds demonstrated high total binding energy −73.20 to −105.85 kJ/mol), and low root mean square deviation (0.194–0.202 nm), root mean square fluctuation (0.0985–0.1136 nm), radius of gyration (2.12 nm), number of H-bonds (0.778–5.436), and eigenvector values (2.39–3.54 nm^2) in the molecular dynamic simulation, signifying restricted motion of Cα atoms, proper folding and flexibility, and highly stable with compact of the BACE1 receptor with the ligands. Docking and simulation studies concluded that rutin, 3,4-dicaffeoylquinic acid, nemorosone, and luteolin are plausibly used as novel inhibitors of BACE1 to combat AD, but further in-depth experimental investigations are warranted to prove these in silico findings.

Keywords ADMET · Alzheimer's disease · BACE1 · Honeybee products · Repurposing · Molecular dynamics

Introduction

Alzheimer's disease (AD) is an irreversible progressive neurodegenerative disorder leading to deterioration in cognitive functions and changes in behavior and personality (Martins et al. 2018). AD causes cognitive and functional impairment, including dementia and disability in the older people and it is documented as a public health precedence by the WHO (Scott et al. 2016; WHO 2021). Aging is the main

Nisekhoto Nisa and Vikas Kumar Roy contributed equally to this work.

Responsible Editor: Lotfi Aleya

✉ Guruswami Gurusubramanian
gurus64@yahoo.com; mzut036@mzu.edu.in

[1] Department of Zoology, Mizoram University, Aizawl, Mizoram 796004, India

Published online: 20 February 2023

Environmental Science and Pollution Research
https://doi.org/10.1007/s11356-023-26018-0

RESEARCH ARTICLE

Long-term consumption of fermented pork fat-based diets differing in calorie, fat content, and fatty acid levels mediates oxidative stress, inflammation, redox imbalance, germ cell apoptosis, disruption of steroidogenesis, and testicular dysfunction in Wistar rats

Sailo Lalrinzuali[1] · Maurya Khushboo[1] · Roy Dinata[1] · Baishya Bhanushree[1] · Nisekhoto Nisa[1] · Rema Momin Bidanchi[1] · Saeed-Ahmed Laskar[1] · Bose Manikandan[1] · Giri Abinash[1] · Buragohain Pori[1] · Vikas Kumar Roy[1] · Guruswami Gurusubramanian[1]

Received: 1 July 2022 / Accepted: 15 February 2023

Abstract

There is a dearth of experimental evidence available as to whether the consumption of fermented pork fat (FPF) food has any harmful effects on metabolism and reproduction due to its excessive calories, high fat content, and fatty acid methyl ester (FAME) levels. We hypothesized that exposure to a FPF-diet with excessive calories, a high fat content, and high FAME levels alters testicular physiology and metabolism, leading to permanent damage to the testicular system and its function. Thirteen-week-old male rats ($n = 20$) were assigned to a high-calorie, high-fat diet (FPF-H, fat-60%, 23 kJ/g), a moderate-calorie, moderate-fat diet (FPF-M, fat-30%, 17.5 kJ/g), a low-calorie and low-fat diet (FPF-L, fat-15%, 14.21 kJ/g) compared to the standard diet (Control, fat-11%, 12.56 kJ/g) orally for 90 days. GC–MS analysis of the three FPF-diets showed high quantities of saturated fatty acids (SFAs) and polyunsaturated fatty acids-ω6 (PUFA-ω6) and low levels of monounsaturated fatty acids (MUFAs) and polyunsaturated fatty acids-ω3 (PUFA-ω3) compared to the control diet. Consequently, the levels of serum FAMEs of the FPF-diet fed rats were significantly increased. In addition, a high level of n-6:n-3 PUFA towards PUFA-ω6 was observed in the serum of FPF-diet fed rats due to the high content of linoleic, γ-linolenic, and arachidonic acid. Long-term consumption of FPF-diets disturbed the anthropometrical, nutritional, physiological, and metabolic profiles. Furthermore, administration of FPF-diets generated metabolic syndrome (dyslipidemia, leptinemia, insulin resistance, obesity, hepato-renal disorder and function), increased the cardiovascular risk factors, and triggered serum and testis inflammatory markers (interleukin-1↑, interleukin-6↑, interleukin-10↓, leukotriene B4↑, prostaglandin↑, nitric oxide↑, myeloperoxidase↑, lactate dehydrogenase↑, and tumor necrosis factor-α↑). Activated testis oxidative stress (conjugated dienes↑, lipid hydroperoxides↑, malondialdehyde↑, protein carbonyl↑, and fragmented DNA↑) and depleted antioxidant reserve (catalase↓, superoxide dismutase↓, glutathione S-transferase↓, reduced glutathione↓, glutathione disulfide↑, and GSH:GSSG ratio↓) were observed in FPF-diet fed rats. Disrupted testis histoarchitecture, progressive deterioration of spermatogenesis, poor sperm quality and functional indices, significant alterations in the reproductive hormones (serum and testis testosterone↓, serum estradiol↑, serum luteinizing hormone↓, and follicle-stimulating hormone↑), were noted in rats fed with FPF diets than in the control diet. Severe steroidogenic impairment (steroidogenic acute regulatory protein, StAR↓; 3β-hydroxysteroid dehydrogenase, 3β-HSD↓; and luteinizing hormone receptor, LHR↓), deficiency in germ cells proliferation (proliferating cell nuclear antigen, PCNA↓), and abnormally enhanced testicular germ cell apoptosis (terminal deoxynucleotidyl transferase dUTP nick end labeling, TUNEL assay↑; B-cell lymphoma-2, BCL-2↓; Bcl-2-associated X protein, BAX↑; and BAX/BCL-2 ratio↑) were remarked in the FPF-diet administered rats in comparison with the control diet. In conclusion, the long-term feeding of an FPF-diet with excessive calories, a high fat content, and high FAME levels induced oxidative stress, inflammation, and

Responsible Editor: Mohamed M. Abdel-Daim

Sailo Lalrinzuali, Maurya Khushboo and Vikas Kumar Roy contributed equally to this work.

Extended author information available on the last page of the article

Published online: 25 February 2023

Indian Journal of Biochemistry & Biophysics
Vol. 60, May 2023, pp. 365-384
DOI: 10.56042/ijbb.v60i5.552

A Review

Pharmacological and therapeutic potential of honey bee antimicrobial peptides

Dinata Roy[1], Chettri Arati[1], Bose Manikandan[1], Giri Abinash[1], Nisekhoto Nisa[1], Baishya Bhanushree[1], Laskar Saeed-Ahmed[1], Rema Momin Bidanchi[1], Buragohain Pori[1], Maurya Khushboo[1], Sonar Indira[1], Vikas Kumar Roy[1], KRS Sambasiva Rao[2]* & Guruswami Gurusubramanian[1]*

[1]Department of Zoology; & [2]Department of Biotechnology, Mizoram University (A Central University), Aizawl-796 004, Mizoram, India

Received 13 April 2023; revised 09 June 2023

Honey bees (Apidae: Apini) and stingless bees (Apidae: Meliponini) act as the main pollinators for many wild and cultivated tropical plants, playing a vital role in the ecology, economy, and culture. Honey bees and stingless bees are one of the major sources of antimicrobial peptides/proteins (AMPs) synthesized in fat bodies and blood cells of bees. Bee AMPs are a class of small peptides having amino acid residues between 9 and 340, classified based on source, activity, structural characteristics, and amino acid-rich species. AMPs have a wide range of inhibitory effects against bacteria, fungi, parasites, and viruses. Four antimicrobial peptide families, *i.e.*, apidaecins (proline-rich), abaecin (proline-rich), hymenoptaecin (glycine-rich), and defensin (cystine-rich) are synthesized in the haemolymph, signifying a broad spectrum of antimicrobial activity. Jelleines (I-IV), royalisin, apisimin (serine-valine-rich peptide), 10 HDA, apalbumin, and apisin, which are present in royal jelly, have antimicrobial, mast cell degranulating, and hemolysis activity. Bee venom also contains several bioactive peptides, such as apamin (leucine-cystine-rich), melittin (leucine-alanine-rich), melectin (lysine-rich), adolapin, secapin (proline-rich), and tertiapin (cystine-lysine-rich). Currently, AMPs databases are displaying an essential role in exploration, identification, characterization, and annotation. Several AMPs databases (CAMP, DRAMP, APD, InverPep, LAMP, ADAPTABLE, ADAM, AntiBP, AMPer, AVPpred, EFC-FCBF, and class AMP) are open-access resources that have been developed to enhance research on antimicrobial peptides. Bee immune responses are composed of a multifaceted group of individual immune mechanisms and special types of behavioral adaptations. Given the importance of drug discovery from honey bee AMPs, this review is aimed at providing an exhaustive screening of the AMPs detected in honey and honeybee products and their classification, databases, computational tools, physicochemical properties, signaling pathways, pharmaceutical and clinical uses, application status, prospects, and problems to be solved.

Keywords: AMPs, Databases, Honey bees, Signaling pathways, Therapeutic applications

Introduction

Honey bees and stingless bees, act as one of the major pollinators in wild forest and agriculture systems, are indispensable for conserving ecological biodiversity, global ecological stability, productivity and economy[1]. Besides, both honey bees and stingless bees are capable to produce different types of honey, royal jelly, bee wax, propolis, bee bread and bee venom based on diverse floral resources visit and can yield significant contributions to human society (Fig. 1). Nevertheless, several factors seemingly lead to bee depopulation and colony/brood loss events, including pathogens (parasites, fungi, bacteria and viruses), ecosystem alteration or loss, and the use of pesticides and antibiotics intimidate wild plant diversity, terrestrial ecosystem stability, crop production, global food supply, and human welfare[2]. The immune system of bees is capable of changing its defence mechanisms, so it is essential to understand how it works in order to examine how it reacts to various pathogenic and stressful situations that affect the health and behaviour of bee colonies (Fig. 1).

Bee immunity serves as an example of the superorganism theory since it relies on both individual and colony-level defence mechanisms to protect bees from infections and stressful situations[3]. Additionally, bees' social immunity—a network of behavioural, physiological, and organizational responses that prevents the admission, establishment, expansion, and transmission of parasites and microbial diseases in the colony—supplements their physiological immune systems. Bee immune responses are comprised of distinctive categories of behavioral adaptations, evolutionary conserved defense strategies (cellular and humoral responses) and assemblage of multifaceted discrete immune mechanisms that afford

*Correspondence:
Phone: +91-7630079075; +91-9862399411 (Mob)
E-mail: krssrao@yahoo.com (KRSSR); gurus64@yahoo.com (GG)

PARTICULARS OF THE CANDIDATE

NAME OF THE CANDIDATE	: BIDANCHI R. MOMIN
DEGREE	: DOCTOR OF PHILOSOPHY
DEPARTMENT	: ZOOLOGY
TITLE OF THESIS	: Biological fingerprinting and therapeutic efficacy of *Lannea coromandelica* and *Trevesia palmata* in trinitrobenzene sulfonic acid induced ulcerative colitis rat model
DATE OF ADDIMISSION	: 19.03.2018

APPROVAL OF RESEARCH PROPOSAL

1.	D.R.C.	: 12.04.2018
2.	B.O.S.	: 27.04.2018
3.	SCHOOL BOARD	: 03.05.2018
MZU REGISTRATION No.		: 7120 of 2014
Ph.D. REGISTRATION No. & DATE		: MZU/Ph.D./1105 of 03.05.2018
EXTENSION (IF ANY)		: No. 16-2/MZU(Acad)/21/313-318 Dated 12 July 2023 (2 years Extention): 20.03.2023-19.03.2025

(**Prof. G. GURUSUBRAMANIAN**)
Head
Department of Zoology
Mizoram University

PAPER NAME

Compiled Thesis (1) (1) bidanchi.pdf

AUTHOR

Bidanchi Momin

WORD COUNT

79590 Words

CHARACTER COUNT

446164 Characters

PAGE COUNT

318 Pages

FILE SIZE

3.8MB

SUBMISSION DATE

Mar 27, 2024 5:58 PM GMT+5:30

REPORT DATE

Mar 27, 2024 6:01 PM GMT+5:30

8% Overall Similarity

The combined total of all matches, including overlapping sources, for each database.

- 6% Internet database
- 6% Publications database
- Crossref database
- Crossref Posted Content database
- 3% Submitted Works database

Excluded from Similarity Report

- Bibliographic material
- Quoted material
- Cited material
- Small Matches (Less then 14 words)

ABSTRACT

BIOLOGICAL FINGERPRINTING AND THERAPEUTIC EFFICACY OF *LANNEA COROMANDELICA* AND *TREVESIA PALMATA* IN TRINITROBENZENE SULFONIC ACID INDUCED ULCERATIVE COLITIS RAT MODEL

AN ABSTRACT SUBMITTED IN PARTIAL FULFILLMENT OF THE REQUIREMENTS FOR THE DEGREE OF DOCTOR OF PHILOSOPHY

BIDANCHI R. MOMIN
MZU REGISTRATION NO.: 7120 of 2014
Ph.D. REGISTRATION NO.: MZU/Ph.D./1105 of 03.05.2018

DEPARTMENT OF ZOOLOGY
SCHOOL OF LIFE SCIENCES
MARCH, 2025

BIOLOGICAL FINGERPRINTING AND THERAPEUTIC EFFICACY OF *LANNEA COROMANDELICA* AND *TREVESIA PALMATA* IN TRINITROBENZENE SULFONIC ACID INDUCED ULCERATIVE COLITIS RAT MODEL

BY

BIDANCHI R. MOMIN

Department of Zoology

SUPERVISOR

Prof. GURUSWAMI GURUSUBRAMANIAN

Submitted

In partial fulfillment of the requirement of the Degree of Doctor of Philosophy in Zoology of Mizoram University, Aizawl.

I. INTRODUCTION

Ulcerative colitis (UC) is a chronic inflammatory bowel disease (IBD) characterized by inflammation and ulceration of the colonic mucosa. It is one of the two main forms of IBD, with higher rates reported in Western countries. The exact aetiology of UC remains incompletely understood, but it is believed to result from a complex interplay between genetic susceptibility, environmental factors, dysregulated immune responses, and alterations in the gut microbiota (Mendell et al., 2023).

UC typically presents with a relapsing-remitting course, characterized by periods of active inflammation interspersed with periods of remission. The severity and extent of disease vary among patients, ranging from mild to severe. The diagnosis of UC is based on a combination of clinical symptoms, endoscopic findings, histopathological evaluation, and exclusion of other causes of colonic inflammation. Treatment strategies vary depending on disease severity, extent, and patient factors (Juliao-Banos et al., 2020).

Ulcerative colitis is associated with various complications, including toxic megacolon, intestinal perforation, strictures, colorectal cancer, and extraintestinal manifestations such as arthritis, dermatologic conditions, and hepatobiliary disorders. Close monitoring and appropriate management are essential to prevent and mitigate these complications (Gordon et al., 2024).

Trinitrobenzene sulfonic acid (TNBS) is a well-established chemical agent used to induce experimental colitis in animal models, particularly rats, to mimic the pathophysiological features of human UC. The TNBS-induced colitis model serves as a valuable tool for preclinical drug development in UC, allowing researchers to evaluate the efficacy and safety of potential therapeutic interventions in a controlled experimental setting. However, it is essential to acknowledge the limitations of the model and consider complementary approaches to ensure the translational relevance of preclinical findings to human disease (Antoniou et al., 2016).

Sulfasalazine, a classic disease-modifying anti-rheumatic drug (DMARD), has been a cornerstone of UC therapy for decades, with its efficacy in treating UC well-documented. It is composed of sulfapyridine and 5-aminosalicylic acid (5-ASA),

which modulates inflammatory pathways within the intestinal mucosa and inhibits pro-inflammatory cytokines. 5-ASA also has antioxidant properties, reducing oxidative stress within the colonic mucosa (Choi and Fenando, 2020).

Clinical trials and observational studies consistently demonstrate the efficacy of sulfasalazine in inducing and maintaining remission in patients with mild to moderate UC. However, its efficacy may be limited in patients with severe disease or those who are refractory to treatment (Yoshino et al., 2016).

Lannea coromandelica and *Trevesia palmata* in Mizoram, India, hold particular significance due to their diverse pharmacological properties and traditional uses in managing various ailments (Swathi and Lakshman, 2022; Manoharan et al., 2023). *L. coromandelica* and *T. palmata* have been traditionally employed as important remedies for generations, with roots used to treat digestive ailments, while *T. palmata* is used for wound healing and inflammation reduction (Ahmed, 2019). However, scientific research on the efficacy and safety of these plants is still limited. Further studies are needed to validate their traditional uses, identify active compounds, and understand their pharmacological mechanisms. Caution should be exercised when using herbal remedies, and consultation with healthcare professionals is advisable, especially for serious or chronic health conditions (Hassen et al., 2022).

L. coromandelica and *T. palmata* are rich sources of bioactive compounds, including polyphenols, flavonoids, terpenoids, alkaloids, and saponins. Their diverse chemical composition highlights their potential therapeutic versatility and importance in traditional medicine systems. Studies have demonstrated the beneficial effects of these plants, including anti-inflammatory, antioxidant, antimicrobial, antidiabetic, analgesic, and wound healing properties (Swathi and Lakshman, 2022; Manoharan et al., 2023). Their traditional uses, phytochemical composition, and pharmacological activities highlight their importance in indigenous healthcare systems and underscore the need for further research to explore their full therapeutic potential. By integrating traditional knowledge with modern scientific approaches, efforts can be made to harness the medicinal value of these plants for the benefit of the population in Mizoram and beyond, thereby preserving traditional healing practices and promoting public health.

In recent years, there has been an increasing interest in investigating the therapeutic potential of *L. coromandelica* and *T. palmata* in experimental models of UC (Islam et al., 2022; Wang et al., 2023; Ha et al., 2024; Manoharan et al., 2023). Trinitrobenzene sulfonic acid (TNBS)-induced colitis in rats is a well-established model that closely mimics the pathophysiology and clinical features of human UC (Modesto et al., 2022). Both plants have demonstrated significant anti-inflammatory effects in TNBS-induced colitis rats, as evidenced by a reduction in colonic inflammation, histological damage, and levels of pro-inflammatory cytokines such as TNF-α, IL-6, and IL-1β.

In conclusion, the biological fingerprinting and therapeutic efficacy of *L. coromandelica* and *T. palmata* in the TNBS-induced UC rat model offer promising prospects for the development of novel therapeutic agents for UC management.

The isolation, characterization, and identification of bioactive compounds from *Lannea coromandelica* and *Trevesia palmata* involves a multi-step process that includes extraction, chromatographic separation, and spectroscopic analysis (Sasidharan et al., 2011). Techniques such as gas chromatography-mass spectrometry (GC-MS), liquid chromatography-mass spectrometry (LC-MS), and infrared spectroscopy (IR) are commonly employed for this purpose (Salerno et al., 2020; Junaedi et al., 2021; Ardrey, 2003).

Extraction involves extracting bioactive compounds from plant material, while fractionation and purification involve fractionation using chromatographic techniques. Chromatographic analysis (GC-MS) is used for the separation and identification of volatile and semi-volatile compounds, while LC-MS is used for non-volatile and polar compounds. Infrared spectroscopy (IR) is used to analyze the molecular structure and chemical composition of compounds (Abubakar et al., 2020).

Computational studies have emerged as valuable tools for predicting and evaluating the phytochemical composition and pharmacological bio-activities of medicinal plants. These methods, including molecular docking, molecular dynamics simulations, and quantitative structure-activity relationship (QSAR) modelling, allow for in-silico analysis of plant-derived compounds and their interactions with biological targets (Wu et al., 2020).

In this experiment, computational approaches can be used to predict the phytochemical profile of *L. coromandelica* and *T. palmata* leaves by screening their chemical constituents against databases of known natural products. Molecular docking studies can help identify potential biological targets of the bioactive compounds present in *L. coromandelica* and *T. palmata* leaves, while pharmacophore modelling and virtual screening techniques can be employed to identify lead compounds with desired pharmacological properties.

In conclusion, computational studies provide valuable insights into the phytochemical composition and pharmacological bio-activities of *L. coromandelica* and *T. palmata* leaves, offering a rational approach for the discovery and development of new therapeutic agents. Integrating computational and experimental approaches enables a more comprehensive understanding of these plants' medicinal properties and accelerates the drug discovery process for the treatment of various diseases.

Lannea coromandelica and *Trevesia palmata* are medicinal plants used in traditional medicine for therapeutic purposes. However, it is crucial to assess their safety profiles, particularly regarding acute and sub-acute toxicity, before considering their therapeutic applications in humans. Acute toxicity refers to the adverse effects of a single exposure to a substance, while sub-acute toxicity involves repeated exposures over a relatively short duration, typically up to 28 days in animal studies (Lawal et al., 2016). Understanding the toxicological effects of these plants is crucial for determining safe dosage regimens and potential risks associated with their use (Mensah et al., 2019).

Toxicity studies in animal models, such as rats, provide valuable insights into the adverse effects of these plants on various organ systems and help establish the margin of safety for human consumption (Ugwah-Oguejiofor et al., 2019). These studies help identify safe dosage ranges and potential toxic effects of the extracts, guiding their appropriate use in traditional medicine and therapeutic applications (Wang et al., 2023).

Phytocompounds derived from *Lannea coromandelica* and *Trevesia palmata*, such as polyphenols, flavonoids, and terpenoids, have shown potential in modulating various cellular pathways involved in inflammation, oxidative stress, and cell survival.

However, their specific effects and mechanisms of action in the context of UC pathology require further investigation (Swathi and Lakshman, 2022; Manoharan et al., 2023).

Several biomarkers have been shown to correlate with disease activity in UC, such as calprotectin (FC), which predicts endoscopic activity with a high sensitivity. Phytocompounds with antioxidant and free radical scavenging properties may counteract oxidative and nitrosative stress, protect against colonic injury, modulate immune responses and pro-inflammatory cytokine production, and regulate apoptosis of colonic epithelial cells (Tatsumi et al., 2023).

This study investigates the modulatory, anti-inflammatory, and antioxidant effects of phytocompounds isolated from *L. coromandelica* and *T. palmata* in a trinitrobenzene sulphonic acid (TNBS)-induced ulcerative colitis rat model. In this experiment, cold extraction technique was used to extract phytocompounds from the leaves of these plants. The rats were divided into different treatment groups, including a control group, TNBS-induced colitis group, sulfasalazine treated group, and two groups receiving phytocompounds of 10 mg/kg and 20 mg/kg. The phytocompounds were administered orally at various doses for a specified duration. The effects of phytocompounds on colonic inflammation, mucosal damage, and histopathological changes were evaluated. The anti-inflammatory effects of phytocompounds were assessed by measuring levels of pro-inflammatory cytokines and antioxidant enzyme activities. The findings may elucidate the therapeutic potential of these medicinal plants and guide the development of novel treatments for ulcerative colitis targeting multiple pathological pathways. The gut-microbiota dependence of the protective effects of main active components from *L. coromandelica* and *T. palmata* against UC holds significant therapeutic implications, and further research elucidating the mechanisms underlying these interactions will pave the way for the development of novel microbiota-targeted therapies for UC management.

II. OBJECTIVES

- Isolation, characterization and identification of bioactive compounds from *Lannea coromandelica* and *Trevesia palmata* through chromatographic and spectroscopic analyses (GC-MS, LC-MS and IR)
- Computational study of the phytochemical and pharmacological bio-activities of *Lannea coromandelica* and *Trevesia palmata* leaves
- To appraise the modulatory, anti-inflammatory and antioxidant effects of phytocompounds isolated from *Lannea coromandelica* and *Trevesia palmata* in trinitrobenzene sulphonic acid (TNBS)-induced ulcerative colitis rat model
- Main active components of *Lannea coromandelica* and *Trevesia palmata* protects against ulcerative colitis through gut-microbiota dependence

III. MATERIALS AND METHODS

3.1. Identification and collection of the plants sample

The leaf of *L. coromandelica* and *T. palmata* was collected from Tanhril forest in Aizawl, Mizoram. The sample was identified, confirmed and submitted in the Department of Environmental Science's herbarium, Mizoram university, Aizawl, Mizoram, India under accession number 653 (A1481) and 1543 (3575).

3.2. Preparation and processing of leaves

L. coromandelica and *T. palmata* leaves were collected, cleaned, chopped and dried in shade by air at room temperature (22ºC), after which they were powdered using a fine blender for extraction. The cold extraction process of the powdered plant samples was then carried out. Briefly, 100 gm of plant samples were dissolved in 500 ml of 100 % methanol and kept in a conical flask at room temperature for 72 h. The samples are then filtered using Whatman No. 1 filter papers and a rotary evaporator was used to condense the filtrate into a dark brownish-green semi-solid extract. The dried extract obtained was then stored for further use at 4ºC.

3.3. Gas chromatography-mass spectrometry (GC–MS) analytical conditions and analysis

Lannea coromandelica leaf extract (LCLE) and *Trevesia palmata* leaf extract (TPLE) were analyzed on a GCMS-2010 Shimadzu system (Shimadzu, Japan) in EI mode at 70 eV with a Restek-5MS column (30 0.25 mm film thickness 0.25 m). The carrier gas was pure helium gas (99.99 percent pure), flowing at a constant rate of 1 mL/min. For GC-MS spectrum detection, an electron ionisation energy technique was chosen, with a high ionisation energy of 70 eV (electron Volts), a scan length of 0.2 s, and fragments ranging from 40 to 650 (m/z). The injector temperature was maintained at 260°C, and the injection volume was 2 µL (split ratio: 10:1). The flow control mode was linear at a pressure of 99.3 kPa. The total and column flow rates were 16.3 mL/min and 1.21 mL/min, respectively. The temperature of the column oven was initially set at 120°C for two minutes, then increased by 10°C every minute until it reached 280°C, and finally to 300°C for 20 minutes. The chromatogram and mass spectra were assessed using the Xcalibur™ software included in the GC-MS/LC-MS system. The phytochemical contents of the test samples were determined by comparing their retention time (min), peak area, peak height, and mass spectral patterns to those of authentic compounds stored in the National Institute of Standards and Technology (NIST) library, which contains over 62,000 patterns and Dr. Duke's ethnobotanical phytochemical databases12. The spectra of the unknown component were compared to those of the known components in the NIST collection. The phytochemicals' names, molecular weights, and structures were determined.

3.4. Liquid chromatography-mass spectrometry (LC-MS/MS) classification

The Acquity Ultra Performance Liquid Chromatography (ACQUITY UPLC H-Class) equipment was used with an auto sampler and a binary pump (Waters, USA) connected to a 10L loop. The separation of phytocompounds from LCLE and TPLE was studied under a variety of chromatographic conditions, such as mobile phase composition, flow rate, and injection volume at various gradient programmes. Several mobile phase mixtures, including acetonitrile-water,

methanol-water, and acetonitrile-0.1% (v/v) formic acid aqueous solution, were evaluated in the gradient programme at a flow rate of 1.5 mL/min. The best separation conditions were determined to be 0-300 bar column pressure and 30°C column temperature. The compounds were separated at 30°C with an Acquity CSH C18 column (2.1 mm x 100 mm x 1.7 m). Two solvents, 0.1% (v/v) formic acid in water (A) and methanol (B), were used to accomplish gradient elution at a flow rate of 1.5 ml/min. The gradient programme started with 5% (B) at 0-1 min, then increased to 30% (B) at 6-12 min, 60% (B) at 12-16 min, 80% (B) at 16-20 min, and 5% (B) at 26-30 min. The sample injection volume was 10 µL. The MS analysis on the Water UPLC-TQD Mass Spectrometer (XEVOTQD#QCA1232) was carried out using data-dependent automated switching between MS and MS/MS acquisition modes. Positive and negative ionization modes were used to record the spectra, with a mass acquisition range of 150-2000 m/z.

3.5. FT-IR Analysis

Functional groups were identified using Fourier transform infrared spectroscopy (FTIR). The methanolic leaf extracts were analyzed using FTIR (Shimadzu, Kyoto, Japan, IR Affinity1), with a scan range of 400 to 4000 cm-1 and a resolution of 4 cm-1.

A total of 31 phytocompounds of *Lannea coromandelica* and 26 phytocompounds of *Trevesia palmata* leaves were identified and collected from various research papers from PubMed (https://pubmed.ncbi.nlm.nih.gov). PubMed is a free search engine that mainly accesses the MEDLINE database, which contains references and abstracts on biomedical and life sciences subjects. The database is managed by the National Institutes of Health's United States National Library of Medicine as part of the Entrez information retrieval system. PubChem is a public chemical information resource created and managed by the National Centre for Biotechnology Information (NCBI) at the National Library of Medicine (NLM), which is part of the National Institutes of Health (NIH) in the United States. It compiles descriptions of chemical compounds and their biological activity from more than 500 data sources and makes this knowledge available to the public for

free. The SMILES format, as well as the PubChem CID, Class of Compound, Chemical Formula, and Molecular Weight of a total of 31 phytocompounds of *L. coromandelica* and 26 phytocompounds of *T. palmata*, were collected and retrieved from PubChem (National Institutes of Health's open chemistry database).

3.6. Toxicity Prediction by QSAR TEST Toolbox

All the 27 phytocompounds identified from plant leaves of *Lannea coromandelica* against the giant, free-living ciliate, the fathead minnow, and rat using Toxicity Estimation Software Tool (TEST), (https://epa.figshare.com/articles/software/Toxicity_Estimation_Software Tool TEST /21379365) was developed to allow users to easily estimate the toxicity of chemicals from the structure of a compound using Quantitative Structure Activity Relationships (QSARs) methodologies. Mathematical models called Toxicity Estimation Software Tool (TEST) QSARs are used to predict amounts of toxicity based on molecular descriptors, or the physical properties of chemical structures. Here, the research was conducted using NOAEL of repeated dosage toxicity and reproductive toxicity. For this investigation, the consensus technique was used since it incorporates all of the previously mentioned models for toxicity prediction.

3.7. Prediction of activity spectra for substances (PASS)

PASS is an online software that may be used to assess the potential binding affinity of organic drug-like molecules based on their structural properties. All phytochemicals underwent PASS analysis (Filimonov et al., 2014). It uses multilevel neighbourhood of atom (MNA) descriptors and a Bayesian algorithm to predict the activity of organic compounds using a structure-activity relationship (SAR) model for a large number of pharmaceutical drugs.

3.8. Protein retrieval and preparation

The three-dimensional structures of COX-2 (PDB ID: 3NTG, Fig.), TNF-α (PDB ID: 2AZ5, Fig.), IL-6 (PDB ID: 1ALU, Fig.), and iNOS (PDB ID: 1M8D, Fig. 1) were retrieved from the Research Collaboratory for Structural Bioinformatics (RCSB) Protein Data Bank (PDB) at a resolution of 1.62 Å. UCSF Chimaera 1.15

(https:// www. cgl. ucsf. edu/ chime ra/) was used to construct the crystal structures of COX-2, TNF-α, IL-6, and iNOS receptors prior to docking (Pettersen et al. 2004). The co-crystallized ligand, water molecules, and metal ions were all removed from the target proteins. Polar hydrogen atoms and partial charges have been introduced into the formations. The shortened side chains were restored and Gasteiger charges were added to the target proteins using the in-built dock prep programme (Opo et al. 2021).

3.9. Physicochemical properties of the receptors

Expasy-ProtParam was used to assess the physicochemical parameters of COX-2, TNF-α, IL-6, and iNOS receptors (http://web. expasy. org/protparam/). The amino acid sequence of COX-2, TNF-α, IL-6, and iNOS receptors was downloaded in FASTA format from RCSB PDB and used as input for the webserver to compute several parameters such as theoretical PI, amino acid composition, atomic composition, extinction coefficient, estimated half-life, instability index, aliphatic index, and grand average of hydropathicity (GRAVY) (Gasteiger et al., 2005).

3.10. Protein active site prediction

The discovery and characterisation of pockets in a protein structure is a critical step in a molecular docking investigation. The fpocket web server (https://biose rv. rpbs. univ- paris- dider ot. fr/ services/ fpock et/) was used to identify the active site or pocket of the prepared COX-2, TNF-α, IL-6, and iNOS receptors. The fpocket tool uses Voronoi tessellation and α-spheres to identify protein active pockets. The fpocket successfully detected 94% and 92% of known protein binding sites inside the top three pockets (Schmidtke et al., 2010). The receptor was assigned to the best-ranked pocket (Pocket 0) from the fpocket results. The results were visualised using Schrödinger's Pymol 2.4.0 (http:// www. pymol. org/ pymol).

3.11. Molecular docking

The molecular docking was done in PyRx - Python prescription 0.8 using the AutoDock Vina plug-in programme (Trott and Olson 2010). GA run (number of genetic algorithms, 250) and eval (number of energy evaluations, 25000000) were

altered, while other choices docking parameters remained unchanged. The AutoGrid programme was used to create the grid box for grid mapping. The "Vina wizard control" option loaded the target COX-2, TNF-α, IL-6, and iNOS receptors, as well as ligand molecules. The active pocket residue of the receptor molecule was named, shown, and classified using the PyRx virtual screening software's "molecules" function to perform point-specific molecular docking. Following categorization, a grid box was mapped on the receptor. The centre point's measurements for COX-2 are x (45.3951), y (22.7384), and z (30.0723), while the grid area's dimensions are x (30.0191), y (30.0609), and z (30.0723). The centre point's measurements for iNOS are x (124.213), y (112.677) and z (22.3046), while the grid area's dimensions are x (30.0328), y (30.0078) and z (30.0557. The centre point's measurements for IL-6 are x (11.2608), y (33.7931), and z (5.9736), while the grid area's dimensions are x (30.0298), y (30.0613), and z (30.0479). The centre point's measurements for TNF-α are x (12.4509), y (114.6905), and z (95.7405), while the grid area's dimensions are x (30.0609), y (30.0335), and z (30.5265). Following the grid mapping generation, the AutoDock Vina programme was created and executed. The AutoDock Vina Lamarckian algorithm (LGA) uses a tight clustering technique with an RMSD tolerance of 1.0 Å to generate 200 conformers for each ligand (Fuhrmann et al., 2010). The generated clusters were accurately sorted by the lowest binding energy (the most stable conformer) and arranged hierarchically. The docking results were examined on the "analyse results" page and saved in CSV format (Comma Separated Values). The interaction with the lowest binding affinity (kcal/mol) was chosen as the optimal conformation for each ligand. The top four protein-ligand interactions were selected for further investigation. The chosen interactions were visualised using BIOVIA Discovery Studio Visualizer v21.1.0.20298 (https:// disco ver.3ds. com/ disco). very-studio-visualizer-download (Biovia, 2015) and PyMol software (Schrodinger and DeLano, 2020).

3.12. Evaluation of various Pharmacokinetics (PK) and pharmacodynamics properties

Lannea coromandelica, and *Trevesia palmata* ligand compounds were retrieved from the PubChem database (https://pubchem.ncbi.nlm.nih.gov/) using the standard SMILES format. SwissADME (http://www.swissadme.ch) and Molinspiration Cheminformatics (https://www.molinspiration.com) tools were used to predict the ADMET features, lipophilicity, water solubility, drug likeness bioactivity score (DLBS), and pharmacokinetics-bioactivity, as well as medicinal chemistry, drug likeness bioavailability score and pharmacokinetics. SWISSADME and Molinspiration Cheminformatics tools evaluate the ligand molecules using the Lipinski rule of 5 (LOR5), which states that an active oral medication must meet the following criteria: ADMET default range—Molecular weight (MW): 100-600 hydrogen atoms; number of hydrogen bond acceptors (nHA): 0–12; number of hydrogen bond donors (nHD): 0-7; number of rotatable bonds (nRot): 0-11 (amide C-N bonds are excluded from being taken into account in certain contexts because of their high rotational energy barrier); number of rings (nRing): 0-6; number of rigid bonds as opposed to rotatable bonds (nRig): 0-30; flexibility: Flexibility = nRot / nRig; Topological polar surface area (TPSA) (Å2): 0-140, based on Veber rule; logarithm of aqueous solubility value (LogS): -4 to 0.5 log mol/L; logarithm of the n-octanol/water distribution coefficient (LogP): 0 to 3 log mol/L; logarithm of the n-octanol/water distribution coefficients at pH=7.4 (LogD7.4): 1 to 3 log mol/L (Daina et al., 2014; Ertl et al., 2000; Lipinski, 2004; Lipinski et al., 2001; Veber et al., 2002). The drug-likeness bioactivity score (DLBS) of the ligand molecule was predicted using the criteria of GPCR ligand, ion channel modulator, nuclear receptor ligand, kinase inhibitor, protease inhibitor, enzyme inhibitor, and cytochrome P450 inhibitors and scored as follows: The Molinspiration cheminformatics server (Daina & Zoete, 2016) classified medicines as active (score >0), moderately active (5.0 to 0.0), or inactive (scoring <5.0). The SwissADME programme was used to calculate pharmacokinetic bioactivity parameters such as gastrointestinal (GI) absorption, blood brain barrier (BBB) permeability, and P-glycoprotein substrate (P-gp). The SwissADME

method was used to forecast skin permeability (Log Kp), and a lower Log Kp value indicates less penetration to the skin, making it an attractive medication candidate (Potts and Guy, 1992). The zero alert of PAINS and the Brenk filter (which aids in categorising the ligand molecule) indicate whether or not the ligand molecule responds to the biological assays (PAINS), as well as ensuring the accepted toxic level, chemical reactivity, and metabolically unstable or enduring properties that are responsible for poor pharmacokinetics (Brenk) (Baell and Holloway, 2010; Brenk et al., 2008). The synthetic accessibility score is a metric for assessing the ease of synthesis of drug-like compounds, with a value of 1 indicating extremely easy synthesis and a score of 10 indicating very difficult synthesis (Ertl and Schuffenhauer, 2009). A bioavailability score of greater than 0.10 indicates oral bioavailability according to Lipinski's principles and is deemed a suitably absorbable molecule orally (Doak et al., 2014).

3.13. Toxicity Studies

Acute and sub-acute toxicity tests were performed based on the OECD (Organisation for Economic Co-operation and Development) - Guidelines 425 and 407 (OECD 2008a, 2008b).

3.14. Acute toxicity (LD50 test)

The study conducted oral acute toxicity research on male rats, following OECD guideline No. 425. The rats were divided into treatment groups (2000 and 5000 mg/kg body weight) and given a single dose of methanolic leaf extracts from *Lannea coromandelica* and *Trevesia palmata*. The study recorded signs of acute toxicity, deaths per dosage, and daily water and feed consumption. After observation, animals were anaesthetized with ketamine and xylazine, and blood samples were taken for analysis, while organs were removed, weighed, and preserved in Bouin's fixative for histological study.

3.15. Sub-acute toxicity

The study involved four experimental groups of male animals, each given three doses of *Lannea coromandelica* and *Trevesia palmata* orally for 28 days. The

animals were monitored for body weight, food and water consumption, and potential toxicity indicators according to OECD Guideline 407, (OECD, 2008b). After 28 days, they were starved and anesthetized, and blood samples were collected for further investigation.

3.16. Body weight, organ indices, food and water intake and rectal temperature

Body weight (g), food consumption (g) and water consumption (mL) were computed everyday between 08:00 h and 11:00 h for 7 days all throughout the experiment. The absolute organ weight of colon tissue samples was recorded.

3.17. Sample collection

After 24 hours of final treatment, all animals were sacrificed with an intraperitoneal injection of Ketamine (90 mg/kg body weight) and Xylazine (10 mg/kg body weight). Serum was obtained after centrifugation of whole blood at 1000 × g at room temperature for 10 minutes. Colon tissues were obtained after removing the adhering connective tissues of each animal and kept immediately at -20°C. The tissue was fixed in Bouin's fixative, which contained 75% saturated picric acid, 25% formaldehyde, and 5% glacial acetic acid, for at least 24 hours before being transferred to 70% ethanol for further testing. All dissection techniques were carried out under aseptic conditions.

Total protein lysate was prepared by weighing colon pieces. The tissue fragments were homogenized in an ice-cold suspension buffer containing 50 mM Tris-Hydrochloric acid, pH 8.0; 150 mM Sodium Chloride (NaCl); 0.1% Sodium Dodecyl Sulphate (SDS); 1 g/ml Aprotinin; 1 mM Phenylmethylsulfonyl fluoride (PMSF) and 1mM Ethylenediaminetetraacetic acid (EDTA) disodium salt dehydrate (cat# E5134; Sigma-Aldrich, St. Louis, MO, USA) to yield 10% homogenate (w/v). The supernatants were centrifuged at 10000 × g at 4 °C for 10 minutes and kept at -20 °C for western blot analysis. Tissues were homogenized with the above-mentioned SDS-free buffer for the enzyme assay.

3.18. Haematological analysis

Haematological assays were done on all surviving animals at the conclusion of the trial, on the 15th day for acute toxicity and the 29th day for sub-acute toxicity. Animals were sacrificed, and their blood was collected in tubes.

The hematologic parameters were assessed for white blood cell (WBC), red blood cell (RBC), haemoglobin (Hb), haematocrit, mean corpuscular volume (MCV), mean corpuscular haemoglobin (MCH), and mean corpuscular haemoglobin concentration (MCHC).

3.19. Serum Biochemical Analysis

The biochemical assay was performed on all surviving animals at the end of the experiment. The blood was collected into tubes and centrifuged at 3500 rpm for 30 minutes. Serum from each sample was collected and kept at -80ºC until analysis. Serum alanine aminotransferase (ALT), aspartate aminotransferase (AST), alkaline phosphatase (ALP), total protein, globulin (Glo), albumin (Alb), urea, blood urea nitrogen (BUN), creatinine, triglycerides, total cholesterol, and calcium activity were measured using a coral clinical diagnostic kit.

3.20. Histological Analysis

The organs were fixed using Bouin's fixative, embedded in paraffin, sectioned at 5 µm, stained with haematoxylin and eosin, and studied under light microscopy (Martey et al., 2010). The histological analysis intended to determine the organs' tissue integrity. The characteristics studied included degeneration, necrosis, apoptosis, leukocyte infiltration, congestion, blood extravasation, and fibrosis (Fabia et al., 1993).

3.21. Animal Care and Handling

The animal care and handling (CPCSEA Registration No. 1999/GO/ReBi/S/18/CPCSEA, valid from 16/02/2018 to 15/02/2023) was carried out in accordance with the rules allowed by Mizoram University's Institutional Animal Ethics Committee in Aizawl, India (Permit No. MZU-IAEC/2018/11).

Three-month-old male/female Wistar albino rats weighing 150 to 180 g were selected from an inbred colony maintained under controlled conditions of temperature (23 ± 2º C), humidity (50 ± 5%), and light (12 hours of light and dark, respectively). The animals were given sterile food and drink. Throughout the experiment, five animals were confined in a polypropylene cage with bedding made from locally sourced wood powder. All efforts were made to alleviate the suffering and misery of male Wistar albino rats.

3.22. Induction of colitis and drug treatment schedule

Colitis was induced according to the procedure described by Li et al., 2011. Briefly, rats were slightly anaesthetized with ether following a 24 h fast, and then TNBS dissolved in 50 % ethanol were instilled into the colon of the animals (150 mg/kg in a volume of 0.25 mL) using a medical-grade polyurethane catheter for enteral feeding (external diameter 2 mm) inserted 8 cm into the anus. Control group were made for comparison with TNBS/ethanol instillation: rats in the sham group received an enema of physiological saline instead of the TNBS solution. Rats were randomly divided into following 10 groups as follows (Table 1 and 2):

3.23. Assessment of Disease activity index, colonic damage, ulcer area and ulcer index

3.24. Disease activity index (DAI)

Disease activity index (DAI) was based on body weight loss, stool consistency and blood in stools. Body weight loss, stool consistency and blood in stools were recorded daily for the study. Briefly, scores were assigned for each item to calculate DAI as follows:

Scoring system for loss in body weight was as follows: no weight loss = 0; weight loss of 1% to 5% = 1; weight loss of 6% to 10% = 2; weight loss of 11% to 20% = 3; and weight loss 20% and above = 4.

Scoring levels for stool consistency was as follows: normally formed pellets = 0; pasty and semiformed pellets = 2; and liquid stools = 4.

Occult bleeding was scored as stated: negative hemoccult = 0; positive hemoccult = 2; and visible blood/gross bleeding from the rectum = 4.

The scoring parameters were added together resulting in a total score ranging from 0 to 12 divided by 3.

Body weight of rat was measured daily from the start of the experiment to the termination day. All animals were monitored daily for the duration of the study to assess DAI changes in response to treatment (Yang et al., 2014).

3.25 Morphological Evaluation

The removed colons were excised free of adherent adipose tissue, rinsed with ice-cold saline and dissected longitudinally. It was examined visually immediately and the macroscopic scoring of the colonic damage was assessed using the criteria shown in Table 34, on a scale of 0–5 as previously described by Morris et al., 1989.

Table 3. Criteria for scoring of macroscopic damage.

Score	Macroscopic Morphology
0	No damage.
1	Localized hyperemia, but no ulcers.
2	Linear ulcers with no significant inflammation*.
3	Linear ulcer with inflammation at one site.
4	Two or more sites of ulceration and/or inflammation.
5	Two or more major sites of inflammation and ulceration or one major site of inflammation and ulceration extending >1 cm along the length of the colon.

*Inflammation was defined as regions of hyperemia and bowel wall thickening.

The ulcer area and ulcer index were assessed according to Dengiz and Gursan's method. The ulcer index was calculated by using the following formula (Kandhare et al., 2013; Kumar et al., 2014; Rachmilewitz et a., 1989):

Table 1: Induction of ulcerative colitis using experimental rat model of trinitrobenzene sulphonic acid (TNBS) - *Lannea coromandelica* bioactive compounds

Group no.	Animal group	Treatment	Dose	Route of Administration	No. of Animals	Days of Treatment		
						0 day	1-7th days	8th day
I	Sham control	Dimethyl sulfoxide (DMSO) (1 %)	1 ml	p.o.	5	-	√	Blood sample were collected and animals were sacrificed for bio-chemical, molecular and histo-pathological examination
II	TNBS induced control	DMSO (1%)	1 mL	p.o	5	-	√	
		Trinitrobenzensulfonic acid (TNBS)	150 mg/kg	intrarectally		√	-	
III	TNBS induced and Sulfasalazine treated	Sulfasalazine in DMSO (1%)	1 mL	p.o	5	-	√	
		Trinitrobenzensulfonic acid (TNBS)	150 mg/kg	intrarectally		√	-	
IV	TNBS induced and Lannea coromandelica (Lc) bioactive compounds (10 mg/kg)	10 mg/kg Lc leaf extract in DMSO (1%)	1 mL	p.o	5	-	√	
		Trinitrobenzensulfonic acid (TNBS)	150 mg/kg	intrarectally		√	-	
V	TNBS induced and Lannea coromandelica bioactive compounds (20 mg/kg) treated	20 mg/kg Lc leaf extract in DMSO (1%)	1 mL	p.o	5	-	√	
		Trinitrobenzensulfonic acid (TNBS)	150 mg/kg	intrarectally		√	-	

Table 2: Induction of ulcerative colitis using experimental rat model of trinitrobenzene sulphonic acid (TNBS) - *Trevesia palmata* bioactive compounds

Group no.	Animal group	Treatment	Dose	Route of Administration	No. of Animals	Days of Treatment		
						0 day	1-7th days	8th day
I	Sham control	Dimethyl sulfoxide (DMSO) (1 %)	1 mL	p.o.	5	-	√	Blood sample were collected and animals were sacrificed for bio-chemical, molecular and histo-pathological examination
II	TNBS induced control	DMSO (1%)	1 mL	p.o	5	-	√	
		Trinitrobenzensulfonic acid (TNBS)	150 mg/kg	intrarectally		√	-	
III	TNBS induced and Sulfasalazine treated	Sulfasalazine in DMSO (1%)	1 mL	p.o	5	-	√	
		Trinitrobenzensulfonic acid (TNBS)	150 mg/kg	intrarectally		√	-	
IV	TNBS induced and *Trevesia palmata* (Tp) bioactive compounds (10 mg/kg)	10 mg/kg Tp leaf extract in DMSO (1%)	1 mL	p.o	5	-	√	
		Trinitrobenzensulfonic acid (TNBS)	150 mg/kg	intrarectally		√	-	
V	TNBS induced and Trevesia palmata (Tp) bioactive compounds (20 mg/kg) treated	20 mg/kg Tp leaf extract in DMSO (1%)	1 mL	p.o	5	-	√	
		Trinitrobenzensulfonic acid (TNBS)	150 mg/kg	intrarectally		√	-	

Ulcer index (UI) = Total area of ulcer (mm^2)/Total area of colon (mm^2)

and the inhibition rate was calculated by using the formula:

$$\% \text{ Inhibition} = [(UI_{control} - UI_{treated}/UI_{control})] \times 100$$

5.26. ELISA assays

Determination of Nitric oxide content (NO), myeloperoxidase (MPO), Calprotectin (CALP), Interleukin-6 (IL-6), Interleukin-1 (IL-1), Leukotriene-B4 (LT-B4), FAD-Linked sulfhydryl oxidase ALR, Prostaglandin E2 (PG-E2), Total Antioxidant (T-AOC) and Interleukin-10 (IL-10) was done using ELISA kits (Bioassay Technology Laboratory Rat ELISA kit) as per manufacturer's protocol.

3.27. Measurement of Lipid Peroxidation

The malondialdehyde (MDA) level in the colon was determined using the approach previously published by Ohkawa et al., 1979, with slight modifications (Aboul-Soud et al., 2011). Briefly, 75 µl of colon lysates were combined with the equivalent amount of 10% Trichloroacetic acid. Freshly made 0.2% Thiobarbituric acid was then added at a 1:2 ratio and heated for 45 minutes. The solutions were allowed to cool before the optical densities were measured at 532 nm against a blank, and the MDA concentration was expressed as nM/mg protein. A mixture devoid of colon protein lysate served as a blank.

3.28. Assessment of GSH, SOD, CAT, GPx

Superoxide dismutase (SOD) assay. The previously published approach was used in the superoxide dismutase assay (Kakkar et al., 1984). To prepare the mixture, add 50 µl of 10% tissue homogenate, 600 µl of 52 mM sodium pyrophosphate buffer (pH 8.3), 50 µl of 186 µM phenazine methosulphate (PMS), and 150 µl of 300 µM Nitroblue tetrazolium (NBT). To begin the reaction, add 100 µl of 750µMml NADH and incubate at 30°C. After 90 seconds of incubation, the reaction was stopped by adding 500 µl glacial acetic acid. 2 ml of n-butanol were added, vortexed and left to stand for ten

minutes. The mixture was centrifuged at 10000 × g for 10 minutes at room temperature, then the supernatant was collected. Colour intensity was measured at 560 nm.

Glutathione reduced (GSH) assay. A previously established principle and method were used for the Glutathione reduction assay (Rahman et al., 2006). Briefly, A mixture with 2.0 M Pyrophosphate buffer (pH 7.4), 0.2 M of 5,5′-dithio-bis-[2-nitrobenzoic acid], and 50 µl of 10% tissue homogenate. The experiment was based on the rate of TNB-chromophore production following the reaction of DTNB with intracellular GSH concentration. The TNB complex has a maximum absorbance of 412 nm. The TNB complex production rate was thought to be related to the GSH level of the tissue samples, with GSH concentration represented as U/mg protein. The reaction mixture free of tissue homogenate served as a blank.

Catalase assay. A previously published approach was used to determine Catalase activity (Sinha, 1972). The assay mixture consisted of 1 ml of PBS (pH 7), 100 µl of testis tissue lysate, and 400 µl of 2 M hydrogen peroxide (H_2O_2). After 1 minute, the reaction was stopped by adding 2.0 ml of dichromate-acetic acid reagent (5% potassium dichromate and glacial acetic acid in a 1:3 ratio). Absorbance was measured at 570 nm with a spectrophotometer. The activity was measured as U/mg of H_2O_2 consumed per minute per mg of protein (H_2O_2/min/mg protein). A mixture devoid of tissue homogenate was used as a blank.

Glutathione Peroxidase (GPx) assay. Sazuka et al.'s (1985) approach was used to determine GPx activity. To prepare the mixture, 100 µl of homogenate was combined with 200 µl of EDTA, sodium azide, GSH, H2O2, and 400 µl buffer. The reaction mixture was incubated at 37ºC for 10 minutes before adding 10% trichloroacetic acid (TCA). After centrifugation, the supernatant was collected and mixed with 3 ml disodium hydrogen phosphate and 1000 µl of 5,5'-dithio-bis(2-nitrobenzoic acid) (DTNB). A spectrophotometer was used to measure the absorbance of the sample/s in comparison to the blank at 412 nm. The activity was calculated as micromoles GSH per milligram protein.

3.29. Histopathological examination of gastric lesions and measurement

3.29.1 Hematoxylin and eosin staining (H&E)

Colon tissues were fixed in Bouin's fixative for 24 h in Bouin's fixative. The fixed specimen was processed through the conventional paraffin embedding technique, sectioned at 5µm and stained with hematoxylin and eosin (Bancroft and Gamble, 2002), for histopathological studies. Microscopic scoring was assessed using the criteria illustrated in table 2 (Fabia et al., 1993).

Table 35. The variables used for microscopic scoring.

Variables	**Severity of changes**			
	0	1	2	3
Ulceration	No ulcer	Erosion or single ulceration not exceeding lamina muscularis mucosa	Multifocal ulcerations not exceeding the submucosa	Ulcerations exceeding the submucosa
Mucus cell depletion	Preserved mucus cell	Mild depletion in a few cell	Moderate depletion (less than 50% complete disappearance of cells)	Severe depletion or complete disappearance of cells mucosa
Cyrpt abcesses	No abcesses	1–3 abscesses/slide	4–9 abscesses/slide	10 or more abscesses/slide
Inflammatory cysts	No cysts	1–3 cysts/slide	4–9 cysts/slide	10 or more cysts/slide
Mucosal atrophy	Normal thickness	Mild atrophy (less than 10%)	Moderate atrophy (10–50%)	Severe atrophy (>50%)
Edema (submucosa)	Normal thickness	Mild edema (submucosal expansion less than 10%)	Moderate edema (submucosal expansion, 10–100%)	Severe edema (submucosal expansion, >100%)
Inflammatory cell infiltration	No inflammatory	Mild inflammatory cell infiltration	Moderate (distributed but not dense)	Dense inflammatory cell infiltration

	cell infiltration		inflammatory cell infiltration	
Vascular dilatation	Normal blood vessels	Mild dilatation of single blood vessel	Moderate dilatation of several blood vessels	Severe dilatation of several blood vessels

3.30. Western blotting

Western blot analysis was performed on colon protein lysates, as previously described (Jeremy et al., 2017). Briefly, the total protein concentration of each lysate was determined using Bradford techniques (Bradford, 1976). Proteins (50 µg) were electrophoresed using 10% sodium dodecyl sulfate-polyacrylamide gel electrophoresis (SDS-PAGE) at 150 V. The resolved proteins were transferred to a polyvinylidene difluoride (PVDF) membrane using the Medox-Bio Mini SemiDry Blotting MX-1295-01 device for 20-30 minutes. Membranes were then blocked for at least 1 hour at room temperature in a blocking solution containing 0.05% Tween 20 in Phosphate-buffered saline (PBS) and 10% non-fat skimmed milk (Cat# GRM1254-500G HiMedia Laboratory Private Limited, Mumbai, India). The membranes were next probed with BCL-2 (1:2000, Mouse polyclonal antibody, Cat#sc-7382, Santa Cruz Biotechnology, INC., Dallas, USA), BAX (1:1000, Mouse polyclonal IgG, Cat#sc-7480, Santa Cruz Biotechnology INC. Dallas, USA), Anti-Active Caspase-3 (1:1000, Mouse monoclonal antibody, Cat# E-AB-22115, Elabscience), Tumour Necrosis Factor Alpha (TNF-α) (1:1000, Rabbit polyclonal IgG, Cat# BS-2081R, BIOSS), Interleukin-6 (IL-6) (1:1000, Rabbit monoclonal IgG, BIOSS), Nuclear Factor Kappa B p65 (NFkB p65) (1:2000, Mouse monoclonal IgG, Cat# E-AB-22066, Elabscience), NOX2 (NADPH OXIDASE 2), also called CYBB (CYTOCHROME b (-245) (1:1000, Rabbit Polyclonal antibody, Cat# E-AB-60387, Elabscience) and Peroxisome Proliferator Activated Receptor gamma (PPARG) (1:1000, Rabbit polyclonal IgG, Elabscience) for overnight inside humidified chamber at 4 °C. Membranes probed with rabbit raised primary antibody were incubated with Horse-radish Peroxidase (HRP) conjugated goat-anti-rabbit secondary IgG antibody (1:4000, Cat#E-AB-1003, Elabscience), and membranes probed with mouse raised primary antibody were incubated with HRP

conjugated goat-anti-mouse secondary IgG antibody (1:4000, Cat#E-AB-1001, Elabscience) for 3 hours with constant agitation at room temperature. The membranes were rinsed four times with PBST before being immersed in Enhanced Chemiluminescence (ECL) solutions (Cat #1705061, BioRad, Hercules, CA, USA) according to the manufacturer's instructions and developed on X-ray film in a dark room. The band intensities were quantified using ImageJ software. A probe was created for β-Tubulin (1:1500, Rabbit monoclonal IgG, Cat#E-AB-20070, Elabscience), which served as a loading control for all antibodies utilised in this investigation.

3.11. Statistical analysis

All data were expressed as mean ± standard error of the mean (SEM). Comparison and analysis were performed using one way ANOVA. The P values <0.05 were considered significant.

IV. SUMMARY

- This experiment outlines the analysis of phytocompounds from two plant sources, *Lannea coromandelica* and *Trevesia palmata*, focusing on their metabolic interactions, repeated dose toxicity, reproductive toxicity, and predicted biological activities using various computational tools such as QSAR Tool Software, ADMETLab 2.0, and PASS Online.
- In summary, the molecular docking studies provide promising candidates from *Lannea coromandelica* and *Trevesia palmata* for further exploration as potential anti-inflammatory agents targeting COX-2, iNOS, TNF-α, and IL-6 receptors.
- Histological Changes: Both LCLE and TPLE treatments induced histological alterations in the liver and kidneys, including congestion, sinusoidal dilation, bile duct proliferation, lumen atrophy, and tubular enlargement.
- The provided data elucidates the effects of *Lannea coromandelica* and *Trevesia palmata* methanolic extracts on various inflammatory markers in the context of TNBS-induced colitis, shedding light on their potential as

therapeutic agents for inflammatory bowel diseases like ulcerative colitis (UC).

- The results outline the therapeutic efficacy of *Lannea coromandelica* leaf extract (LCLE) and *Trevesia palmata* leaf extract (TPLE) in mitigating oxidative stress, improving antioxidant status, influencing histological changes in the colon, and modulating protein expression related to apoptosis and inflammation in TNBS-induced colitis in rats.

V. REFERENCES

Juliao-Banos, F., Torres-Amaya, M., Otero-Regino, W., Vallejo, M. T., Galiano, M. T., Feliciano, J., ... & Gil-Parada, F. (2020). Guidelines for the management of ulcerative colitis in the adult population (update). Revista colombiana de Gastroenterología, 35, 2-62.

Vavricka, S. R., Schoepfer, A., Scharl, M., Lakatos, P. L., Navarini, A., & Rogler, G. (2015). Extraintestinal manifestations of inflammatory bowel disease. Inflammatory bowel diseases, 21(8), 1982-1992.

Gordon, H., Burisch, J., Ellul, P., Karmiris, K., Katsanos, K., Allocca, M., ... & Kucharzik, T. (2024). ECCO guidelines on extraintestinal manifestations in inflammatory bowel disease. Journal of Crohn's and Colitis, 18(1), 1-37.

Antoniou, E., Margonis, G. A., Angelou, A., Pikouli, A., Argiri, P., Karavokyros, I., ... & Pikoulis, E. (2016). The TNBS-induced colitis animal model: An overview. Annals of medicine and surgery, 11, 9-15.

Choi, J., & Fenando, A. (2020). Sulfasalazine.

Yoshino, T., Sono, M., & Yazumi, S. (2016). Usefulness of sulfasalazine for patients with refractory-ulcerative colits. BMJ Open Gastroenterology, 3(1), e000103.

Ahmed, M. (2019). Medicinal plants. MJP Publisher.

Hassen, G., Belete, G., Carrera, K. G., Iriowen, R. O., Araya, H., Alemu, T., ... & DEBELE, T. K. (2022). Clinical implications of herbal supplements in conventional medical practice: a US perspective. Cureus, 14(7).

Swathi, S., & Lakshman, K. (2022). Photochemistry and Pharmacological Bio-Activities of Lannea coromandelica: A Review. Innovare Journal of Medical Science, 10(5).

Manoharan, A. L., Jagadeesan, G., Nataraj, G., Muniyandi, K., Guruswami, G., Arunachalam, K., & Thangaraj, P. (2023). Efficacy of Trevesia palmata (Roxb. ex Lindl.) Vis. Extract on MG 63 cell lines and arthritis-induced animal models. Journal of Ethnopharmacology, 300, 115742.

Islam, F., Mitra, S., Nafady, M. H., Rahman, M. T., Tirth, V., Akter, A., ... & El-Kholy, S. S. (2022). Neuropharmacological and antidiabetic potential of lannea coromandelica (houtt.) merr. Leaves extract: an experimental analysis. Evidence-Based Complementary and Alternative Medicine, 2022.

Wang, K., Mao, T., Lu, X., Wang, M., Yun, Y., Jia, Z., ... & Shi, R. (2023). A potential therapeutic approach for ulcerative colitis: targeted regulation of macrophage polarization through phytochemicals. Frontiers in Immunology, 14, 1155077.

Ha, H. A., Al-Sadoon, M. K., Saravanan, M., & Jhanani, G. K. (2024). Antibacterial, antidiabetic, acute toxicity, antioxidant, and nephroproductive competence of extracts of Lannea coromandelica fruit through in-vitro and in-vivo animal model investigation. Environmental Research, 242, 117767.

Manoharan, A. L., Jagadeesan, G., Nataraj, G., Muniyandi, K., Guruswami, G., Arunachalam, K., & Thangaraj, P. (2023). Efficacy of Trevesia palmata (Roxb. ex Lindl.) Vis. Extract on MG 63 cell lines and arthritis-induced animal models. Journal of Ethnopharmacology, 300, 115742.

Modesto, R., Estarreja, J., Silva, I., Rocha, J., Pinto, R., & Mateus, V. (2022). Chemically induced colitis-associated cancer models in rodents for pharmacological modulation: A systematic review. Journal of clinical medicine, 11(10), 2739.

Sasidharan, S., Chen, Y., Saravanan, D., Sundram, K. M., & Latha, L. Y. (2011). Extraction, isolation and characterization of bioactive compounds from plants' extracts. African journal of traditional, complementary and alternative medicines, 8(1).

Salerno, T. M., Donato, P., Frison, G., Zamengo, L., & Mondello, L. (2020). Gas chromatography—Fourier transform infrared spectroscopy for unambiguous determination of illicit drugs: a proof of concept. Frontiers in Chemistry, 8, 624.

Junaedi, E. C., Lestari, K., & Muchtaridi, M. (2021). Infrared spectroscopy technique for quantification of compounds in plant-based medicine and supplement. Journal of advanced pharmaceutical technology & research, 12(1), 1-7.

Ardrey, R. E. (2003). Liquid chromatography-mass spectrometry: an introduction (Vol. 2). John Wiley & Sons.

Abubakar, A. R., & Haque, M. (2020). Preparation of medicinal plants: Basic extraction and fractionation procedures for experimental purposes. Journal of Pharmacy and Bioallied Sciences, 12(1), 1-10.

Wu, F., Zhou, Y., Li, L., Shen, X., Chen, G., Wang, X., ... & Huang, Z. (2020). Computational approaches in preclinical studies on drug discovery and development. Frontiers in chemistry, 8, 726.

Lawal, B., Shittu, O. K., Oibiokpa, F. I., Mohammed, H., Umar, S. I., & Haruna, G. M. (2016). Antimicrobial evaluation, acute and sub-acute toxicity studies of Allium sativum. Journal of Acute Disease, 5(4), 296-301.

Mensah, M. L., Komlaga, G., Forkuo, A. D., Firempong, C., Anning, A. K., & Dickson, R. A. (2019). Toxicity and safety implications of herbal medicines used in Africa. Herbal medicine, 63(5), 1992-0849.

Ugwah-Oguejiofor, C. J., Okoli, C. O., Ugwah, M. O., Umaru, M. L., Ogbulie, C. S., Mshelia, H. E., ... & Njan, A. A. (2019). Acute and sub-acute toxicity of aqueous extract of aerial parts of Caralluma dalzielii NE Brown in mice and rats. Heliyon, 5(1).

Wang, H., Chen, Y., Wang, L., Liu, Q., Yang, S., & Wang, C. (2023). Advancing herbal medicine: enhancing product quality and safety through robust quality control practices. Frontiers in Pharmacology, 14, 1265178.

Tatsumi, Y., Kakimoto, K., Hara, A., Mizuta, N., Numa, K., Kinoshita, N., ... & Nishikawa, H. (2023). Biomarkers for Monitoring of Changes in Disease Activity in Ulcerative Colitis. Journal of Clinical Medicine, 12(22), 7165.

Opo, F. A. D. M., Rahman, M. M., Ahammad, F., Ahmed, I., Bhuiyan, M. A., & Asiri, A. M. (2021). Structure based pharmacophore modeling, virtual screening, molecular docking and ADMET approaches for identification of natural anti-cancer agents targeting XIAP protein. Scientific reports, 11(1), 4049.

Gasteiger, E., Hoogland, C., Gattiker, A., Duvaud, S. E., Wilkins, M. R., Appel, R. D., & Bairoch, A. (2005). Protein identification and analysis tools on the ExPASy server (pp. 571-607). Humana press.

Schrodinger, L., & DeLano, W. (2020). The PyMOL molecular graphics system, version 2.0 Schrodinger, LLC (2017). Google Scholar There is no corresponding record for this reference.

Zoete, V., Daina, A., Bovigny, C., & Michielin, O. (2016). SwissSimilarity: a web tool for low to ultra high throughput ligand-based virtual screening.

Baell, J. B., & Holloway, G. A. (2010). New substructure filters for removal of pan assay interference compounds (PAINS) from screening libraries and for their exclusion in bioassays. Journal of medicinal chemistry, 53(7), 2719-2740.

Brenk, R., Schipani, A., James, D., Krasowski, A., Gilbert, I. H., Frearson, J., & Wyatt, P. G. (2008). Lessons learnt from assembling screening libraries for drug discovery for neglected diseases. ChemMedChem: Chemistry Enabling Drug Discovery, 3(3), 435-444.

Ertl, P., & Schuffenhauer, A. (2009). Estimation of synthetic accessibility score of drug-like molecules based on molecular complexity and fragment contributions. Journal of cheminformatics, 1, 1-11.

Doak, B. C., Over, B., Giordanetto, F., & Kihlberg, J. (2014). Oral druggable space beyond the rule of 5: insights from drugs and clinical candidates. Chemistry & biology, 21(9), 1115-1142.

Creton, S., Dewhurst, I. C., Earl, L. K., Gehen, S. C., Guest, R. L., Hotchkiss, J. A., ... & Billington, R. (2010). Acute toxicity testing of chemicals—opportunities to avoid redundant testing and use alternative approaches. Critical reviews in toxicology, 40(1), 50-83.

OECD. (2008a). Guidance document on acute inhalation toxicity testing. Series on Testing and Assessment.

OECD. (2008b). Test Guideline 425: Acute Oral Toxicity: Up-and-Down Procedure. OECD Guidelines for the Testing of Chemicals.

Fabia, R., Ar'Rajab, A., Johansson, M. L., Andersson, R., Willen, R., Jeppsson, B., ... & Bengmark, S. (1993). Impairment of bacterial flora in human ulcerative colitis and experimental colitis in the rat. Digestion, 54(4), 248-255.

Yang, Y., Smith Jr, D. L., Keating, K. D., Allison, D. B., & Nagy, T. R. (2014). Variations in body weight, food intake and body composition after long-term high-fat diet feeding in C57BL/6J mice. Obesity, 22(10), 2147-2155.

Morris, G. P., Beck, P. L., Herridge, M. S., Depew, W. T., Szewczuk, M. R., & Wallace, J. L. (1989). Hapten-induced model of chronic inflammation and ulceration in the rat colon. Gastroenterology, 96(2), 795-803.

Kandhare, A. D., Ghosh, P., Ghule, A. E., Zambare, G. N., & Bodhankar, S. L. (2013). Protective effect of Phyllanthus amarus by modulation of endogenous biomarkers and DNA damage in acetic acid induced ulcerative colitis: Role of phyllanthin and hypophyllanthin. Apollo Medicine, 10(1), 87-97.

Kumar, V. S., Rajmane, A. R., Adil, M., Kandhare, A. D., Ghosh, P., & Bodhankar, S. L. (2014). Naringin ameliorates acetic acid induced colitis through modulation of endogenous oxido-nitrosative balance and DNA damage in rats. Journal of biomedical research, 28(2), 132.

Rachmilewitz, D., Simon, P. L., Schwartz, L. W., Griswold, D. E., Fondacaro, J. D., & Wasserman, M. A. (1989). Inflammatory mediators of experimental colitis in rats. Gastroenterology, 97(2), 326-337.

Ohkawa, H., Ohishi, N., & Yagi, K. (1979). Assay for lipid peroxides in animal tissues by thiobarbituric acid reaction. Analytical biochemistry, 95(2), 351-358.

Kakkar, P., Das, B., & Viswanathan, P. N. (1984). A modified spectrophotometric assay of superoxide dismutase.

Rahman, I., Kode, A., & Biswas, S. K. (2006). Assay for quantitative determination of glutathione and glutathione disulfide levels using enzymatic recycling method. Nature protocols, 1(6), 3159-3165.

Sinha, A. K. (1972). Colorimetric assay of catalase. Analytical biochemistry, 47(2), 389-394.

Sazuka, Y., Tanizawa, H., & Takino, Y. (1989). Effect of adriamycin on the activities of superoxide dismutase, glutathione peroxidase and catalase in tissues of mice. Japanese journal of cancer research, 80(1), 89-94.

Bradford, M. M. (1976). A rapid and sensitive method for the quantitation of microgram quantities of protein utilizing the principle of protein-dye binding. Analytical biochemistry, 72(1-2), 248-254.